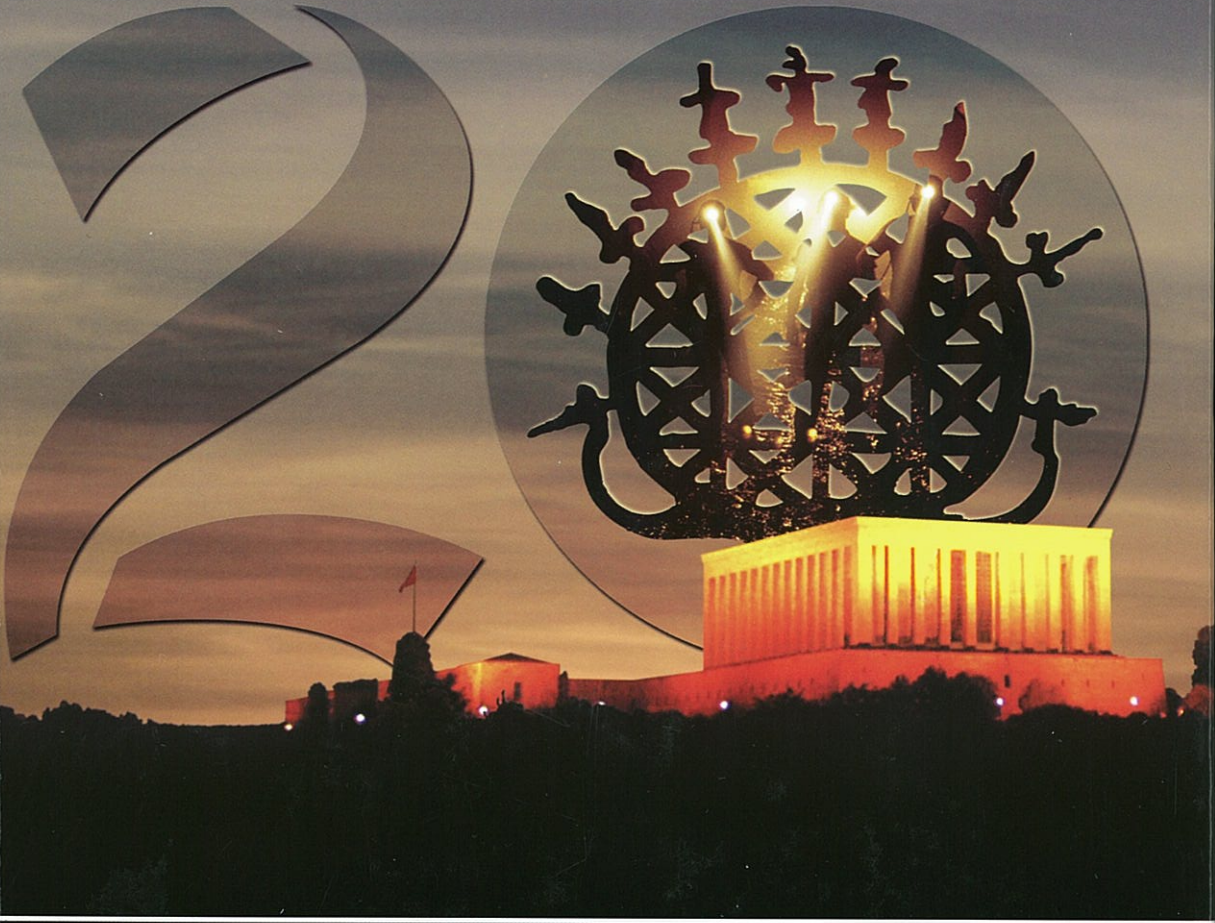


PROCEEDINGS OF THE 20TH INTERNATIONAL MINING CONGRESS OF TURKEY

6-8 June 2007-ANKARA



EDITORS

Dr. Celal KARPUZ

Dr. Mehmet Ali HINDİSTAN

Dr. A. Erhan TERCAN



UCEAT

CHAMBER OF MINING ENGINEERS OF TURKEY

SPONSORS

The Scientific and Technological Research Council of Turkey (TÜBİTAK)

Turkish Coal Enterprises (TKİ)

Eti Mine Works General Management

Turkish Hardcoal Enterprises (TTK)

Yıldızlar Holding

Black Sea Copper Works

Eti Copper Corporation

Dedeman Holding

IMCET2007 / ANKARA, TURKEY / 6-8 JUNE 2007

Proceedings of the 20th International Mining Congress of Turkey

Edited by

Dr. Celal KARPUZ

Middle East Technical University, Ankara, Turkey

Dr. Mehmet Ali HİNDİSTAN

Hacettepe University, Ankara, Turkey

Dr. A. Erhan TERCAN

Hacettepe University, Ankara, Turkey

THE CHAMBER OF MINING ENGINEERS OF TURKEY

This volume of the proceedings of the 20th International Mining Congress of Turkey is sponsored by DEMİR EXPORT A.Ş. of Turkey

All rights reserved © 2007

No parts of this book may be reproduced in any form or by any means, without written permission of the Chamber of Mining Engineers of Turkey.

Published by Ümit Ofset Matbaacılık San. ve Tic. Ltd. Şti.
Ankara, Turkey
Tel: +90 (312) 384 26 27

ISBN : 978-9944-89-288-9

Publication No : 133

© UCEAT the Chamber of Mining Engineers of Turkey

Address : Selanik Cad. No : 19/4
06650 Kızılay-Ankara, Turkey

Phone : +90 (312) 425 10 80

Fax : +90 (312) 417 59 90

URL : www.maden.org.tr

e-mail : maden@maden.org.tr

EXECUTIVE BOARD OF THE CHAMBER OF MINING ENGINEERS OF TURKEY

President : Mehmet TORUN
Vice President : Berna Fatma VATAN
Secretary : Nahit ARI
Treasurer : Ahmet SARDAR
Members : Mehmet Ali HİNDİSTAN
Cemalettin SAĞTEKİN
Hüseyin Can DOĞAN

ORGANIZING AND EXECUTIVE COMMITTEE

Chairman : Dr. Celal KARPUZ
Vice Chairman : Dr. A. Erhan TERCAN
Secretary : Dr. Mehmet Ali HİNDİSTAN
Treasurer : Yusuf Ziya AKGÖK
Members : Nejat TAMZOK
Ali ÖNEMLİ
Aysen ERTEN
Mehtap KILIÇ
Savaş ÖZÜN
Güneş ERTUNÇ

SCIENTIFIC AND ADVISORY COMMITTEE

Dr. Hüriyet AKDAŞ	Dr. Levent ERGÜN	Dr. Gündüz ÖKTEN
Dr. Okay AKSOY	Müfit ERDİL	Mustafa ÖNDER
Dr. Raşit ALTINDAĞ	Ömer ERKOÇ	Dr. Muammer ÖNER
Dr. Ergin ARIOĞLU	Dr. Adem ERSOY	Dr. Bahri ÖTEYAKA
Dr. Ali İhsan AROL	İlker ERTEM	Dr. Gülhan ÖZBAYOĞLU
Dr. Ümit ATALAY	Dr. Hasan GERÇEK	Dr. Yılmaz ÖZÇELİK
Dr. Mustafa AYHAN	Dr. Kemal GÖKAY	Dr. Hüseyin ÖZDAĞ
Yusuf AYDIN	Dr. R.Mete GÖKTAN	Dr. Saim SARAÇ
Dr. İrfan BAYRAKTAR	Dr. Özcan Y. GÜLSOY	Burhanettin ŞAHİN
Dr. A.Hakan BENZER	Dr. Lütfullah GÜNDÜZ	Dr. Ahmet ŞENTÜRK
Dr. Aydın BİLGİN	Dr. Tevfik GÜYAGÜLER	Dr. M. Gürel ŞENYUR
Dr. Nuh BİLGİN	Dr. Çatin HOŞTEN	Dr. Ferhan ŞİMŞİR
Dr. Naci BÖLÜKBAŞI	İbrahim İŞCEN	Dr. Levent TEZCAN
Dr. Atilla CEYLANOĞLU	Dr. Sair KAHRAMAN	Dr. Levent TUTLUOĞLU
Dr. Neşe ÇELEBİ	Dr. Ali KAHRİMAN	Dr. Bülent TÜTMEZ
Dr. Sabri ÇELİK	Hakan KAYA	Sait ULUIŞIK
Dr. Hanifi ÇOPUR	Muammer KAYA	Dr. Reşat ULUSAY
Dr. Ahmet DEMİRCİ	Dr. Ayhan KESİMAL	Dr. Tuğrul ÜNLÜ
Dr. Nuray DEMİREL	Çetin KOÇAK	Dr. Bahtiyar ÜNVER
Dr. Vedat DİDARİ	Dr. Adnan KONUK	Ömer ÜNVER
Dr. Şebnem DÜZGÜN	Dr. Halil KÖSE	Dr. Mahir VARDAR
Dr. İ.Göktay EDİZ	Dr. Seyfi KULAKSIZ	Dr. Ercüment YALÇIN
Dr. Zafir EKMEKÇİ	Köksal MUCUK	Dr. Ergül YAŞAR
Dr. Kaan ERASLAN	Dr. Yadigar MÜFTÜOĞLU	Dr. Hüseyin YAVUZ
Dr. Selamet ERÇELEBİ	Dr. Erkin NASUF	Dr. Necati YILDIZ
Dr. Bülent ERDEM	Dr. Turgay ONARGAN	Dr. Ekrem YÜCE
Dr. Hasan ERGİN	Dr. A.Hakan ONUR	

PREFACE

Importance of natural resources in human life is well known. Mining operations are a must for a contemporary life. Almost all the products that we used in our life are a consequence of mining operations. Mines are formed in millions years and nonrenewable as consumed.

Production and evaluation of worthy resources require surely an efficient planning and control. The importance of mining increases as mines are produced and used in its own industry as end product. For this purpose it is necessary to integrate mining sector to other sectors such as industry, energy, chemistry, agriculture and building. There is no country in the world that has developed by importing raw materials. The importing income obtained from all of our mines in 2006 is \$2 Billion while foreign money paid for coal at the same year is \$1.5 Billion. For this reason it is important to plan mines so that they can be used in our industry. Construction and application of policies that will reduce unemployment; rise national income and overcome regional inequalities have a vital importance.

The presence of at least one mining engineer at every stage of mining activity is required to increase efficiency and use recent technology. The Chamber of Mining Engineers believes that an arrangement that will be formed on the basis of National Mining Policy will be successful. In this respect, developing a policy that puts human and labor into center, provides an effective control of the public in mining activities, bears in mind, at the same time, environmental and ecological factors in these activities, aims at improving income distribution by reducing poverty has considerable importance in terms of both public benefit and development of mining sector.

In the light of these assessments, the papers presented in the 20th International Mining Congress of Turkey will contribute to solving the problems of mining sector. For this reason, we thank to public and private establishments supporting the Congress, and those who contribute with presentation of the papers and finally spend effort to achieve the Congress.

**The Executive Board of
The Chamber of Mining Engineers of Turkey**

FOREWORD

It is an honor and a great pleasure for me, as the chairman of the Organizing Committee of IMCET 2007 to welcome you to the congress and Turkey.

The 20th International Mining Congress and Exhibition of Turkey (IMCET 2007) organized by the Chamber of Mining Engineers of Turkey will be held in Ankara on **June 6-8, 2007**. The IMCET series of congress has been well recognized by the mining society from around the world. The primary objective of the Congress is to present and discuss the problems in mining industry, to transfer scientific and technological developments to a wide range of people and to provide communication among scientists, operators, mine owners and engineers. The IMCET 2007 also presents an opportunity for fruitful encounter of the Turkish culture and some examples of the ancient history of Turkey. I am quite positive that all the participants can taste the cultural, historical and social aspects of the Turkey in addition to their professional experience.

The 60 papers were chosen from more than 80 abstracts and compiled in two volumes. The first volume includes the 31 papers in English and the second volume includes 31 papers in Turkish. The 62 papers are presented and included in the proceedings volume have been grouped under eleven specific themes including Underground Mining, Mineral Processing, Drilling&Blasting, Geostatistics, Rock Testing, Cuttability, Mining&Environment, Geotechnical Engineering, Safety&Environment, Education and Miscellaneous. They are going to be presented 15 different technical sessions in addition to the two plenary papers.

The success of the IMCET 2007 is mainly due to the efforts of the Organizing Committee, Executive Board of the Chamber, the Scientific Committee and chairpersons of the sessions. I believe that they have tried to do their own bests and will continue to do so. It is obvious that the IMCET 2007 and these proceeding volumes would not come to reality without contribution of the authors and speakers. Our thanks also go to the delegates for their interest and contributions to the success of the congress.

Special thanks to Dr. R. Güner Gürtunca and Mehmet Torun for being our invited speakers and for their excellent presentations. It was also a great pleasure for us that the International Executive Board of the World Mining Congress honored the IMCET 2007.

Our sponsors and exhibitors have also provided invaluable support. We also thank them with gratitude.

Once again, I thank to all participants of the IMCET 2007 for their invaluable contributions for the success of the Congress. Once again it is a great pleasure for me to welcome all the delegates to IMCET in Ankara and hope that you will find the congress technically stimulating and your stay in Ankara socially enjoyable.

Dr. Celal Karpuz
Chairman
Organizing Committee

CONTENTS

Preface	vi
Foreword	vii
Invited Paper	
Recent Developments in Coal Mining Safety in the United States <i>R.G. Gürtunca, J.A. Breslin</i>	1
Underground Mining	
The Importance of Bolt Profile Spacing on Load Transfer Mechanism <i>N. Aziz, H. Jalalifar</i>	15
Numerical Modelling of Mining Induced Subsidence <i>W. Keilich, N.I. Aziz</i>	21
Application of Quantitative and MADM Methods in MMS <i>K. Shahriar, H. Dezyani, A. Afshar</i>	33
Investigation of Factors Affecting Floor Heave and Convergence of Galleries in Tabas Coal Mine <i>A. Royanfar, K. Shahriar</i>	41
Utilisation of Bow Tie Analysis for Ground Control Risk Assessment <i>G.V. Kızıl, J. Joy, C. Strawson</i>	47
Mineral Processing	
Investigation of Breakage Properties of Chromites at Kayseri Region <i>V. Deniz, E. Tank, E. Boz, Y. Umucu</i>	57
New Developments of the Separation Equipments for Aggregate Beneficiation <i>E. Garbarino, M. Cardu, R. Mancini</i>	67
The Improvement of Mill Throughput Using Barmac Pregrinding Technology at Cement Plants <i>S. Esen, H. Benzer</i>	79
Utilization of Some Industrial Wastes as Abrasive in Surface Preparation Processes <i>N. Ataman, G. Özbayoğlu</i>	85
Laboratory-Based Flowsheet Development of Iranian Ilmenite Upgrading <i>M. Irannajad, A. Mehdilo</i>	93
Computer-Based Optimization of Air Separators <i>S. Rashidi, M. Irannajad, A. Farzanegan</i>	103
Floatability of Barite <i>R. Albuquerque, R. Papini, A. Peres</i>	113
Drilling and Blasting	
Effect of Blasted Rock Particle Size on Excavation on Machine Loading Performance <i>M. Sari, P. J.A. Lever</i>	121
Two-Component Bulk Emulsions: A Revolution in the Explosives Manufacturing <i>M. Cardu</i>	127

Geostatistics

A Geostatistical Approach for Estimation of the Permeability and Groundwater Path in Rocks 137

A. Majdi, Y. Pourrahimian, B. Kushavand

Mining Method Selection of Chahar Gonbad Deposit Based on Fuzzy Decision Making (FDM) 143

K. Shahriar, F.S. Namin, H.D.J. Abadi

Lignite Thickness Estimation via Adaptive Fuzzy-Neural Network 151

B. Tütmez, A. Dağ, A.E. Tercan, U. Kaymak

Cuttability

Full-Scale Linear Cutting Tests Towards Performance Prediction of Chain Saw Machines 161

H. Çopur, C. Balcı, N. Bilgin, D. Tumaç, İ. Düzyol

Predicting the Cuttability of Rock using Artificial Neural Networks and Regression Trees 171

B. Tiryaki

Mining and Environment

Sources of Mining Effluents and Suitable Treatment Options 185

N. Kuyucak

Economic and Environmental Constraints Relevant to Building Aggregates Beneficiation Plants 197

V. Badino, G.A. Blengini, E. Garbarino, K. Zavaglia

Online Information Management on Coal and Gas Outburst 209

N. Aziz, R. Caladine, L. Tome, D. Vyas

Geotechnical Engineering

Effect of Confining Stress on Rock Mass Deformation Modulus in Javeh Dam Site 217

H. Aliasghari, R. Berry

Technique on Optimization of Geomechanical Monitoring in an Underground Construction 221

A.V. Man'ko

Investigation of Jet Grouting Effect on Slope Stability 229

B. Nikbakhtan, Y. Pourrahimian, H. Aghababaei

Education

"Miners – Fireman" First Empire at the Beginning of the Ancient Historical Times 241

H. Sauku

Virtual Reality - A Toy or a New Way of Training 247

M. Kızıl

Miscellaneous

Physical modelling of Joints Spacing Effects on Penetration Rate of Rotary Drilling in Open Pit Mines 259

H. S. Hoseinie, Y. Pourrahimian, H. Aghababaei

Dragline Dynamic Modeling for Efficient Excavation 265

N. Demirel, S. Frimpong

Work of Mining Machines in Fault Tectonic Zones for the Conditions of Assarel Mine 277

L. Tsotsorkov, D. Nikolov, A. Kostov

Author Index

285

Invited Paper

Recent Developments in Coal Mining Safety in the United States

R.G. Gürtunca & J.A. Breslin

Pittsburgh Research Laboratory, National Institute for Occupational Safety and Health, Pittsburgh, PA, USA

This paper briefly describes the progress in mine safety in the United States, with emphasis on recent events that have followed since the explosion at the Sago Mine in January 2006. Legislation following the mine accidents last year and areas of work carried out by the National Institute for Occupational Safety and Health (NIOSH) related to the accidents are discussed.

American coal production in 2006 was 1,150 million short tons. Most of this coal is consumed domestically, with annual exports of coal about 50 million tons. One third of annual production is produced at surface mines and the rest from underground. This coal is produced by about 82,000 miners working at 1,400 coal mines. Major improvements in coal mine safety have been made in the US since the Federal Mine Safety and Health Act of 1977. The fatal injury rate in underground coal mines between 1977 and 2004 was reduced by 47.8% to 0.036. The annual number of fatalities dropped from 112 to 14 during that period. Likewise, the non-fatal days-lost injury rate was reduced by 42.6% from 10.87 to 6.24.

The improvements in mine safety during this period can be seen in the graph of underground coal mine explosion fatalities and injuries from 1980 to present, which is shown in Figure 1. Between 1984 and 1993 (9 year period) there were 5 explosions and one major mine fire, for a total of 55 fatalities. Over the seven year period from 1993 to 1999 there were no fatalities from coal mine fires and explosions. However, in the six years since 2000 there have been 5 explosions and one fire, which have caused 37 fatalities.

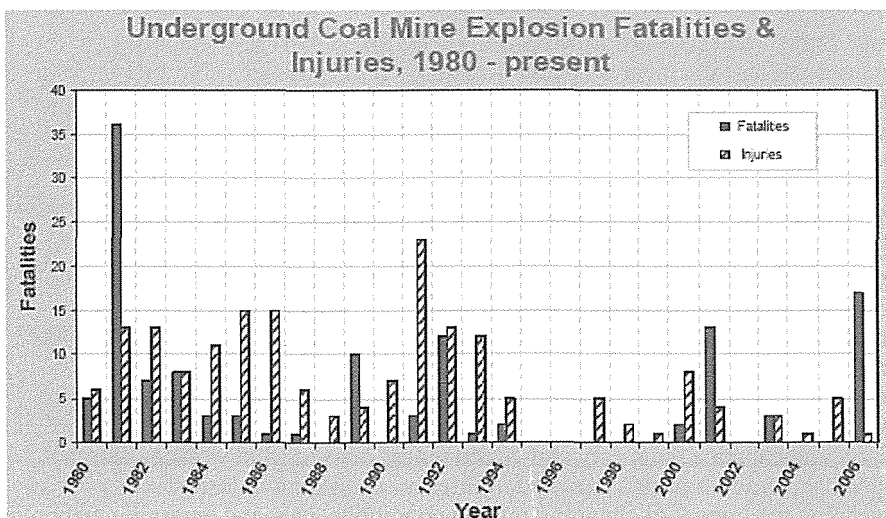


Figure 1. Underground Coal Mine Explosion Fatalities and Injuries, 1980 to Present.

The most recent mine incidents began last year with an explosion on January 2 at the Sago mine in West Virginia which killed 12 miners. A fire at the Aracoma Alma No. 1 Mine in West Virginia on January 19 caused 2 fatalities. On May 20 there was an explosion at the Darby No. 1 Mine in Kentucky which resulted in 5 more deaths. These major mine accidents caused great public concern and led the US Congress to pass the Mine Improvement and New Emergency Response Act of 2006 (MINER Act) on May 24, 2006. The Congress also passed an Emergency Supplemental Appropriation (ESA), which was signed in June. The ESA included funding of an additional \$10 million to NIOSH to develop critical disaster response technologies in areas of oxygen supply, refuge chambers, and communications and tracking.

MINER ACT

The coal mining disasters in early 2006 and the MINER Act have had very significant effects on the coal mining industry in US. Some of the major provisions of the MINER Act include:

- Requires each covered mine to develop and continuously update a written emergency response plan;
- Requires wireless two-way communications and an electronic tracking system within three years, permitting those on the surface to locate persons trapped underground;
- Requires each mine to have available two experienced rescue teams capable of a one hour response time;
- Requires mine operators to make notification of all incidents or accidents which pose a reasonable risk of death within 15 minutes;
- Requires new safety standards relating to the sealing of abandoned areas in underground coal mines, increasing the requirements for strength of the seals;
- Establishes a competitive grant program for new mine safety technology to be administered by NIOSH;
- Establishes an interagency working group to provide a formal means of sharing Government-developed technology that would have applicability to mine safety;
- Establishes a Technical Study Panel for Belt Air to investigate the use of air from conveyer belt mine entries to ventilate the mine face;
- Raising the financial penalties for safety violations;
- Establishes a permanent Office of Mine Safety & Health in NIOSH, which helps ensure a viable and long-term focus on mining safety and health.

The Mine Safety and Health Administration (MSHA) has responsibility in the U.S. for promulgation and enforcement of Federal mine safety regulations. NIOSH is responsible for research to improve occupational safety and health for all workers including miners. NIOSH assumed the sole Federal responsibility for research on mine safety after the closure of the US Bureau of Mines in 1996. NIOSH inherited from the Bureau of Mines the mining research laboratories in Pittsburgh, PA and Spokane, WA. The NIOSH mining program currently has about 256 employees and a budget for 2007 of \$31 million.

NIOSH does research in mining aimed toward seven major strategic goals. These are:

1. Reduce respiratory diseases in miners by reducing health hazards in the workplace associated with coal worker pneumoconiosis, silicosis, and diesel emissions.
2. Reduce noise-induced hearing loss (NIHL) in the mining industry.
3. Reduce repetitive/cumulative musculoskeletal injuries in mine workers.
4. Reduce traumatic injuries in the mining workplace.
5. Reduce the risk of mine disasters (fires, explosions, and inundations); and minimize the risk to, and enhance the safety and effectiveness of, emergency responders.
6. Reduce ground failure fatalities and injuries in the mining industry.
7. Determine the impact of changing mining conditions, new and emerging technologies, training, and the changing patterns of work on worker health and safety.

ON-GOING INTRAMURAL RESEARCH

The intramural research done by NIOSH related to prevention and response to mine fires and explosions is directed toward strategic goal number 5 above. This research is done primarily at the NIOSH Pittsburgh Research Laboratory (PRL). The NIOSH strategy in this area is in order of priority: prevention, escape, and rescue. Our research is aimed first at preventing explosions or fires that could endanger the lives of miners, second at technology to allow miners to escape if a serious incident occurs, and third at technology that would facilitate the rescue of miners who might be trapped underground.

Several of the current research projects at PRL have direct relevance to preventing the types of mining accidents which occurred last year. These include:

Mine explosion prevention: This project studies explosion propagation and explosion combustion mechanisms through full-scale tests at the Lake Lynn Experimental Mine (LLEM) and through laboratory tests. The LLEM research includes flame propagation in large volumes of non-uniformly mixed methane, the effects of non-uniform zones of coal and rock dust along an entry, and the effects of coal dust on the ribs/roof compared to floor dust. Researchers also study the amount of rock dust necessary to inert typical mine size dust for both high and low volatile coals. Basic research on the explosion mechanisms and flame propagation attempts to reach a more fundamental understanding of mine explosions.

NIOSH and MSHA conducted joint research to evaluate explosion blast effects on mine ventilation stoppings at the LLEM. After mine explosion accidents, MSHA conducts investigations to determine the causes as a means to mitigate or eliminate future occurrences. As part of these post-explosion investigations, the condition of underground stoppings, including the debris from damaged stoppings, is documented as evidence of the strength and direction of the explosion forces (Figure 2). These results assist investigators in determining the explosion forces that destroy or damage stoppings during actual coal mine explosions. (Weiss et al, 2006)

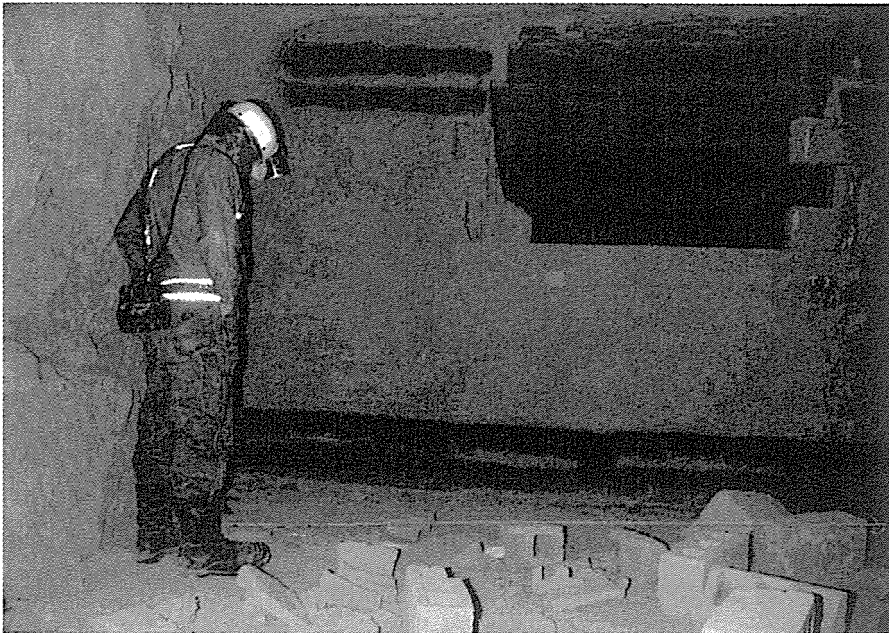


Figure 2. Ventilation stopping partially destroyed by explosion pressure.

Improving methane control practices in coal mines: The project goal is to identify and model methane emissions on longwall faces and continuous miner sections. This should improve the effectiveness of methane control technology, and reduce the explosion hazard for underground miners. The effectiveness of methane drainage on longwall and room and pillar face emission rates is assessed through underground methane emissions monitoring, borehole production evaluations and methane content measurements. Analytical, non-site specific algorithms are produced to predict face methane emission rates. Methane prediction methodologies are packaged for technology transfer to the mining industry. Methane drainage practices for continuous miner room and pillar operations are reviewed to evaluate potential application to abandoned or sealed workings. A surface borehole monitoring experiment is in progress for a Pennsylvania longwall panel. Figure 3 shows a surface borehole monitoring station. The adaptation of commercially available reservoir modeling software has successfully simulated gas flows for various borehole configurations and longwall mining scenarios. Two empirical methods for predicting longwall face emissions for increased face lengths have been developed and published. (Krog et al, 2006; Schatzel et al, 2006).

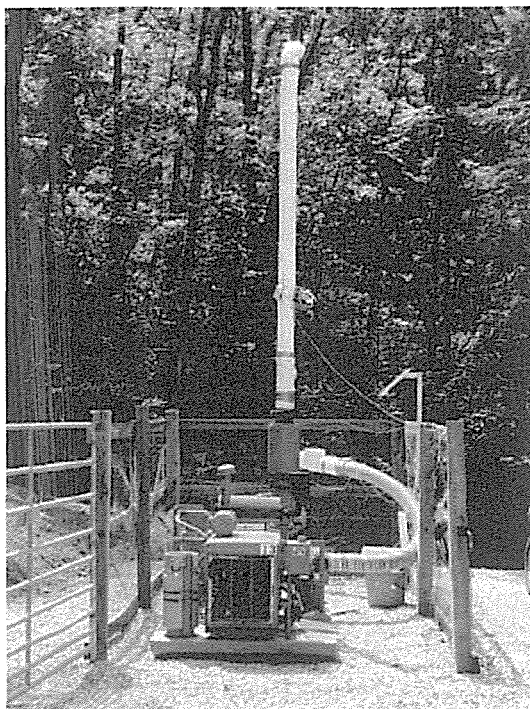


Figure 3. Instrumenting gob vent boreholes for monitoring.

Rescue Training and Technology: In cooperation with state mining agencies and mining companies, realistic training exercises for mine rescue teams have been developed, conducted, and evaluated at the LLEM. These training simulations require teams to make strategic decisions while they explore smoke filled entries, rescue injured miners, navigate around obstacles such as bad roof and water, conduct equipment checks, and reestablish ventilation controls. Mine rescue teams have evaluated a variety of rescue technologies during realistic training exercises at the LLEM. Technologies that have been evaluated with more than 50 different rescue teams include a lighted team linkline, lifeline pulleys, various communication

systems, thermal imaging cameras, retractable stretchers, high-intensity LED lights, chemical light sticks, and handheld lasers. (Conti, 2001) Some of these technologies, such as lifeline pulleys and chemical light sticks, have already been adopted by many of the rescue teams. Further work is planned to make the lighting technologies and lasers intrinsically safe for use in mine rescue applications. Efforts are also continuing to find a licensee for the NIOSH patent on the lighted rescue linkline. (Conti and Chasko, U.S. Patent #6,742,909)

RECENT OOUTPUTS FROM INTRAMURAL RESEARCH

Some of the on-going research which was being done prior to the accidents in early 2006 have already produced relevant results which are ready for transfer to the coal mining industry. These include:

Coal Dust Explosibility Meter: The Coal Dust Explosibility Meter (CDEM), shown in Figure 4, is the first device that provides an immediate capability for determining if coal dust concentrations in active areas of underground coal mines have been sufficiently mixed with rock dust to prevent risk of explosion. This meter will quickly determine the explosibility and the incombustible content of coal and rock dust mixtures in coal mines, thereby improving sample analysis and rock dusting practices. The CDEM measures the explosibility of a coal and rock dust mixture by an optical reflectance method. Since rock dust is white and coal dust is black, the intensity of the reflected light depends on the concentration of rock dust in the mixture. The CDEM, when calibrated with actual mine dust mixtures, can be used to determine the approximate percentage of rock dust in the coal and rock dust mixture. PRL developed the theory and technology behind the device, and a prototype was developed in collaboration with the Geneva College Center for Technology Development. NIOSH and partners recently received the prestigious R&D 100 Award for the PRL-developed meter.



Figure 4. Coal Dust Explosibility Meter (CDEM).

Fine Coal Dust: NIOSH research has examined the adequacy of the 65% rock dust requirement for mine intakes. NIOSH and MSHA recently conducted a joint survey to determine the range of coal particle sizes found in dust samples collected from intake airways of U.S. coal mines. The last comprehensive survey of this type was performed in the 1920s. The size of the coal dust is relevant to the amount of rock dust required to inert the coal dust, with more rock dust needed to inert finer sizes of coal dust. Dust samples were collected by MSHA inspectors from underground coal mines throughout the U.S. Samples were normally collected in several intakes at each mine. The laboratory analysis procedures included acid leaching of the sample to remove the limestone rock dust, sonic sieving to determine the dust size, and low temperature ashing of the sieved fractions to correct for any remaining incombustible matter. The results indicate that particle sizes of mine coal dust in intake airways are finer than those measured in the 1920s. (Sapko, 2006)

Explosion Pressure Design Criteria for New Seals in U.S. Coal Mines: A new project was begun last year to study mine seals. Mine seals are structures built in underground coal mines to isolate abandoned mining panels or groups of panels from the active workings. Figure 5 shows a mine seal under construction. Recent explosions in the U.S. underground coal mining industry suggest that currently accepted seal construction and design methodologies are inadequate. Historically, mining regulations required seals to withstand a 140 kPa (20 psi) explosion pressure; however, the 2006 MINER Act requires MSHA to increase this design standard by the end of 2007. NIOSH has produced a new report that provides a sound scientific and engineering justification to recommend a three-tiered explosion pressure design criteria for seals in coal mines in response to the MINER Act.

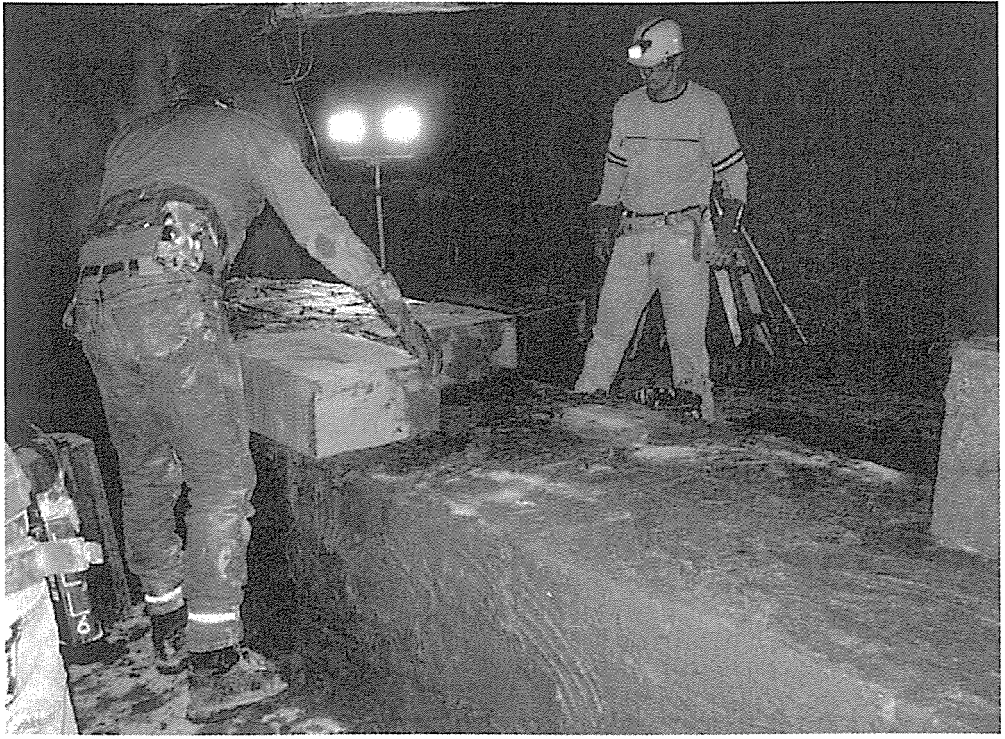


Figure 5. Construction of a mine seal.

NIOSH engineers considered various kinds of explosive atmospheres that can accumulate within sealed areas and used simple gas explosion models to estimate worst case explosion pressures that could impact seals. Three design pressure pulses were developed for the dynamic structural analysis of new seals under the three conditions in which those seals may be used. For the first condition, an unmonitored seal where there is a possibility of methane-air detonation behind the seal, the recommended design pulse rises to 4.4 MPa (640 psi) and then falls to the 800 kPa (120 psi) constant volume explosion overpressure. For unmonitored seals without the possibility of detonation, a less severe design pulse that simply rises to the 800 kPa (120 psi) constant volume explosion overpressure, but without the initial spike, may be employed. For monitored seals, engineers can use a 345 kPa (50 psi) design pulse if monitoring can assure that the maximum length of explosive mix behind a seal does not exceed 5 m (15 ft) and also that the volume of explosive mix does not exceed 40% of the total sealed volume. Use of this 345 kPa (50 psi) design pulse requires monitoring and active management of the sealed area atmosphere.

NIOSH used these design pressure pulses along with the Wall Analysis Code from the U.S. Army Corps of Engineers and a simple plug analysis to develop design charts for the minimum required seal thickness to withstand each of these explosion pressure pulses. These design charts consider a range of practical construction materials used in the mining industry and specify a minimum seal thickness given a certain seal height. These analyses show that resistance to even the maximum 4.4 MPa (640 psi) design pulse can be achieved using common seal construction materials at reasonable thickness.

NIOSH will continue research to improve underground coal mine sealing strategies and prevent explosions in sealed areas of coal mines. In collaboration with the U.S. National Laboratories, NIOSH researchers will further examine the dynamics of methane and coal dust explosions in mines and the dynamic response of seals to these explosion loads. This should lead to better understanding of the detonation phenomena and simple techniques to protect seals from transient pressures. Additional work will include field measurements of the atmosphere within sealed areas. This work will improve the monitoring of gob atmospheres to reduce the likelihood that an explosive methane/air gas mixture accumulates behind the seal line.

Methane Control Handbook: This is a summary handbook published last year that compiles in one document the results of several decades of research by the US Bureau of Mines and NIOSH on methods to control methane in underground coal mines. This handbook describes effective methods for the control of methane gas in mines and tunnels. It describes methane control methods primarily for U.S. coal mines, but also for metal and nonmetal mines and tunnels. (Kissell 2006)

NEW INTRAMURAL PROJECTS

NIOSH has initiated a pilot project to evaluate the potential for risk assessment and management in the US for disaster prevention. Recent mine disasters focused attention on the need to improve the operation and management of mine emergency response, from communications to rescue operations. Experience in other countries indicates that mine safety can be dramatically improved by implementing risk management methods, including hazard identification, risk assessment, implementation of controls, emergency response plans and a system to manage the process. The project time frame is approximately 15 months to conduct a series of case studies across mining sectors, with interim reports and evaluations to assess the need to continue or expand the effort. The case studies will lead mine personnel through a formal risk assessment of mine site hazards with the potential for multiple fatalities. The process will evaluate prevention, initial response, communications, escape, refuge and

emergency response capacities and identify gaps in protection. The purpose is to build interest in and validation for the wider use of the risk assessment and management process and to identify any obstacles to its success in the US mining industry. To date, nine major hazard risk assessment case studies have been completed. A NIOSH report will soon be written detailing the strengths and weaknesses of this approach.

A Mine Emergency Communications Partnership was organized by NIOSH to facilitate the development, evaluation, and implementation of communication system technology that would allow workers in mines to communicate with personnel on the surface after an accident. Included is post-accident worker tracking technology. The primary goals of the Mine Emergency Communications Partnership are to: establish general performance expectations for mine emergency communications systems; establish uniform and fair criteria for testing and evaluating systems; conduct in-mine tests on systems under consistent conditions; and report the findings. A secondary goal is to identify gap areas that should be addressed through research. The Mine Emergency Communications Partnership includes representatives from state and national mining associations, labor unions, state and federal regulatory agencies, manufacturers, and university and government researchers.

PROGRESS ON THE EMERGENCY SUPPLEMENTAL APPROPRIATION (ESA)

The Emergency Supplemental Appropriation (ESA) made available an additional \$10 million to NIOSH with the goal to facilitate the adaptation and movement of oxygen supply, communications, tracking, and refuge chamber technologies from other industries or from prototype stage to commercialization, and into the mines as rapidly as possible. The intent of Congress was to overcome the small market barrier, by providing some government funding to solve unique application issues associated with in-mine use. The relatively small mining market in the US provides little incentive for expensive research and development of new safety technology for mining without some assistance from the government.

The ESA funds target technologies that could be available for mine use within 36 months. The focus is on moving demonstrated prototypes to commercialization, or adapting technologies from other military or civilian sectors into mining. While longer term R&D activities are important to develop new concepts and conduct experimental investigations of possible innovations, they aren't the focus of the ESA.

To address needs in a timely and cost-effective manner, the primary focus of the ESA has been on competitive contracts. The appropriated funds became available in September 2006. However, preliminary work had already begun. NIOSH scientists and engineers have been studying promising technologies that could meet the urgent needs of mineworkers. They continue to meet with manufacturers, inventors and innovators, trade and labor organizations, academia, and industry to discuss options, alternatives, and needs. They are examining installations in underground mines, and meeting with constituents and experts in the U.S. and other mining countries. Communications and tracking technologies are being tested in the lab and underground to evaluate the efficacy of systems purported to work in underground mines.

A number of opportunities were identified that have a reasonable likelihood of being commercialized and available for in-mine use within 36 months. However, it's unlikely that all of these are doable for \$10 million. Therefore, a competitive process is being used to prioritize the most promising technologies based on significant positive impact on mine worker safety, and also on reasonable chance of commercial availability within 36 months.

Five new contracts are planned in the communications and tracking area. These include:

- Development of a "hardened" leaky-feeder-type system
- Development of a node or mesh-based system
- Study of communications standards for compatibility

- Agreement with Department of Defense to adapt military technology to mining communication systems
- Development of a general communication and/or tracking system.

Refuge chambers are one option for safety protection in the event of explosions or fires. In the United States, the use of refuge chambers in coal mines has generated debate. While refuge chambers can save lives, it is also argued that they may cause miners to seek refuge rather than attempt to escape their hazardous situation. There are a number of considerations involved with this approach, including the capabilities of stations, the type and location of structures, design criteria, and maintenance and training issues. Recent discussions have generated some consensus among stakeholder groups on refuge concepts as part of an escape strategy. Specifically, the merits of at least two concepts have emerged: inflatable, portable devices for use at the face, and "refuge rooms" for use outby the face. The refuge rooms could serve as "way stations" or "safe havens" as escaping miners make their way out of the mine. Being somewhat more permanent in nature, these rooms could in some cases be connected to the surface with a borehole, which would offer many other benefits. NIOSH plans to address the engineering issues associated with the construction and application of the various refuge alternatives through contract research. The knowledge developed through this contract will be used to develop recommended practices documents and other practical guidelines for mines, and to establish potential criteria for a possible approval and certification process for refuge chambers.

Researchers at NIOSH's National Personal Protective Technology Laboratory (NPPTL) will facilitate the development and commercialization of the next generation of self-contained self-rescuers (SCSRs) through competitive contracts. The new SCSRs will provide more reliable oxygen supplies to miners in escape situations. The new and improved SCSRs could be developed, tested, and submitted for certification within the next 24 months.

Five contracts are planned for oxygen supplies and refuge chambers, including:

- A Hybrid SCSR
- A Dockable SCSR
- Development of overall escape strategies utilizing refuge chambers
- Survey and document refuge products, standards, and usage worldwide.
- Development of recommended practices for refuge rooms.

Some of these contracts have already been awarded and the last of these is expected to be awarded by June of this year.

SUMMARY

In conclusion, the provisions of the MINER Act and the funding provided by the ESA give us the best opportunity for "revolutionary" improvements to mining safety in nearly three decades. They can lead to potentially significant improvements for all of mining, not just coal. We are engaged in a mix of intramural and extramural activities to help realize the opportunities.

REFERENCES

- Conti-RS (2001). Emerging Technologies: Aiding Responders in Mine Emergences and During the Escape from Smoke-Filled Passageways. In: Proceedings of Northwest Mining Association 107th Annual Meeting, Exposition and Short Courses (December 3-7, 2001; Spokane, WA); :14 pp
- Conti-RS; Chasko-LL. Lighted Line. U.S. Patent #6,742,909
- Kissell-FN (2006). Handbook for Methane Control in Mining. Pittsburgh, PA: U.S. Department of Health and Human Services, Public Health Service, Centers for Disease Control and Prevention, National Institute for Occupational Safety and Health, DHHS (NIOSH) Publication No. 2006-127, Information Circular 9486, 2006 Jun; :1-184

- Krog-RB, Schatzel-SJ, Garcia-F, Marshall-JK (2006). Predicting Methane Emissions from Longer Longwall Faces by Analysis of Emission Contributors. In: Proceedings of the 11th U.S./North American Mine Ventilation Symposium. Mutmanski JM, Ramani RV, eds. Leiden, Netherlands: Balkema Publishers, pp. 383-392.
- Sapko-MJ, Cashdollar-KL, Green-GM, Verakis-HC (2006). Coal Dust Particle Size Survey of U.S. Mines. In: Proceedings of the Sixth International Symposium on Hazards, Prevention, and Mitigation of Industrial Explosions (Halifax, NS, Canada, Aug 27 – Sept 1, 2006). Halifax, Canada: Dalhousie University, 2006 Aug; 2:676-682
- Schatzel-SJ, Krog-RB, Garcia-F, Marshall-JK, Trackemas-J (2006). Prediction of Longwall Methane Emissions and the Associated Consequences of Increasing Longwall Face Lengths: A Case Study in the Pittsburgh Coalbed. In: Proceedings of the 11th U.S./North American Mine Ventilation Symposium. Mutmanski JM, Ramani RV, eds. Leiden, Netherlands: Balkema Publishers, pp. 375-382.
- Weiss-ES; Cashdollar-KL; Harteis-SP; Shemon-GJ; Beiter-DA; Urosek-JE (2006). Explosion Evaluation of Mine Ventilation Stoppings. In: Proceedings of the 11th U.S./North American Mine Ventilation Symposium, University Park, Pennsylvania, June 5-7, 2006. Mutmanský JM, Ramani RV. eds., London, U.K.: Taylor & Francis Group, 2006 Jun; :361-366.

Underground Mining

The Importance of Bolt Profile Spacing on Load Transfer Mechanism

N. Aziz

University of Wollongong, NSW, Australia

H. Jalalifar

Shahi Bahonar University of Kerman, Iran

ABSTRACT A series of laboratory based push and pull tests were carried out to investigate how profile configuration influences the load transfer mechanism of bolt/resin interface. Tests were carried out in both 75 mm and 150 mm long steel sleeves. Three types of bolts were examined; they were bolts most commonly used for strata reinforcements in underground coal mines in Australia. The bolts had near equal core diameter but of different profile configurations. The change in the length of the encapsulation sleeve was examined in light of the small number of profiles encapsulated effectively in short 75 mm long sleeves. The results showed that peak loads and displacements were directly related to the height and the spacing of the bolt surface profiles. Profile spacing appears to have greater influence on load transfer capacity than the profile height.

1 INTRODUCTION

Rock bolt plays important role in ground support in both civil and mining engineering. Since it was first introduced, various studies have been undertaken to gain better knowledge about how rock bolts perform in different strata conditions. These studies incorporate both the laboratory and field tests. In laboratory test, several methods of testing have been designed to evaluate the load transfer properties of rock bolts. These methods are known as conventional short encapsulation pull test, which involved pulling bolt anchored in a hole either cast in concrete or drilled in rock. Another approach involves push and pull testing of bolts in steel sleeves, which is now known as short encapsulation steel tube test in a laboratory based environment. Each of these test methods has its own advantages and limitations; however steel tube tests have been proven to eliminate most of the problems encountered in the conventional short pull tests carried out in concrete blocks or in the field.

With the recent shift from mechanical point anchors to full encapsulation cement or chemical resin anchors, the focus of attention has shifted towards bolt surface profile configurations as being a relevant parameter for load transfer mechanism interaction between the bolt and encapsulation medium. Fabjanczyk et al. (1992) were the early researchers that recognised the importance of bolt surface configurations influencing the load transfer mechanism between resin and bolt interfaces. However, they made no reference on profile spacing. This was left to Aziz, Dey and Indraratna (2001) and their work on bolt profile configurations under constant normal stiffness conditions. They reported that both bolt profile height and profile spacing were important parameters influencing the load transfer mechanisms. In their later work in short encapsulations tests, Aziz and Webb (2003) examined the load transfer characteristics of both profile and non profiles bolts which established the effectiveness of profile spacing as an important parameter in load transfer

capabilities. Their initial work was conducted by push testing of bolts in 75 mm steel sleeves with hole diameters being 27 mm. All the bolts used were of equal core diameter of 21.7 mm. In most recent work, Aziz (2004), Aziz and Jalalifar (2005) carried out the tests under both push and pull test conditions, and that the bolts were conducted in centrally located positions with uniform resin annulus thickness. This work was later extended to include; the resin encapsulation thickness variations; changes to bolt profile spacing; and the three dimensional modelling of both pull and push testing of bolts in 75 mm encapsulation.

In an attempt to address the limited length of the bolts encapsulated in 75 mm steel sleeve, additional comparative study has been undertaken using 150 mm encapsulation length, with the tests being carried out under both push and pull conditions. The details of this study form the subject of discussion in this paper.

2 LOAD TRANSFER MECHANISM

Load is transferred from the bolt to the rock via grout by the mechanical interlock between the surface irregularities in the interface and friction. When shearing, the load is transferred to the bolt via shear stress in the grout. The nature of bolt failure in

field test is different from laboratory test. In field test, failure is dependent upon the characteristics of the system and the material properties of individual elements. Slippage may occur at either rock/grout or grout/bolt interfaces, which is called decoupling behaviour. Decoupling takes place when the shear stress exceeds the strength of the interface. In the laboratory test, failure usually occurs along the bolt/grout interface. However, if real rock or concrete is used, instead of steel tube as an outer casing element, then failure may happen along the rock/grout interface, depending on the strength of rock /concrete strength and hole wall profiling. Kilic (1999) and Kilic et al. (2002) reported that when surface friction of a borehole decreases, slippage occurs at the grout/rock interface. In addition, when the borehole and bolt length exceeds a critical value, failure takes place at the bolt. As shown in Figure 1, the mechanical interlocking occurs when the irregularities move relative to each other. Surface interlock will transfer shear forces from one element to another. When the shear forces exceed the ultimate capacity of the medium, failure occurs and only frictional and interlocking resistance will control the load transfer characteristics of the bolt.

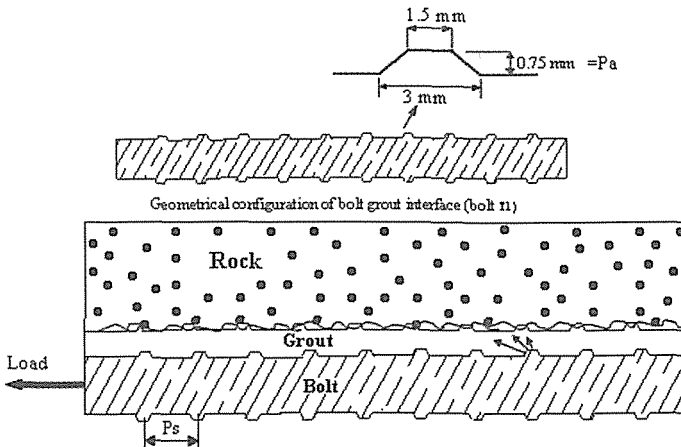


Figure 1. Sketch of bolt-grout interface in pull and push test for bolt type T1 (P_a and P_s are profile height and profile spacing respectively).

3 EXPERIMENTAL STUDY

Pull and push tests were carried out in two short encapsulation, 75 mm, and 150 mm length steel sleeves. Bolts were encapsulated in sleeves using Mix and Pour resin. As can be seen in Figure 2, the bolts were located centrally with uniform resin annulus thickness, and every effort was made to ensure the bolts were also set axially parallel to the sleeve hole axis. Figure 3 shows the general view of pull test set-up in both 75 and 150 mm cylinders

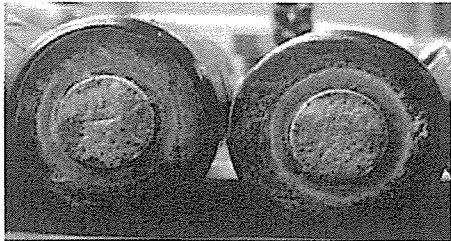


Figure 2. Uniform resin annulus thickness around the bolt.

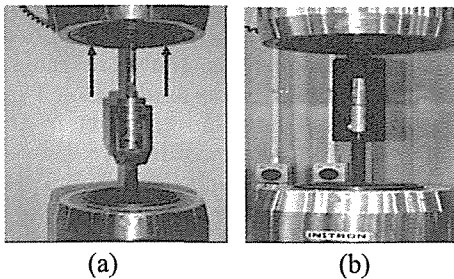


Figure 3. Pull test arrangement; (a) 75 mm sleeve (b) 150 mm sleeve.

Because of the limited encapsulated length in 75 mm sleeve, there was insufficient number of bolt profiles embedded in resin encapsulation column, particularly for Bolt Type T3 with wider profile spacing of 25 mm. Accordingly, the length of the steel sleeve was doubled by having two 75 mm sleeves butted at ends to form 150 mm long sleeve. Figure 4 shows the post-test samples with the bolts being pulled out of steel sleeves in 75 mm long steel sleeves with 45 mm outer and 27 mm inner diameters.

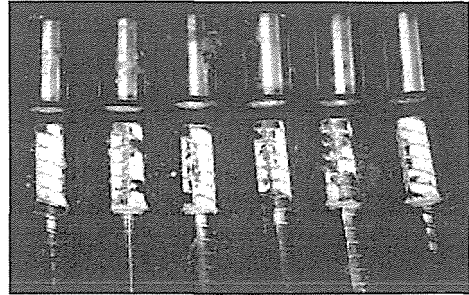


Figure 4. Failure along the bolt/grout interface in pull test, in 75 mm steel sleeve.

Figure 5 shows the laboratory set-up for push tests, both 75 mm and 150 mm cylinder with the bolts being pulled out of the steel sleeves in 150 mm long, 45 mm outer and 27 mm inner diameters. All failures occurred along the bolt / grout interface. The grout and bolt properties are illustrated in Table 1, Table 2 and 3 show various bolt parameters and experimental results for 75 and 150 mm encapsulation length, respectively.

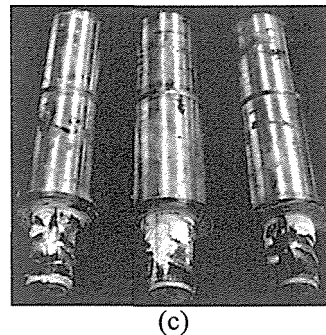
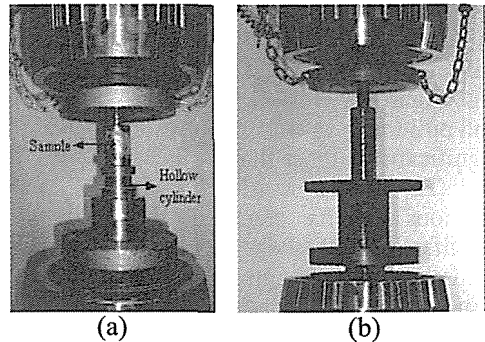


Figure 5. Push test device in (a) 75 mm sleeve (b) 150 mm sleeve (c) failure in push test at 150 mm encapsulation length.

Table 1. Grout and steel properties.

	grout	steel
UCS (MPa)	71	-
Ave. Shear strength (MPa)	16.2	645
E (GPa)	12	200
Poisson's ratio	0.25	0.3

Table 2 Laboratory results in 75 mm encapsulation length.

Measured parameters	Pull			Push		
	Bolt type			Bolt type		
	T1	T2	T3	T1	T2	T3
Ave. Profile Height (mm)	0.75	1.35	1.2	0.75	1.35	1.2
Ave. Profile Spacing (mm)	11.0	12.0	25	11	12.0	25
Ave. Max Load (kN)	114.8	131.7	160	129	139.2	172
Ave. Max Displ (mm)	4.10	4.51	8.2	3.3	3.86	7.4
Ave. Shear Stress Capacity (MPa)	22.2	25.4	31	24.8	26	33.2

Table 3. The laboratory results in 150 mm encapsulation length.

	Pull			Push		
	Bolt type			Bolt type		
	T1	T2	T3	T1	T2	T3
Ave. Profile Height (mm)	1	1.35	1.2	0.75	1.35	1.2
Ave. Profile Spacing (mm)	11.0	12	25.0	11.0	12.0	25
Ave. Max Load (kN)	132.5	200	253.2	143	222.5	281
Ave. Max Displacement (mm)	4.26	5.3	14.85	4.1	4.1	10
Ave. Shear Stress Capacity (MPa)	12.78	19.5	24.42	13.8	21.5	27.1

As can be observed from both Table 2 and 3 and Figure 6, Bolt Type T3 has both push and pull loads as well shear resistance values significantly higher than both Bolt Types T1 and T2. These results are in line with previous results reported by Aziz and Jalalifar (2005). Post peak residual shear load and shear strength of Bolt Type T3 was also higher than the other two bolts. Table 4 shows the different values between the results of pull and push tests in both 75 and 150 mm sleeves.

The average shear stress values in long sleeve push test on each bolt showed a reduction of 44.2%, 20.2% and 18.2% in Bolt Types T1, T2 and T3, respectively. Clearly, the level of reduction in push load in Bolt Type T1 was more significant than the other two bolts. This was also true for pull test in which shear stress was reduced by 42.4% for Bolt Type T1 and 20.9% for Bolt Type T3. No pull tests were made on Bolt Type T2 in 150 mm long sleeve. Table 4 shows the results of comparative tests by pull and push tests carried out in both 75 mm

and 150 mm sleeves. There is significant increase in shear load as shown in Table 4, when 150 mm sleeve was used in Bolt Types T2 and T3, but not so significant in Bolt Type T1. The average difference between push and pull test, for all three Bolt Types, T1, T2 and T3 was between 7 to 11% as deduced from Figure 6. The reason for higher load difference in 150 mm sleeve between push and pull in Bolt Type T3 was due to fact that the shear load was greater than the steel elastic yield load of around 260 kN. This caused relatively large bolt diameter reduction and the possible loss of bond connection, eventually dropping in a shear load. The effect of excessive bolt elongation and diameter loss yield would be significantly reduced with the length of encapsulation (sleeve length) is reduced to 120 mm in length, particularly for Bolt Type T3. However, the anchorage length for Bolt Type T1 can be exceeded up to 300 mm. The peak load/shear displacement in each bolt type was different, with Bolt Type T3 was significantly higher than the other two

short spaced profiled bolts. Clearly, the profile spacing appears to have greater impact on the load transfer mechanism of the bolt/resin interaction than the profiles height has. This supports the earlier findings under constant normal stiffness conditions reported by Aziz (2002). Also, increased profile

spacing causes greater peak load displacement. This is advantageous as it facilitates greater rock displacement and hence improves ground control capability particularly in soft rock conditions.

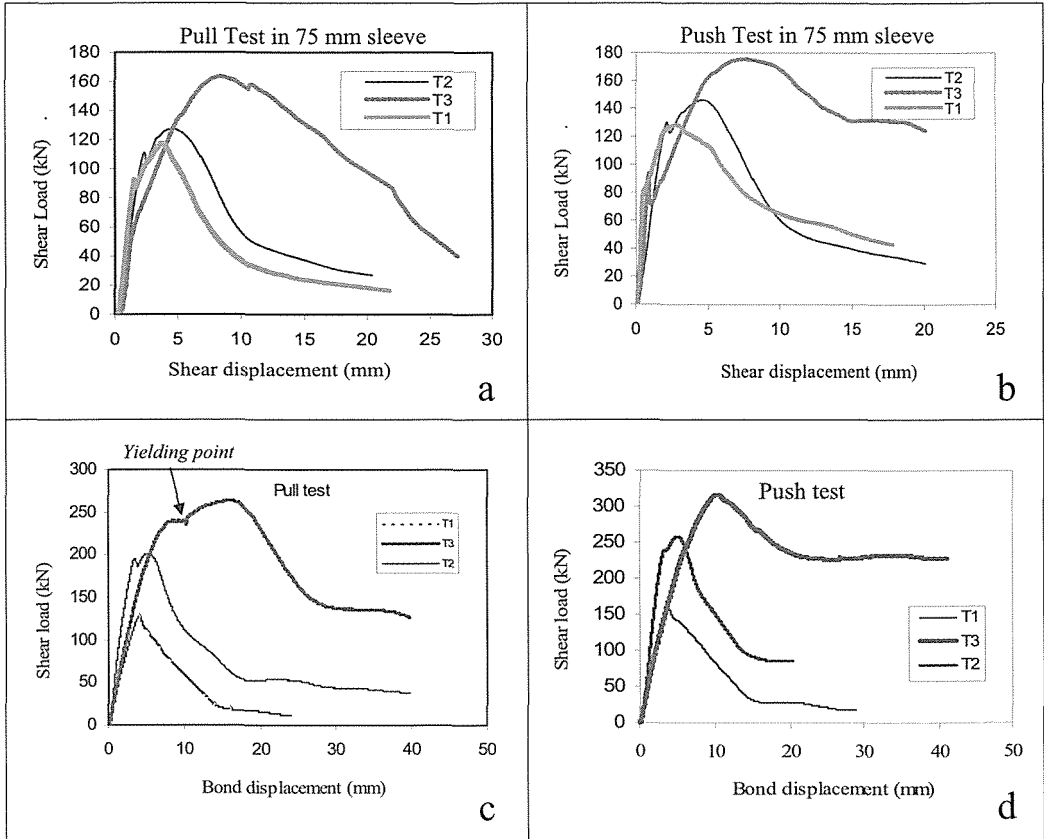


Figure 6. Shear load as a function of displacement in (a) pull test in 75 mm sleeve, (b) push test in 75 mm sleeve, (c) pull test in 150 mm sleeve, (d) push test in 150 mm sleeve.

Table 4. Differences in load between pull and push in 75 mm and 150 mm sleeves.

Bolt Type	Push load increase, from 75mm to 150mm sleeve length (%)	Pull load increase, from 75mm to 150mm (%)	Load difference between push and pull test at 75 mm (%)	Load difference between push and pull test at 150 mm (%)
T1	11	15.4	11	7.6
T2	59	51.9	5.4	11
T3	63.4	58.2	7	10

4 CONCLUSION

The experimental results have lead to the following conclusions:

- The average shear stress capacity of a bolt in a push test is greater than in a pull test.
- Yielding and necking is unlikely to occur in bolts tested in 75 mm long steel sleeves as the peak shear load was around 40% of the maximum tensile strength of the steel. However, it occurs in 150 mm in Bolt Type T3 as the pull load is greater than the peak elastic yield load.
- Bolt-resin interface failure occurred by initially shearing of the grout at the profile tip in contact with the resin. The load failure of the resin /bolt surface contact is dependent on the profile height as well as spacing.
- Increased profile spacing causes greater peak load displacement. This is advantageous as it facilitates greater rock displacement and hence improved ground control capability particularly in soft rock conditions.
- Bolt Type T3 produced higher shear resistance, followed by Bolt Type T2 and then T1.
- Post peak load displacement profile of Bolt Type T3 is greater than the other Bolt Types T1 and T2 respectively.
- The length of steel sleeves used for load transfer mechanism study should facilitate a sufficient number of profiles encapsulation and in parity with the profile spacing of the bolt tests. Particular care must be taken to ensure that each bolt is centrally located in the sleeve and with the uniform resin annulus thickness.

REFERENCES

- Aziz, N.I., Dey, D. and Indraratna, B., 2001, New approach to study load transfer mechanisms of fully grouted bolts, *Proc of 17th International Mining Congress and exhibition, The Chamber of Mining Engineers of Turkey*, Ankara, June 19-22, pp. 143-154.
- Aziz, N., 2004, Bolt surface profiles- an important parameter in load transfer capacity appraisal. *Proceedings of the fifth International Conference on Ground Control and Mining Construction*, September, Perth, pp. 221-230.
- Aziz, N. and Jalalifar, H., 2005, Investigation into the transfer mechanism of loads in grouted bolts. *Australian Geomechanics Journal. Vol. 40, No.2.* pp.99-113.
- Aziz, N. and Webb, B., 2003, Load transfer Appraisal of bolts using short encapsulation push test. *4th Underground Coal Operators, Conference*. Wollongong. pp. 72-81.
- Fabjanczyk, M, Hurt. K.and Hindmarsh D., 1998, Optimization of roof bolt performance. *Proceedings of the International Conference, Geomechanics/ground control in Mining and Underground Construction*, UOW, NSW, July,pp.413-424.
- Kilic A. M., 1999, The effects of grout properties to the bolt capacity, *Proceedings of the sixteenth Mining Congress of Turkey*, Ankara, Kozan press, pp. 189-196.
- Kilic, A, Yasar. E. & Atis, C.D., 2002, Effect of bar shape on the pull out capacity of fully grouted rock bolts, *Tunneling & Underground Space Technology*, Vol 18 No 1, February, pp.1-6.

Numerical Modelling of Mining Induced Subsidence

W. Keilich, N.I. Aziz
University of Wollongong, Australia

ABSTRACT A methodology of subsidence prediction for isolated single longwall panels using the Distinct Element code UDEC has been developed as an alternative for subsidence modelling/prediction in the Southern Coalfield of New South Wales, Australia. The models have been validated by comparison with empirical results, observed caving behaviour for isolated single panels in flat terrain and the application of the Voussoir Beam analogue.

1 INTRODUCTION

Ground subsidence due to mining has been the subject of intensive research for several decades, and it remains to be an important topic confronting the mining industry today.

Subsidence prediction in Australia is currently limited to empirical and numerical techniques. The empirical techniques are suitable for flat lying or gently sloping areas but are unsuitable for areas of large topographical relief. From the available numerical techniques, FLAC (Fast Lagrangian Analysis of Continua) has been commonly used for assessing the impacts of longwall mining on river valleys. FLAC has limited application as the code is not capable of modelling discontinuous rock masses effectively.

In this project, a methodology of subsidence prediction using the Distinct Element code UDEC (Universal Distinct Element Code) has been developed as an alternative for subsidence modelling/prediction in the Southern Coalfield. The UDEC models have been validated by comparison with empirical results, observed caving behaviour, and the application of Voussoir Beam theory.

The expected outcome will be a reliable subsidence prediction tool capable of simulating ground deformations and subsurface movements in flat terrain.

2 SUBSIDENCE IN THE SOUTHERN COALFIELD

During longwall mining, a large void in the coal seam is produced and this disturbs the equilibrium conditions of the surrounding rock strata, which bends downward while the floor heaves.

When the goaf reaches a sufficient size, the roof strata will fail and cave. Seedsman (2004) reports that caving does not necessarily occur vertically above the extracted coal panel, but in many cases, caving is defined by a goaf angle that fades over the goaf. This angle is most likely a function of the bedding structure of the roof and the orientation of the goaf with respect to sub vertical jointing.

In the Newcastle Coalfield the average goaf angle is 12° with a standard deviation of 8°. Numerical modelling by CSIRO Exploration and Mining and Strata Control Technology (1999) of the caving in the Southern Coalfield appears to support a goaf

angle value of 12°. Further numerical modelling by Gale (2005) in an unspecified coalfield also supports this value. Caving will cease when the goaf angle encounters a stratigraphic unit strong enough to bridge what is now the effective span. This concept is illustrated in Figure 1. The goaf and overburden strata will then compact over time and become stabilised.

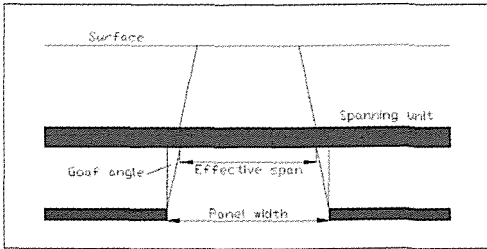


Figure 1. Relationship between panel width, goaf angle and effective span.

The caving of the roof strata as previously described, gives rise to several zones within the overburden strata. The number of zones varies in the literature with Kratzsch (1983) describing six zones, Peng (1992) describing four zones, and Kapp (1984) describing three zones. These zones are not distinct but there is a gradual transition from one to another.

Seedsman (2004) reported on the existence of a massive unit in the strata of the Newcastle Coalfield and presented an alternative way of predicting subsidence based on the Voussoir Beam analogue. For this method to be applied, it is assumed that the massive unit remains elastic and all goafing takes place underneath the massive unit. Therefore the developed subsidence is a function of the deflection of the massive unit, provided the massive unit remains elastic and does not fail.

Unfortunately, the amount of information on the caving characteristics in the Southern Coalfield is somewhat limited. Microseismic results from the CSIRO Exploration and Mining Division, and Strata Control Technology, in an Australian Coal Association Research Program (ACARP) project provided some useful information on the caving behaviour at Appin Colliery,

which is located in the Southern Coalfield (CSIRO Exploration & Mining & Strata Control Technology 1999). The longwall panel that was monitored was 200 m wide and extracted the 2.3 m thick Bulli Seam at a depth of about 500 m. The monitoring included the installation of 17 triaxial geophones and nine geophones in a borehole drilled from the surface to the Bulli Seam and two perpendicular surface strings of four geophones each. The period of monitoring was approximately four months, during which there was 700 m of face retreat. From the monitoring it was seen that the majority of fracturing extended approximately 50 m to 70 m above the Bulli Seam with no fracturing exceeding approximately 290 m, and to a depth of 80 m to 90 m into the floor. Figure 2 illustrates the microseismic events in a cross section of the monitored longwall.

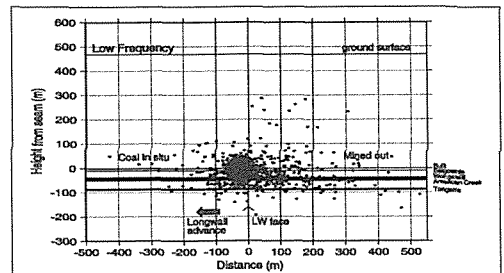


Figure 2. Cross section of longwall with microseismic event location (CSIRO Exploration & Mining & Strata Control Technology, 1999).

An analysis of the stratigraphic details in the subsidence handbook by Holla and Barclay (2000) shows that the Bulgo Sandstone is the most massive unit in the stratigraphy of the Southern Coalfield, with a thickness ranging from approximately 90 m to 200 m, and located at a distance between 90 m and 120 m above the Bulli Seam at Appin Colliery. It is also the strongest of the larger upper units as indicated by a geotechnical characterization (MacGregor & Conquest 2005). If the position of the Bulgo Sandstone were overlain onto Figure 2, it would be seen that the majority of the fracturing in the goaf is contained by the Bulgo Sandstone. This

would seem to suggest that the Bulgo Sandstone is acting as the massive spanning unit, therefore all potential subsidence development can be theoretically derived from a voussoir analysis of the Bulgo Sandstone.

3 EMPIRICAL PREDICTIONS

The method devised by the New South Wales Department of Primary Industries has been in existence since 1985 and is available as a handbook (Holla & Barclay 2000). Since then, the method has been refined with the addition of subsidence data, and a discussion on the effects of mining induced subsidence on public utilities, dwellings and water bodies. Whilst not accounted for in the prediction technique, there is also a discussion on the major factors modifying the theoretical subsidence behaviour such as faults, dykes, and gullies. Several case studies were also presented to illustrate these factors in action.

The subsidence data and resulting graphs in this method were obtained from collieries in the area between the Illawarra Escarpment and the Burratorang Valley. This data was collected over a period of thirty years. The majority of the mines included in the analyses were mining the Bulli seam except in two cases for which the workings were in the Wongawilli seam. The predominant method of mining was by longwall mining, although some pillar extraction data has been included. The relationship between S_{\max}/T and W/H for single panels is illustrated in Figure 3.

It can be seen from Figure 3 that the lower curve represents the relationship between the width to cover depth (W/H) and subsidence factor (S_{\max}/T) for longwall extraction, where S_{\max} is the maximum developed subsidence and T is the extracted thickness. It can also be seen from Figure 3 that the largest longwall W/H ratio still falls into the sub-critical category ($W/H < 1.4$). This is a result of the deep mining conditions in the Southern Coalfield, and although data exists for W/H ratios between 0.5 and 0.9, the resulting scatter suggests that subsidence

prediction would be more accurate for W/H ratios less than 0.5.

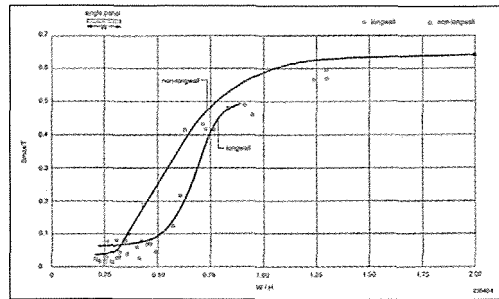


Figure 3. Relationship between S_{\max}/T and W/H for single longwall panels (Holla & Barclay 2000).

4 DEVELOPMENT OF A NUMERICAL MODELLING APPROACH

The development of a numerical modelling approach for isolated single longwall panels is based on the principles outlined in Hudson, Stephansson and Andersson (2005). The principles stipulate that the numerical modelling itself is not the most important aspect, but the conceptualisation of the problem, material properties and parameters should be paramount in any investigation. It is also stressed that the engineering problem at hand should be subjected to “soft” and “hard” audits.

The soft audit establishes an overview of the modelling work and determines whether well known issues of importance and difficulty in characterising and modelling rock masses have been addressed at the outset. The hard audit is similar to the soft audit but requires justifications to the answers given. The audits are designed to ensure that the numerical modelling is transparent and traceable through the audit trail.

A literature review on the numerical modelling of mining subsidence related problems was also undertaken. It was found that continuum codes like FLAC were popular but required calibration of material properties to work effectively, thereby introducing increased uncertainty into the numerical modelling. In effect, the

continuum codes worked best when used to back-analyse subsidence results. As a result of this, the continuum codes could not be considered as a true predictor of subsidence.

It was concluded after the literature review and the auditing procedure that a discontinuum code such as UDEC would be a better choice in producing a true subsidence prediction tool as they are able to model blocky rock masses therefore allowing evaluation of sub-surface behaviour as well as surface subsidence. Furthermore, UDEC has the advantage of being able to incorporate field properties directly into the model without calibration, eg. stress field, bedding plane spacing, joint spacing, sub vertical joint orientation, material and joint properties.

5 NUMERICAL MODELLING STRATEGY

The approach used in the numerical modelling was to try and replicate the longwall subsidence curve in Figure 3.

Holla and Barclay (2000) contain a list of mines and extraction details, from which the ground movement data were collected and the subsidence curves derived (single panel only). The majority of the mines extracted the Bulli Seam using the longwall method of mining. The data that was derived from pillar extraction and Wongawilli Seam extraction was excluded from the modelling. It should be noted that the extraction details are approximate figures only.

Holla and Barclay (2000) also contain the thickness of the stratigraphic units in the overburden, grouped according to colliery. This was used for the derivation of the thickness of rock units above the Bulli seam for different mines.

Excluding mines that utilise pillar extraction, and extract the Wongawilli Seam, it was concluded that a minimum of four models can be created from the available data (Table 1).

It must be noted that although 18 potential models can be created with the available data, four models was considered sufficient to cover the range of W/H ratios represented

in the single panel subsidence curve in Figure 3. At the time of writing, another model with a W/H ratio of 0.81 was running but early indications suggest a model this large is impractical to run, with the current run time of this model exceeding two weeks.

Table 1. Basic details of models.

Model	Panel Width W (m)	Cover Depth H (m)	Extracted Thickness T (m)	W/H
1	105	413	2.7	0.25
2	158	450	2.5	0.35
3	160	288	3.0	0.56
4	175	288	3.0	0.61

5.1 Model Geometry

Symmetry has been utilised to halve the size of the models needed, with the right hand side of the model representing the centreline of the panel. Each model has the left hand boundary fixed at five times the excavation width, as indicated by the UDEC user's manual (Itasca 2000), or the predicted range of ground movement as indicated by the 29° angle of draw (Holla & Barclay 2000), or whichever is the greater value. The finalised dimensions for each model are given in Table 2. Bedding planes were assumed as horizontal and vertical joints were placed with a 90° dip and offset to form a brickwork style pattern.

Table 2. Finalised width and depth for each model.

Model	Model Width (m)	Model Depth (m)
1	315	509.8
2	474	546.6
3	480	385.1
4	525	385.1

5.2 Material Properties

A great deal of information has been published on the material properties of the stratigraphic units above and including the Bulgo Sandstone by Pells (1993). Most of this data is derived from civil engineering

works in and around Sydney, not specifically the Southern Coalfield. Most recently, a drilling program has been completed which contains the geotechnical characterisation of several boreholes that were drilled over Appin and Westcliff collieries (MacGregor & Conquest 2005). As a result of this geotechnical characterisation and a survey of the literature (CSIRO Petroleum 2002; Williams & Gray 1980; & McNally 1996) a complete set of material properties have been derived. The material properties that have been derived from laboratory testing have been used directly in the models without calibration or modification.

5.3 Bedding Planes and Properties

Bedding, stratification or layering is one of the most fundamental and diagnostic features of sedimentary rocks. In numerical modelling, it is important to correctly distinguish what constitutes bedding planes and intrabed structures as bedding planes are the major source of shear and slip in a discontinuous rock mass.

Bedding is due to vertical differences in lithology, grain size, grain shape, packing or orientation. Generally, bedding is layering within beds on a scale of about 1 or 2 cm, and lamination is layering within beds on a scale of 1 or 2 mm (Tucker 2003; & Selley 2000). Limited information exists about bedding planes in the Southern Coalfield. Most of the information has been derived from civil engineering works and visual examination of outcrops along the coast by Ghobadi (1994). It is also recognised that strata thickness and bedding plane thickness will vary from site to site, so it would be advantageous to derive the required information from a complete geotechnical investigation at one site, if possible.

The drill cores that were obtained for the geotechnical characterisation (MacGregor & Conquest 2005) were logged for discontinuities, but unfortunately bedding planes or drilling induced fractures were not specifically identified. The authors were allowed access to the logs and laboratory reports. Neutron and gamma logging was

also performed on holes. A site visit was conducted by the authors and a visual examination of the core, along with a comparison of the logs was carried out for the Bulgo Sandstone. It was found that there was a good correlation between major bedding planes and partings identified in the core and the corresponding logs. When compared to data provided by Pells (1993) and Ghobadi (1994), there was good agreement apart from the Newport Formation and Bald Hill Claystone. In these instances, it was decided to use the values provided by Pells (1993).

Information on specific bedding plane properties are scarce and if the discontinuities are not directly laboratory tested, estimates or values from field studies have to be used. Derivation of the joint and normal and shear stiffness was done in accordance to the procedures described by Itasca (2000). It seems that the shear stiffness can be approximated as one-tenth of the normal stiffness. This approach has been used by Itasca (2000), and has been used by Coulthard (1995) and Badelow et al (2005). The joint and bedding plane strength parameters have been derived from Chan, Kotze and Stone (2005), and Barton (1976) has been used to calculate cohesion based on the JRC and JCS values given by Chan, Kotze and Stone (2005).

5.4 Vertical Joints and Properties

Very little data exists on the vertical joint spacing in rock units in the Southern Coalfield, and even where geotechnical characterisations have been completed; vertical joint spacing simply cannot be assessed from HQ cores.

Price (1966) reports on work done in Wyoming, USA, which suggests for a given lithological type, the concentration of joints is inversely related to the thickness of the bed. Examples were given for dolomite where joints in a 10 ft. thick bed occurred at every 10 ft.; and joints in a 1 ft. thick bed occurred every 1 ft. Similar results were also reported for sandstone and limestone. The mechanism proposed by Price (1966)

assumed that the cohesion between adjacent beds is non-existent and that friction angle; normal stress and tensile strength are all constant. It was suggested that while these parameters will change in reality, these factors cause only second-order variations in the relationship between joint frequency and bed thickness. A comprehensive review of the Price model was performed by Mandl (2005). In addition, this review also included Hobbs' model, which is a more complex model that takes into account the elastic modulus and bedding plane cohesion of adjacent beds. Both models predict a joint spacing that scales with bed thickness.

Ghobadi (1994) reports that the vertical joint spacing in the Hawkesbury Sandstone is observed to be 2 – 5 m, the Scarborough Sandstone 1 – 4 m, the Bulgo Sandstone 0.5 – 1.5 m, the Stanwell Park Claystone 0.1 – 0.5 m, and the Wombarra Claystone 0.2 – 0.6 m apart. It was noted that many of the joints on the escarpment and coastline are filled with calcite and/or clay. These values are not in good agreement with the Price joint model.

Pells (1993) reports that the vertical joint spacing in the Hawkesbury Sandstone is 7 – 15 m in the Southern catchment area, the Newport Formation 1 – 3 m, Bald Hill Claystone 1 m, and the Bulgo Sandstone 2 – 13 m. These values are in good agreement with the Price joint model, therefore it was assumed that vertical joint spacing is equal to bed thickness and this assumption was used in the numerical models. Vertical joint properties have been estimated in the same manner as for bedding planes.

5.5 In-Situ Stress

A thorough review of regional and local in-situ stress has been compiled by the CSIRO Petroleum (2002) for their numerical modelling. From 206 measurements across the Sydney Basin, the ratio of horizontal stress to vertical stress was found to be in the range of 1.5 – 2.0. For the numerical models, a horizontal to vertical stress ratio of two was implemented.

5.6 Mesh Generation

The mesh employed was relatively simple. Each block was subdivided into four constant strain zones. It was noted by Coulthard (1995) that this may result in a unit of large blocks excessively stiffer than a unit of smaller blocks. This is particularly noticeable where the larger unit overlies the smaller one. If this occurs in the models, the mesh density will be increased in the areas of interest.

5.7 Constitutive Models

The constitutive model employed is the Mohr-Coulomb model. The constitutive model used for the joints is the Mohr-Coulomb residual strength model. This joint model has the capability to reduce or increase friction, cohesion, dilation and tensile strength.

6 RESULTS

Four models (Models 1, 2, 3 and 4) have been run and analysed. A fifth model representing a W/H ratio of 0.81 was running at the time of writing but its excessive run times may rule it out in any further analysis.

The results have been analysed and plots produced for:

- S_{max}/T (subsidence factor),
- S_{goaf}/S_{max} ,
- K1 (maximum tensile strain constant),
- K2 (maximum compressive strain constant),
- K3 (maximum tilt constant), and
- D/H (position of inflection point relative to goaf).

Strain and tilt are defined by Equation 1 (Holla & Barclay 2000):

$$+E_{max}, -E_{max}, G_{max} = 1000 \times K \times \frac{S_{max}}{H} \quad [1]$$

Where,

- +E_{max} : Max tensile strain (mm/m)
- E_{max} : Max comp. strain (mm/m)
- G_{max} : Max tilt (mm/m)
- K : Constant
- S_{max} : Max developed subsidence (m)
- H : Depth of cover (m)

Horizontal strain is the change in length per unit of the original horizontal length of ground surface. Tensile strains occur in the trough margin and over the goaf edges. Compressive strains occur above the extracted area. Holla and Barclay (2000) noted that maximum tensile strains are generally not larger than 1 mm/m and maximum compressive strains 3 mm/m, excluding topographical extremes.

Tilt of the ground surface between two points is found by dividing the difference in subsidence at the two points by the distance between them. Maximum tilt occurs at the point of inflection where the subsidence is roughly equal to one half of S_{max} .

The point of inflection is the location where tensile strains become positive and vice versa. It has been found by Holla and Barclay (2000) that the inflection point lies inside the goaf for W/H ratios greater than 0.5.

The respective maximum values were readily picked from the model outputs. The strain profiles for Models 2 and 3 contained anomalies where strain turned compressive in two sections of the profile above unmined coal. However, the magnitude of the strains was extremely low and this behaviour has been ascribed to the modelling technique.

Block failure and the formation of the caved zone can be seen in Figure 4. Block failure trends inward over the goaf at an angle of approximately 12° to 15°. This is in good agreement with CSIRO Exploration & Mining & Strata Control Technology (1999) and Gale (2005). The caved zone also stops abruptly at the base of the Bulgo Sandstone; this is in general agreement with the microseismic monitoring (CSIRO Exploration & Mining & Strata Control Technology 1999).

Slip occurs on every bedding plane up to the surface, and vertical joints open up in the caved zone and also along the surface, outside the goaf edge.

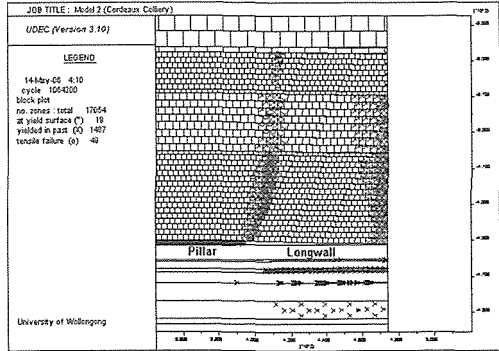


Figure 4. Typical cave zone above longwall panel.

The analysed results from Models 1, 2, 3 and 4 are shown in Table 3 (Model 1 = M1, Model 2 = M2 etc).

Table 3. Results.

Parameter	M1	M2	M3	M4
W (m)	105	158	160	175
H (m)	413	450	288	288
T (m)	2.7	2.5	3.0	3.0
W/H	0.25	0.35	0.56	0.61
S_{max} (mm)	41.12	162.39	312.72	455.85
S_{goaf} (mm)	39.64	82.64	87.24	89.05
+ E_{max} (mm/m)	0.092	0.139	0.690	1.218
- E_{max} (mm/m)	0.065	0.287	0.516	0.686
G_{max} (mm/m)	0.086	1.275	3.731	5.432
D (m)	-96.00	5.50	18.50	26.00
S_{max}/T	0.015	0.065	0.104	0.152
S_{goaf}/S_{max}	0.964	0.509	0.279	0.195
K1	0.924	0.386	0.635	0.770
K2	0.653	0.794	0.475	0.434
K3	0.864	3.533	3.436	3.432
D/H	-0.232	0.012	0.064	0.090

To put the results into perspective, the results from Table 3 are reproduced on the corresponding empirical curves from Holla and Barclay (2000). These are shown in Figures 5, 6, 7, 8, 9 and 10.

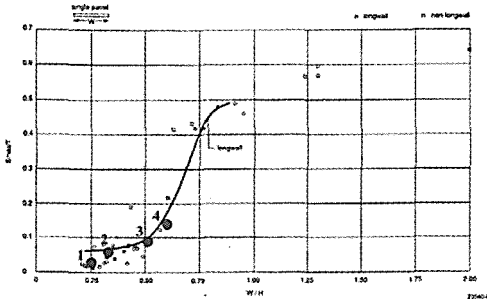


Figure 5. Model results for S_{max}/T (after Holla & Barclay 2000).

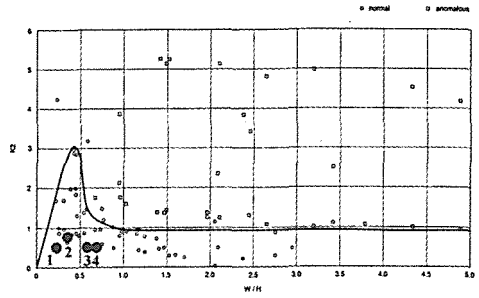


Figure 8. Model results for $K2$ (after Holla & Barclay 2000).

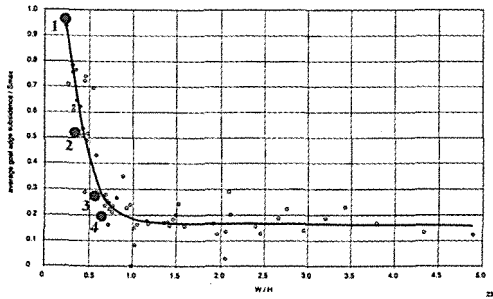


Figure 6. Model results for S_{goaf}/S_{max} (after Holla & Barclay 2000).

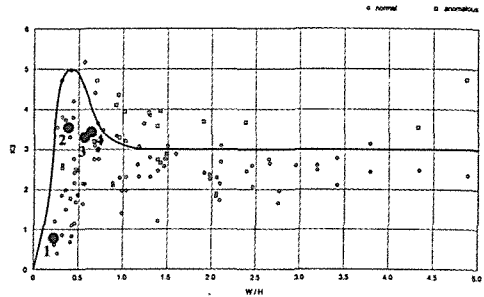


Figure 9. Model results for $K3$ (after Holla & Barclay 2000).

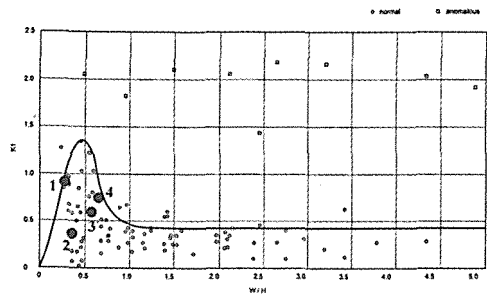


Figure 7. Model results for $K1$ (after Holla & Barclay 2000).

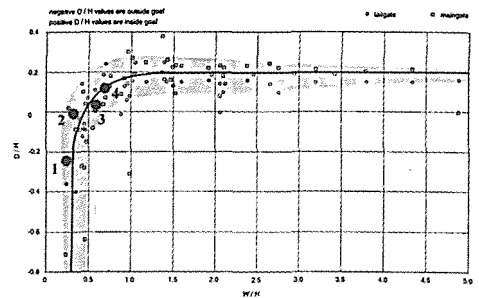


Figure 10. Model results for D/H (after Holla & Barclay 2000).

It can be seen from Figures 5 and 6 that the numerical models predict maximum developed subsidence and goaf edge subsidence quite well. Given the amount of scatter in the empirical data for the subsidence factor, this is a good result. Another preliminary model with a W/H ratio of 0.81 was run but was halted due to excessive run times (in excess of two weeks).

In this model, complete failure of the Bulgo Sandstone had occurred, leading to a sharp increase in the subsidence factor. This characteristic is evident in Figure 5, where the subsidence factor increases dramatically for W/H ratios greater than 0.5. Even though the model had not been run to completion, the results provided further verification of the proposed theory that the Bulgo Sandstone

is the major control for sub-critical subsidence in the Southern Coalfield.

Horizontal strain has been previously defined as the change in length per unit of the original horizontal length of ground surface. Tensile strains occur in the trough margin and over the goaf edges. Compressive strains occur above the extracted area. Holla and Barclay (2000) noted that maximum tensile strains are generally not larger than 1 mm/m and maximum compressive strains 3 mm/m, excluding topographical extremes. Strain has been recognized as one of the most difficult parameters to predict due to vertical joints potentially opening up on the surface and the large effect that variations in topography has on the strain profile. Observed strain profiles in the field are never as perfect as theoretical strain profiles due to these factors.

It can be seen from Figures 7 and 8 that the model results contain considerable scatter in the data points, as do the empirical results for the strain constants. Part of the problem is the use of the K1 and K2 constants which normalize strains to depth and S_{max} – this may not be valid for sub-critical extraction. Another part of the problem is the magnitude of movements being predicted and modelled. Since the magnitude of the movements are in the order of a few millimetres over a distance of several hundred metres, the scatter in the predicted strain constants can be attributed to modelling “noise”. Even though there may be difficulty in predicting surface strains, it is encouraging to note that the predicted strains from the numerical models lie within the empirical curves.

As defined previously, tilt of the ground surface between two points is calculated by dividing the difference in subsidence at the two points by the distance between them. Maximum tilt occurs at the point of inflection where the subsidence is roughly equal to one half of S_{max} . It can be seen in Figure 9 that the model results for the tilt

constant produced good matches with the empirical predictions.

The point of inflection is the location where tensile strains become positive and vice versa. The results of the position of the inflection point relative to the goaf can be seen in Figure 10. It is noted by Holla and Barclay (2000) that the position of the inflection point falls inside the goaf for W/H ratios greater than 0.5 or outside the goaf for W/H ratios less than 0.5. It can be seen that this observation holds true for Model 1 (W/H = 0.25), Model 3 (W/H = 0.56) and Model 4 (W/H = 0.61), although the predicted location of the inflection point falls within the range of empirical data scatter. The location of the inflection point is within 32 m of the position of maximum tilt for all four models. The predicted subsidence at the inflection point is roughly one half of predicted S_{max} for all models and this is in agreement with Holla and Barclay (2000).

The calculated angle of draw for the models varied between 19° and 56°. This produced an average value of 37°. The angle of draw was calculated using the 20 mm cut-off limit. Given that there seems to be no apparent relationship between angle of draw and W/H ratio, the predicted values can only be compared to the empirical values (average angle of draw from empirical database is 29°) and not be verified in any way.

Caving and cracking events are also contained below the base of the Bulgo Sandstone. In Models 3 and 4, the cave zone penetrates through the base of the Bulgo Sandstone which suggests that the Bulgo Sandstone is the major control on subsidence up to W/H ratios of around 0.6. Once the Bulgo Sandstone fails, it is no longer the massive spanning unit that controls subsidence, resulting in a large increase in the subsidence factor. This trend was noticed in the fifth preliminary model which had a W/H ratio of 0.81 and also is evident in the empirical prediction curve (see Figure 5). It was also noticed that the caving of the goaf

was not really a massive combination of block failures and rotations, but more a gradual settling and deflection of the roof strata. This would have resulted in substantially less bulking in the goaf, but does not seem to be an issue as far as subsidence predictions are concerned. The failure to produce bulking in the goaf was also noted by Coulthard (1995).

From the results it can be seen that the numerical models are satisfactorily verified by the empirical results when it comes to subsidence predictions and the prediction of the shape of the subsidence trough over single longwall panels.

7 APPLICATION OF VOUSSOIR BEAM THEORY

The derivation and instructions on how to use Voussoir Beam theory can be found in Sofianos (1996), Sofianos and Kapenis (1998) and Nomikos, Sofianos and Tsoutrelis (2002). This theory has been used to calculate the theoretical deflection of the Bulgo Sandstone in Models 2 to 4.

The results from Models 1 to 4 indicate that the Bulgo Sandstone is the massive spanning unit in the overburden and the majority of the caving is confined below the base of the massive unit. This is the case for Model 2, whilst failure extends into the Bulgo Sandstone in Models 3 and 4. It was noted that caving was not sufficient enough to produce any measurable goaf angle in Model 1, therefore this model cannot be analysed with the Voussoir Beam method. The geometry of the cave zone is defined by a goaf angle of between 14° to 25° for Model 2, 12° to 25° for Model 3 and 10° to 25° for Model 4.

In order to perform an analysis, the following parameters must be known:

- Panel width (m),
- Cover depth (m),
- Hawkesbury Sandstone thickness (m),
- Newport Formation thickness (m),
- Bald Hill Claystone thickness (m),
- Bald Hill Claystone density (kg/m³),

- Bulgo Sandstone thickness (m),
- Bulgo Sandstone density (kg/m³),
- Bulgo Sandstone Young's Modulus (MPa),
- Cave zone height (m), and
- Goaf angle (°).

It is important to note that the analysis is actually performed on the base of the Bulgo Sandstone as defined by the bedding plane spacing and extent of failure into the spanning unit, and using the notion that thinner bedded layers load thicker bedded layers (Obert & Duvall 1967), it is only the Bald Hill Claystone that acts as a surcharge on the Bulgo Sandstone.

For example, if the Bulgo Sandstone is 92 m thick with a bedding plane spacing of 9 m, the Bald Hill Claystone 12 m thick and the cave zone penetrates 64 m into the Bulgo Sandstone, the analysis would be performed on the bottom 9 m of unbroken Bulgo Sandstone with that layer being loaded by a surcharge of 31 m. The area and weight of the surcharge is defined by the goaf angle and the weighted average density of the surcharge.

Using the procedure described in the above mentioned references, a simple spreadsheet was set up to calculate the deflection of the Bulgo Sandstone according to each model geometry. It was found that the calculated deflections were highly sensitive to the goaf angle value. As a result of this sensitivity, it was decided to back calculate the goaf angle from the observed Bulgo Sandstone deflection from the UDEC models. As can be seen from Table 4, this approach was successful and demonstrated the validity of the UDEC models in simulating the deflection of the Bulgo Sandstone.

Table 4. Analytical and numerical deflection of the Bulgo Sandstone.

Model	UDEC Deflection (mm)	UDEC Goaf Angle (°)	Back-Calculated Goaf Angle (°)
2	275	14 – 25	20.0
3	345	12 – 25	11.6
4	506	10 – 25	12.5

8 CONCLUSIONS

In this project, a set of UDEC numerical models were developed to simulate single panel longwall extractions. The process of creating the models, including the compilation of material/joint properties and the determination of the geometry for each individual model was discussed. It was emphasised that all the material/joint properties should be transparent and fully traceable to minimise the appearance of “adjusting” certain parameters to fit a predefined outcome.

From the results, it was seen that the numerical models provided quite a good match to the empirical results, the caving development evident in the numerical models agreed with the observed caving characteristics and supports the theory that the Bulgo Sandstone is the control on sub-critical subsidence, and the results from the Voussoir Beam calculation further enhanced the credibility of the models. Overall, it was concluded that the numerical models were satisfactorily verified and a major outcome of this modelling was the creation of a tool that can be used for isolated single panel predictions.

ACKNOWLEDGEMENTS

The authors wish to express their thanks to Seedsman Geotechnics Pty. Ltd. for financial support, BHP Illawarra Coal Pty. Ltd. for access to drill cores, and Strata Control Technology Operations Pty. Ltd. for their cooperation and helpful insights with core logging data and laboratory results. Thanks are also extended to Michael Coulthard of M.A Coulthard and Associates Pty. Ltd. for his technical guidance on the use of UDEC.

RERERENCES

- Badelow, F, Best, R, Bertuzzi, R & Maconochie, D 2005, ‘Modelling of defect and rock bolt behaviour in geotechnical numerical analysis for Lane Cove Tunnel’, *Proceedings Geotechnical Aspects of Tunnelling for Infrastructure Projects, Mini-Symposium*, 12th October 2005, Milsons Point, Australia, 9 p.
- Barton, N., 1976, ‘The shear strength of rock and rock joints’, *International Journal of Rock Mechanics and Mining Sciences and Geomechanics Abstracts*, vol. 13, issue 9, September 1976, pp. 255 – 279.
- Chan, K F, Kotze, G P & Stone, P C 2005, ‘Geotechnical modelling of station caverns for the Epping to Chatswood rail line project’, in *Proceedings Geotechnical Aspects of Tunnelling for Infrastructure Projects, Mini-Symposium*, 12th October 2005, Milsons Point, Australia, 15 p.
- Coulthard, M A, 1995, ‘Distinct element modelling of mining-induced subsidence – a case study’, in Myer, L R et al. (eds.), *Proceedings of the Conference on Fractured and Jointed Rock Masses*, 3 – 5 June 1992, Lake Tahoe, California, USA, Balkema, Rotterdam, pp. 725 – 732.
- CSIRO Exploration & Mining & Strata Control Technology, 1999, ‘Ground behaviour about longwall faces and its effect on mining’, ACARP Research Project No. C5017, *Australian Coal Association Research Program, Brisbane, Queensland, Australia*.
- CSIRO Petroleum 2002, ‘Numerical Modelling Studies’, in Waddington Kay & Associates, ‘*Research into the impacts of mine subsidence on the strata and hydrology of river valleys and development of management guidelines for undermining cliffs, gorges and river systems*’, ACARP Research Project No. C9067, *Australian Coal Association Research Program, Brisbane, Queensland, Australia*.
- Gale, W. J., 2005, ‘Application of computer modelling in the understanding of caving and induced hydraulic conductivity about longwall panels’, *Proceedings of the Coal2005 6th Australasian Coal Operators’ Conference*, 26 – 28 April 2005, Brisbane, Australia, pp. 11 – 15.
- Ghobadi, M H 1994, ‘Engineering geologic factors influencing the stability of slopes in the Northern Illawarra region’, PhD thesis, University of Wollongong, Australia.

- Holla, L & Barclay, E 2000, *Mine Subsidence in the Southern Coalfield, NSW, Australia*, New South Wales Department of Mineral Resources, pp. 1 – 16.
- Hudson, J A, Stephansson, O & Andersson, J 2005, 'Guidance on numerical modelling of thermo-hydro-mechanical coupled processes for performance assessment of radioactive waste repositories', *International Journal of Rock Mechanics and Mining Sciences*, vol. 42, issues 5 – 6, July – September 1999, pp. 850 – 870.
- Itasca 2000, *UDEC User's Guide*, Itasca Consulting Group, Inc: Minneapolis, Minnesota, USA.
- Kapp, W A 1984, 'Mine subsidence and strata control in the Newcastle District of the Northern Coalfield New South Wales', PhD thesis, University of Wollongong, Australia.
- Kratzsch, H 1983, *Mining Subsidence Engineering*, Springer – Verlag, p. 41, 153.
- MacGregor, S & Conquest, G 2005, 'Geotechnical characterization and borehole completion logs for surface boreholes: Endeavour 3 (WCC DDH29), Endeavour 4 (WCC DDH 30) and Endeavour 5 (WCC DDH 31)', Report No. BHPC2843, *SCT Operations Pty. Ltd.*
- Mandl, G 2005, *Rock Joints – The Mechanical Genesis*, Springer – Verlag, Germany, pp. 55 – 97.
- McNally, G H 1996, 'Estimation of the geomechanical properties of coal measure rocks for numerical modelling', in McNally, G M & Ward, C R (eds.), *Proceedings of the Symposium on Geology in Longwall Mining*, 12 – 13 November 1996, University of New South Wales, pp. 63 – 72.
- Nomikos, P P, Sofianos, A I & Tsoutrelis, C E 2002, 'Structural response of vertically multi-jointed roof rock beams', *International Journal of Rock Mechanics and Mining Sciences*, vol. 39, issue 1, January 2002, pp. 79 – 94.
- Obert, L & Duvall, W I 1967, *Rock Mechanics and the Design of Structures in Rock*, John Wiley and Sons, Inc., pp. 518 – 522.
- Pells, P J N 1993, 'The 1993 E.H Davies Memorial lecture, rock mechanics and engineering geology in the design of underground works', *Australian Geomechanics Society*, pp. 3.1 – 3.33.
- Peng, S S 1992, *Surface Subsidence Engineering*, Society for Mining, Metallurgy, and Exploration, Inc. (AIME), Braun-Brumfield, Inc., pp. 1 – 20.
- Price, N J 1966, *Fault and Joint Development in Brittle and Semi-Brittle Rock*, Pergamon Press Ltd., London, pp. 144 – 147.
- Seedsman, R W 2004, 'Back analysis of sub-critical subsidence events in the Newcastle Coalfield using voussoir beam concepts', *Proceedings of the 6th Triennial Conference on Subsidence Management Issues*, Mine Subsidence Technological Society, Newcastle, Australia, pp. 65 – 74.
- Selley, R C 2000, *Applied Sedimentology*, 2nd edn, Academic Press, California, p. 142.
- Sofianos, A I 1996, 'Analysis and design of an underground hard rock voussoir beam roof', *International Journal of Rock Mechanics and Mining Sciences*, vol. 33, issue 2, February 1996, pp. 153 – 166.
- Sofianos, A I & Kapenis, A P 1998, 'Numerical evaluation of the response in bending of an underground hard rock voussoir beam roof', *International Journal of Rock Mechanics and Mining Sciences*, vol. 35, issue 8, December 1998, pp. 1071 – 1086.
- Tucker, M E 2003, *Sedimentary Rocks in the Field*, 3rd edn, John Wiley & Sons Ltd, England, pp. 88 – 94.
- Williams, W A & Gray, P A 1980, 'The nature and properties of coal and coal measure strata', in Hargraves, A J (ed.), *Proceedings of Support in Coal Mines, The Aus. I.M.M., Illawarra Branch Roof Support Colloquium*, September 1980, The Australasian Institute of Mining and Metallurgy, Parkville, Victoria, Australia, pp. 1 – 12.

Application of Quantitative and MADM Methods in MMS

K. Shahriar

Dept. of Mining and Metallurgical Engng., Amirkabir University of Technology, Tehran, Iran

H. Dezyani

Senior Engineer (Mining), Tehran, Iran

M. Afshar

Kavoshgaran Consulting Engineers, Tehran, Iran

ABSTRACT Mining method selection is among the most critical and problematic points in mining engineering profession. Choosing a suitable method for a given ore-body is very important for the economics, safety and the productivity of the mining work.

In this paper, Technique for Order Preference by Similarity to Ideal Solution (TOPSIS) and AHP with 18 criteria and quantitative methods are used to develop a suitable mining method for the Reza Abad ballclay & bauxite ore deposit in Damqan. Three alternatives (Open pit, Shrinkage stoping and cut and fill stoping) are evaluated. The studies show that the suitable mining method appropriate mining technique for this deposit with regard to the present situation is cut and fill method.

1 INTRODUCTION

Selection of an appropriate mining method is a complex decision that requires the consideration of many technical, economic and environmental factors. There is no single appropriate mining method for a deposit; there are usually two or more feasible methods. Each method entails some inherent problems. Consequently, the optimum method is that method with the least problems (Nicholas, 1992).

Until now, different researches dealing with mining method selection subject have been done by many investigator such as Boshkov and Wright (1973), Morrison (1976), Laubscher (1981), Hartman (1987), Nicholas (1981 and 1992), Miller et al. (1995), Clayton et al. (2002).

In this paper those method selections, which include both surface and underground mining method selection, have been studied, such as, modified Nicholas approach, modified UBC (MMS system), AHP and TOPSIS for the Ballclay and Bauxite Reza Abad of Damqan ore deposit.

1.1 Objective

The main aim of the present study is to determine the optimal mining methods for exploitation of the Ballclay and Bauxite of RAD ore deposit. The Ballclay and Bauxite of RAD ore deposit which is situated in east of Iran.

Physical parameters such as deposit geometry (general shape, ore thickness, dip and ore depth) grade distribution and rock mechanics characteristics and all other necessary data needed for evaluation all collected using field and laboratory tests, which are given in table 1.

2 QUANTITATIVE METHODS

2.1 Nicholas Approach

The classification proposed by Nicholas (1981 and 1992) determines feasible mining methods by numerical ranking and thus is truly quantitative. The Nicholas Method is based on an analysis of characteristics of the deposit that include ore geometry and geomechanical properties of the

hangingwall, ore zone, and footwall rocks. The Nicholas Method uses a system of four rankings. The rankings are summed with the highest rankings indicating the most favourable mining methods. The rankings range from 0 to 4. A value of 0 strongly suggests a particular characteristic is unfavourable, while a value of 4 indicates a characteristic that is highly favourable. A value of -49 is used to eliminate a particular mining method from being feasible.

Table 1. Input paramrters for mining method selection in Ballclay and Bauxite of RAD ore deposit.

	Parameters	Description
Ore zone	General deposit shape	Layer
	Ore thickness	1 meters
	Ore dip	70 degree
	Grade distribution	Graditional
	Depth	100 meters
	Uniaxial Compressive Strength (UCS)	1 – 5 MPa
	RQD	20 - 40
	Rock Substance Strength (RSS)	0.1
	Rock Mass Rating (RMR)	42
	Uniaxial Compressive Strength (UCS)	50 – 100 MPa
Hangwall	RQD	40 – 70
	Rock Substance Strength (RSS)	1.85
	Rock Mass Rating (RMR)	65
	Uniaxial Compressive Strength (UCS)	1 – 5 MPa
Foot wall	RQD	20 - 40
	Rock Substance Strength (RSS)	0.1
	Rock Mass Rating (RMR)	42

A recent modification to the system is the weighting of the categories for the ore geometry, ore zone, hanging wall, and footwall. To give each of these categories weight, the ore zone, hanging wall, and footwall need to be multiplied by 1, 1, 0.8, 0.5 However, this weighting can be changed based on personal experience (Table 2). The net weighting is then multiplied by each of the categories. Using this method for the Ballclay and Bauxite of RAD ore deposit resulted in cut and fill and open pit mining methods respectively.

2.2 Modified UBC (MMS System)

The MMS system proposed by Clayton et al. (2002). This approach is similar the UBC mining method selection algorithm, but incorporated fuzzy logic in analysis procedure.

Table 2. Summary of evaluation using Nicholas (1992) Method for Ballclay and Bauxite of RAD ore deposit.

Method	Rank
Open pit	32,5
Cut and fill	34,4
shrinkage	22,9
Sublevel stoping	15,2
Top slicing	20,1
Square set	33,4
Block caving	28,4
Sublevel caving	21,6

Unfortunately neither of these methods takes account of the uncertainty associated with boundary conditions of the categories used to describe input variables. This paper details the development of a Knowledge based System Mining Method Selection (MMS) that incorporates the uncertainty associated with these boundary conditions, and uses these uncertainties to modify the input parameter rankings to adjust the rating values for each method. The system is based on the UBC Mining Method Selection Algorithm but provides the opportunity to describe the parameters using Fuzzy Logic. The ratings for Geometry and Grade Distribution, Rock Mass Rating, and Rock Substance Strength are modified by multiplying the Degree of Beliefs in membership determined from the above associative memory maps by the respective ranking weights. A single rule is used for each output state, where the output states are the individual mining methods considered.

$$\text{Total Rating} = f(S, G, D, P, \text{RMR}, \text{RSS}) = \sum \{ \text{DoB}(s, g, d, p, \text{rmr}, \text{rss}) \times \text{RANK}(s, g, d, p, \text{rmr}, \text{rss}) \}$$

where;

DOB: Membership degree

S : Deposit Shape

G : Deposit Grade
 D : Deposit Depth
 P : Deposit Plunge, or Dip
 RMR : Rock Mass Rating of Hanging wall, Ore Zone, and Footwall respectively
 RSS : Rock Substance Strength of Hanging wall, Ore Zone, and Footwall respectively

Therefore it can be written:

$$\text{Depth (100 m)} = \{0.5/\text{shallow}, 0.5/\text{intermediate}, 0/\text{deep}\} = \{0.5/\text{shallow}, 0.5/\text{intermediate}\}$$

Therefore in this deposit, the deposit depth in the final ranking for cut and fill would be:
 Ore depth rating (cut and fill) =
 2*membership degree (ore depth: shallow)
 +3*membership degree (ore depth: intermediate)+ 4* membership degree (ore depth: deep)

$$\text{Ore depth rating (cut and fill)} = 2 * 0.5 + 3 * 0.5 + 4 * 0 = 2.5$$

The RMR evaluation in this system according to fuzzy set distribution shown in Figure 1, which shown that RMR of ore zone and foot wall (42) membership degree is 0.42 of "poor" and 0.58 of "fair"

$$\text{RMR of ore zone (42)} = \{0.42/\text{poor}, 0.58/\text{fair}\}$$

RMR of ore zone and hanging wall (65) membership degree is 0.77 of "good" and 0.23 of "fair"

$$\text{RMR of ore zone (65)} = \{0.77/\text{good}, 0.23/\text{fair}\}$$

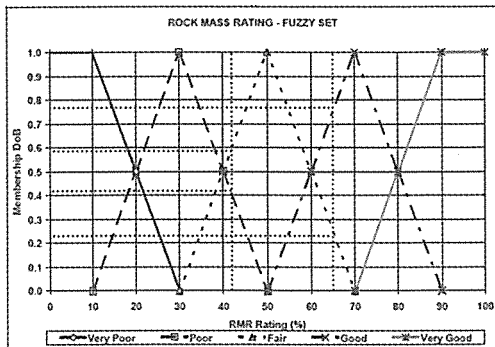


Figure 1. Fuzzy set for RMR in MMS system.

After calculation, the RMR rank of Ballclay and Bauxite of RAD ore deposit for each method's has been shown in Table 3.

For the other ranking parameters such as deposit dip, thickness, RSS of walls there was no difference between MMS system and UBC method in Ballclay and Bauxite of RAD ore deposit because their rate was far from boundaries.

Table 3. MMS system ranking for Ballclay and Bauxite of RAD ore deposit.

Method	Rank
Open pit	29.58
Cut and fill	27.63
shrinkage	23.86
Sublevel stopping	13.65
Top slicing	18.27
Square set	22.91
Block caving	-18.85
Sublevel caving	-21.27

Finally by comparing the results, it has been found that open pit and cut and fill mining method was more suitable than others, while based on RMR and RSS open pit mining method has the highest rank and based on geometry condition cut and fill method is the most suitable one (Table 3).

3 MADM METHODS

3.1 AHP Method

To deal with a complex, hierarchical MADM problem, Saaty [Saaty, 1980] proposed a method for selecting the available alternatives by decomposing a complex MADM problem into a system of hierarchy. His method, well known as the analytic hierarchy process (AHP), structures the decision problem into levels corresponding to goals, criteria, sub-criteria and alternatives, making it possible for the decision maker to focus on a smaller set of decisions. Commonly, a hierarchy has at least three levels, comprising the global or overall goal of the problem at the top, multiple criteria that define alternatives in the middle and the competing alternatives at the bottom. For the abstract criteria, such as

the concept of comfort and security when comparing the performances of cars in the case of buying a car, sub-criteria are generated sequentially through a multilevel hierarchy to provide the operationalization of the respective criteria.

The main feature of AHP is its using the pairwise comparison to elicit the relative importance of the alternatives in terms of each criterion. It deals with the decision $m \times n$ matrix, which is constructed by using the relative importance of the alternatives with respect to each criterion. The vector $(a_{i1}, a_{i2}, \dots, a_{in})$ represents the principal eigenvector of an $n \times n$ reciprocal matrix which is determined by pairwise comparisons of the impact of the m alternatives on the i^{th} criterion.

The global value of an alternative can be obtained by aggregating the contribution of each criterion to the overall goal through the summation of the product of the criteria weight and the performance of the alternative with respect to each criterion. The best alternative can be determined by comparing the aggregated value. The calculation of the aggregated score for each alternative can be obtained from the following equation:

$$A_{AHPscore} = \max_i \sum_{j=1}^n a_{ij} w_j \quad \text{for } i = 1, 2, 3, \dots, m. \quad (1)$$

Where a_{ij} represents the relative value of alternative A_i and w_j denotes the respective weight when it is considered in terms of criteria C_j . Moreover, it is necessary to normalize the alternative rating and the weight to result in $\sum a_{ij} = 1$ and $\sum w_j = 1$.

The strength of the AHP approach lies in its ability to hierarchically structure a complex, multi-attribute problem into a comprehensive structure representing the decision maker's perception of the decision problem. The similarity between the Simple Additive Weighted and the AHP method is also obvious. It is essentially the formalization of the intuitive understanding of a complex problem using a hierarchical structure, and therefore can be attributed also to a hierarchical SAW method. By using the relative value instead of the actual value, the AHP approach is also applicable for single,

as well as multi-dimensional, multi-criteria decision making problems.

First step in AHP trend is to demonstrate the hierarchy structuring of real complex problem which the general objective is positioned at the highest level. The parameters and alternatives are shown in next level (Saaty, 1990; 1994). If the purpose of using the AHP technique is to select the suitable mining method for ore deposit, then one must positioned the suitable mining method at highest level and the most effective mining method parameters located in next level, finally the mining methods as a alternative will be located at the lowest level. In AHP technique the elements of each level compared to its related element in upper level inform of pair-wise comparison method. The results of these comparisons are shown in matrix form as:

$$A = \begin{bmatrix} a_{11} & \dots & a_{1n} \\ \vdots & a_{22} & \dots & \vdots \\ a_{n1} & \dots & a_{nn} \end{bmatrix} \quad (2)$$

Or

$$A = [a_{ij}] \quad i, j = 1, 2, \dots, n \quad (3)$$

where:
 a_{ij} is the priority of element i compared to element j

It must be noted that, in pair comparison of criterion if the priority of element i compared to element j is equal to w_{ij} then the priority of element j compared to element i is equal to $1/w_{ij}$. The priority of element compared to it is equal to one. After calculation of alternative weight compared to criterion weight and criterion compared to objective, overall priority of each alternative can be calculated (Chan and Lyn, 2001; Gole, 2001; Chu and Kalaba, 2000).

This method contained the following three stages:

1- Recognition of objective, criterions, sub-criterions and alternatives for creation of hierarchy structure. At this stage gathering all available information of ore deposit, the major factors affected on selection of mining methods were determined. Based upon study of this stage three criterion, 18 sub-criterions

and three alternatives were recognized as an ingredient of hierarchy structure (Fig.2).

2- In this stage based up on experiences, engineering judgment and knowledge, pairwise comparison of parameters was used to build up the matrix.

$$A_2 = \begin{bmatrix} 1 & 1.4 & 1.4 & 2 & 1 & 2 \\ 0.7 & 1 & 1.4 & 1.7 & 1.2 & 2 \\ 0.7 & 0.7 & 1 & 1 & 1 & 1 \\ 0.5 & 0.6 & 1 & 1 & 1 & 0.5 \\ 1 & 0.8 & 1 & 1 & 1 & 2 \\ 0.5 & 0.5 & 1 & 2 & 0.5 & 1 \end{bmatrix} \quad A_4 = \begin{bmatrix} 1 & 1/6 & 1/3 & 1/9 & 1/9 & 1/6 \\ 6 & 1 & 3 & 1/3 & 1/5 & 1/5 \\ 3 & 1/3 & 1 & 1/6 & 1/7 & 1/3 \\ 9 & 3 & 6 & 1 & 1/5 & 1/2 \\ 9 & 5 & 7 & 5 & 1 & 1 \\ 6 & 5 & 3 & 2 & 1 & 1 \end{bmatrix}$$

$$A_5 = \begin{bmatrix} 1 & 1/2 & 3 & 1 & 1/2 & 4 \\ 2 & 1 & 3 & 2 & 1 & 2 \\ 1/3 & 1/3 & 1 & 1/4 & 1/2 & 1 \\ 1 & 1/2 & 4 & 1 & 1/2 & 4 \\ 2 & 1 & 2 & 2 & 1 & 2 \\ 4 & 1/2 & 1 & 1/4 & 1/2 & 1 \end{bmatrix} \quad A = \begin{bmatrix} 1 & 2/3 & 2 \\ 3/2 & 1 & 3 \\ 1/2 & 1/3 & 1 \end{bmatrix}$$

$$A_1 = \begin{bmatrix} 1 & 1 & 5 \\ 1 & 1 & 8 \\ 1/5 & 1/8 & 1 \end{bmatrix} \quad A_2 = \begin{bmatrix} 1 & 1.1 & 1.3 \\ 0.91 & 1 & 1.2 \\ 0.77 & 0.83 & 1 \end{bmatrix} \quad A_3 = \begin{bmatrix} 1 & 2 & 4 \\ 1/2 & 1 & 3 \\ 1/4 & 1/3 & 1 \end{bmatrix}$$

$$A_{14} = \begin{bmatrix} 1 & 3 & 2 \\ 1/3 & 1 & 2 \\ 1/2 & 1/2 & 1 \end{bmatrix} \quad A_5 = \begin{bmatrix} 1 & 1 & 1/3 \\ 1 & 1 & 1/3 \\ 3 & 3 & 1 \end{bmatrix} \quad A_{16} = \begin{bmatrix} 1 & 4 & 1/2 \\ 1/4 & 1 & 1/5 \\ 2 & 5 & 1 \end{bmatrix}$$

$$A_6 = \begin{bmatrix} 1 & 3 & 1/2 \\ 1/3 & 1 & 1/4 \\ 2 & 4 & 1 \end{bmatrix} \quad A_{22} = \begin{bmatrix} 1 & 4 & 8 \\ 1/4 & 1 & 2 \\ 1/8 & 1/2 & 1 \end{bmatrix} \quad A_{23} = \begin{bmatrix} 1 & 7 & 1 \\ 1/7 & 1 & 1/5 \\ 1 & 5 & 1 \end{bmatrix}$$

$$A_7 = \begin{bmatrix} 1 & 2 & 2 \\ 1/2 & 1 & 1/4 \\ 2 & 4 & 1 \end{bmatrix} \quad A_{25} = \begin{bmatrix} 1 & 9 & 6 \\ 1/9 & 1 & 1/4 \\ 1/6 & 4 & 1 \end{bmatrix} \quad A_{26} = \begin{bmatrix} 1 & 1/3 & 2 \\ 3 & 1 & 3 \\ 1/2 & 1/3 & 1 \end{bmatrix}$$

$$A_8 = \begin{bmatrix} 1 & 2 & 1 \\ 1/2 & 1 & 1/2 \\ 1 & 2 & 1 \end{bmatrix} \quad A_9 = \begin{bmatrix} 1 & 2 & 3 \\ 1/2 & 1 & 3/2 \\ 1/3 & 2/3 & 1 \end{bmatrix} \quad A_{13} = \begin{bmatrix} 1 & 1 & 1/2 \\ 1 & 1 & 1/3 \\ 2 & 3 & 1 \end{bmatrix}$$

$$A_{15} = \begin{bmatrix} 1 & 1 & 1/2 \\ 1 & 1 & 1 \\ 2 & 1 & 1 \end{bmatrix} \quad A_{17} = \begin{bmatrix} 1 & 2 & 1 \\ 1/2 & 1 & 1/2 \\ 1 & 2 & 1 \end{bmatrix} \quad A_{18} = \begin{bmatrix} 1 & 1/2 & 1/3 \\ 2 & 1 & 1/2 \\ 3 & 2 & 1 \end{bmatrix}$$

3- The third stage of studies was the calculation of local and overall priorities of parameters and mining method by Expert Choice software.

The output of phase one was the selection of two mining methods:

1. Cut & fill, and
2. Open pit (Table 4).

As indicated in Table 5, cut & fill mining has highest priority and shrinkage has lowest priority.

3.2 TOPSIS Method

TOPSIS method is a technique for order preference by similarity to ideal solution and proposed by Hwang and Yoon (1981). The ideal solution (also called positive ideal solution) is a solution that maximizes the benefit criteria/attributes and minimizes the cost criteria/attributes, whereas the negative ideal solution (also called anti-ideal solution) maximizes the cost criteria/attributes and minimizes the benefit criteria/attributes. The so-called benefit criteria/attributes are those for maximization, while the cost criteria/attributes are those for minimization. The best alternative is the one, which is closest to the ideal solution and farthest from the negative ideal solution.

Suppose a MCDM problem has m alternatives, A_1, \dots, A_m , and n decision criteria/attributes, C_1, \dots, C_n . Each alternative is evaluated with respect to the m criteria/attributes.

All the values/ratings assigned to the alternatives with respect to each criterion form a decision matrix denoted by $X = (x_{ij})_{n \times m}$. Let $W = (w_1, \dots, w_n)$ be the relative weight vector about the criteria, satisfying $\sum_{i=1}^n w_i = 1$.

Table 4. Final result of mining method selection of Reza Abad ball clay & bauxite ore deposit by AHP technique.

Parameter	weight	CUT & FILL	SHRINKAGE	OPEN-PIT
geometries	0.333	0.396	0.319	0.285
operational	0.500	0.482	0.245	0.273
geomechanic	0.167	0.379	0.248	0.373
Final weight		0.436	0.270	0.294

Then the TOPSIS method can be summarized as follows:

A- Calculate the decision matrix (D) as

$$D = \begin{bmatrix} X_{11} & \dots & X_{1n} \\ \vdots & \dots & \vdots \\ X_{m1} & \dots & X_{mn} \end{bmatrix} \quad (4)$$

B- Calculate the normalized decision matrix or R matrix. The normalized value r_{ij} is calculated as

$$r_{ij} = \frac{x_{ij}}{\sqrt{\sum_{i=1}^m x_{ij}^2}} \quad i = 1, \dots, n, \quad j = 1, \dots, m \quad (5)$$

$$R = \begin{bmatrix} r_{11} & \dots & r_{1n} \\ \vdots & \dots & \vdots \\ r_{m1} & \dots & r_{mn} \end{bmatrix} \quad (6)$$

C- Calculate the criteria weighted matrix as

$$W = \begin{bmatrix} w_1 & \dots & 0 \\ \vdots & w_2 & \dots \\ 0 & \dots & w_n \end{bmatrix} \quad (7)$$

D- Calculate the weighted normalized decision matrix. The weighted normalized value v_{ij} is calculated as

$$v_{ij} = w_i r_{ij} = W \times R \quad j = 1, \dots, m, \quad i = 1, \dots, n \quad (8)$$

Where w_i is the weight of the i th attribute or criterion, and $\sum_{i=1}^n w_i = 1$.

E- Determine the positive ideal and negative ideal solution.

$$A^+ = \{v_1^+, \dots, v_n^+\} = \{(\max_j v_{ij} | i \in I), (\min_j v_{ij} | i \in J)\} \quad (9)$$

$$A^- = \{v_1^-, \dots, v_n^-\} = \{(\min_j v_{ij} | i \in I), (\max_j v_{ij} | i \in J)\} \quad (10)$$

Where I is associated with benefit criteria, and J is associated with cost criteria.

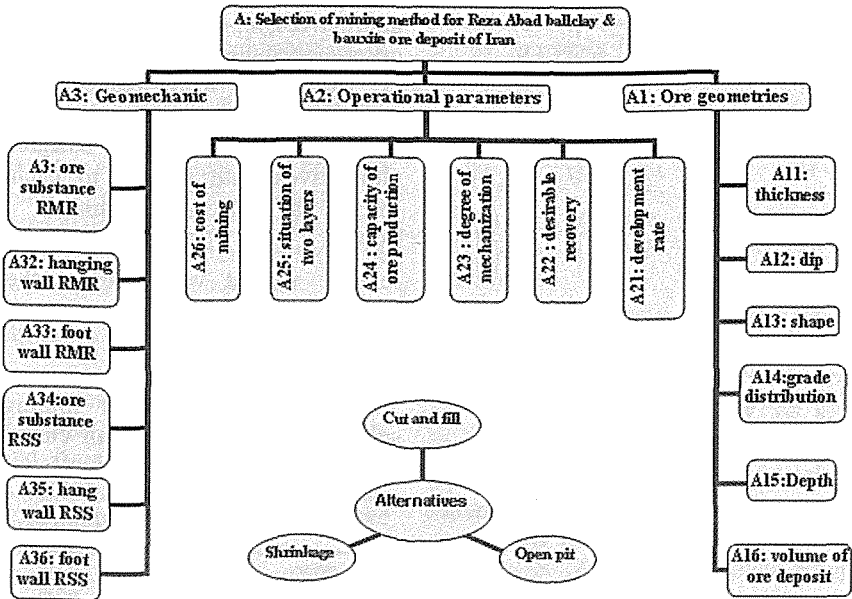


Figure 2. Hierarchy structuring of Reza Abad ball clay & bauxite ore deposit based on technical parameters.

A)

$$D = \begin{bmatrix} 6 & 9 & 9 & 8 & 3 & 4 & 6 & 8 & 8 & 6 & 9 & 3 & 6 & 7 & 4 & 3 & 6 & 2 \\ 8 & 7 & 4 & 4 & 3 & 4 & 2 & 4 & 1 & 2 & 1 & 5 & 2 & 3 & 2 & 5 & 3 & 3 \\ 1 & 2 & 1 & 1 & 7 & 6 & 8 & 1 & 6 & 7 & 2 & 1 & 6 & 1 & 6 & 7 & 6 & 5 \end{bmatrix}$$

B)

$$R = \begin{bmatrix} 0.6 & 0.78 & 0.91 & 0.89 & 0.37 & 0.48 & 0.59 & 0.89 & 0.8 & 0.63 & 0.97 & 0.51 & 0.69 & 0.91 & 0.53 & 0.33 & 0.67 & 0.32 \\ 0.8 & 0.6 & 0.4 & 0.44 & 0.37 & 0.48 & 0.2 & 0.44 & 0.1 & 0.21 & 0.11 & 0.84 & 0.23 & 0.39 & 0.27 & 0.55 & 0.33 & 0.49 \\ 0.1 & 0.17 & 0.1 & 0.11 & 0.85 & 0.73 & 0.78 & 0.11 & 0.6 & 0.74 & 0.21 & 0.17 & 0.69 & 0.13 & 0.8 & 0.77 & 0.67 & 0.81 \end{bmatrix}$$

C)

$$W = \begin{bmatrix} 0.075 & 0 & 0 & 0 & 0 & 0 & 0 & 0 & 0 & 0 & 0 & 0 & 0 & 0 & 0 & 0 & 0 & 0 & 0 \\ 0 & 0.067 & 0 & 0 & 0 & 0 & 0 & 0 & 0 & 0 & 0 & 0 & 0 & 0 & 0 & 0 & 0 & 0 & 0 \\ 0 & 0 & 0.047 & 0 & 0 & 0 & 0 & 0 & 0 & 0 & 0 & 0 & 0 & 0 & 0 & 0 & 0 & 0 & 0 \\ 0 & 0 & 0 & 0.040 & 0 & 0 & 0 & 0 & 0 & 0 & 0 & 0 & 0 & 0 & 0 & 0 & 0 & 0 & 0 \\ 0 & 0 & 0 & 0 & 0.059 & 0 & 0 & 0 & 0 & 0 & 0 & 0 & 0 & 0 & 0 & 0 & 0 & 0 & 0 \\ 0 & 0 & 0 & 0 & 0 & 0.044 & 0 & 0 & 0 & 0 & 0 & 0 & 0 & 0 & 0 & 0 & 0 & 0 & 0 \\ 0 & 0 & 0 & 0 & 0 & 0 & 0.012 & 0 & 0 & 0 & 0 & 0 & 0 & 0 & 0 & 0 & 0 & 0 & 0 \\ 0 & 0 & 0 & 0 & 0 & 0 & 0 & 0 & 0.044 & 0 & 0 & 0 & 0 & 0 & 0 & 0 & 0 & 0 & 0 \\ 0 & 0 & 0 & 0 & 0 & 0 & 0 & 0 & 0 & 0.025 & 0 & 0 & 0 & 0 & 0 & 0 & 0 & 0 & 0 \\ 0 & 0 & 0 & 0 & 0 & 0 & 0 & 0 & 0 & 0 & 0.089 & 0 & 0 & 0 & 0 & 0 & 0 & 0 & 0 \\ 0 & 0 & 0 & 0 & 0 & 0 & 0 & 0 & 0 & 0 & 0 & 0.195 & 0 & 0 & 0 & 0 & 0 & 0 & 0 \\ 0 & 0 & 0 & 0 & 0 & 0 & 0 & 0 & 0 & 0 & 0 & 0 & 0.133 & 0 & 0 & 0 & 0 & 0 & 0 \\ 0 & 0 & 0 & 0 & 0 & 0 & 0 & 0 & 0 & 0 & 0 & 0 & 0 & 0.029 & 0 & 0 & 0 & 0 & 0 \\ 0 & 0 & 0 & 0 & 0 & 0 & 0 & 0 & 0 & 0 & 0 & 0 & 0 & 0 & 0.043 & 0 & 0 & 0 & 0 \\ 0 & 0 & 0 & 0 & 0 & 0 & 0 & 0 & 0 & 0 & 0 & 0 & 0 & 0 & 0 & 0.011 & 0 & 0 & 0 \\ 0 & 0 & 0 & 0 & 0 & 0 & 0 & 0 & 0 & 0 & 0 & 0 & 0 & 0 & 0 & 0 & 0.031 & 0 & 0 \\ 0 & 0 & 0 & 0 & 0 & 0 & 0 & 0 & 0 & 0 & 0 & 0 & 0 & 0 & 0 & 0 & 0 & 0.039 & 0 \\ 0 & 0 & 0 & 0 & 0 & 0 & 0 & 0 & 0 & 0 & 0 & 0 & 0 & 0 & 0 & 0 & 0 & 0 & 0.013 \end{bmatrix}$$

D)

$$V = \begin{bmatrix} 0.045 & 0.052 & 0.043 & 0.036 & 0.022 & 0.021 & 0.007 & 0.039 & 0.02 & 0.056 & 0.189 & 0.068 & 0.02 & 0.039 & 0.006 & 0.01 & 0.026 & 0.004 \\ 0.08 & 0.04 & 0.019 & 0.018 & 0.022 & 0.021 & 0.002 & 0.019 & 0.002 & 0.019 & 0.021 & 0.112 & 0.006 & 0.017 & 0.003 & 0.017 & 0.013 & 0.007 \\ 0.007 & 0.011 & 0.005 & 0.004 & 0.05 & 0.032 & 0.009 & 0.005 & 0.015 & 0.066 & 0.041 & 0.023 & 0.018 & 0.006 & 0.009 & 0.024 & 0.016 & 0.01 \end{bmatrix}$$

E)

$$A^+ = \{0.08 \ 0.052 \ 0.043 \ 0.036 \ 0.05 \ 0.032 \ 0.009 \ 0.039 \ 0.02 \ 0.066 \ 0.189 \ 0.112 \ 0.02 \ 0.039 \ 0.009 \ 0.024 \ 0.026 \ 0.01\}$$

$$A^- = \{0.007 \ 0.011 \ 0.005 \ 0.004 \ 0.022 \ 0.021 \ 0.002 \ 0.005 \ 0.002 \ 0.019 \ 0.021 \ 0.023 \ 0.006 \ 0.006 \ 0.003 \ 0.017 \ 0.013 \ 0.004\}$$

F- Calculate the separation measures, using the n-dimensional Euclidean distance. The separation of each alternative from the ideal solution is given as

$$S_j^+ = \sqrt{\sum_{i=1}^n (V_{ij} - V_i^+)^2} \quad j = 1, \dots, m \quad (11)$$

Similarly, the separation from the negative ideal solution is given as

$$S_j^- = \sqrt{\sum_{i=1}^n (V_{ij} - V_i^-)^2} \quad j = 1, \dots, m \quad (12)$$

G- Calculate the relative closeness to the ideal solution. The relative closeness of the alternative A_j with respect to A^+ is defined as

$$C_j = \frac{S_j^-}{S_j^+ + S_j^-} \quad j = 1, \dots, m \quad (13)$$

Since $S_j^- \geq 0$ and $S_j^+ \geq 0$, then, clearly, $C_j \in [0,1]$.

H- Rank the alternatives according to the relative closeness to the ideal solution. The bigger the C_j , the better the alternative A_j . The best alternative is the one with the greatest relative closeness to the ideal solution.

The obtained results of mining method selection of Reza Abad ball clay & bauxite ore deposit by TOPSIS technique shown in Table 5.

Table 5. The obtained results of mining method selection of Reza Abad ball clay & bauxite ore deposit by TOPSIS technique.

Alternatives	S_j^+	S_j^-	C_j
CUT & FILL	0.070	0.203	0.743
SHRINKAGE	0.185	0.124	0.401
OPEN-PIT	0.200	0.064	0.242

4 CONCLUSIONS

Typically, systems used to select potential mining methods based on a finite number of defined input parameters do not account for the inherent uncertainty associated with the selection process. This uncertainty is particularly relevant and meaningful at the boundaries between the categories. The MMS system is a method built on the UBC mining method selection algorithm that incorporates fuzzy logic in the analysis which can be used as, a remediation tools for above mentioned short-comings. Using MMS system for selecting optimum and

most suitable method according conditions of Ballclay and Bauxite of RAD ore deposit, cut and fill and open pit mining methods has been identified as more suitable methods. Fuzzy MADM has found wide applications in the solution of real world decision making problems. The MADM methods are based on an aggregating function representing "closeness to the ideal". the basic principle of the TOPSIS method is that the chosen alternative should have the "shortest distance" from the ideal solution and the "farthest distance" from the "negative-ideal" solution.

TOPSIS (Technique for Order Preference by Similarity to Ideal Solution) was used to select the suitable mining method for Reza Abad ball clay & bauxite mine of Iran. 18 technical and economical parameters were chosen for selection of mining method. Based upon the mentioned parameters, three mining methods were selected as following:

1. Cut & fill,
2. Shrinkage, and
3. Open-pit

Finally, by using TOPSIS and AHP methods the cut & fill mining method was selected to be the most suitable mining method for Reza Abad ball clay & bauxite mine of Iran.

REFERENCES

- Dezyani, H., 2006, "*Mining Method Selection in Ball Clay and Bauxite mine of Reza Abad*", M.S. thesis, Islamic Azad University Science and Research Branch, Tehran, Iran, pp.75-100.
- Lai, Y.J, Liu, T.Y, Hwang, C.L,1994, "*TOPSIS for MODM*", European Journal of Operational Research 76 (3) (1994) 486-500.
- Wang, Y.M, Taha M.S. 2006, Elhag, "*Fuzzy TOPSIS method based on alpha level sets with an application to bridge risk assessment, Expert Systems with Applications*", 31 (2006) 309-319.
- Dezyani.H, Shahriar, K, Ataei, M, Afshar .M, 2006, "*Mining Method Selection by TOPSIS Approach*", VI-th International Scientific Conference SGEM 2006, Modern Management of Mine Producing, Geology and Environmental Protection, Albena, Bulgaria, PP19-25
- Clayton, C., Pakalnis, R., Meech, J., 2002, "*A Knowledge-based System for Selecting a Mining Method*", IPPM conference, University of British Columbia.
- Nicholas D.E., 1992. "*Selection Procedure*". Society of Mining, Metallurgy, and Exploration, Inc- PP.2090-2106.
- M.A. Abo-Sinna, A.H. Amer, 2005, "*Extensions of TOPSIS for multi-objective large-scale nonlinear programming problems*", Applied Mathematics and Computation 162 (2005) 243-256.

Investigation of Factors Affecting Floor Heave and Convergence of Galleries in Tabas Coal Mine

A. Royanfar & K. Shahriar

Amirkabir University of Technology, Tehran, Iran

ABSTRACT In Tabas coal mine (Parvade 5), the heave and convergence are ever known subjects of the ground control problems that have caused significant deficiencies particularly in the reuse of tailgates. The abutment pressure, the horizontal stress, the ground water, the exploitation method and the nature of layers in roof and floor of coal strata could be considered as the most effective factors in floor heave and sidewalls convergence in galleries. Detailed investigations in Tabas coal mine (Parvade 5) showed that the abutment pressures are major factors for increasing the length of packs and their reinforcing in downside of the stop along with the usage of rib pillar and pack in upside of the stop in addition to the blasting of roof in gob zone have been selected here to overcome the problem. Applying these techniques resulted in the reduction of the intensity of floor heave and sidewall convergence. Thus deformation of height and width has reduced 64.58% and 40%, respectively.

1 INTRODUCTION

In longwall mining a very common ground control problem, is the floor heave and sidewall convergence in gate roads. Reduction of galleries cross section will have considerable effects on transporting system, ventilation of mine and totally will reduce the efficiency of production process.

In Tabas coal mine (Parvade 5) severe floor heave and sidewall convergence in the gate roads, occur due to presence of soft floor rocks and high stress field affected by abutment pressure as the longwall face advances. Gate roads particularly reused tailgates are very difficult to maintain.

This paper was firstly started with describing of longwall mining system in Tabas and followed by study of effective factors in galleries deformation and finally proposed suitable technique to reduce the intensity of the problem.

2 TABAS COAL MINE (PARVADE 5)

The exploration area of the Parvade 5 is about 18 km^2 that is located south 75 kilometer far from the Tabas city. There are five coal seams which three of them are not exploitable due to large amount of sulphur. The reserve of other two seams named C1 and B2 is around 10600000 tons. The location of Tabas is shown in Figure 2.

In order to better understanding the gate road behavior, it is important to briefly review the longwall mining system used in this mine and the type of support used in gate roads.

2.1 Geology of Mine

In Tabas coal mine, two, 1.00-1.15 m thick 10-12 degree dip seams, named C1 and B2 with a distance about 29 meters between them are being extracted. This paper is focused on floor heave and sidewall convergence problem and its consequence

remediation in Eastern Level 5 in seam C1 at the depth of about 120 meter.

The immediate roof of coal seam C1 is consisted of two kind of siltstone with thickness of 1.7 and 2.5 meter respectively. The strength of layers increases with the decrease in layer's depth in Tabas coal field. The immediate floor is a weak seatearth mudstone 0.4 m thick and then a layer of siltstone 0.8 m thick becoming stronger with depth.

There are not considerable joint and fractures in coal seam and adjacent layers and in most parts the layers are almost intact. On the other hand, existence of joints or fractures except in faulty zone do not create any major problem in support of galleries or stopes. There is not also considerable ground water flow in this mine, except in a faulty zone, which water inflow to galleries and intensify the swelling of floor layer.

2.2 Longwall Mining System in Tabas Coal Mine

The longwall layout in Tabas coal mine (Parvade 5) is advance longwall with reuse of previous gate (Figure 1). On the other hand, there is one gallery between adjacent stopes which is used for two purposes, at first it is the tailgate of stope 1 and then it is used as the headgate for stope 2.

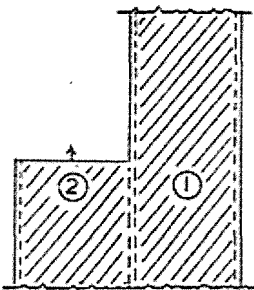


Figure 1. Longwall advance with reuse of previous gate (Yoginder&Chugh, 1982).

In this condition the gate which is reused, has already experienced deformation behind face (1) due to stress redistribution. Consequently, its residual condition after face (1) will influence its subsequent

efficiency during reuse with face (2). Such roadway layout has needed extensive repair work behind face (2) and has led to major restriction to transport and ventilation (Yoginder&Chugh, 1982).

The length of Longwall faces is in the range of 40 -140 meters. The gate roads are usually excavated to an 8.2 m² cross section and the final cross section is 6 m².

Yielding-type 7.2 TH profile steel sets with 1 meter spacing are used as permanent support. The coal in a panel is fully extracted with no rib pillar leaving between them.

3 FACTORS AFFECTING THE DEFORMATION IN GALLERIES

In this mine, there are severe deformations in galleries which restrict transporting system; therefore it is necessary to dig the floor. The most effective factors leading to this problem in galleries should be considered as:

a. The magnitude and orientation of horizontal stresses relative to entry orientation. (Mark *et al.*, 1998)

b. The stresses acting on the roadways, resulting from redistribution of geostatic stresses during excavation of coal from the longwall working that are named abutment pressures. (Peng&Chiang, 1984; Farmer, 1985)

c. The presence of ground water particularly in weak rocks such as clay. (Farmer, 1985)

d. The exploitation method in longwall faces that can affect magnitude of roadway deformation. (Yoginder&Chugh, 1982)

e. The strength of floor rocks. (Farmer, 1985; Chaojing&Shudong, 1996)

f. Proximate geology including the presence of major discontinuities. (Farmer, 1985; Chaojing&Shudong, 1996)

The orientation of the principal horizontal stresses relative to the mine layout can have a significant effect on the stability of mine workings. Entries that are parallel to the maximum horizontal stress will suffer less damage than those are perpendicular to it. (Mark *et al.*, 1998)

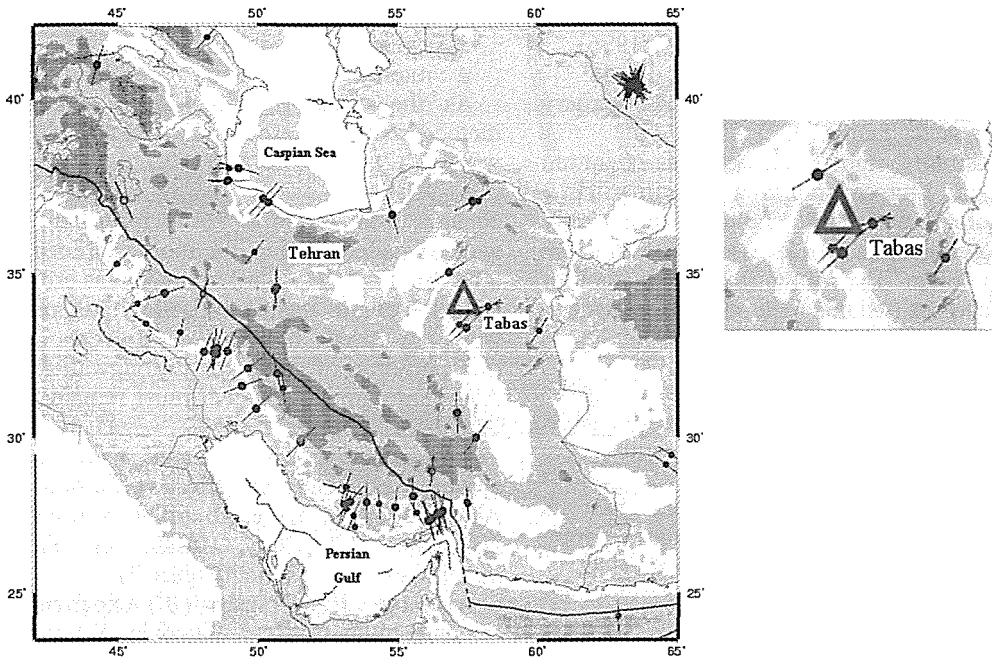


Figure 2. Stress data of the near field region around Tabas (IRITEC, 2002).

Referenced to the world stress map project data displays the location and orientation of numerous stress indicators within Iran, all of which are derived from earthquake records (Figure 2). From the neighborhood region very close to the Tabas mine, the data have been obtained from five earthquakes where thrust fault conditions prevail and about eight earthquakes where strike-slip conditions prevail. It is possible to deduce that the major horizontal stress orientated from north east to south west. (IRITEC, 2002)

The orientation of galleries in this mine is north west to south east that is perpendicular to major horizontal stress orientation. But before the start of coal extraction in longwall faces, the galleries do not exhibit any support problem. It means that horizontal stress is not a major factor of gallery deformation.

Floor heave and sidewalls deformations have been observed in all levels with different depth and face length. Also immediate roof is caved continuously with advancing of faces. (Royanfar&Shahriar, 2006)

Consequently, to reduce the effect of the lateral pressure, we must change the current exploitation method with more suitable ones or make some improvement and corrections in current method.

Changing the method from advance longwall mining to multi-entry retreat longwall mining could reduce deformations of galleries considerably. In this system design of chain pillars and yield pillars in multi-entries can reduce the effect of abutment pressures on galleries and beside panels and another mine working. Also in retreat longwall mining the maintenance of galleries in caving area is not necessary since they are not reused.

The changing and replacement of the mining system has extensive costs. Also the production of coal simultaneously with development of galleries is the main factor in choosing the advance system.

Consequently, to reduce the intensity of floor heave and sidewall convergences, following techniques have been proposed:

a. installation of the rock bolt system in gallery (Unal *et al.*, 2001; Stephen, 2004)

- b. replacing of the steel rings with arch one in gallery (Chaojing&Shudong, 1996)
- c. reinforcing of packs (Farmer, 1985)
- d. use of rib pillar in both sides of gallery (Yoginder&Chugh, 1982)

Feasibility studies showed that operation costs and time consumption regarding item c is more less than a, and b. Consequently reinforcing of the packs is selected to solve this problem. The results from application of this idea verified this method as successful.

4 CONTROL OF GALLERY DEFORMATION

To reinforce the packs, several points have considered:

- a. Existence of critical zone that is generally defined as 0.01-0.06 times depth, from the ribside. (Yoginder&Chugh, 1982)
- b. use of rib pillars with 0.1 x depth width (Yoginder&Chugh, 1982; Brady&Brown, 1992)
- c. Use of the packs with low compressibility (Farmer, 1985)
- d. In the case of the pack of low compressibility or use of rib pillar, the direction of deformation will be determined by the edge of the pack or pillar side and deformation of the actual roadway will be limited. (Farmer, 1985; Brady&Brown, 1992)
- e. A pack length several times the seam height would be required to give any useful support to the roadway. (Farmer, 1985)

At first rib pillars in both sides of gallery were designed with Wilson's (1978, 1981) analysis method. Data for C1 coal seam has been shown in Table 1 in which values of both *C* and ϕ parameters were obtained from Roclab software (2002).

Table 1. C1 Coal seam characteristics (Royanfar, 2006).

Coal seam	σ_c (MPa)	RMR (%)	<i>C</i> (MPa)	ϕ (Degree)
C1	16	40	0.322	36.32

Where:

σ_c : uniaxial compressive strength

- RMR : rock mass rating
- C* : cohesion coefficient
- ϕ : internal friction angle

As the width of pillar from Wilson's method was calculated as 13.4 m and also it will be 12 m according to 0.1 times depth rule. Also the critical zone in this level changes from 1.2 m to 7.2 m from the side wall of gallery which for more confidence, 0.08 times depth (9.6 m) was taken as critical zone length. In upside of gallery, rib pillar was not used because it prevents the transportation of conveyor in longwall face. Also large amount of coal must remain due to use of rib pillars.

Consequently a 10 meter wide pack system in both sides of gallery was proposed. Also a 2 meter wide rib pillar is used in downside of gallery, inside of above mentioned pack system. (Figure 3).

Average vertical stress ($\bar{\sigma}$) experienced by such pillar was calculated by Whittaker and Sing equation (1981).

$$\bar{\sigma} = \frac{9.81\gamma}{1000.P^2} \{[(P+W).D - \frac{1}{4}W^2 . \cot \Phi]P\}$$

for $W/D < 2 \tan \Phi$

Where:

- γ : average density of the overburden
- P* : width of rib pillar
- W* : width of longwall extraction
- D* : depth below surface
- Φ : angle of shear of roof strata at edge of longwall extraction and measured to vertical.

The values of above parameters are given in Table 2.

Table 2. Characteristics of rib pillar (Royanfar, 2006).

γ (MN/m ³)	<i>P</i> (m)	<i>W</i> (m)	<i>D</i> (m)	Φ (Deg)	$\bar{\sigma}$ (MPa)
0.0245	2	100	120	31	0.971

In this condition, coal pillar strength was calculated as 5.7 MPa using Mark and Chaz (1997) equation. Therefore, the pillar can resist against vertical stress.

$$\sigma_p = \sigma_1(0.64 + 0.54 \frac{P}{h} - 0.18 \frac{P^2}{hL})$$

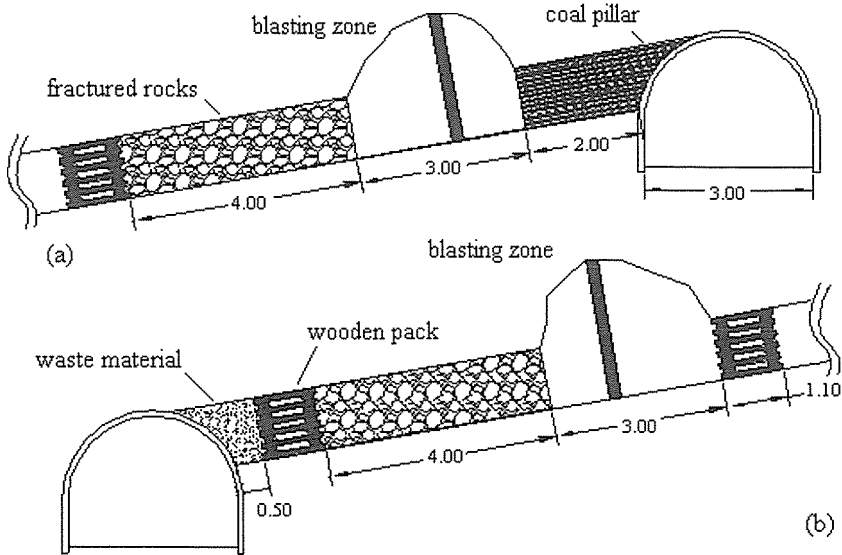


Figure 3. The System of packs around of gallery (a) downside of gallery, (b) upside of gallery

Where:

σ_p = coal pillar strength

σ_1 = strength of a cubical specimen of critical size or greater (e.g. about 1 m for coal)

$$\sigma_1 = \frac{\sigma_c \sqrt{d}}{\sqrt{36}}$$

σ_c = specimen uniaxial strength

d = specimen diameter (2.13 inch)

L and h , pillar length and height are 4 and 1.10 m respectively.

Consequently timber and rock packs have been used. The required rock supplied by blasting the roof in short distance of gallery. Holes 1.8 m long was used because the thickness of immediate roof measured 1.6 meter.

Before the use of this system, the maximum overall reduction of gallery height was 96 cm (i.e. 41.74% of overall height) and the maximum overall reduction of the gallery width was 1.05 meter (i.e. 35% of overall width). Study of the results, shows that the new system of packs is very suitable in reduction of intensity of deformations. Deformation measurements of the galleries after using of new idea showed that the

maximum overall reduction in height and width are 34 cm (i.e. 14.78% of overall height) and 63 cm (i.e. 21% of overall width), respectively.

It means the reduction of the height and width are reduced 64.58% and 40%, respectively.

5 CONCLUSIONS

The main findings of this study are as follows:

a. The major effective factor in heave and convergence in this mine were abutment pressures.

b. The use of packs with low compressibility, keeps away maximum abutment pressure and deformations from galleries.

c. Use of blasting in roof, causes reduction of load of immediate roof to gallery supports.

d. Application of proposed method provides the aim of extraction of maximum amount of coal from longwall faces.

e. Measurements of deformations in galleries showed that deformation in height and width reduced 64.58% and 40%, respectively.

REFERENCES

- Brady, B.H.G. and Brown, E.T., 1992, Rock Mechanics For Underground Mining , Chapman and Hall, pp.399-415.
- Chaojing, H. and Shudong, Z., 1996, Control of Gateroad Floor Heaves by a New Type of Ring Support, Mining Science and Technology, Balkema, Rotterdam, pp.147-158.
- Farmer, I., 1985, Coal Mine Structures, London, Chapman and Hall, New York, pp.192-215.
- IRITEC, 2002, Iran International Engineering Company, Tabas Coal Mine Project Basic Design, pp.56-69.
- Mark, C., Mucho, T.P. and Dolinar, D., 1998, Horizontal Stress and Longwall Head Gate Ground Control, SME annual meeting.
- Peng, S. and Chiang, H.S., 1984, Long wall Mining, Wiley and Sons, New York. pp.50-70.
- Royanfar, A., 2006, Study of Heave and Convergence and Their Control Methods in Tabas Coal Mine Entries (Parvade 5), Msc Thesis, Amirkabir University of Technology, Tehran, Iran, pp.90-130.
- Royanfar, A. and Shahriar, K., 2006, Strata Control Design in Galleries of Tabas Coal Mine (Parvade 5), 2nd International Conference on Geo-Resources in The Middle East and North Africa (Submitted)
- Stephen, C., 2004, The Effect of Standing Support Stiffness on Primary and Secondary Bolting Systems, National Institute for Occupational Safety and Health
- Unal, E., Ozkan, İ. and Cakmakci, G., 2001, Modeling the Behavior of Longwall Coal Mine Gate Roadways Subjected to Dynamic Loading, International Journal of Rock Mechanics & Mining Science, pp.181-197.
- Yoginder, P. and Chugh, 1982, State-Of-The-Art of Ground Control in Longwall Mining and Mining Subsidence, pp.79-82.

Utilisation of Bow Tie Analysis for Ground Control Risk Assessment

G.V. Kızıllı & J. Joy

Minerals Industry Safety and Health Centre (MISHC)

The Sustainable Minerals Institute (SMI), The University of Queensland, Brisbane, Australia

C. Strawson

Group Geotechnical Engineer, Anglo Coal Australia, Brisbane, Australia

ABSTRACT Rockfall related incidents account for a significant number of the fatalities and injuries in Australian underground mines. Proactive analysis of designs and operations to determine the causal factors of rockfall incidents is vital. One method that is becoming increasingly popular is the Bow Tie Analysis. A detailed introduction to the 'Bow-Tie' concept is given. The paper describes how such a concept could be utilised as a decision making tool for risk assessments at mine sites. An example of the use of the Bow Tie hazard analysis technique is included for illustration. For this purpose, a hypothetical rockburst scenario is developed, and a Bow Tie Diagram is built. The practical application of the bow tie approach is demonstrated. Two recently developed risk assessment techniques, Risk Spider and Open Risk are also overviewed.

1 INTRODUCTION

Mining is a hazardous occupation in terms of safety and health but the risks should be unacceptable. Mining hazards include ground control, equipment operation, changes in production methods blasting, etc.

During the past decade, the Australian mining industry has recorded 144 fatalities, an average of more than 14 deaths a year. Ground control issues constitute a significant risk within the mining industry. In 2002 - 03, of the 12 fatalities recorded in the industry, five were due to operation of mobile plant, four to rockfalls or strata failure (25%), and the balance to machine accidents (MCA 2003).

Mine health and safety is improving, however new technology may introduce new hazards. How will the mining industry meet the challenges of the 21st Century?

This paper focuses on a risk assessment method, demonstrated using a hypothetical ground control incident. Proactive analysis of relevant designs and operations is carried out to determine the causal factors of the

rockburst incident. Pre-event and post-event controls are also identified.

Ground control risk assessment would assist with:

- a. Identifying methods of measuring hazards magnitude,
- b. Describing how and why hazards get out of control, including inadequate monitoring, and poor inspections,
- c. Determining potential consequences such as people/equipment/production loss,
- d. Identifying potential risks such as roof fall/rib fall resulting from inadequate ground support, poor mining design and layout,
- e. Identifying technical details of risks such as pillar/roof deformation, strata weathering,
- f. Identifying the presence, likelihood and severity of the risks, and
- g. Establishing effective control measures to reduce the risks to acceptable levels.

Improvement at each stage leads to significant improvements in risk management, safety, and reduction in losses.

2 RISK ASSESSMENT TECHNIQUES

Risk assessment techniques range from simple qualitative approaches to detailed quantitative assessments. When a major incident is identified by using comparatively simple techniques, such as a Risk Matrix Method (qualitative), the unwanted event is then subject to detailed and comprehensive risk assessment (semi quantitative, quantitative risk assessment).

The two relatively recently developed techniques, which are also applicable to ground control risk assessment are briefly introduced. Both of these methods are based on global historical data collected over the last 15 years. The database represents a compilation of the Ground Control accidents / incidents occurring over this time period.

This study focuses on the Bow Tie Analysis method which is explained in more detail below following a brief overview of two other methods.

2.1 Risk Spider

The Risk Spider technique assists with underground ground control risk assessments. This semi quantitative risk assessment technique utilises a system where risks are grouped and assessed using a similar rating system to the matrix system. Each risk element is therefore allocated a distinct value, generally between '0' (Low potential, and/or probability) and '10' (high potential and/or probability). The results are then plotted on the spokes of a wheel, where '0' is the centre, and '10' the outer perimeter. High potential/likelihood events are then easy to identify. The objective of using the risk spider is to identify the high potential risks, and to reduce them to below a value of '5' by using risk reduction measures.

The Risk Spider is currently being evaluated in the field for the purpose of Ground Control risk assessment. Applications of this method are not only

limited to Ground Control, but are applicable to other areas.

2.2 Open Risk

The semi quantitative Open Risk method is designed to carry out open pit geotechnical (or strata control) risk assessment. It is a computer based assessment tool that allows a number of pre formatted questions to be asked of the person/s undertaking the risk assessment. These questions are structured to ensure that all open pit geotechnical risk elements are identified.

The answers are rated on a scale of '0' to '10', and the various possible events are weighted to provide a computer output, which identifies the high risk activities. The Open Risk allows the user to add risk reduction techniques thereby reducing the rating of a particular event. This is a valuable tool, as relatively unskilled operators are able to undertake a risk assessment ensuring that all risk elements are identified. From this perspective, development of the 'Open Risk' was particularly onerous.

The Open Risk method is currently being evaluated in Australia. This is a standard operational tool in South African open cut mines. This methodology is applicable in all areas where risk assessments are conducted.

2.3 Bow Tie Analysis

The enormous role played by ground support and the potential negative consequences of rock falls have driven a need to develop ways to improve the prediction and prevention of rockfalls. The initiatives have the potential to save numerous lives as well as millions of dollars (Dal Santo 2002). Complete and in depth assessments and evaluations of the causes, and preventative and mitigative control measures are important. This would assist with identifying "critical controls" and the allocation of often limited resources to these critical areas.

One risk assessment method that is becoming increasingly popular is the Bow Tie Analysis. The Bow Tie concept (Mark M

2005) is not particularly new, however its use has become popular in a number of industries (particularly onshore major hazard industries) in recent years. The US Federal Aviation Authority (FAA) requires employing the 'Bow Tie Diagram' as the main mechanism for "safety analyses" (FAST 2004). Other organisations responsible for safety in air traffic control recommend using this technique (EuroControl 2004). The Bow Tie Analysis model (semi-quantitative) is also a common method applied for Major Hazard Facilities Safety Assessments (Worksafe 2006). The Major Hazard Facilities Regulations - Guidance Note GN 14 – Safety Assessment provides description of the Bow Tie analysis model as "... provides a method of assessing, and communicating hazards and the relevant linkages to control measures. It provides for focused monitoring and auditing of controls. The model describes the hazards and causes that may lead to an event and describes the potential outcomes. An event is where "loss of control" may occur that may result in a significant impact". The Guidance Note further states that "The bow tie model allows a range of prevention layers to be examined, which may eliminate or minimise the likelihood of specific causes that may lead to an event. It also highlights mitigation layers that may reduce the consequence of an event, after a loss of control has occurred" (Worksafe 2006).

A presentation of the Bow Tie Analysis model for an unwanted event is given in Figure 1.

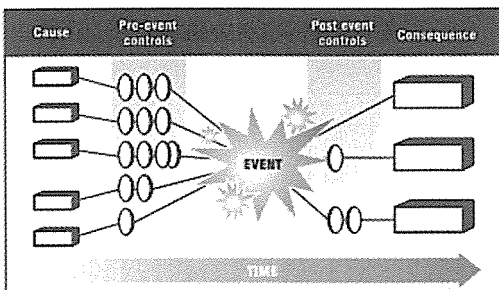


Figure 1. The bow tie analysis diagram (Lawson, 2003).

Bow Tie Analysis diagrams provide a graphical representation of the dynamics of each risk scenario.

The 'unwanted event' is shown in the centre of the Bow Tie Analysis. The left side of the diagram describes the causes and hazards. The controls or barriers to the event occurring are also shown. These are Proactive controls. The right hand side of the diagram describes various consequences that can occur. The controls or barriers that are in place after an event has occurred are also shown. These are Reactive Controls, classified as Reduction or Mitigation. The preference is for proactive control, however reactive control is essential to minimise harm after an event (Joy et al., 2004).

3 HYPOTHETICAL ROCKBURST SCENARIO

For the purpose of illustrating the Bow Tie Analysis, a hypothetical rockburst scenario is developed. Based on this scenario, the background is explained as follows:

Background

A small underground nickel mine was successfully operated in the early 1990's, utilising the narrow vein mining method. Falling commodity prices, and increasing input costs forced it to be placed under care and maintenance in 1996. In 2000, increases in metal prices resulted in the mine re opening, and development in an area previously deemed uneconomic. Miners were sent back into this area to extend old development and recommence mining.

A normal re-entry procedure was followed which included visual inspections of the area to be mined, re-ventilating, gas testing to determine gas accumulations, and pumping out of excess water. The area appeared stable during an assessment. There was no visible fretting or slabbing of the roof or sides. Secondary support was not considered necessary.

Available historical data included old workings survey plans which assisted with evaluation of possible flooded and gaseous areas.

What happened?

As a part of the resumption of mining operations, a charging crew was required to load blast holes at the brow of an uphole bench. A seismic event, likely to be associated with the recommencement of stopping and increase in stresses stored in a local fault zone occurred. This resulted in a fall of ground in the ore drive in which the charging crew was operating.

The charging crew was loading blast holes at the brow of an uphole bench. Two of the mine workers were in the basket of the machine, and another was operating the machine.

Impacts of the Event

The rockfall (approx. 50 t) landed on the basket of the charging machine. One of the men in the basket died instantly. The operator was not injured, but was unable to access the area where the rock fell. The operator alerted the surface controller and the surface controller immediately dispatched rescue teams.

Why it Happened?

Although a normal re-entry procedure was followed, no geotechnical assessment was carried out prior to re-entry. The existing ground support was not monitored as there appeared to be no visible fretting or slabbing of the roof or sides. As a result of this assessment, secondary support was not considered necessary. Saline water in the roof strata may have caused corrosion of the bolts, reducing their effective strength. When the seismic event occurred, the bolts are likely to have failed at reduced loads.. Further, due to budget cuts no additional exploratory drilling was undertaken. The existing exploratory drilling had been done on a 100m spacing, which though was sufficient to identify the orebody, was insufficient to delineate a fault structure. There was limited information available on the overall stability of the area to be mined. Data relating to 'as mined' layouts and previous geotechnical investigations was not available.

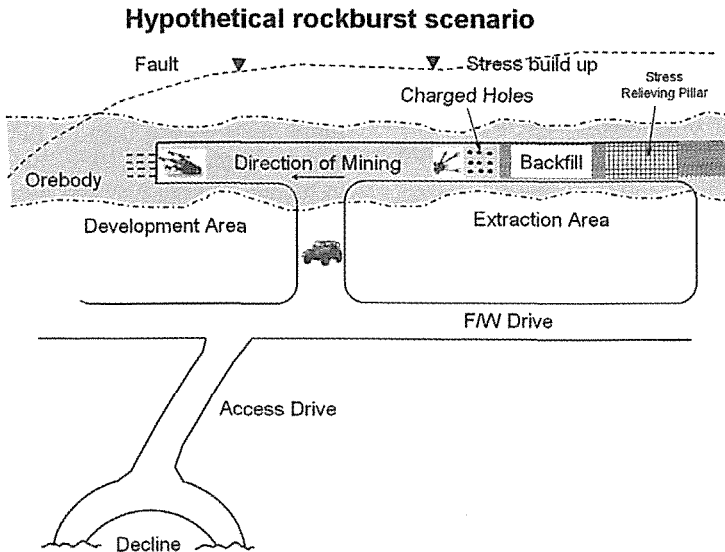


Figure 2. Hypothetical rockburst scenario is presented.

Ground Control Risk Management BOW TIE PRINCIPLE

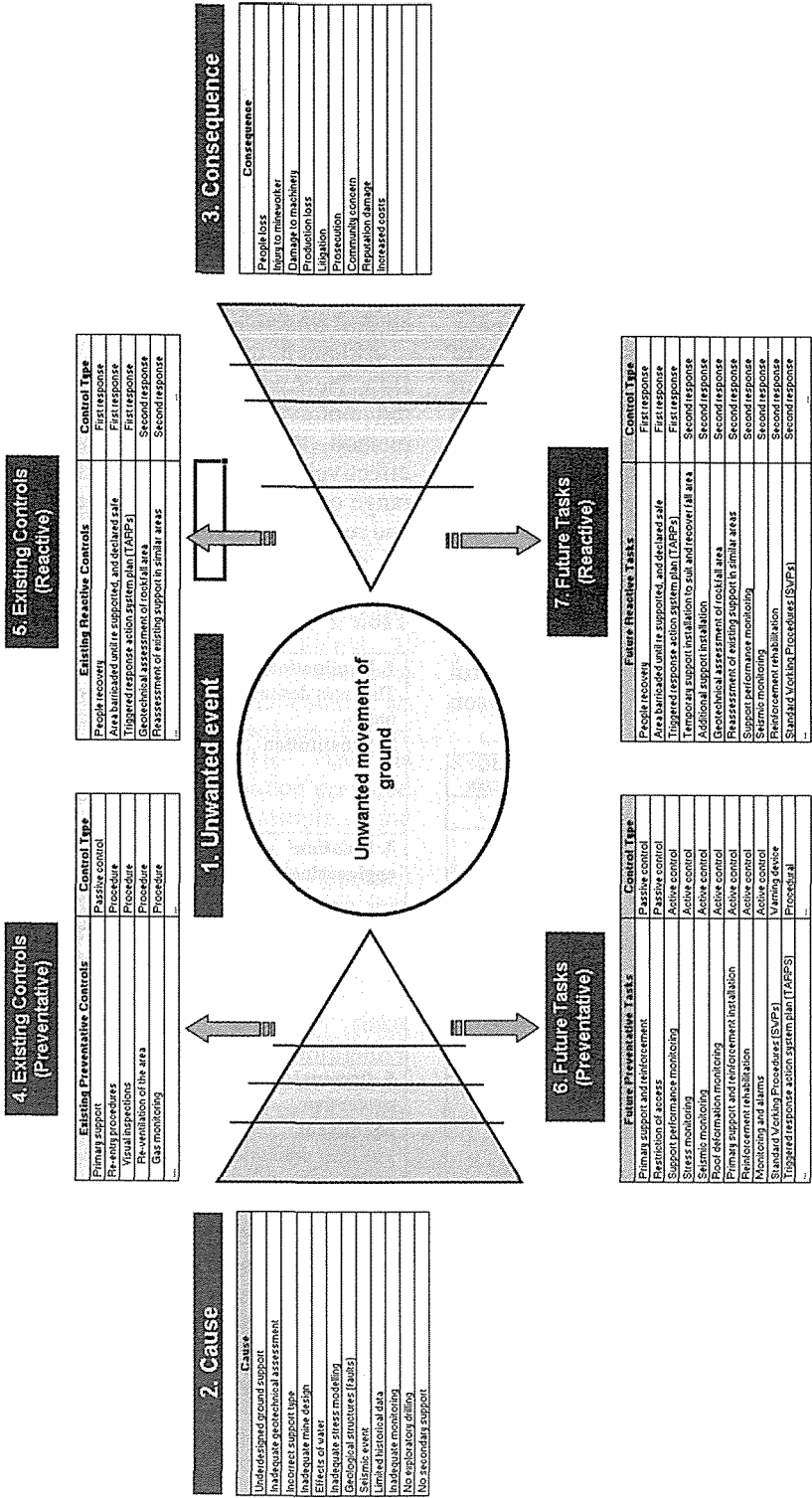


Figure 3. Bow tie analysis diagram illustrating the graphical representation of the rockburst scenario.

The initiating ground control event, rockburst, is shown in the centre (1) of the Bow Tie Analysis diagram. The causes (2) and consequences (3) of the event are identified, and included in the Diagram. It should be noted that the illustration, in the figure above, is incomplete. The lists are compiled for demonstration only.

For each identified cause, based on the hypothetical scenario, controls are identified. The control measures used to control risks are chosen based on their effectiveness. Controls should fit within the hierarchy of controls. The order of the hierarchy of controls indicate that control measures which are higher in the hierarchy provides improved levels of risk control. In practice, a number of control options are usually used in combination.

The Major Accident Control Analysis, MACA tool (Lawson 2003) is useful to

Table 1. MACA (Major Accident Control Analysis) control type classification (Lawson 2003).

MACA Control Type Classification (Lawson 2003)		Hierarchy of Controls
Control type	Description	
Design Change	Engineering type controls that potentially eliminate the hazard.	Elimination Substitution
Passive Control	Controls that are in place that do not require human intervention.	Isolation Engineering
Active Control	Controls that are in place that require humans to activate them.	Engineering
Warning Device	Alarms or monitoring that indicate a hazardous situation.	Engineering
Procedure	Documented SOPs that control the hazardous situation.	Administrative (PPE)

conduct a more detailed assessment of the effectiveness of controls in place for identified risks.

In this approach, MACA Control Type Classification (Lawson 2003,) as shown in Table 1, is adopted to classify and value prevent controls (proactive). The MACA control type classification is based on Hierarchy of Controls as demonstrated in Table 2. Reactive controls are also valued to give an overall image of pre and post event control effectiveness.

Although the process of developing the Bow Tie Analysis for this particular scenario did not value controls like the MACA method, the more basic Bow Tie Analysis effectively allowed us to identify the full range of causes, consequences and, proactive and reactive controls.

Table 2. Hierarchy of controls.

1. Elimination The most desirable option	If you eliminate a hazard you completely eliminate the associated risk.
2. Substitution	You can substitute something else (a substance or a process) that has less potential to cause injury.
3. Isolation/ engineering	You can make a structural change to the work environment or work process to interrupt the path between the worker and the risk.
4. Administrative	You may be able to reduce risk by upgrading training, changing rosters or other administrative actions.
5. Personal protective equipment The least desirable option	When you can't reduce the risk of injury in any other way, use personal protective equipment (gloves, goggles, etc.) as a last resort.

The Bow Tie Analysis is applicable to common mining issues to identify a range of good practice controls. The Bow Tie Analysis method can also be included in strategic planning. Advantages of using the Bow Tie Analysis approach are identified as:

- Provision of a clear and concise collation of the possible potential hazards

- Detailing of the causes of each of the potential hazards,
- Determining the consequences of the unwanted event/s,
- Formulating effective controls for the possible causes, for each scenario, and identifying critical controls,
- Communicating the controls currently in place,
- Demonstrating how improvements would reduce risk and increase safety, and
- Presentation, using the Bow Tie Analysis method allows for easy visual interpretation of the entire risk scenario.

4 CONCLUSIONS

This paper attempted to present some of the risk assessment techniques that are applicable to ground control issues, explaining some of the key points of different approaches. This paper developed a hypothetical scenario to demonstrate an example of a practical application of the selected method, Bow Tie Analysis approach. The analysis information provided in this paper only represent a sample of the results identified.

The use of a Bow Tie Analysis approach allows segregation of risk assessment into smaller, discrete, and independent components. The simplicity of the Bow Tie Analysis method is its capability to identify the complexities of mining risks, consequences and possible mitigative measures. The relationship between causes, the unwanted event, consequences and their controls is clearly documented and easier to communicate in a meeting room. The ability to visualise the interaction of the various elements allows it to be used by all in an operational environment. The simple, pictorial approach greatly aids decision makers without necessitating extensive training in its use, and interpretation.

It is important to note that there is no single procedure for evaluating risk that is appropriate for all stages of mine operations. Different types of analysis or combination of

methods are often required at different stages of a mine life. This study is intended as general guidance only. Detailed guidance will require consideration to be given to the objective of the risk assessment, the detail required as a result of the risk assessment, and site specific conditions.

REFERENCES

- Dal Santo L 2002, *Decision Making to Manage Risks in Ground Control*, New South Wales Health and Safety Conference, Terrigal Australia.
- EUROCONTROL 2004, *Review of Techniques To Support The EATMAP Safety Assessment Methodology Volume 4*, European Organization for the Safety of Air Navigation.
- FAST 2004, *Toolsets / System Safety Management Program- Section 4*, Federal Aviation Authority Acquisition System Toolset.
- Joy J & Griffiths D 2004, *National Minerals Industry Safety and Health Risk Assessment Guideline (NMISHRAG)*, Viewed April 2007, <http://nmishrag.mishc.uq.edu.au/NMISHRAG_Content.asp>.
- Kizil G, Joy J & Strawson C 2006, *Improving Ground Control Risk Management Strategies*, Queensland Mining Industry Health and Safety Conference, 6 - 9 Aug 06, Townsville.
- Kizil G, Joy J & Strawson C 2006, *Improving Ground Control Risk Management Practices*, Queensland Minerals Industry Safety and Health Conference, Townsville.
- Lawson S 2003, *Formal safety assessment methodology utilizing control effectiveness evaluation*, Newmount Australia.
- Mark M 2005, *Bow tie analysis*, Riskline News, Autumn 2005.
- Minerals Council of Australia (MCA) 2003, *Australian Minerals Industry Safety and Health, Safety Survey Report for 1 July 2002 – 30 June 2003*.
- Worksafe 2006, *Major Hazard Facilities Regulations - Guidance Note GN 14 – Safety Assessment*, Viewed March 2007, <<http://www.worksafe.vic.gov.au/wps/wcm/resources/file/ebd5bc450dccb9/GN14.pdf>>.

Mineral Processing

Investigation of Breakage Properties of Chromites at Kayseri Region

V. Deniz, E. Tank, E. Boz & Y. Umucu

Department of Mining Engineering, Suleyman Demirel University, Isparta, Turkey

ABSTRACT In this study, the breakage properties of nine different chromite minerals, originated from the Kayseri region (Turkey), are investigated at batch grinding conditions based on a kinetic model. For this purpose, firstly, samples taken from nine different mines have examined mineralogical by using thin and polish sections then these sections have been investigated texture of chromite mineral and gangue mineral. Secondly, Standard Bond's grindability tests were made for nine samples. Thirdly, experiments were carried out with five different mono-size between 2.8 mm and 0.075 mm formed by a 2 sieve series fraction. Then, parameters of S_i and B_{ij} equations were determined from the size distributions at different grinding times, and the model parameters were compared for nine different chromite samples, and the relationship between the Bond's grindability (G_{bg}) and chromite grade with breakage parameters (S_b , a_T , γ and ϕ_j) were examined. The validity of the obtained relationship parameters of a_T and ϕ_j has been confirmed with correlation, through a regression analysis of samples of chromite.

1 INTRODUCTION

Determination of degrees of liberation, comminution process and mineralogical properties before concentration of the ore are most important for mineral processing.

Chrome, one of the most important from metals using of modern world, is important in especially stainless steel production. From saleability chromite ore want to obtain over 42–44 % Cr_2O_3 of grades (Deniz, 1992). Chromite is being produced in various regions of Turkey where the majority of chromite ores treated are disseminated in structure, mainly in Kayseri region. Kayseri chromite is produced mostly by Dedaman Co. In Kayseri region (Turkey), chromite deposits have different chemical and mineralogical properties.

Comminution is know to be a large consumer of the energy, which consumes 3–4% of the electricity generated world-wide

and comprises up to 70% of all energy required in a typical mineral processing plant, and is one of the most important unit operations in mineral processing. The grinding process has many variables, some of which are difficult to understand (Deniz, 2004; Deniz, 2005).

Bond's grindability can be empirically related to the energy required for comminution and thus is useful for the design and selection of crushing and grinding equipment (Deniz et al., 1996).

In the recent years, matrix model and kinetic model, which are suggested by investigators, have been used in the laboratory and in the industrial areas. Kinetic model which an alternative approach is considered comminution as a continuous process in which the rate of breakage of particles size is proportional to the mass present in that size (Deniz and Onur, 2002).

The analyses of size reduction in tumbling ball mills, using the concepts of specific rate of breakage and primary daughter fragment distributions, have received considerable attention in years. Austin has reviewed the advantages of this approach and the scale-up of laboratory data to full-scale mills has also been discussed in a number of papers (Austin et al., 1984).

This paper presents a comparison of the breakage parameters of nine different chromite minerals under standard conditions in a batch laboratory ball mill, and relationships between Bond's grindability values with breakage parameter values of samples for different mineralogical properties chromite are investigated.

2 THEORY

When breakage is occurring in an efficient manner, the breakage of a given size fraction of material usually follows a first-order law (Austin, 1972). Thus, the breakage rate of material that is in the top size interval can be expressed as:

$$\frac{-dw_1}{dt} = S_1 w_1(t) \tag{1}$$

Assuming that S_1 does not change with time (that is, a first-order breakage process), this equation integrates to

$$\log(w_1(t)) - \log(w_1(0)) = \frac{-S_1 t}{2.3} \tag{2}$$

where, $w_1(t)$ is the weight fraction of the mill hold-up that is of size 1 at time t and S_1 is the specific rate of breakage. The formula proposed by Austin et al. (1984) for the variation of the specific rate of breakage S_i with particle size is

$$S_i = a_T X_i^\alpha \tag{3}$$

where, X_i is the upper limits of the size interval indexed by i , mm, and a_T and α are model parameters that depend on the properties of the material and the grinding conditions.

On breakage, particles of given size produce a set of primary daughter fragments, which are mixed into the bulk of the powder

and then, in turn, have a probability of being re-fractured. The set of primary daughter fragments from breakage of size j can be represented by $b_{i,j}$, where $b_{i,j}$ is the fraction of size j material, which appears in size i on primary fracture, $n \geq i > j$. It is convenient to represent these values in cumulative form.

$$B_{i,j} = \sum_{k=n}^i b_{k,j} \tag{4}$$

where, $B_{i,j}$ is the sum fraction of material less than the upper size of size interval i resulting from primary breakage of size j material: $b_{i,j} = B_{i,j} - B_{i+1,j}$. Austin et al. (1981) have shown that the values of $B_{i,j}$ can be estimated from a size analysis of the product from short time grinding of a starting mill charge predominantly in size j (the one-size fraction BII method). The equation used is,

$$B_{i,j} = \frac{\log[(1-P_i(0))/\log(1-P_i(t))]}{\log[(1-P_{j+1}(0))/\log(1-P_{j+1}(t))]} \quad n \geq i \geq j+1 \tag{5}$$

where, $P_i(t)$ is the fraction by weight in the mill charge less than size X_i at time t . $B_{i,j}$ can be fitted to an empirical function (Austin and Luckie, 1972).

$$B_{i,j} = \phi_j [X_{i-1}/X_j]^\delta + (1-\phi_j) [X_{i-1}/X_j]^\beta \quad n \geq i \geq j \tag{6}$$

where

$$\phi_j = \phi_1 [X_1 / X_1]^{-\delta} \tag{7}$$

where, δ , ϕ , γ , and β are model parameters that depend on the properties of the material. It is found that, B functions are the same for different ball filling ratios, mill diameters, etc. (Austin et al., 1984). If $B_{i,j}$ values are independent of the initial size, i.e. dimensionally normalizable, then δ is zero.

3 MATERIALS AND METHOD

3.1 Materials

Nine different chromite samples taken from deposits belongs to Dedaman Co. were used as the experimental materials. The grade of the chromite samples are presented in Table 1.

Table 1. Cr₂O₃% grades of chromite samples used in experiments.

Samples	Cr ₂ O ₃ , %	Spec. Gravity
AC1	8.55	1.85
A2	3.79	1.70
B4	37.50	2.49
B5	40.81	2.53
T2	34.36	2.39
A3	4.06	1.73
B1	36.16	2.42
B2	19.41	1.93
B3	41.23	2.57

3.2 Mineralogical Analysis

Lump samples which are taken from nine different mines were made thin and polish sections and then these sections have been investigated texture of chromite mineral and gangue mineral.

3.2.1 Mineralogical Properties of AC1

This sample is full formed from serpentine and chromite minerals. Chromite crystals are seen as subhedrall, unhedrall crystals and different particle size. Wall-rock is fully serpentinized ultrabasic rock. Addition, This sample are seen fine band opaque minerals to think over magnetite mineral. The ore contains approximately 10%-15% of chromite, and about 80%-90% of serpentine.

3.2.2 Mineralogical Properties of A2

Wall-rock is dunite. Local remnants of olivine crystals may be seen. Chromite crystals generally are broken due to tectonic effects to get catalastic texture. For this reason, the chromite crystals are seen as broken-off grains and subhedrall, unhedrall crystals. The ore contains approximately 70%-80% of serpentine, 10%-15%, of olivine and about 5%-10% of chromite.

3.2.3 Mineralogical Properties of B4

Rock is from serpentine and chromite minerals. Chromite grains are seen as

catalastic texture and mostly unhedrall crystals form.

3.2.4 Mineralogical Properties of B5

Wall-rock consists dominantly of serpentinized dunite. Chromite crystals generally are broken due to tectonic effects to get catalastic texture. The ore contains approximately 30%-40% of chromite.

3.2.5 Mineralogical Properties of T2

Rock consists serpentine and chromite minerals. Olivine minerals are fully serpentinized. Chromite grains are seen as catalastic texture and mostly unhedrall crystals form. The ore contains approximately 50%-60% of chromite and backward serpentine minerals.

3.2.6 Mineralogical Properties of A3

Rock is from serpentine, pyroxene and chromite minerals. The ore contains approximately 70%, nearly 20 % chromite mineral and backward pyroxene minerals.

3.2.7 Mineralogical Properties of B1

Wall-rock is dunite. This sample is formed from serpentine, olivine and chromite minerals. The ore contains approximately 35%- 40% of chromite. Chromite crystals generally are broken due to tectonic effects to get catalastic texture. For this reason, the chromite crystals are seen as broken-off coarse grains.

3.2.8 Mineralogical Properties of B2

Rock consists more olivine than serpentine and chromite. The ore contains approximately 35%-40% of olivine. Chromite crystals generally are form subhedrall, unhedrall crystals.

3.2.9 Mineralogical Properties of B3

Rock consists olivine, serpentine and chromite. The ore contains approximately 10%-15% of olivine. Quite amounts of serpentine occurrences are seen along the

fractures of olivine. Intercrystalline porosity of the subhedrall chromite crystals is filled with unhedrall and frequently fractured olivine crystals. Chromite grains are seen as cataclastic texture and mostly unhedrall crystals form.

3.3 The test of standard ball mill Bond grindability

The standard Bond grindability test is a closed-cycle dry grinding and screening process, which is carried out until steady state condition is obtained. This test was described as follow (Bond and Maxson, 1943; Yap et al., 1982; Austin and Brame, 1983; Magdalinovic, 1989):

The material is packed to 700 cc volume using a vibrating table. This is the volumetric weight of the material to be used for grinding tests. For the first grinding cycle, the mill is started with an arbitrarily chosen number of mill revolutions. At the end of each grinding cycle, the entire product is discharged from the mill and is screened on a test sieve (P_i). Standard choice for P_i is 106 micron. The oversize fraction is returned to the mill for the second run together with fresh feed to make up the original weight corresponding to 700 cc. The weight of product per unit of mill revolution, called the ore grindability of

the cycle, is then calculated and is used to estimate the number of revolutions required for the second run to be equivalent to a circulating load of 250%. The process is continued until a constant value of the grindability is achieved, which is the equilibrium condition. This equilibrium condition may be reached in 6 to 12 grinding cycles. After reaching equilibrium, the grindabilities for the last three cycles are averaged. The average value is taken as the standard Bond grindability.

4 EXPERIMENTS

Firstly, Standard Bond's grindability tests were made for nine chromite samples. Result of tests, Bond grindability values of chromite samples are shown in Table 3. Then, the standard sets of grinding conditions used are shown in Table 2, for a laboratory mill of 6283 cm³ volume. Five mono-size fractions (-2.36+1.18, -1.18+0.600, -0.600+0.300, -0.300+ 0.150, -0.150+0.075 mm) were prepared and ground batch wise in a laboratory-scale ball mill for determination of the specific rate of breakage. Each sample was taken out of the mill and dry sieved product size analysis.

Table 2. The standard set of grinding conditions.

Mill	Diameter	200 mm									
	Length	200 mm									
	Volume	6283 cm ³									
Mill Speed	Critical	101 rpm									
	Operational ($\phi_c = 75\%$)	76 rpm									
Balls	Diameter (mm)	25.4 mm									
	Specific gravity	7.8									
	Quality	Alloy Steel									
	Assumed porosity	40 %									
	Ball filling volume fraction ($J\%$)	20 % ($J = 0.2$)									
Material	Powder gravity, g/cm ³	AC1	A2	A3	B1	B2	B3	B4	B5	T2	
		1.85	1.70	1.73	2.42	1.93	2.57	2.49	2.53	2.39	
	Interstitial filling ($U\%$)	50 % ($U = 0.5$)									
	Powder filling volume ($f_c\%$)	4 % ($f_c = 0.04$)									

4.1 Determination of the specific rate of breakage

The first-order plots for various feed sizes of chromite samples are illustrated in Figures 1-9. The results indicated that grinding of all size fractions, nine samples could be described by the first-order law. In additional, parameters of specific rate of breakage to supply by first-order plots are present in Table 3. The specific rates of breakage of each mono-size fraction that exhibited first-order grinding kinetic behaviour were determined from the slope of straight-line of first-order plots. Additional, Figure 10 and Figure 11 are shown as two groups of S_i values for grinding of the nine different chromite samples, as a function of size.

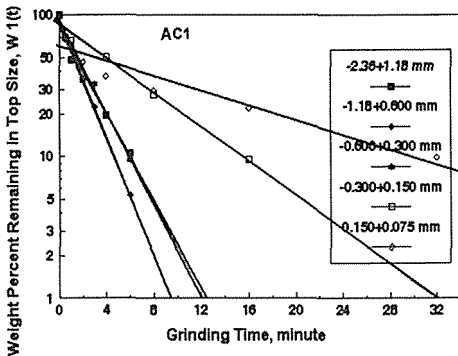


Figure 1. First-order plots for AC1.

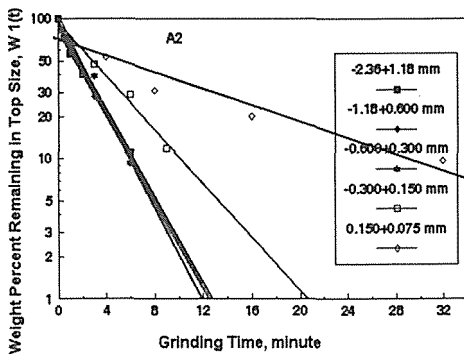


Figure 2. First-order plots for A2.

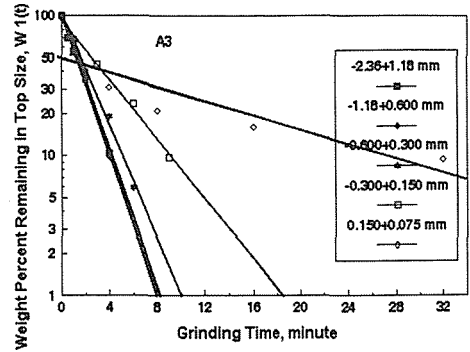


Figure 3. First-order plots for A3.

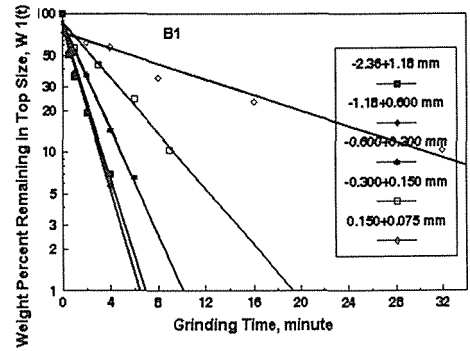


Figure 4. First-order plots for B1.

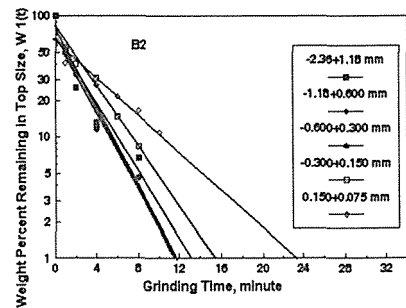


Figure 5. First-order plots for B2.

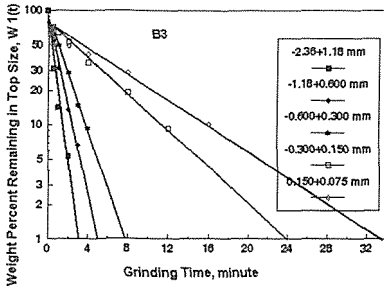


Figure 6. First-order plots for B3.

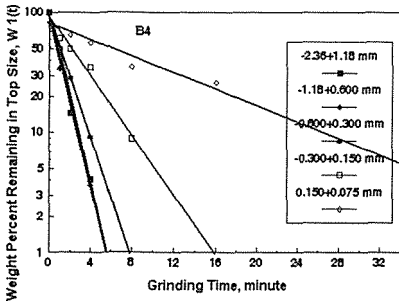


Figure 7. First-order plots for B4.

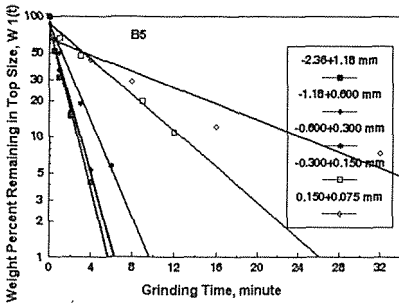


Figure 8. First-order plots for B5.

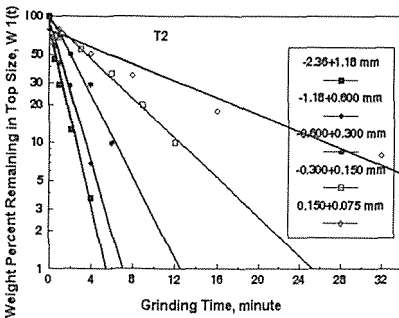


Figure 9. First-order plots for T2.

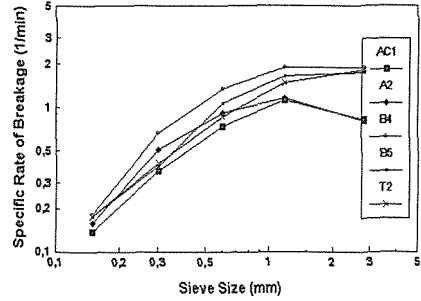


Figure 10. Variation of specific rates of breakage with particle size for Group-I chromite samples.

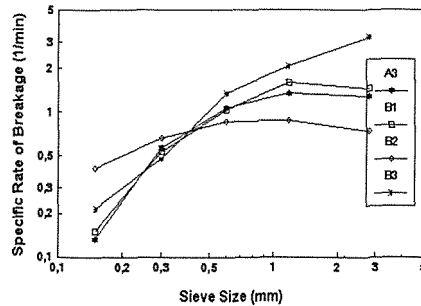


Figure 11. Variation of specific rates of breakage with particle size for Group-II chromite samples.

4.2 Determination of B function

By definition, the values of B were determined from the size distributions at short grinding times. The parameters were determined according to the BII method (Austin et al, 1984), and show the graphical representation on Figures 12-13, as two groups. Chromite samples show a typical normalized behaviour, and the progeny distribution does not depend on the particle size, and it followed that the parameter δ was zero. Model parameters supply by cumulative distribution and these parameters are presented in Table 3.

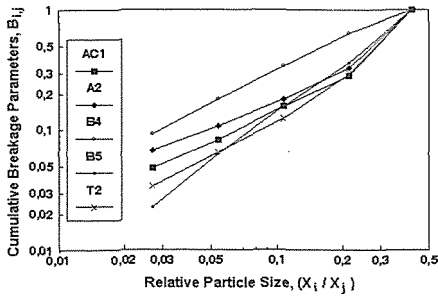


Figure 12. Cumulative breakage distribution functions for Group-I chromite samples.

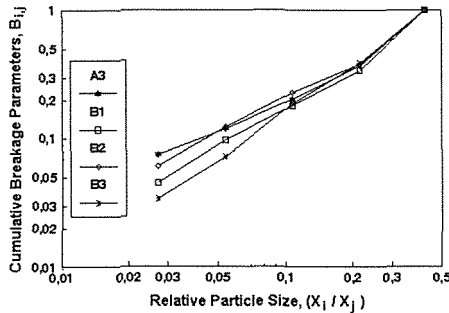


Figure 13. Cumulative breakage distribution functions for Group-II chromite samples.

Table 3. Bond's grindability values and characteristic breakage parameters for chromite samples.

Material	G_{bg} g/rev	a_T	α	γ	ϕ_i
AC1	1.17	1.01	1.208	0.865	0.48
A2	0.71	0.85	1.262	0.703	0.47
A3	1.25	1.29	1.502	0.719	0.51
B1	2.39	1.51	1.386	1.011	0.77
B2	1.39	0.84	0.538	0.961	0.82
B3	1.54	1.85	1.322	1.238	0.71
B4	2.34	1.80	1.442	0.947	1.24
B5	1.74	1.52	1.293	1.404	1.05
T2	1.27	1.30	1.141	0.940	0.49

5 VALIDATION OF THE RELATIONSHIPS BETWEEN BOND'S GRINDABILITY AND CHROMITE GRADE WITH BREAKAGE PARAMETERS

5.1 Variation of cumulative breakage parameter (ϕ_i) and first-order breakage constant (a_T) with Bond's grindability values (G_{bg})

For the same purposes, variation of cumulative breakage parameter (ϕ_i) and first-order breakage constant (a_T) with Bond's grindability (G_{bg}) for Group-I chromite samples was investigated, and is shown in Figure 14. The values of ϕ_i and a_T seem to satisfy a linear relationship with G_{bg} with a correlation coefficient, respectively 0.86 and 0.96 that can be expressed as follows:

$$a_T = 0.603 * G_{bg} + 0.422 \quad (8)$$

$$\phi_i = 0.556 G_{bg} - 0.06 \quad (9)$$

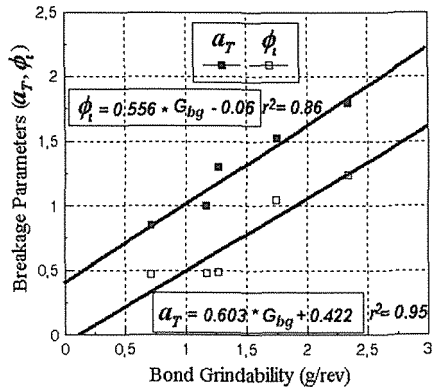


Figure 14. Variation of a_T and ϕ_i with G_{bg} .

5.2 Variation of first-order breakage constant (a_T) with chromite grade (Cr_2O_3 , %)

The values reported in Table 3 have been plotted in Figure 15 referring to relation for different Cr_2O_3 . The values of a_T seem to satisfy a linear with $Cr_2O_3\%$ with a correlation coefficient 0.94 that can be expressed as follows:

$$Cr_2O_3, \% = 23.54 * a_T - 46.58 \quad (10)$$

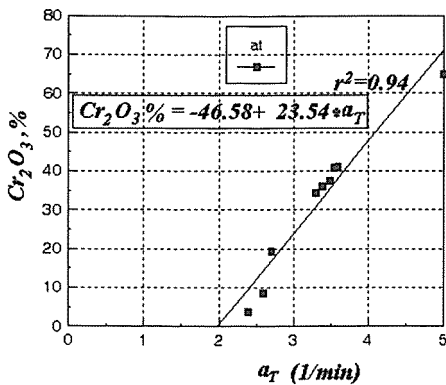


Figure 15. Variation of a_T with Cr_2O_3 %

6 CONCLUSIONS

In result of investigation of thin and polish section; Group-I samples (AC1, A2, B4, B5 and T1) are come into view same mineralogical properties. These samples contain chromite and serpentine minerals. However, Group-II samples (A3, B1, B2, and B3) have been appeared same characteristic. The ore contains approximately 45%- 50% of olivine and about 35% - 45% of chromite.

In grinding tests, samples of these groups have been different grinding properties. Therefore, grinding process knows to most important in respect to energy cost.

The dry grinding of size intervals of chromite samples showed that these samples followed the first-order breakage law with constant normalized primary breakage distribution function.

The values of the primary daughter fragment distributions and the values of α in $S_i = a_T X^\alpha$ are different in the samples of chromite minerals. As the amount of S_i or a_T values increase, the effective breakage increases, and breaks as very fast in the undersize of original particle size. The experimental values show that grinding is not faster for samples as value of Bond grindability values (G_{bg}) increase. Reason of this state, chromite samples have different mineralogical properties.

The γ value, which is the fineness factor, is higher for B5 than the other samples of

chromite, indicating that fewer fines are produced in chromite grinding. Another, the Bond's grindability value (G_{bg}) for B5, which has a high grindability, is higher than the other samples of chromite. Reason of this state, B5 has a larger grain chromite crystal.

The ϕ_j value is higher for B4 than other samples, indicated that breakage of the top size showed acceleration, and deceleration for A2. Similarity, the Bond's grindability value for B4, which has a high grindability, is higher than the other samples.

As a result of these comparisons for a_T and ϕ_j breakage parameters, a high correlation coefficient is obtained. These variations may be used to provide an estimate of Bond's grindability and Cr_2O_3 % for Kayseri region.

REFERENCES

Austin, L.G.,1972. A review introduction to the description of grinding as a rate process. *Powder Technology*. Vol.5: 1-7.

Austin, L.G. and Luckie, P.T., 1972. Methods for determination of breakage distribution parameters. *Powder Technology*. Vol. 5: 215-222.

Austin, L.G. and Bagga, R., Çelik, M., 1981. Breakage properties of some materials in a laboratory ball mill. *Powder Technology*. Vol. 28: 235-241.

Austin, L.G. and Brame, K., 1983. A comparison of the Bond method for sizing wet tumbling mills with a size-mass balance simulation method. *Powder Technology*. Vol. 34: 261-274.

Austin, L.G., Klimpel, R.R. and Luckie, P.T., 1984. *Process Engineering of Size Reduction: Ball Milling*. SME-AIME. NewYork. USA.

Bond, F.C. and Maxson, W.L., 1943. Standard grindability tests and calculations. *Trans. SME-AIME*, Vol. 153. 362-372.

Deniz, V, 1992. Beneficiation of Chromite Ores in Burdur Yeşilova Region, MSc. Thesis, (Supervisor; Prof.Dr. Hüseyin ÖZDAĞ) *Anadolu University*, Eskişehir, Turkey, 101 p.

Deniz, V., Balta, G. and Yamık, A., 1996. The interrelationships between Bond grindability of coals and impact strength index (ISI), point load index (Is) and Friability index (FD). *Changing Scopes in Mineral Processing*. Kemal et al. (Editors). *A.A. Balkema*, Rotterdam, Netherlands: 15-19.

- Deniz, V. and Onur, T., 2002. Investigation of the breakage kinetic of pumice samples as dependent on powder filling in a ball mill. *Int. Journal of Mineral Processing*. Vol. 67: 71-78.
- Deniz, V., 2004. Relationships between Bond's grindability (G_{b2}) and breakage parameters of grinding kinetic on limestone. *Powder Technology*. Vol. 139: 208-213.
- Deniz, V., 2005. Breakage properties of porous materials by ball milling, *The 19th International Mining Congress of Turkey, IMCET2005, İzmir, Turkey, 207-211*.
- Magdalinovic, N., 1989. A procedure for rapid determination of the Bond work index. *Int. Journal of Mineral Processing*, Vol. 27. 125-132.
- Yap, R.F., Sepulude, J.L. and Jauregui, R., 1982. Determination of the Bond work index using an ordinary laboratory batch ball mill. *Design and Installation of Comminution Circuits*. A.L. Mular (Co-Editor). Soc. Min. Eng. *AIME*, USA: 176 - 203.

New Developments of the Separation Equipments for Aggregate Beneficiation

E. Garbarino

Politecnico di Torino, Land, Environment and Geo-Engineering Department, Torino, Italy

M. Cardu & R. Mancini

*Politecnico di Torino, Land, Environment and Geo-Engineering Department, Torino, Italy
CNR-IGAG, Torino, Italy*

ABSTRACT The paper deals with aggregate processing, in order to improve their performances, and takes into consideration the crushing methods, as a means to improve the shape features of the aggregate, and the wet separation process (jigging or water flowing film), as a means to remove unwanted materials. Low grade sources, both natural and artificial (rock excavation muck pile, building rubble), whose exploitation is due to become popular in compliance with EU Recommendations, are the main subject of the analyzed processes. End uses are in road-making and in concrete production.

The problems posed by the wet processes introduction in small mobile plants, implying the respect of space constraints in the water recycling and sludge disposal systems, are dealt with. An experimental case of recycled aggregate production by dry sifting followed by wet processing to obtain an improved product is analyzed, and the design principles of compact mobile plant performing wet processing are exposed.

1 INTRODUCTION

Rocks and alluvials suitable to aggregate production are a widespread resource; therefore, when undesirable substances show up in the product, the most common and reasonable option is to switch to another source.

Consequently, in aggregates preparation, mineral dressing techniques are usually limited to comminution and classification by size, preferably using dry processes, even when the use of some simple separation techniques (such as sink-float) can be traced, in the aggregates literature, since the first half of the 20th century.

A different picture becomes apparent when low grade, usually neglected, sources, such as building rubble and excavation muck pile from civil works, are to be exploited, as a part of a waste recycling operation. In these cases, recycling is mainly made necessary by dumping problems rather than by the scarcity

and / or cost of the natural source, and the mineral dressing technique is confronted with two conditions, having no counterpart in natural sources exploitation:

- a variable, low grade orebody, which poses a practical limit to the process optimization concept and to long term planning;
- a "mobile orebody", which strongly supports the mobile plant option.

In the field of aggregates, what is called recycling is, to a great extent, down recycling: the product is mostly employed in less demanding applications than the original natural raw material.

EU Recommendations make an effort to counteract this natural tendency, by setting objectives represented by desired percentages of substitution of natural aggregates with recycled aggregate, but, even to attain such an (apparently) modest objective the conventional process (crushing

and sieving) falls short. It can be easily perceived that a randomly taken sample of simply crushed and sieved and not otherwise processed rubble or mixed face excavation muck, when mixed to natural aggregate, in most cases simply lowers the performances of the end product (concrete, embankment, road paving layer) to unacceptable levels.

Unwanted components separation stages must be added to the process and, though being the principles of mineral separation the same both for natural and for man made substances, machinery has often to be purposely redesigned (coal washing however, due to same similarity of the grain size and specific gravity ranges of the processed materials, is the main source of ideas in rubble processing).

This paper mainly deals with researches underway in the Land, Environment and Geo-Engineering Department of the Politecnico of Torino on wet processing of poor aggregates to be recycled in concrete, in particular with rubble recycling through wet process; the analysis and discussion of the experimental results and of the suggestions issuing from the tests is preceded by some consideration of particular problems typically found in recycling; the re-bars recovery by magnetic separation, being covered by a mature technology, is not considered.

2 AGGREGATES BENEFICIATION

2.1 Optimal crushing method

Both impact and jaw crushers are popular. Advocates of impact methods maintain that impact crusher produces a lower percentage of platy fragments, undesired in aggregates irrespective of intended use. Our tests confirm the asserted tendency (Fig. 1)

But platy fragments are quite well discarded by subsequent separation stages, unavoidable when an acceptable aggregate for concrete manufacturing has to be obtained from rubble. A more important advantage of impact breaking lies in the fact that, being an open circuit crushing system (no upper limit size is fixed to the output of

the machine), impact crushing makes more efficient the separation of brittle components through a differential comminution effect. Actually most recycling plants resort on impact machines for primary crushing.

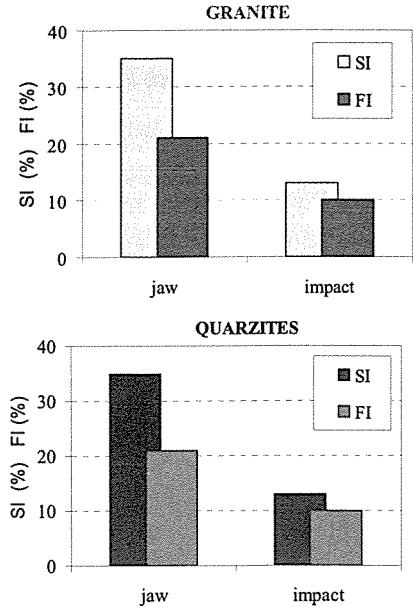


Figure 1. Shape index (SI) and flakiness index (FI) of natural aggregates produced by different crushing methods from different rocks.

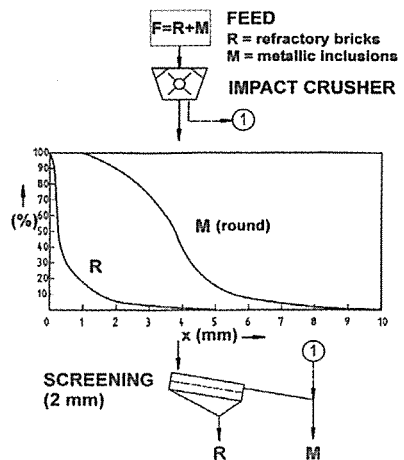


Figure 2. Example of separation by differential comminution (Beenken, 1992).

2.2 Unwanted components

Rubble and to a different extent excavation muck, are rich of unwanted components practically unknown to producers of aggregates from natural sources (which means, sound rock bodies or selected alluvials).

Unwanted components are to be removed because of chemical or physical-chemical properties (reactivity, release of noxious soluble salts, poor adhesion to mortar due to hydro-phobicity of the surface, proneness to rotting), because of physical properties (lack of strength, plastic or viscous behavior under stress, exceedingly high porosity), because of geometrical properties (platy or elongated shape), or because more than one of the above quoted defects. Most of them are man made; in the raw rubble a part of them is contained in mixed grains, but crushing to centimetric size usually leaves unwanted components in the state of free grains, and, moreover, helps to get rid of a part of the weak components by simply sieving the crushed material and discarding the fines, through a “preferential comminution” effect (for the same reason, fines are usually unsuitable to produce an acceptable sand for concrete mixtures).

Figure 3 shows an example of composition of a crushed and sieved rubble sample (size

classes 50 mm to 4 mm), determined by hand picking.

In the case of excavation waste, most abundant unwanted materials are clay, schists, weathered rock (and minor amounts of man made contaminants).

According to the behavior analogy in the treatment, to the composition and to the employment possibilities, the materials composing building rubble can be classified into these categories:

- organic lightweight materials, as paper, wood, plastics, characterized by specific gravity low values and sufficiently good resistances to tumbling;
- mineral lightweight materials, as bituminous mixtures, mortars, cement agglomerates and lightweight bricks and baked clays, characterized by specific gravity low values, poor resistances to tumbling and small abrasiveness;
- mineral heavy materials, as concrete, stone, glass, heavy bricks and baked clays (id est the materials that have to be recovered in order to produce aggregates for “noble” employment, as the concrete production), characterized by specific gravity acceptable values, medium resistances to tumbling and high abrasiveness;
- metal scrap, that is directly recycled to smelters.

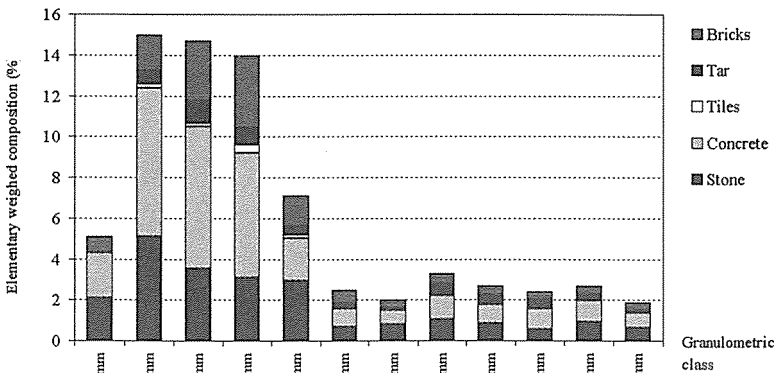


Figure 3. Composition of a crushed and sieved rubble sample (4-50 mm).

Concerning the materials features, even variable in the single species and often evaluated through not comparable methodologies, the most interesting characteristics from the treatment point of view have been considered and their variation ranges are reported in Table 1. In particular, there have been considered:

- the mechanical behaviours, indicated as elastic-brittle (EF), elastic-plastic or elastic-ductile (EP), plastic (P);
- the elastic modulus E, negligible with a plastic behaviour, low if lower than 10^3 MPa, medium if included from 10^3 to 10^4 MPa, high if included from 10^4 to 10^5 MPa and very high if greater than 10^5 MPa;
- the tensile strength, classified as very low if lower than 1 MPa, low if included from 1 to 10 MPa, medium if included from 10 to 10^2 MPa, high if included from 10^2 to 10^3 MPa and very high if greater than 10^3 MPa;
- the abrasiveness, respect to the treatment machine iron parts, classified as negligible if the materials doesn't hold elements capable to scratch the iron (Mohs hardness < 5), considerable if some abrasive elements are hold and notable if the abrasive elements are abundant (Mohs hardness > 5);
- the shape, polyhedric (P), rounded (R), irregular (I), fibrous (F), shaped as splits (S), sherds (C), rags (B), shaving (T);
- the specific gravity, with materials very light, if lower than 1 kg/dm^3 , light, if included from 1 to 2 kg/dm^3 , medium, if included from 2 to 2.4 kg/dm^3 , heavy, if included from 2.4 to 3 kg/dm^3 and very heavy, if greater than 3 kg/dm^3 ;
- other characteristics, as swelling (S), dissolution (B) and so on.

Possible separation methods practically reduce to gravity separation, air sifting, different comminution, and, possibly, differential rebound (experimental).

2.3 Combined shape factor – specific gravity – Los Angeles index criteria to evaluate separation processes

Natural aggregates are mainly tested through Los Angeles test (resistance to tumbling in the normalized testing machine); but a pure wood plus plastics concentrate passes the test, though being unsuitable to concrete manufacturing. Natural aggregates are also checked for average shape, which probably leads to a negative judgment of the wood-plastics concentrate, but the shapes of the fragments of man made materials make them by for more noxious than platy natural stone fragments (think, for instance, a plastic foil imbedded in the concrete). Moreover, expanded plastics and bituminous matter can pass the Los Angeles and the shape test and be very noxious.

Gravimetric analysis is not routinely performed on natural aggregates, but is necessary to fairly evaluate recycled rubble. All tests (Los Angeles, shape, gravimetric analysis) plus a careful inspection are needed to evaluate the success of a separation process.

In Figure 4 the results of a set of separation tests by jiggging at different specific gravity of rubble from a civil demolition are presented and evaluated according to the combined Los Angeles – shape index criterion.

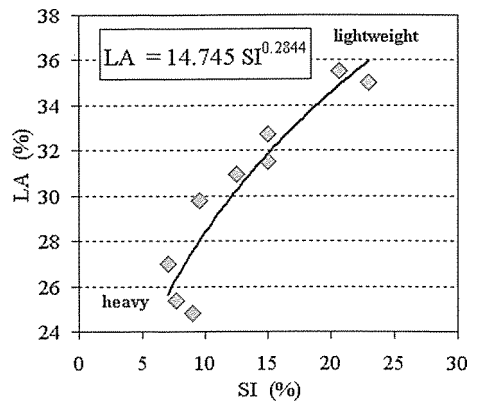


Figure 4. Los Angeles LA vs shape index SI relationship for different specific gravity.

Table 1. Rubble materials subdivision and properties interesting for the treatment.

	Mechanical properties				Shape	Sp. gravity (kg/dm ³)	Other
	Behaviour	E (MPa)	Tensile (MPa)	Abrasion			
ORGANIC LIGHTWEIGHT MATERIALS							
Paper and cardboard	EP	$0 < 10^3$	$10 \div 10^2$	-	B	<1	S
Wood, plywood, shaving wood "Plastics"	EP	$10^3 \div 10^4$	$10 \div 10^2$ $10^2 \div 10^3$	-	F, T	<1	S
Slabs	EP, e. EF	$10^3 \div 10^4$	$10 \div 10^2$ $10^2 \div 10^3$	-, +	B, C	1÷2	
Pipes	EF, ev. EP	$10^3 \div 10^4$	$10 \div 10^2$ $10^2 \div 10^3$	-, +	S, C	1÷2	
Sheets	EP	< 10^3	$10 \div 10^2$ $10^2 \div 10^3$	-	B	1÷2, <1	
Foam polystyrene	P or EP	0	<1	-		<1	
MINERAL LIGHTWEIGHT MATERIALS							
Bitumen	P, EP	$0 < 10^3$	<1, 1÷10	-, +	P, R	2÷2.4	C
Mortar, lime	EF	< 10^3	<1, 1÷10	-, +	P, R	2÷2.4	
Gypsum based materials	EF	< 10^3	<1, 1÷10	-, +	P, R	2÷2.4	B
Cement agglomerate	EF	$10^3 \div 10^4$	1÷10	+, ++	P	2÷2.4	
Lightweight brick and baked clay	EF	$10^3 \div 10^4$	1÷10	+, ++	S, C	2÷2.4 1÷2	
MINERAL HEAVY MATERIALS							
Concrete	EF	$10^3 \div 10^4$ $10^4 \div 10^5$	<1	+, ++	P, R	2÷2.4 2.4÷3	
Stone	EF	$10^4 \div 10^5$ > 10^5	$10 \div 10^2$ $10^2 \div 10^3$	+, ++	P, S, R	2.4÷3 >3	
Heavy brick and baked clay	EF	$10^4 \div 10^5$ > 10^5	$10 \div 10^2$ $10^2 \div 10^3$	++	S, C	2.4÷3	
Glass	EF	$10^4 \div 10^5$ > 10^5	$10 \div 10^2$ $10^2 \div 10^3$	++	S, C, P	2.4÷3	
METALLIC SCRAP							
Ferrous	EP, EF	> 10^5	$10^2 \div 10^3$, > 10^3	++	I, C	>3	D
Aluminium and other lightweight alloys	EP	$10^4 \div 10^5$ > 10^5	$10^2 \div 10^3$	-	I	2.4÷3 >3	
Other not ferrous alloys	EP	$10^4 \div 10^5$ > 10^5	$10^2 \div 10^3$	-, +	I	>3	
Copper	EP	> 10^5	$10^2 \div 10^3$	-	I	>3	
Lead	P		1÷10	-	I	>3	
LEGEND	EP elastic-plastic or elastic- ductile	0 = negligible < 10^3 low $10^3 \div 10^4$ medium	<1 negligible 1÷10 low $10 \div 10^2$ medium	- negligible + considerable ++ notable	P polyhedral S splits R round C sherds B rags F fibrous I irregular T shaving	<1 very light 1÷2 light 2÷2.4 medium 2.4÷3 heavy >3 very heavy	S swelling B dissolution C softening D ferrous- magnetic
	EF elastic-brittle	$10^4 \div 10^5$ high > 10^5 very high	$10^2 \div 10^3$ high > 10^3 very high				
	P plastic						

2.4 Yield – Grade Relationship

Any separation is characterized by a negative correlation between the yield (percentage of the feed that the process makes marketable) and the grade of the product: the cleaner we want the concentrate, the smaller is the amount of concentrate obtained from a given amount of feed.

It is a long way to find a reliable mathematical model for that correlation (which is important to optimize the beneficiation process, roughly speaking to avoid over-beneficiation). We present some results from an experimental study (carried out on the demolition rubble already described in the example at the Paragraphs 2.2 and 2.3) (Fig. 5).

In particular, in rubble processing, however, the concept of the concentrate “grade” is not easy to define. It could be defined by the percentage of replacement of natural aggregate with recycled aggregate (RA), in the composition of a concrete, without noticeable performances impairment (100% grade should therefore represent a recycled aggregate equivalent to the natural product) (Fig. 6).

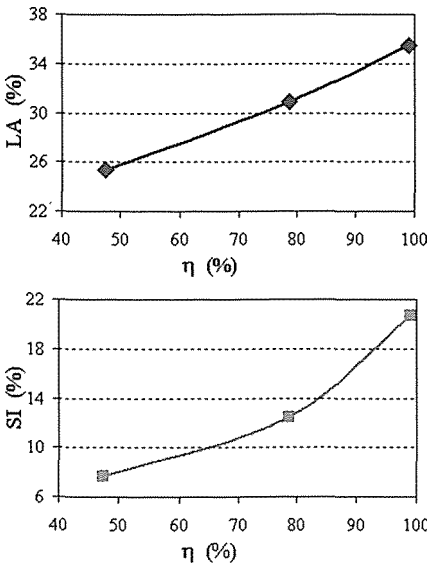


Figure 5. Los Angeles (LA) and shape index (SI) vs yield (η) relationships.

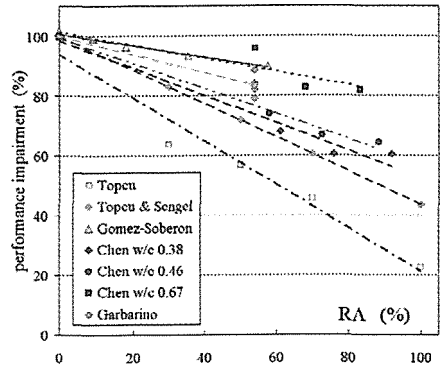


Figure 6. Performance impairment vs replacement percentage of natural aggregate with recycled aggregate (RA).

3 SEPARATION EQUIPMENTS. DRY OR WET PROCESSES?

Basically, separation machines employed in rubble processing rely on:

- wet processing: sink-float (with autogenous heavy medium), jigging, tabling (with table belts and similar);
- dry processing: air sifting;

Differential comminution effects a sort of pre-concentration.

Benefits and drawbacks:

- coming to dry processing, air sifting, the most popular, is simple and productive, but fails to warrant the aggregate quality required by concrete use, apart from cases where a carefully selected feed is processed (Fig. 7.a). More sophisticated systems such as zig zag air separators (Fig. 7.b), however, claim some success in delicate separations, such as concrete-brick debris. Air tabling has a quite low productivity and requires a carefully sized feed;
- sink float machinery is highly productive, but separation specific gravity attainable with autogenous heavy medium is quite low (1.2 kg/dm³), and platy fragments are not rejected (Fig. 8);
- table belts and similar are in intermediate position (Fig. 9). They are simple and productive, but separation

accuracy seldom attains the levels required by concrete aggregates;

- jiggling is conceptually the optimal system, allowing to set the separation specific gravity at any desired value and to remove platy fragments, but requires a quite sophisticated and expensive machinery (Fig. 10);

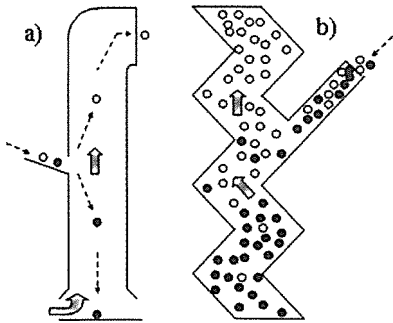


Figure 7. a) air separator scheme; b) zig zag air separator scheme.

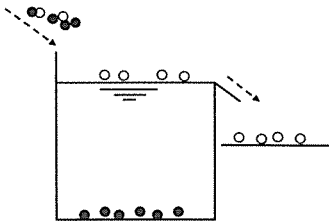


Figure 8. Sink float scheme.

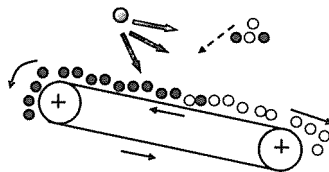


Figure 9. Table belt scheme.

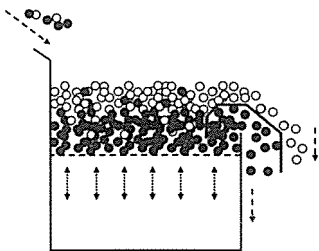


Figure 10. Jig scheme.

All wet processing systems obviously, have the problems of water supply, process water recycling and sludge disposal.

Wet processing option is probably unavoidable when the concrete production is the foreseen use of recycled aggregate, both from rubble and from excavation muck, being able to remove slimes adhering to the grains. Just a simple wet screening step significantly improves the product, as shown by the example in Table 2, that shows the values of yield (η), Los Angeles index (LA), shape index (SI) and saturated surface dried average specific gravity (γ_{ssd}) of different products obtained through different wet treatments at different cut points.

Table 2. Parameters of products from different processes performed on raw rubble.

Treatment	η (%)	LA (%)	SI (%)	γ_{ssd} (kg/dm^3)
Feed	100.0	37.7	-	-
Wet sieving	99.0	35.5	21	2.37
Jigging	78.7	30.9	13	2.50
Jigging	47.4	25.4	8	2.66

4 PROCESS WATER RECYCLING AND SLUDGE DISPOSAL PROBLEM IN STATIONARY AND MOBILE PLANTS

In demolition rubble and excavation muck recycling, the source of the material to be processed (which could be termed the “orebody”) is represented, in most cases, by a succession of separate operation sites, each one providing an amount of raw material in the 1000-5000 t range, as a rule: very large operations take place too, but the cumulated output of small operations largely exceeds the one coming from large operations. Production comes mostly from small, variable and mobile orebodies, which has not counterpart in natural rock bodies exploitation.

Processing facilities can concentrate in large stationary plants fed by a multitude of sources, but a valid option is too represented by compact mobile processing plants, processing the “small mobile orebodies”.

In this case, the general tendency is towards a simplification of the process (in the demolition rubble case: crushing, rebar removal, sieving; in the excavation case: muck crushing and sieving). So doing a low grade product is accepted, as a counterpart of processing and plant simplicity. As a rule, wet processing, which could give rise to acceptable concrete aggregates, is only effected in stationary plants, endowed with the necessary large waste water and sludge disposal systems.

Wet processing in a mobile plant, which could give rise to true recycling (concrete aggregate production) of the demolition material and to an improved valorisation of the excavation muck material, can only become a practicable option through the development of a compact water clarifying and sludge disposal system. To this aim two researches are underway at our Department (Land, Environment and Geo-Engineering Department, Politecnico of Torino):

- for the water clarifying, a research on the capabilities of a compact system formed by a sieve-bend (Fig. 11), a lamella clarifier (Fig. 12) and an hydro-cyclone;
- for the sludge disposal, a research on the geotubes technology (Fig. 13);

The optimal layout of a mobile plants is shown in Figure 14.

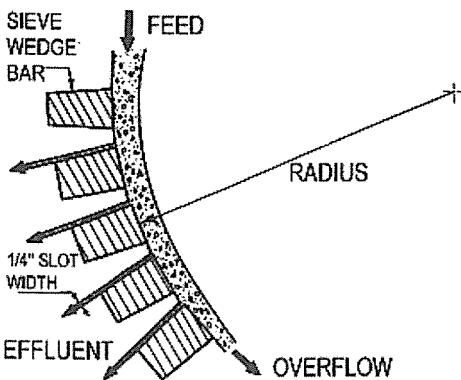
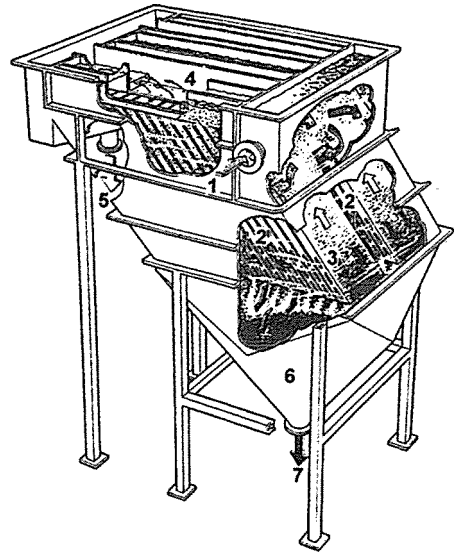


Figure 11. Working scheme of sieve bend (Leonard, 1979).



- Pulp feed (1)
- Pulp distribution chamber (2)
- Lamella packs (3)
- Overflow channels (4)
- Treated water overflow (5)
- Slurry collection tank (6)
- Thick slurry discharge (7)

Figure 12. Example of lamella clarifier (Marmor, 1995).

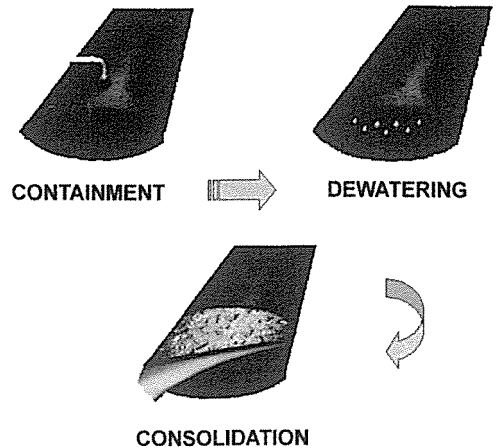


Figure 13. Working principle scheme of geotubes (Miratech, 2004).

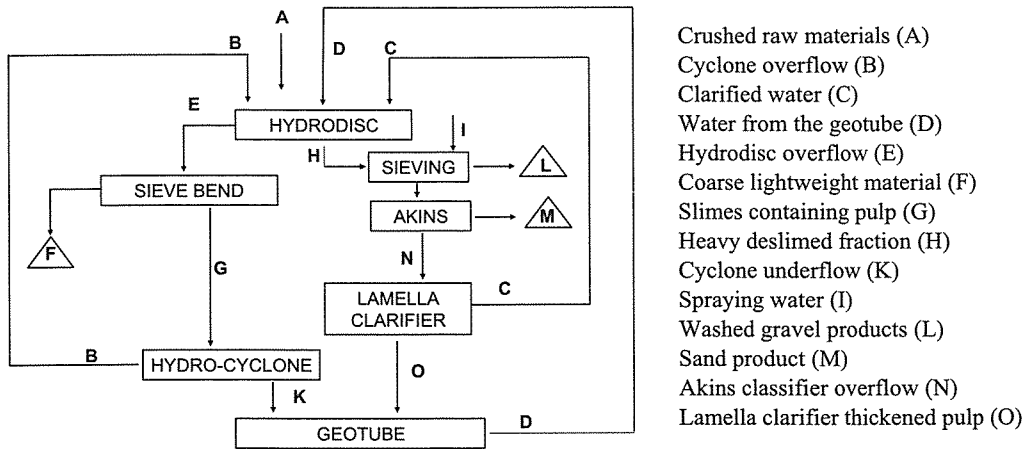


Figure 14. A proposed layout for a mobile wet processing plant for demolition rubble, presently under study.

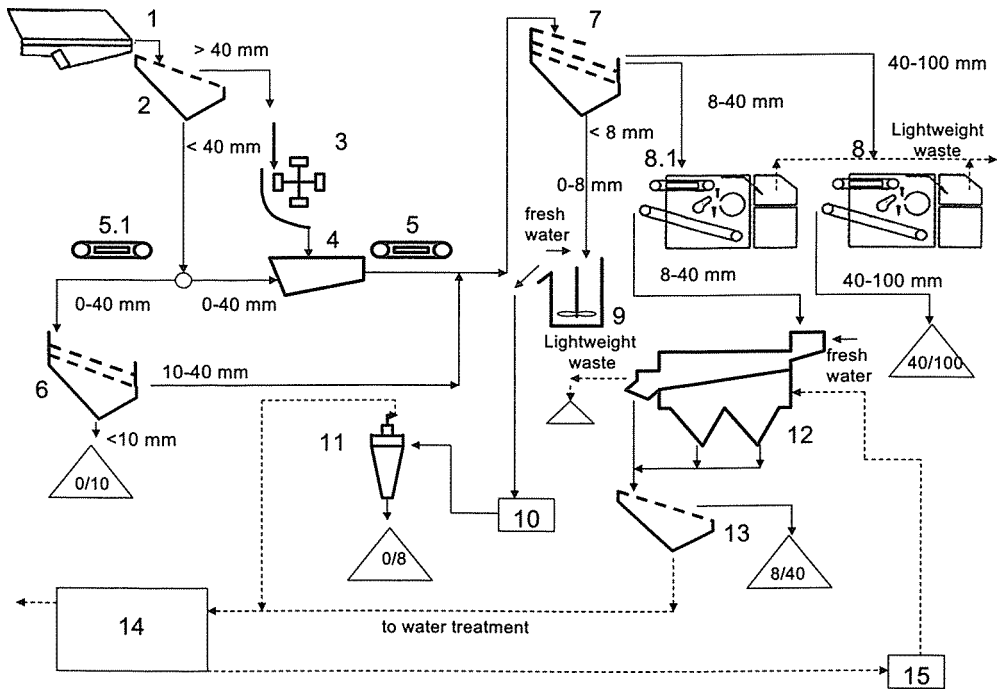
The crushed raw material, coming from a separate crushing – scrap iron removing mobile plant, is fed, in (A), to a hydrodisc or to an equivalent flowing film washing apparatus. Overflow, containing slimes and lightweight particles, is fed (E) to a sieve bend, separating coarse lightweight material (F), representing possibly a source of recycled fuel, while the slimes containing pulp (G) flows to an hydraulic cyclone. Cyclone overflow (B) comes back as process water to the primary lightweight matter separator. Thickened overflow from the cyclone represents a waste and is fed to a geotube (K). The heavy, partly deslimed fraction (H) flows to a multi deck, water sprayed vibrating screen, giving rise to the washed gravel products (L). Spraying water to the screen (I) represents the clean water make up of the system; fines from the screen, in the form a pulp, are fed to an Akins spiral hydro-classifier, or equivalent device, recovering a sand product (M), suitable to non demanding uses. The overflow (N) of the hydro-classifier flows to a lamella clarifier, or an equivalent compact clarifier. The clarified water (C) comes back to the primary washing machine, while the thickened pulp (O) goes to the geotube, as a waste material. Water seeping through the geotube walls can be recovered too and recycled to the washing stage (D). Ideally,

the water makeup is equivalent to the amount lost as humidity of the products (L, M) and of the wastes (F, slimes stored in the geotube). A buildup of very fine clay particles is likely to occur in the case of a long lasting operation (which is unlikely in a mobile plant) and can be counteracted by diverting a part of the cyclone fed to the thickener and adding some flocculant reagent.

5 STATIONARY PLANTS FOR RECYCLED AGGREGATE PRODUCTION

For stationary aggregate recycling plants, the most natural solution is to add a recycling section to an existing natural aggregate production plant and this has been done in a number of cases.

The recycling section, as a rule, is a dry processing plant, the most common objective being to produce the top class material from a natural source and a lower class product from recycling. The two plants share, profitably, materials handling machinery, stockage, air de-dusting, product control and, perhaps more important, space. Wet processing can be later added to the rubble recycling section to extend the range of possible uses of the recycled product.



- Processing:
- throughput 150-180 t/h
- Feeding system:
- feed chute (1) 12 m³
 - feed vibrating conveyor (2)
- Crushing unit:
- primary impact crusher (3)
- Screening unit:
- vibratory feeder (4)
 - vibratory screen (6)
 - vibratory screen (7)

- Magnetic separation unit:
- 2 overband separators (5) (5.1)
- Dry separation unit:
- 2 air separators (8) (8.1)
- Wet separation unit:
- 1 feed box (9)
 - 1 solids pump (10)
 - 1 hydro-cyclone (11)
 - 1 pulsator jig (12)
 - 1 dewatering chute (13)
 - 1 sludge basin and filter press system (14)
 - 1 sludge pump (15)

Figure 15. Hypothesis of a wet separation unit in the CAVIT processing plant (Garbarino & Mancini, 2006b)

An example of an operation of this kind is here reviewed and the most important results are exposed.

In 1999 the CAVIT S.p.A. treatment plant rose as the re-conversion of an extractive site, where the wet pit quarry was closed.

The presently operating dry rubble processing plant performs single stage crushing with an impact crusher, steel and reinforced bars removal with two overband magnetic separators and lightweight materials dry separation with two air separators.

The 8-40 mm product, air-sifted, but still unsuitable to use as concrete aggregate, is the candidate for a further improvement by wet processing.

This kind of separation technique implies these innovations:

- the <math>< 8\text{ mm}</math> class will be pulped and cycloned, to obtain a clean 0-8 mm sand, to be used in non demanding concrete (paving blocks);
- the 8-40 class, that has been successfully tested in laboratory for wet

separation of lightweight and platy components will be jigged.

At a supposed feed rate of 80 t/h, 60 t/h of improved aggregate with Los Angeles index 30 can be obtained, the balance being discarded as environmental filling material.

One jigging unit of the pulsator type, fixed screen, with a screen surface of 3.3 m², and a water consumption of 160 m³/h will be needed. However the water consumption will be much lower, perhaps one tenth of said amount, due to recycling.

6 CONCLUSIONS

Recycling and low grade aggregate improvement provide new opportunities to the research and to the processing machinery fabrication industry, that can be important for a "non mining" country as Italy is.

In particular, re-designing processes formerly developed for natural resources valorisation is a novel activity in which our Department is currently engaged, which shows a promise to yield results.

ACKNOWLEDGEMENTS

We express thanks to Dr. C. Colombino, Mr. F. Tomatis and all the technicians of the CAVIT S.A. and to Eng. A. Faraon, Eng. L. Ortoncelli, Dr. S. Carlesso and all the technicians of the OM S.A. for having kindly provided support and data for this report.

REFERENCES

Beenken, W, 1992. Mineral processing technology: the key to recycling, *Aufbereitungs Technik*, volume 33, n. 12, pp.665-672

Chen, H.J., Tsong, Y., Chen, K.H., (ed. Elsevier Science) 2003. Use of building rubble as recycled aggregates, *Cement and Concrete Research*, volume 33, pp.125-132

Garbarino, E, Mancini, R, (ed. Cardu, Ciccu, Lovera & Michelotti), 2006a. Analysis of the shape parameters of crushed rubble components in view of the recycling as aggregate in the building industry, *MPES 2006, XV International Symposium on Mine Planning and Equipment Selection, Torino, Italy* (ISBN 88-901342-4-0) volume 2, pp. 828-835

Garbarino, E, Mancini, R, (ed. Cardu, Ciccu, Lovera & Michelotti), 2006b. Unconventional feed source and products for a quarrying and processing plant system, *MPES 2006, XV International Symposium on Mine Planning and Equipment Selection, Torino, Italy* (ISBN 88-901342-4-0) volume 2, pp. 836-841

Garbarino, E, Mancini, R, (ed. G. Önal, N. Acarkan, M. S. Çelik, F. Arslan, G. Ateşok, A. Güney, A. A. Sirkeci, A. E. Yüce, K. T. Perek, Istanbul Technical University, Mining Faculty, Turkey), 2006c. Beneficiation of rubble from civil demolition work to produce high grade aggregates. Part I: Beneficiation methods tested, *IMPC 2006, XXIII International Mineral Processing Congress, Istanbul, Turkey* (ISBN 975-7946-27-3 (Tk) 7946-30-3) volume 3, pp. 2249-2254

Garbarino, E, Mancini, R, (ed. G. Önal, N. Acarkan, M. S. Çelik, F. Arslan, G. Ateşok, A. Güney, A. A. Sirkeci, A. E. Yüce, K. T. Perek, Istanbul Technical University, Mining Faculty, Turkey), 2006d. Beneficiation of rubble from civil demolition work to produce high grade aggregates. Part II: Criteria for grade assessment of the processed materials, *IMPC 2006, XXIII International Mineral Processing Congress, Istanbul, Turkey* (ISBN 975-7946-27-3 (Tk) 7946-30-3) volume 3, pp. 2109-2114

Gómez-Soberón, JMV, (ed. Elsevier Science) 2002. Porosity of recycled concrete with substitution of recycled concrete aggregate. An experimental study, *Cement and Concrete Research*, volume 32, pp.1301-1311

Leonard, JW, (ed. The American Institute of Mining, Metallurgical and Petroleum Engineers) 1979. *Coal preparation*, INC, New York

Mancini, R, Garbarino, E, Clerici, C, (ed. A. G. Paşamehmetoğlu, A. Özgenoğlu and A. Y. Yeşilay), 2004. Application of the Mineral Dressing Principles to the Beneficiation of Waste Material, *SWEMP 2004, VIII International Symposium on Environmental Issues and Waste Management in Energy and Mineral Production, Antalya, Turkey*, (ISBN 975-6707-11-9), pp.557-562

Mancini, R, Garbarino, E, Michelotti, E, (ed. Singhal, Fytas, Chiwetelu), 2005. Demolition and rubble recycling as new operation fields for mining technologies and machinery, *MPES 2005, XIV International Symposium on Mine Planning and Equipment Selection, Banff, Alberta, Canada* (ISSN 1712-3208), pp. 1712-3208

- Marmor, F, 1995. Process water recovery with lamella clarifiers. Also beneficial for recycling of building material, *Aufbereitungs Technik*, volume 36, n. 4, pp. 169-174
- Miratech, 2004. *Containment and dewatering. Geotubes*, Georgia, USA, www.geotube.com
- Topçu, IB, NF, Günçan, (ed. Elsevier Science) 1995. Using waste concrete as aggregate, *Cement and Concrete Research*, volume 25, n.7, pp.1385-1390
- Topçu, IB, Şengel, S, (ed. Elsevier Science) 2004. Properties of concretes produced with waste concrete aggregate, *Cement and Concrete Research*, volume 34, pp.1037-1312

The Improvement of Mill Throughput Using Barmac Pregrinding Technology at Cement Plants

S. Esen

Metso Minerals Process Technology Asia-Pacific, Brisbane, Australia

H. Benzer

Hacettepe University, Mining Eng. Dept., Beytepe, Ankara, Turkey

ABSTRACT The increasing demand for “finer cement” products, and the need for reduction in energy consumption and green house gas emissions, necessitate the optimization of grinding circuits. Opportunities exist at cement plants to improve energy efficiency while maintaining or enhancing productivity. Several technologies and measures exist that can reduce the energy consumption of the various process stages of cement production including raw and finish milling. This paper presents one of these technologies, which is pregrinding with Barmac B-Series Vertical Shaft Impactors (VSI) in raw and finish milling. Recent pilot plant studies conducted at Metso Minerals show that significant clinker size reduction occurs in Barmac VSI crushers, which can increase the cement mill throughput and decrease the energy consumption in finish milling. In addition, a number of grinding simulations using JKSimMet software conducted to date have been presented. The simulation results show that pregrinding increases mill throughput by 14 to 26%.

1 INTRODUCTION

Cement production is an energy intensive process. It consumes 2% of the global primary energy and 5% of the total global industrial energy. Grinding is a high-cost operation consuming approximately 60% of the total electrical energy expenditure in a typical cement plant. The electrical energy consumed in the conventional cement making process is in the order of 110 kWh/tonne, of which approximately 30% is used for raw materials preparation and 40% for the finish milling (cement clinker grinding). This is the largest single consumption point of electric power in the process of converting raw materials to finished cement (Bhatty, 2004).

The cost of energy as part of the total production costs in the cement industry is significant, warranting the attention for energy efficiency to improve the bottom line. Substantial potential for energy efficient

improvements exist in the cement industry and in individual plants. The cement industry is targeting technologies focusing on:

- Increasing the mill throughput;
- Energy savings;
- Minimising the production costs without negatively affecting product yield or quality.

The industry is looking into energy-efficient technologies to meet these goals. Energy efficiency is an important component of a company’s environmental strategy. Opportunities exist at cement plants to improve energy efficiency while maintaining or enhancing productivity. Ball mills have undergone considerable evolution in the last three or four decades. The trends are reflected in increasing mill size, use of high efficiency separators, adoption of new designs of mill internals, application of innovative control systems, and adoption of hybrid plants.

Several technologies and measures exist that can reduce the energy consumption of the various process stages of cement production including raw materials preparation, clinker production, finish grinding, product and feedstock changes. However, in this paper, the technologies and measures in finish grinding, especially pregrinding technology, were considered. This paper presents the pregrinding technology using Barmac Vertical Shaft Impact crushers manufactured by Metso Minerals including pilot plant results and grinding simulations.

2 CEMENT GRINDING AND PREGRINDING

Portland cement is made by exact proportioning of materials containing calcium, silica, alumina and iron. Approximately 1.5 tonnes of raw materials are required to produce 1 tonne of finished cement. Grinding operation is the major operation and occurs at the beginning and at the end of the cement making process. The last step in the process of manufacturing Portland cement is the finish grinding of clinker together with a small amount of gypsum and some admixtures. The principal objectives of clinker grinding are to promote the hydration of cement and to ensure complete coating of inert aggregates. The fineness of the cement affects the concrete properties in terms of the workability, strength and permeability. The finer the grind the more reactive is the finished cement. Therefore, every type of cement has got its own fineness to meet the required quality.

A cement clinker grinding circuit reduces the feed from an 80% passing size between 10 and 40 mm to 35-40 microns with the size reduction ratio being in the order of 250-1000. Tube mills with multichambers are traditionally used for cement grinding either in open or closed circuit operations. In the first chamber, larger balls (from 50 mm up to 90 mm) are used for coarse grinding while the smaller balls (as small as 12 mm ranging up to 50 mm) are used for fine grinding

(Bhatty, 2004). In recent years, the use of ball mills, and more particularly, of air-swept ball mill systems, is being overtaken by vertical roller mills. Horizontal roller mills have also found applications in cement grinding starting from 1990s (Bhatty, 2004).

The use of the concept of pregrinding to increase production capacity has been the latest technological milestone in the evolution of milling systems starting from 1990s (Bhatty, 2004). The energy efficiency of ball mills for use in finish grinding is relatively low, consuming up to 30-42 kWh/ton clinker depending on the fineness of the cement (Marchal, 1997). Several new mill concepts exist that can significantly reduce power consumption in the finish mill to 20-30 kWh/ton clinker, including roller presses and Vertical Shaft Impactors used for pre-grinding in combination with ball mills (Seebach et al., 1996; Jankovic et al., 2004). The addition of a pre-grinding system to a ball mill will result in savings of 6-22 kWh/ton cement (Scheuer & Sprung, 1990; Jankovic et al., 2004).

In the past 20 years, high pressure grinding roll (HPGR) technology has been predominantly used in pre-grinding of clinker. Presently, many American and European cement grinding circuits have HPGRs which increase grinding capacity and energy efficiency. Vertical Shaft Impactors have started to find applications in the cement sector (mainly in India and China).

3 THE OPERATIONAL PRINCIPLES OF BARMAC VSI CRUSHERS

Barmac B-series VSI (Vertical Shaft Impactor) crushers are applied to a broad range of materials in minerals and aggregate industry. Due to the "autogenous grinding action" it is especially efficient for highly abrasive materials such as cement clinker. The crushing action is schematically presented in Figure 1.

Material fed into the top of the machine is separated into three separate streams in a rock lined rotor, and is continuously discharged into the crushing chamber at velocities up to 85 m/s. Multiple events occur and a variety of forces act on the

individual particles as they are subjected to a rock-on-rock chain reaction of crushing and grinding. A second stream of material can be cascaded in a controlled quantity into the crushing chamber turbulence, causing an increase in the particle population within the chamber, thereby improving the energy transfer.

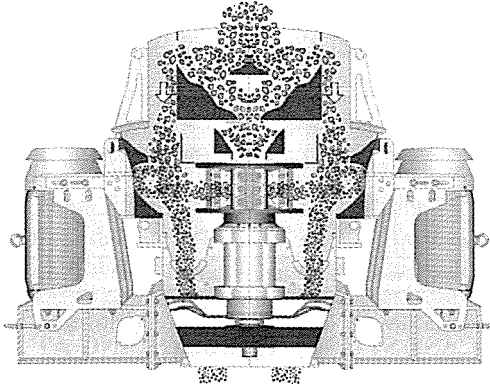


Figure 1. Schematic of Barmac crusher operation.

In this paper, potential benefits of using the Barmac VSI crusher for clinker pre-crushing at cement plants were studied. Figure 2 shows the proposed cement grinding circuit with a pregrinding stage.

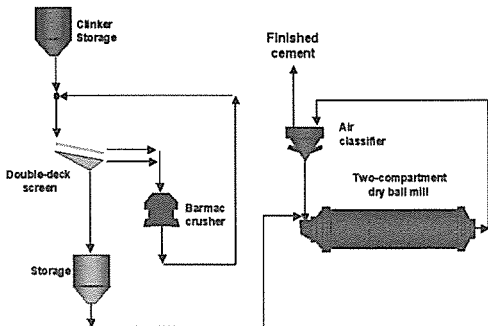


Figure 2. Simplified cement grinding circuit with a precrushing stage.

4 PREGRINDING RESULTS

4.1 Pilot Plant Test Results

On June 23, 2006, pilot crusher tests were conducted at Metso Minerals Mineral

Research and Test Center (MRTC) for Cementos Apasco, Mexico (MRTC, 2006). Test material was clinker. The aim was to investigate the efficiency of the Barmac VSI crusher as a pregrinder. Clinker feed was pre-screened by 2.36 or 4.70 mm screens. The Barmac VSI crusher was operated in a closed circuit arrangement. Rotor tip speed was varied between 55 and 65 m/s. The results are seen in Figure 3.

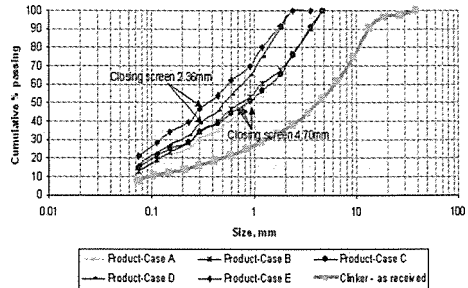


Figure 3. Clinker and the crushed clinker (product) size distributions for Cementos Apasco, Mexico.

It is shown that Barmac VSI product is significantly finer than the feed proving that Barmac is efficiently producing the finer material. In particular, the Barmac VSI produces significant amounts of fine clinker (13-21% -75 μ m), which should increase the performance of the ball mill (Fig. 3). In addition to this, ball mill feed F80 (80% passing size) is reduced significantly (from 10 mm to approximately 1.5-2.5 mm), which should necessitate smaller balls and some other adjustments in the ball mill. The effect of finer ball mill feed on mill throughput and energy consumption will be given in the next section. Note that the finer the final screen cut, the finer the size distribution is. The specific energy consumptions are approximately 1.3 and 1.5 kWh/t for the circuit with 4.70 mm and 2.36 mm respectively. Circulating load was found in the range of 100-163% for the trial tests (Esen & Jankovic, 2006).

4.2 Simulations of Cement Grinding Circuits

In recent years, considerable steps have been taken to improve comminution efficiency both in the development of machines with the ability to enhance energy utilisation and in the optimal design of grinding systems to enable more efficient use of existing machines. But it is still necessary to have a better knowledge of the effects of mill operating variables if optimum performance is to be achieved.

The best way to optimize the grinding circuit to achieve economic plant operation is by simulation, using proven mathematical modeling techniques. Simulation is a valuable tool in process technology if the process models are accurate and if model parameters can be determined in a laboratory or plant. It is now used extensively for the design and optimisation of wet grinding circuits and has brought large economic benefits. It is likely that economic benefits are also attainable in dry grinding.

JKSimMet Simulation package has been a proven tool to optimize the dry grinding line (mill/separator) operating variables. Lynch et al. (2000) and Benzer et al. (2003) developed a modelling approach for the two compartment cement mills using extensive data around and inside the mill. It should be noted that in order to obtain the “site specific” model constants, detailed surveys of the milling circuit are required: the size distribution of the material in each stream as well as from different points inside the mill. In this study the modelling approach and the model parameters were taken from the studies published in Benzer et al. (2003).

Simulations with different feed size distributions (raw clinker, and pre-crushed clinker using the Barmac crusher) were carried out, keeping the product size constant at $P_{80}=0.038$ mm. A number of cement milling simulations were carried out by Metso Minerals Process Technology group located in Brisbane, Australia. These included the simulations for Argos Cement, Green Island, Lafarge cement and Holcim Apasco cement (Jankovic, 2003, 2005, 2006; Esen & Jankovic, 2006). Simulations were carried out

using JKSimMet software and supplied ball mill feeds (with and without pre-grinding). Table 1 summarises the results. It is shown that pre-grinding increases throughput by 14 to 26%. The overall energy efficiency of the circuit could also be improved in the order of 10-15%.

Table 1. Summary of cement milling simulations.

		Argos Cement	Green Island	Lafarge Cement	Holcim Apasco
Ball mill feed – without pre-grinding	F80, mm	20	15.5	32	14
	Tonnage, tph	50	110	125	138
Ball mill feed – with pre-grinding	F80, mm	2.3	3.0	3.5	2.7
	Tonnage, tph	60	135	143	174
Tonnage increase, %		20	23	14	26

5 CASE STUDY – PREGRINDING AT A CEMENT PLANT IN INDIA

An Indian cement plant purchased a Barmac VSI crusher (Barmac B8000) to increase the throughput of the grinding plant. The $P(80)$ clinker sizes with and without Barmac were approximately 25 mm and 3 mm respectively. The Barmac VSI was installed in a closed circuit arrangement (similar to as shown in Figure 2) to produce 100% minus 5mm mill feed (Figure 4). The product obtained from the mill after the inclusion of the Barmac VSI in the circuit has led to a 33% increase in the capacity of the mill, from 45 tph to 60 tph (www.barmac.com).

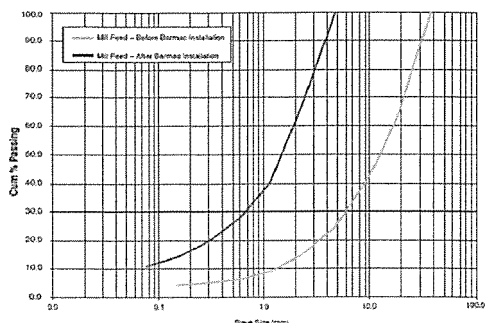


Figure 4. Size distributions of the mill feed before and after pregrinding.

6 COMPARISON OF THE HPGR AND BARMAC VERTICAL SHAFT IMPACTOR IN PREGRINDING APPLICATIONS

It is shown that pre-grinding of cement clinker is advantageous for increased throughput as well as reduced power consumption. There are two main technologies for pregrinding option: high pressure grinding rolls (HPGR) and vertical shaft impactor (e.g. Barmac VSI). Vertical roller mills have also found some applications as a pregrinder. Despite of the fact that HPGR has found extensive applications in cement sector, Barmac crushers have also found applications in this sector due to its low capital cost, low maintenance cost and production of a significant amount of finely ground clinker. On the other hand, the HGPR operating with an air classifier in a closed circuit configuration has been shown to offer substantial energy savings. There are several data published about this in the literature. The major disadvantages of HPGR can be listed as high capital cost (approximately 10 times more expensive under similar tonnage), high maintenance cost (high wear) and low availability (long down time). In addition, wear rate in HPGR applications is a function of the feed size.

In order to make a comparison between an open circuit HPGR and a Barmac VSI crushing circuit, the samples were collected from different cement plants using Barmac crusher and HPGR as a pre-crushing unit for the clinker production. A comparison of the product discharges obtained from these two equipments is given in Figure 5. In these cases, the HGPR is operating as open circuit and the Barmac VSI crushing circuit consists of the machine itself and a screen.

As shown in Figure 5, both the open circuit HPGR discharge and the Barmac VSI circuit discharge have got similar size distribution. The benefits obtained from these two pre-crushing circuits should be the same; however, the cost of the Barmac crushing application would be much lower.

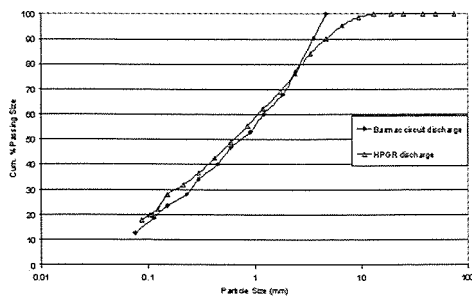


Figure 5. Particles size distributions of the HGPR and Barmac circuit output.

7 CONCLUSIONS

This paper shows that the pre-crushing of cement clinker using a Barmac Vertical Shaft Impactor offers realistic benefits to a cement plant in terms of process efficiency. Pilot plant tests showed that Barmac VSI is efficiently producing finer material. In particular, the Barmac VSI produces significant amounts of fine clinker, which should increase the performance of the ball mill. The cement milling simulations carried out using grinding simulation software showed that pre-grinding increases throughput by 14 to 26%. The overall energy efficiency of the circuit could also be improved in the order of 10-15%.

A few Barmac pregrinding systems have been installed in India and China. It has been reported that the increase in the capacity of the mill has reached up to 33% after the introduction of the pregrinding system.

In order to get the benefit from the finer feed resulting from the pregrinding, necessary circuit optimization should be carried out to achieve the throughput increases. This includes the optimization of a number of parameters in the dry grinding circuit which requires a comprehensive survey and simulations based on the survey. Such a study ensures that a plant would obtain the targeted throughput increases and reduced energy consumption while not affecting the product quality.

REFERENCES

- Benzer, H., Ergun, L., Oner, M. and Lynch, A.J. 2003. Case Studies of Models of Tube Mill and Air Separator Grinding Circuits, *Proceedings: XXII International Mineral Processing Congress*, Chief Editors: L. Lorenzen and D.J. Bradshaw, pp 1524-1533.
- Bhatty, J.I., Miller F.M., Kosmotka, S.H., 2004. *Innovations in Portland Cement Manufacturing*. Portland Cement Association, USA.
- Esen S and Jankovic, A, 2006. *Holcim Apasco Cement Milling Simulations*. Metso Minerals Process Technology Asia-Pacific, Brisbane, Australia. Internal Report.
- Jankovic, A, 2003. *Green Island Cement Milling Simulations*. Metso Minerals Process Technology Asia-Pacific, Brisbane, Australia. Internal Report.
- Jankovic, A, Valery, W, Davis, E. 2004. Cement grinding optimisation. *Minerals Engineering* 17: 1075-1081.
- Jankovic, A, 2005. *Lafarge Cement Milling Simulations*. Metso Minerals Process Technology Asia-Pacific, Brisbane, Australia. Internal Report.
- Jankovic, A, 2006. *Argos Cement Milling Simulations*. Metso Minerals Process Technology Asia-Pacific, Brisbane, Australia. Internal Report.
- Lynch, A.J., Öner, M., Benzer, H., 2000. Simulation of a closed cement grinding circuit. *ZKG International* 10, 560–567.
- Marchal, G. 1997. Industrial Experience with Clinker Grinding in the Horomill. *Proc.1997 IEEE/PCA Cement Industry Technical Conference XXXIX Conference Record*, Institute of Electrical and Electronics Engineers: New Jersey.
- Metso Minerals Mineral Research and Test Center, 2006. *Pilot Plant Crushing Tests on Clinker for Cementos Apasco*. Milwaukee, WI, USA.
- Scheuer, A. and Sprung, S., 1990. Energy Outlook in West Germany's Cement Industry. *Energy Efficiency in the Cement Industry* (Ed. J. Sirchis), London, England: Elsevier Applied Science.
- Seebach, H.M. von, E. Neumann and L. Lohnherr, 1996. State-of-the-Art of Energy-Efficient Grinding Systems. *ZKG International* 2 49 pp.61-67 (1996).

Utilization of Some Industrial Wastes as Abrasive in Surface Preparation Processes

N. Ataman & G. Özbayoğlu

Middle East Technical University, Mining Engineering Department, Ankara, Turkey

ABSTRACT Abrasive blast cleaning involves mechanical cleaning by the continuous impact of abrasive particles at high velocities on to the substrate using compressed air. Materials from different origins can be used as a blasting media including coal slag, smelter slag, mineral abrasives, metallic abrasives, and synthetic abrasives.

Four different slag samples, namely coal furnace slag, ferrochrome slag, granulated blast furnace slag and converter slag, were studied. The samples were prepared by crushing and screening. The chemical composition and physical characteristics of the samples were determined. All the samples were tested in industrial scale. Test results showed that the converter slag meet all the specifications for abrasives and it can be used in blast cleaning operations. However, other tested materials - coal furnace slag, granulated blast furnace slag and ferrochrome slag - are not suitable to be used as abrasive in surface preparation technologies.

1 INTRODUCTION

An essential preliminary to any coating operation is proper surface preparation. There are no coatings which will provide long term protection when applied over a poorly prepared surface. It is believed that of the cost of a coating job, as much as two-thirds goes for surface preparation and labor (NACE 2000).

Abrasive blasting is the most widely used method of surface preparation. It is the process of propelling abrasive particles from a blast machine, using the power of compressed air (Hansel 2000). Its importance has long been known and several researches on blasting pre-treatment have been conducted (Wingen 1988, Momber and Wong 2005, Kambham et al. 2007, Rosenberg et al. 2006) and its effects on adhesiveness of coating systems have been investigated (Amada et al. 1999, Griffiths et al. 1996, Mellali et al. 1994, Amada and

Hirose 1998, Harris and Beevers 1999, Çelik et al. 1999, Staia et al. 2000).

A vital component in successful preparation of surfaces by abrasive blasting is the blasting media (Robinson 2000). Copper slag, coal slag, garnet, steel grit, and steel shot are common blasting abrasives. Traditionally sand was used, but metallic grit and slag abrasives have replaced it due to the adverse health and environmental effects of silica dust associated with sand. There are numerous considerations in selection of suitable media. Quality and performance of an abrasive is determined by its physical properties and chemical cleanliness. Besides the quality and performance aspects, local supply is a critical consideration in selection of a blasting media. Although there exists well known blasting abrasives in market, availability and cost restrict their usage. This situation has led the authors to conduct such a research. The objective of this research is

to produce blasting abrasives from domestic industrial wastes and investigate the usability of produced abrasives in surface preparation technologies.

2 EXPERIMENTAL

2.1 Materials

Four different slag samples of three sources were investigated and tested. A coal furnace slag (CFS) sample from Çayırhan Thermal Power Plant (Ankara), a granulated blast furnace slag (GBFS) and a converter slag (CS) sample from Ereğli Iron and Steel Works (Zonguldak), and a ferrochrome slag (FS) sample from Eti Krom (Elazığ) were investigated.

Coal slag is a coarse, granular, gray colored waste-product that is collected from the bottom of the furnace that burn coal for the generation of steam. It contains white and brownish particles and porous granules of 1.5 cm maximum size. Converter slag is the air-cooled steel furnace slag, sometimes called as BOF slag, and the sample contains brownish grey vesicular lumps with a top size of about 15-20 cm. Granulated blast furnace slag is water-quenched, glassy, yellowish, sand-like granules with a top size of about 5-6 mm. Ferrochrome slag is a by-product from the production of ferrochrome. The sample is composed of grey or brownish grey and white grains with a top size of about 8 cm.

2.2 Materials Characterization

Physical characteristics and chemical cleanliness of the materials was evaluated in accordance with the common specifications stated by Turkish standard TS EN ISO 11126 (2002). Samples were assessed from the aspects of size distribution, apparent density, hardness, moisture content, water soluble contaminants and water-soluble chlorides. Those specifications are determined by the methods described in TS EN ISO 11127 Part 2 to 7 (2002). Chemical composition of the materials was determined by X-ray fluorescence method.

2.3 Sample Preparation

Since original samples have different physical characteristics, pretreatments of test samples before sizing were performed in different ways. Converter and ferrochrome slag samples were first crushed in a jaw crusher to below 3 mm - the maximum allowable size for blasting abrasives - because of their lumpy nature. On the other hand, coal furnace and granulated blast furnace slag samples were air-dried before sizing due to their high moisture content. Samples were sieved for specified sizes, 1.2 mm - 0.3 mm. Oversize materials were re-crushed and undersize materials were rejected.

Besides the sample preparation method mentioned above a coal furnace slag sample was also prepared by wet screening and another granulated blast furnace slag sample was prepared within size range of 1.7 mm - 1.2 mm.

2.4 Industrial Application

The performance and quality of the prepared samples were tested using an industrial scale blasting machine in Sedef Shipyard (İstanbul). Blasting conditions are given in Table 1. Rusted steel panels of a ship in maintenance were blasted until all of the samples were consumed and the surfaces were evaluated. In order to assess the surface cleanliness, Turkish standard TS EN ISO 8501-1 (2000) was used. Surface profile pattern of blasted surfaces were evaluated using Rugotest No:3 surface profile comparator.

Table 1. Blasting conditions during industrial application.

Stand-off distance	~ 60 cm
Blasting angle	60-90°
Air Pressure	700 kPa
Nozzle diameter	10 mm

3 RESULTS AND DISCUSSION

3.1 Chemical Composition

Coal slag is mainly an aluminum silicate material. Chemical analyses of the coal furnace slag sample and Eurogrit coal slag abrasive (Eurogrit BV 2005) are given in Table 2.

Chemical compositions of two coal slags showed that aluminum content of coal furnace slag is quite lower than that of coal slag abrasive used in industry. However, its calcium and magnesium content is higher compared to Eurogrit coal slag abrasive. Those differences are possibly due to the petrographical and mineralogical

compositions of coal and its associated mineral matter. Chemical analysis of coal furnace slag also reveals that there is almost 10 % loss of ignition, which is possibly the indication of unburned coal. Those differences in chemical composition of the sample are expected to cause variations from expected physical properties such as apparent density, hardness, etc.

Results of the chemical analyses of granulated blast furnace slag sample and typical slag composition obtained from National Slag Association –NSA (USA) is given in Table 3.

Table 2. Chemical analyses of coal slag sample and Eurogrit coal slag abrasive.

Components	SiO ₂	Al ₂ O ₃	CaO	Fe ₂ O ₃	MgO	Na ₂ O	K ₂ O	Other	LOI
Eurogrit (%)	45-52	24-31	3-8	7-11	2-3	0-1	2-5	traces	-
Coal Slag (%)	48.1	10.5	13.7	7.4	6.2	1.6	1.6	0.9	9.6

Table 3. Chemical analyses of granulated blast furnace slags.

Components	FeO	SiO ₂	MnO	Al ₂ O ₃	CaO	MgO	S	Other
NSA (%)	0.2-1.6	27-38	0.15-0.76	7-12	34-43	7-15	1.0-1.9	-
GBFS (%)	0.09	36.82	0.56	15.38	40.80	4.91	1.20	0.15

Apart from the little variations, GBFS seems to be a typical calcium silicate slag.

The chemical composition of domestic converter slag and its counterparts from South Africa (Lieuw Kie Song and Emery 2001), Taiwan (Li 1999) and USA (NSA 2005) is given Table 4. High iron and CaO contents of converter slag sample draw attention. The reason may be originated from higher scrap and lime addition to produce a strongly basic slag. Although most of calcium exists in bound crystalline form with the other constituents, converter slag can also contain free lime.

When the chemical composition of Chrome Grit (Gritblasting Equipment Sales 2005) and ferrochrome slag sample is compared (Table 5) it is seen that ferrochrome slag has lower iron, silicon and chromium content. However, its magnesium

content is much higher than that of the ferrochrome slag abrasive used in industry. Those differences might be originated from source materials and fluxing agent used in ferrochrome production, and efficiency of operation.

3.2 Standard Specifications

Turkish standard TS EN ISO 11126 evaluates the materials from the aspects of size distribution, apparent density, hardness, moisture content, water soluble contaminants and water-soluble chlorides.

According to TS EN ISO 11126 abrasive particles should not be coarser than 3.15 mm and amount of particles finer than 0.2 mm and coarser than 2.8 mm should not be higher than 5 %. Sieve analyses of investigated materials are given in Figure 1.

Table 4. The Major components of converter slags.

Components	Total Fe	FeO	SiO ₂	MnO	Al ₂ O ₃	CaO	MgO
Converter Slag (Turkey) (%)	21.87	9.36	9.62	4.66	0.89	49.48	2.39
South Africa (%)	19.2	12.1	12.5	4.8	4.1	36.4	8.9
Taiwan (%)	1-8	5-20	13-16	4-7	0.9-1.7	45-52	4-6
USA (%)	-	24	15	5	5	42	8

Table 5. Chemical analyses of Chrome Grit and ferrochrome slag sample.

Components	Fe ₂ O ₃	SiO ₂	Al ₂ O ₃	CaO	MgO	TiO ₂	Cr ₂ O ₃	Other
Chrome Grit (%)	8	32	26	2	20	1	12	-
Ferrochrome Slag (%)	1.75	25.2	23.6	1.4	41.8	0.3	5.3	0.6

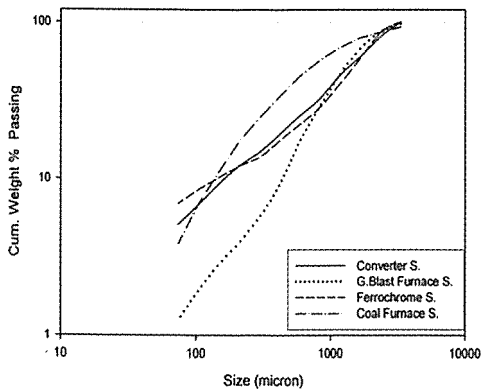


Figure 1. Sieve analyses of converter slag, granulated blast furnace slag, coal furnace slag and ferrochrome slag.

Particle size distributions of coal furnace slag and granulated blast furnace slag samples showed that original materials can not be used as an abrasive in blast cleaning without sizing. However, more than 70 % of original coal furnace slag and almost 90 % of original granulated blast furnace slag can be utilized as abrasive after only a proper sizing if they meet the other specifications requested by the blast cleaning industry. On the other hand, lumpy nature of converter slag and ferrochrome slag necessitated a crushing stage before sizing. After successive

crushing and sizing it is also seen that almost 90 % of converter slag and ferrochrome slag can be used in blast cleaning operations from the point of size distribution.

Measured apparent densities of investigated materials and standard specifications are given in Table 6.

Table 1. Apparent densities of materials.

Material	CFS	GBFS	CS	FS
Standard (kg/dm ³)	2.4-2.6	3.0-3.3	-	3.47*
Sample (kg/dm ³)	2.1	2.4	3.8	3.4

*Chrome Grit, <http://www.gritblasting.co.za/msds.htm>

As it is seen from the 6 coal furnace slag and granulated blast furnace slag samples do not meet the specifications. Both of them are below the required values. Lower apparent density of coal furnace slag is attributed to its chemical composition. Low Al₂O₃ content and unburned coal possibly reduces its apparent density. As to granulated blast furnace slag, its apparent density is much lower than specified values. This might point out a porous structure possibly due to cooling regime. Converter slag has the highest apparent density among studied materials. It might be due to high iron

content in the slag and possibly occur with scrap metal additions during steel production. Compared to ferrochrome slag abrasive used in industry, Turkish ferrochrome slag seems to be suitable to be

utilized in blast cleaning from the density point of view.

Common specifications of non-metallic abrasives covered in TS EN ISO 11126 with the investigated slag samples are compared in Table 7.

Table 7. Specifications of Turkish (ISO) standards with investigated slag samples.

Specification	Standard	GBFS	CS	FS	CFS
Hardness (Mohs)	Min. 6	> 6	> 6	> 6	6 (?)
Moisture Content (%)	Max. 0.2	0.02	0.03	0.04	0.03
Water-Soluble Contaminant (mS/m)	Max. 25	15.7	811	14.3	-
Water Soluble Chloride (%)	Max. 0.0025	0.0004	0.0013	0.0001	-

The results show that hardness of granulated blast furnace slag, converter slag and ferrochrome slag are obviously greater than 6 in Mohs scale. On the other hand, different particles of coal furnace slag sample scratches the glass slide in different levels, therefore the exact hardness value of coal furnace slag is doubtful and it is considered to be low to be used in blast cleaning. While converter slag meets most of the criteria, its conductivity value exceeds the maximum allowable limit. However, this problem may easily be overcome by thorough washing with river water. Pre-treatment of washing not only removes the water soluble contaminants but may also prevent dusting generated by adhering fines. Conductivity of coal slag and its water soluble chloride

content were not determined because of its failure in industrial application. Table 7 reveals that granulated blast furnace slag and ferrochrome slag meet all the common specifications of related standards and appears to be a good candidate to be a blasting abrasive. However, industrial application determines the final decision.

3.3 Industrial Application

Industrial application is the most important stage in determining the success of a material as blasting abrasive since this stage determines the performance of abrasives and quality of the obtained surfaces to be suitable for coating systems. Table 8 gives the results of industrial application of tested materials.

Table 8. Results of industrial application of tested materials.

Material	Degree of Cleanliness (TS EN ISO 8501)	Surface Roughness (Rugotest No.3)	Contamination	Dusting
Converter Slag	Sa 2	B N9a	No residue	Low
G. Blast Furnace Slag	Sa 2 ½	BN9 - B N10	White Spots	Low
Ferrochrome Slag	Sa 2 ½	B N9b	White Spots	High
Coal Furnace Slag	< Sa 1	< B N6	-	High

Industrial application of converter slag showed that the tested sample provided "Sa 2" degree of cleanliness removing most of the mill scale, rust, and foreign matter from the work surface. "Sa 2" is considered, in many cases, satisfactory ensuring that high enough pressure is applied and enough cleaning time is given. The slag sample provided surface roughness of B N9a on Rugotest No.3, which is sufficient for general purpose blast cleaning operations. Therefore, the tested sample was accepted to have a promising cleaning performance meeting the requirements of the industry. It was also observed that the tested sample did not leave residues on the work surface preventing premature failure of coating system due to contamination. It appeared to be a low dusting material, which is an important characteristic for occupational health concerns and from the ergonomics point of view. All those observations show that the converter slag can be a reasonable alternative to standardized and commonly used blasting abrasives in market.

The application of granulated blast furnace slag on the work surface revealed that it provides "Sa 2½" degree of cleanliness and created brighter, near to white, surface than does the converter slag. However, the appearance of blasted surface was misleading. When the worked surface was viewed with magnification, it was realized that the sample leaved local traces of contamination in the form of white spots. The residues smear the surface and gave an extra brightness and white look. In addition, it did not create mush dust during the operation, which gives superiority to an abrasive. Comparison of the worked surface with the surface profile comparator showed that the sample provides surface roughness between the mid point of B N9 and B N10 on Rugotest No.3, which is suitable for all purpose blast cleaning operations. As a result, although granulated blast furnace slag has a good cleaning performance, it can not be utilized as an abrasive due to left residues on the blasted surface.

The application of the ferrochrome slag gave similar results to granulated blast

furnace slag. It provided "Sa 2½" degree of cleanliness and created brighter, near to white, surface. However the appearance of blasted surface was misleading. Because, it leaved local contamination in the form of white spots similar to granulated blast furnace slag. The spots were much larger and greater in number. In contrast to granulated blast furnace slag, ferrochrome slag sample created high amount of dust during the operation due to explosion of particles when they impact the work surface. Surface profile test showed that it provided surface roughness of B N9b on Rugotest No.3, which does not meet the specifications of general purpose blast cleaning operations. As a result, ferrochrome slag sample from Eti Krom is not suitable to be utilized as an abrasive in surface preparation of steel surfaces.

Coal furnace slag was not able to clean the surface from mill scale, rust and paint coatings. Visual assessment of surface cleanliness showed that the tested sample is not applicable in blast cleaning operations. It did not fulfill the requirements of the "Sa 1" degree of cleanliness, which is the lowest degree in blast cleaning. Although the sample created some local roughness, it was not able to provide the lowest degree of roughness, which is B N6 on Rugotest No.3. Hence it does not meet the surface profile requirement by the industry, which is commonly in the range of B N9a-B N10a in industry. Besides, the test sample created high amount of dust during the operation. Therefore it is decided that coal furnace slag from Çayırhan thermal power plant can not be utilized as an abrasive in blast cleaning operations.

4 CONCLUSIONS

This study showed that although the standards do not contain any specifications about chemical composition of the abrasives except for water soluble compounds. It appears that chemical composition affects the quality and performance of an abrasive. Sieve analysis of investigated materials shows that none of the materials can be used

directly as an abrasive in blast cleaning operations. They should be prepared for industrial application by drying, crushing and screening treatments. Washing of abrasives with fresh water improves their quality, since washing not only removes the water soluble contaminants but also prevents dusting generated by adhering fines. Standard specifications are the pre-requests for the materials to be utilized as abrasive. But, industrial application determines the final decision.

The converter slag from Erdemir Iron and Steel Works provides "Sa 2" degree of cleanliness and sufficient surface roughness. Although it has a conductivity value above the allowable limit, this problem may easily be overcome by washing with fresh water and it can be utilized as an abrasive in surface preparation operations before the general purpose application of epoxy paints. Converter slag is mainly utilized as pavements, road construction material and railway ballast. In the literature, there is limited information about the utilization of those materials as blasting abrasive. This study showed that converter slag can be a good alternative to silica sand.

Although the granulated blast furnace slag from Ereğli Iron and Steel Works has a good cleaning performance, it can not be utilized as an abrasive in surface preparation of steel since it leaves local traces of contamination in the form of white spots on the worked surface. The coal furnace slag from Çayırhan thermal power plant can not be utilized as an abrasive in blast cleaning operations in view of the fact that it can not maintain the minimum cleaning performance and creates excessive dust. The ferrochrome slag from Eti Krom A.Ş. can not provide required surface roughness for general purpose blast cleaning operations. It leaves white spots and smears the work surface giving it an extra brightness and white look. Consequently ferrochrome slag can not be utilized as an abrasive in surface preparation of steel substrates.

ACKNOWLEDGEMENT

Financial support from Middle East Technical University (BAP- 2005-07-02-00-84) is gratefully acknowledged.

REFERENCES

- Amada, S., and Hirose, T., 1998. Influence of grit blasting pre-treatment on the adhesion strength of plasma sprayed coatings: fractal analysis of roughness, *Surface and Coatings Technology*, 102, pp 132-137.
- Amada, S., Hirose, T., Senda, T., 1999. Quantitative evaluation of residual grits under angled blasting, *Surface and Coatings Technology*, 111, pp 1-9.
- Çelik, E., Demirkıran, A. Ş., Avcı, E., 1999. Effect of grit blasting of substrate on the corrosion behavior of plasma-sprayed Al_2O_3 coatings, *Surface and Coatings Technology*, 116-119, pp 1061-1064.
- Eurogrit B.V., Products, Eurogrit aluminium silicate (coal slag grit) available at http://www.eurogrit.nl/temp/uk_us/index.html, retrieved 10 January, 2005.
- Griffiths, B.J., Gawne, D.T., Dong, G., 1996. The erosion steel surfaces by grit blasting as a preparation for plasma spraying, *Wear*, 194, pp 95-102.
- Gritblasting Equipment Sales, Chrome Grit, *Material Safety Data Sheet*, available at <http://www.gritblasting.co.za>, retrieved 16 January, 2005.
- Hansel D., 2000. Abrasive Blasting Systems. *Metal Finishing*, 98, 7 (July).
- Harris, A.F., Beevers, A., 1999. The effect of grit blasting on surface properties for adhesion, *Int. Jour. Adhesion and Adhesives*, 19, pp 445-452.
- Kambham, K., Sangameswaran, S., Datar, S.R., Kura, B., 2007. Copper slag: optimization of productivity and consumption for cleaner production in dry abrasive blasting, *Journal of Cleaner Production*, 15, 5, pp 465-473.
- Li, Y.S., 1999. The use of waste basic oxygen furnace slag and hydrogen peroxide to degrade 4-chlorophenol, *Waste Management*, 19, pp 495-502.
- Lieuw Kie Song, E.R., Emery, S., 2001. Preliminary development of slag as a stabilised material for labour intensive construction of roads, *Proceedings of First International Conference on Employment Creation in Development*, South Africa.
- Mellali, M., Grimaud, A., Frauchais, P., 1994. Parameters controlling the sand blasting of substrates for plasma spraying, *Proceedings of the 7th National Thermal Spray Conference*, pp 227-232, Boston.

- Momber, A.W., and Wong, Y.C., 2005. Overblasting effects on surface properties of low-carbon steel, *JCT Research*, 2, 6, pp 453-461.
- NACE International Basic Corrosion Course Handbook, 2000, chp 14, 7-14, Houston.
- National Slag Association (NSA), Steel Slag, available at http://www.nationalslagassoc.org/PDF_files/SSPr emAgg.PDF, retrieved on 20 January, 2005.
- Robinson, J. (Ed.), 2000. What lies beneath – surface preparation, the key to coating performance, *Corrosion Management*, May, pp 16-22.
- Rosenberg, B., Yuan, L., Fulmer, S., 2006. Ergonomics of abrasive blasting: A comparison of high pressure water and steel shot, *Applied Ergonomics*, 37, 5, pp 659-667.
- Staia, M.H., Ramos, E., Carraquero, A., Roman, A., Lesage, J., Chisot, D., Mesmacque, G., 2000. Effect of substrate roughness induced by grit blasting upon adhesion of WC-17%Co thermal sprayed coatings, *Thin Solid Films*, 377-378, pp 657-664.
- TS EN ISO 11126, 2002. Preparation of steel substrates before application of paints and related products - Specification for non - metallic blast cleaning abrasives, *Turkish Standards Institution*, Ankara.
- TS EN ISO 11127, 2002. Preparation of steel substrates before application of paints and related products - Test methods for non-metallic blast cleaning abrasives, *Turkish Standards Institution*, Ankara.
- TS EN ISO 8501-1, 2000. Preparation of steel substrates before application of paints and related products-Visual assessment of surface cleanliness Part 1: Rust grades and preparation grades of uncoated steel substrates after overall removal of previous coatings, *Turkish Standards Institution*, Ankara.
- Wingen, J., 1988. Grit blasting as surface preparation before plasma spraying, *Surface and Coatings Technology*, 34, pp 101-108.

Laboratory-Based Flowsheet Development of Iranian Ilmenite Upgrading

M. Irannajad

Department of Mining, Metallurgical and Petroleum Eng., Amirkabir University of Technology, 424, Hafez Ave. Tehran, 15914, Iran

A. Mehdilo

Mining Eng. Group, Amirkabir Jahad Daneshgahi Unit, Tehran, Iran

ABSTRACT A process root selection was investigated on hard rock titanium deposit of Qara-aghaj, Ueromieh, Iran. The deposit contained ilmenite as valuable mineral with average grade of 8.5% TiO₂.

Mineralogical studies performed by optical microscopy, SEM and XRD, indicated that the ore consists mainly of ilmenite, magnetite, titanomagnetite and some gangue minerals such as pyroxene, olivine and plagioclase. The ilmenite was mainly granules form but some lamellae forms of ilmenite were found inside the magnetite. Also very narrow lamellae of hematite and hemo-ilmenite were found inside the ilmenite. The liberation degree of ilmenite was determined 150 microns.

Several concentrating circuits were investigated for selection of an optimum ilmenite upgrading flowsheet. Among them, the combination of heavy liquid (Clerici solution with SG=4) and low intensity-wet magnetic separator (LIWMS) presented an ilmenite concentrate containing 43.5% TiO₂. An ilmenite concentrate grading 45% TiO₂ was obtained by the combination of shaking table and LIWMS. A modification on latter flowsheet consisting of regrinding of LIWMS tailing and recirculating it on LIWMS a final concentrate could be obtained with 44.5% total recovery.

1 INTRODUCTION

1 INTRODUCTION

Ilmenite, with anatase and rutile, is the main source of TiO₂. Ilmenite, with the general chemical formula, FeTiO₃, is an accessory mineral of igneous rocks, and is found in sedimentary deposits. The theoretical content of TiO₂ in ilmenite is 52.6%. The processing industry separates ilmenite into two main types, hard-rock and beach sand varieties. Ninety percent of TiO₂ pigments production comes from ilmenite. The rest comes from rutile and other minerals. Titanium metal is well known for its resistance to corrosion and its mechanical strength in alloys, however, about 90% of titanium is used in the form of TiO₂ as a white pigment in paint, papers and plastics.

About 10% of titanium is used in metal form, mainly in aerospace industries (Nantel, 2001).

The Qara-aghaj hard rock titanium deposit (one of two-titanium deposit in Iran) is located in the 36 Km at the North-West of Euromieh in Azarbayejan province, Iran (Figure 1). Based on the preliminary exploration, some 1590 meters trenches have excavated throughout in the outcrop of the ultramafic mass. In addition, four exploration faces and two boreholes with overall length about 155 meters have been excavated in this stage. The calculations concerning to the reserve estimation indicate that there are 209 Mt titanium ore with averaging of 8.5% TiO₂ in the deposit. From the reserve viewpoint, the Qara-aghaj deposit can be compared with the other hard rock

deposits such as Tellnes in Norway, by having a low TiO₂ content. In spite of abundant uses of the titanium in different industries, there is not any production of the titanium in Iran. So, the deposit can be considered as a titanium source in the country (Karkkainen and Appelqvist, 1999).

provided and studied. Figure 2 shows sampling from one of the faces.

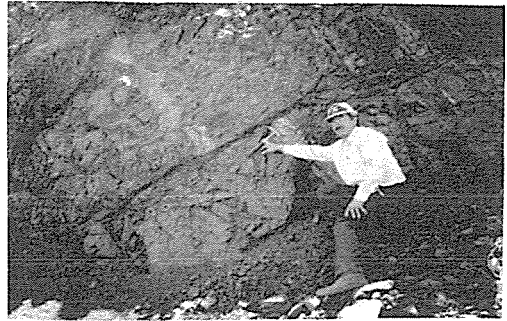


Figure 2. Sampling from one of the faces.

2 SAMPLES CHARACTERIZATION

2.1 Sample Preparation

The procedure in which the sample was prepared for different analysis is illustrated in Figure 3.



Figure 1. Location map of Qara-aghaj deposit.

For the mineral processing tests in the laboratory scale, a representative sample is

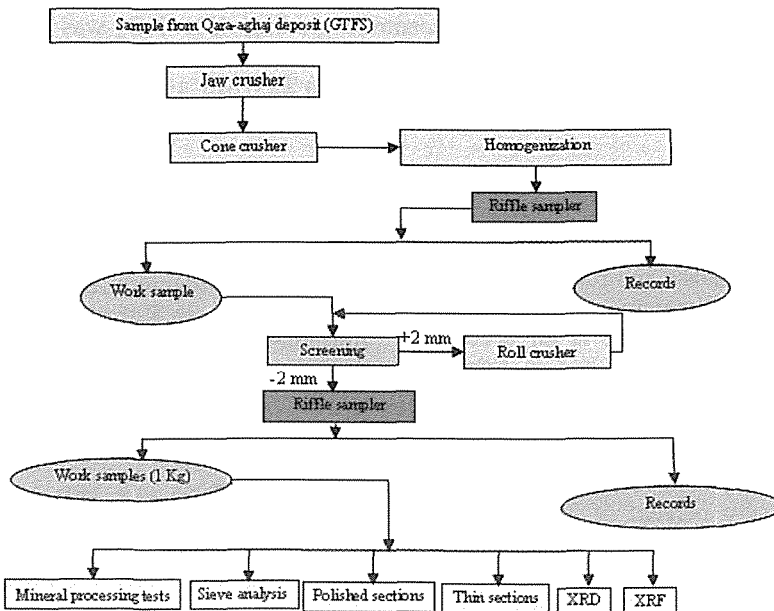


Fig.3. sample preparation procedure.

2.2 Size Analysis

After crushing less than 2 mm, the sample was sieved. According to the results presented in Figure 4 the d_{80} of sample is 1190 μm .

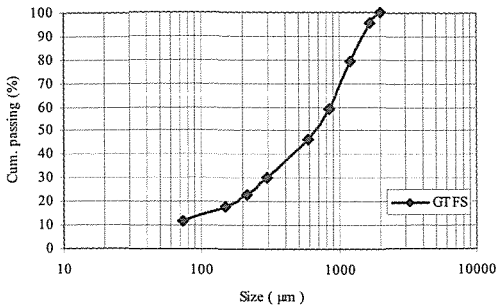


Figure 4. Sieve analysis of sample

2.3 Chemical Analysis

The chemical composition of sample, shown in Table 1, was determined by X-Ray fluorescence (XRF) method. The TiO_2 content of the sample confirmed the results obtained in the exploration stage.

Table 1. Chemical composition of sample

Component	Fe_2O_3	SiO_2	MgO	TiO_2	CaO	Al_2O_3	P_2O_5	MnO	S	V_2O_5	L.O.I
%	34.4	27.4	15.0	9.0	5.9	3.1	2.9	0.41	<<	0.14	0.86

Table 2. Main minerals observed in the thin sections

mineral	considerations
Pyroxene	containing clinopyroxene and orthopyroxene
Olivine	Its content in mineralization zone is more than diorite (gangue) zone
Plagioclase	forming a large portion of low-grade zone of the ore
Amphibole	as hornblende form resulting from alteration of clinopyroxene
Opaque minerals	opaque minerals involve ilmenite and magnetite filling the spaces between silicate minerals
Secondary minerals	such as chlorite, antigorite and serpentine resulting from alteration of clinopyroxene and olivine
Other minerals	apatite, quartz, feldspar

2.5.2 Polished Sections

Some 42 polished sections were prepared and studied; among them, some sections are

2.4 Phase Analysis

According to the X-Ray diffractography, the main valuable minerals consist of the ilmenite (17% approx.) and the magnetite (16% approx.). The other minerals present in the sample are pyroxene, olivine, plagioclase, hornblende, apatite and secondary minerals such as chlorite.

2.5 Ore Microscopy

2.5.1 Thin Sections

Based on the results obtained from 19 thin sections studies, the main minerals observed in the ore are described in the Table 2.

Figure 5 shows interlocking of the main minerals of the ore and quality of the mineralization. The mineralization is taken place in the pyroxenite. The interlocking of minerals in the mineralization and gangue zones is indicated in Figure 6. The plagioclases have formed the main portion of the gangue (dioritic) zone. It is important to mention that the mineralization in the gangue zone is very low with very fine grains.

illustrated in the Figure 7. The main opaque minerals observed in the polished sections are the ilmenite and magnetite that are interlocked and surrounded by the pyroxene

and olivine. There are very fine titanomagnetite grains in the background of the magnetite. The magnetite is found in the spongy and compact forms. The lamellae of

the ilmenite are observed inside the compact type. In addition, the fine grains of the apatite have formed within the ilmenite and magnetite or contacting with them.

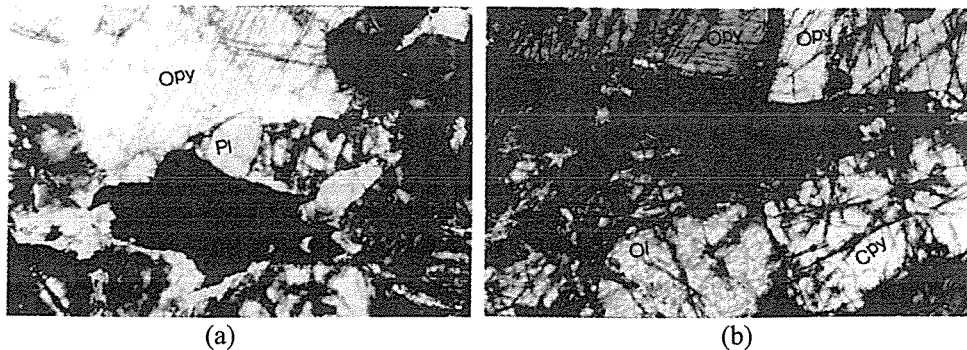


Figure 5. Interlocking of transparent and opaque minerals in the mineralization zone
 a: the plagioclases quantity is very low, and the right cleavage of orthopyroxene is observed
 b: the olivine and the clinopyroxene are altering into the amphibole and chlorite
 (*Opy*: orthopyroxene *Cpy*: clinopyroxene *Ol*: olivine *Pl*: plagioclase)

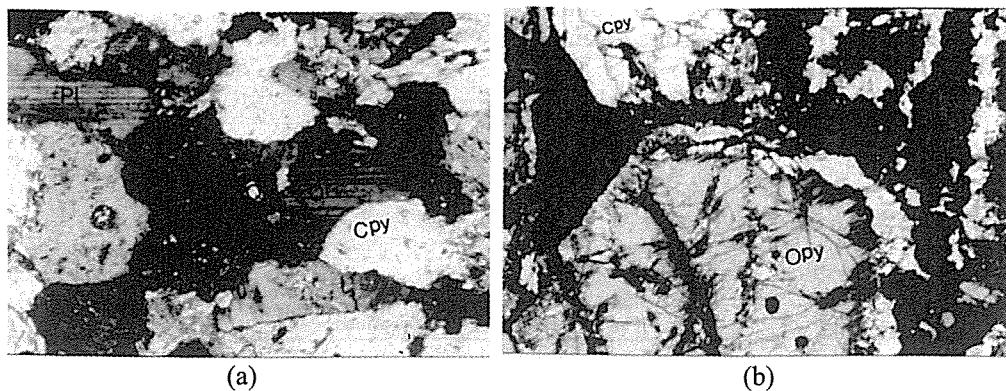


Figure 6. Interlocking of the minerals in the mineralization and gangue (dioritic) zones
 a: gangue (dioritic) zone, mainly formed from plagioclase
 b: mineralization zone (accompanying with clinopyroxene and orthopyroxene)
 (*Opy*: orthopyroxene *Cpy*: clinopyroxene *Ol*: olivine *Pl*: plagioclase)

The sulphide minerals such as pyrite, chalcopyrite and pyrotite appear in the inclusion form inside the ilmenite and magnetite or in the exsolution forms (Figure 7). The quantity of the sulphide minerals being very low in the face sample, its quantity is higher when the depth is increased.

The ilmenite is found in granules form, but some lamellae of the ilmenite are found inside the magnetite. These lamellae are very narrow and so unrecoverable by the physical methods. Some lamellae of the hematite are also observed inside the ilmenite.

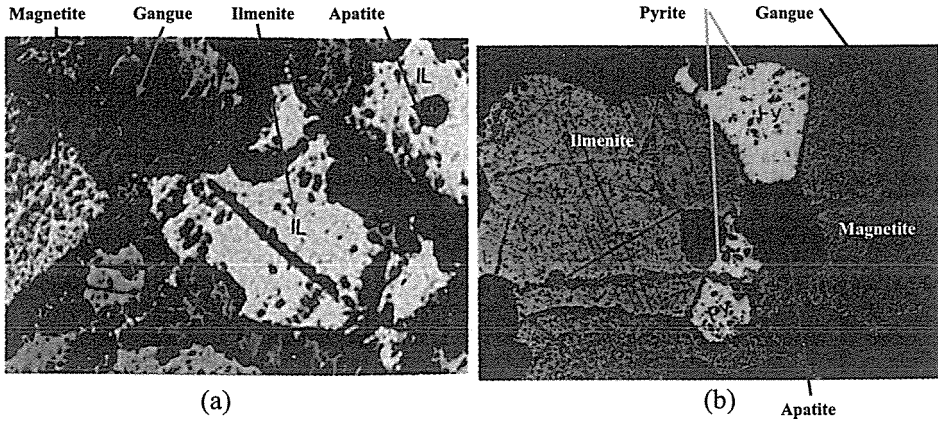


Figure 7. a: presence of apatite inside Ilmenite and magnetite as opaque minerals.
 b: presence of sulphide minerals in borehole sample (interlocking of pyrite and apatite with ilmenite and magnetite)

2.6 Examination by Electron Microscopy (SEM)

The studying by SEM, indicated that the light lamellae are found inside the the ilmenite which based on point analysis, the average of TiO_2 and Fe_2O_3 at them are 32.6% and 60.3% respectively. It is seems that, these lamellae are ilmino-hematite (Figure 8). There are some ilmenite lamellae by thicknes of 0.5-30 microns inside magnetite, which are caused the formation of ilmino-magnetite. In addition, some lamellae of

spinel are observed in the background of magnetite as hersinite ($FeAlO_4$) form and the olvo-spinel form at the ilminite background. Based on point analysis by using SEM, average chemical composition of ilmenite and magnetite minerals are presented in Table 3. Presence of Ti in the magnetite lattice as solid solution form has been caused formation of titanomagnetite. Replacement of Ti by Mg and Mn in ilmenite lattice results in reducing of TiO_2 in ilmenite.

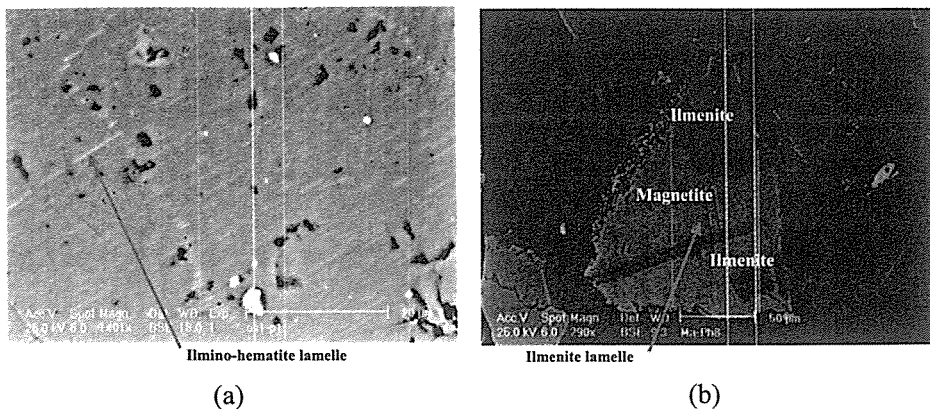


Figure 8. (a) Light lamellae inside the ilmenite (ilmino-hematite or hemo-ilmenite)
 (b) Interlocking of ilmenite and magnetite and relatively a thick lamelle of ilmenite inside magnetite (IL: ilmenite Ma: magnetite He: hematite Py: pyrite Ap: apatite)

Table 3. Chemical analysis of ilmenite and magnetite by SEM

Composition (%)	Fe ₂ O ₃	TiO ₂	V ₂ O ₅	MnO	MgO	SiO ₂	Al ₂ O ₃
Ilmenite	48.33	48.01	0.58	1.14	0.96	0.48	0.47
Magnetite	91.08	1.23	1.46	0.55	-	1.85	-

2.7 Liberation Degree

The results of the ilmenite liberation degree determined by grain counting method are presented in Figure 9. The 80% of the ilmenite is liberated at 150 μm and 50% at 380 μm.

In addition, the control of the liberation degree was performed by the heavy liquid test using methylene iodide (SG=3.3). The results have presented in Figure 10. These results confirm that the liberation degree for this ore is 150 μm.

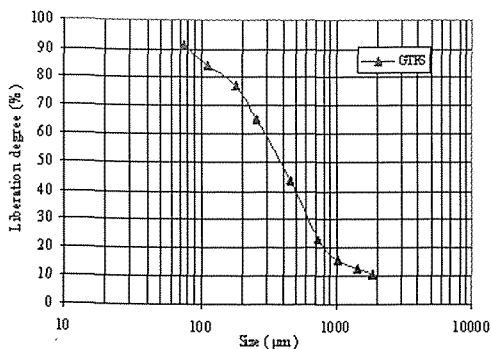


Figure 9. Ilmenite liberation degree by grain counting.

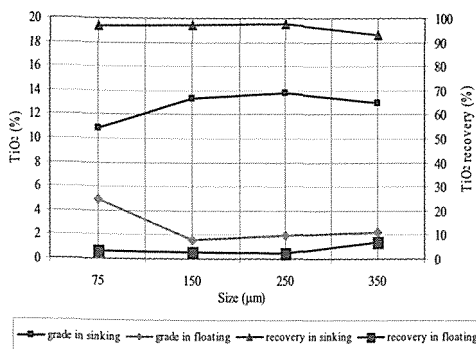


Figure 10. Controlling of liberation degree by heavy liquid tests.

3 SEPARATION TESTS AND DISCUSSION

Due to the physical properties of the ilmenite such as its paramagnetic property, high specific gravity and conductivity, a set of different combination of separation methods can be used. In this regard, the sieve and chemical analysis of the mill products after preliminary grinding tests, performed by the rod and ball mills, showed that the liberation could be obtained in the following conditions: after removing of the particles finer than 30 μm, by losing only 5.4% of TiO₂, the sample is ground in a rod mill with a 65 solid percent for 12 minutes.

Various combination tests that have been programmed and performed in this study are as following:

- 1- Shaking table - Low intensity wet magnetic separator (LIWMS)
- 2- Heavy liquid – permanent magnet (as a LIWMS)
- 3- Low intensity wet magnetic separator - High intensity wet magnetic separator
- 4- Low intensity wet magnetic separator (LIWMS) - Shaking table
- 5- Humphreys spiral - Low intensity wet magnetic separator

Among these tests, the results of the two combinations that have numbered 1 and 2 are described.

3.1 Heavy Liquid – Permanent Magnet (as a LIWMS) Combination Test

The procedure and the results obtained are presented in Figure 11. The test was performed by using a Clerici solution (SG=4) on the face sample discarded of (-75 μm) fraction. A compound concentrate of the ilmenite, magnetite and titanomagnetite grading of 32.2% TiO₂ was obtained. A magnetic separation, by a permanent magnet (as LIWMS) performed on the sink product, provided an ilmenite concentrate (NM)

having 43.5% TiO₂ content by a 61.3% recovery. The magnetic fraction (M) was formed a titanomagnetite product with 20.3% TiO₂ content by a 27.0% distribution. In this

test, a final tailing (floating fraction) forming 69.8% of the feed and having a 1.84% TiO₂ content with only 11.7% loss of TiO₂, could be rejected.

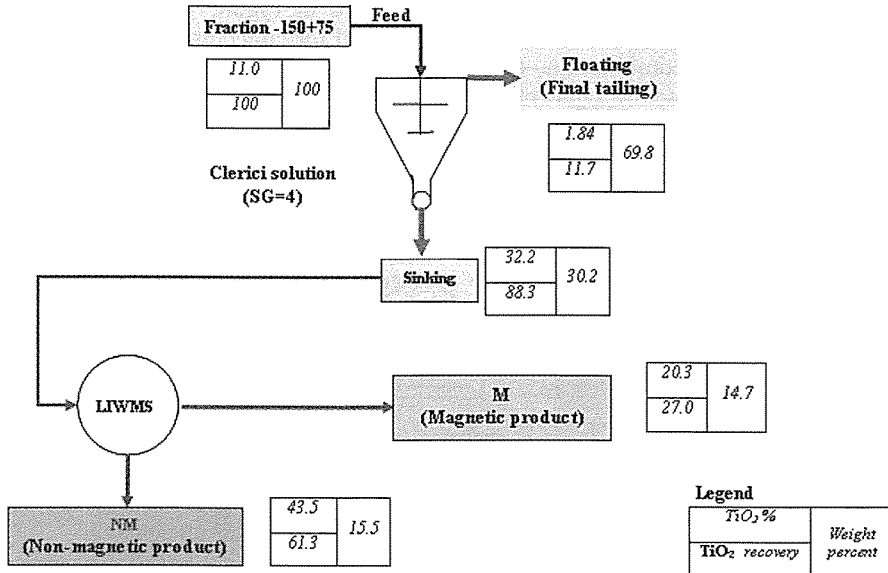


Figure 11. Schematic diagram of heavy liquid- LIWMS separation.

3.2 Shaking Table- LIWMS Combination Test

The procedure in which the test was performed is presented in Figure 12. After grinding of the face sample, the ore was concentrated by shaking table. The middling product (M1) of the first table was retailed by obtaining a concentrate (C2) that mixed with the first table concentrate (C1) and the combination of the two concentrate (C3) were fed a Eriez low intensity wet magnetic drum separator. This magnetic separator produced an ilmenite concentrate (NMP1) grading of 45.2% TiO₂ and a recovery of 39.1%. The magnetic product (MP1) was reground to 80% finer than 75 μm by a ball mill to liberate some of the interlocked ilmenites. The magnetic separation of this reground product provided a second ilmenite concentrate (NMP2) with grade of 40.3% TiO₂ by a recovery of 5.3% of TiO₂. Mixing

of this two concentrates (NMP1 and NMP2) produced a final concentrate (C) having a 44.5% TiO₂ content by a recovery of 44.4%. It is obvious that the middling product of second table (M2), having the same TiO₂ content with the feed (F), can be used as a circulating load in a continuous operation. A final tailing (T), having a 3.19% TiO₂ content, caused 13.5% loss of the total TiO₂. Also, by second magnetic separation on the reground product, a titanomagnetite product (MP2) was obtained. It is a potential by-product to recover V₂O₅.

4 CONCLUSION

Due to a considerable reserve of 209 Mt of the ore with of 8.5% TiO₂ content, the Qaraaghaj rock deposit can be considered as a potential titanium resource in Iran. The valuable products that can be recovered are

the ilmenite and titanomagnetite as the main valuable minerals, the magnetite and the pentaoxides of vanadium and phosphorus as the by-products. The V_2O_5 can be recovered by chemical processing of a titanomagnetite product and the P_2O_5 can be obtained by the flotation of the final tailing of the gravity separator.

Among the various combination tests performed, the suitable ilmenite concentrate

was obtained by the combination of the gravity-magnetic separators. In this regard, an ilmenite concentrate grading about 45% TiO_2 could be produced by a reasonable recovery. So, based on the results obtained from various tests performed, a flowsheet presented in Figure 13 was developed and proposed for concentration of the Qara-aghaj ore.

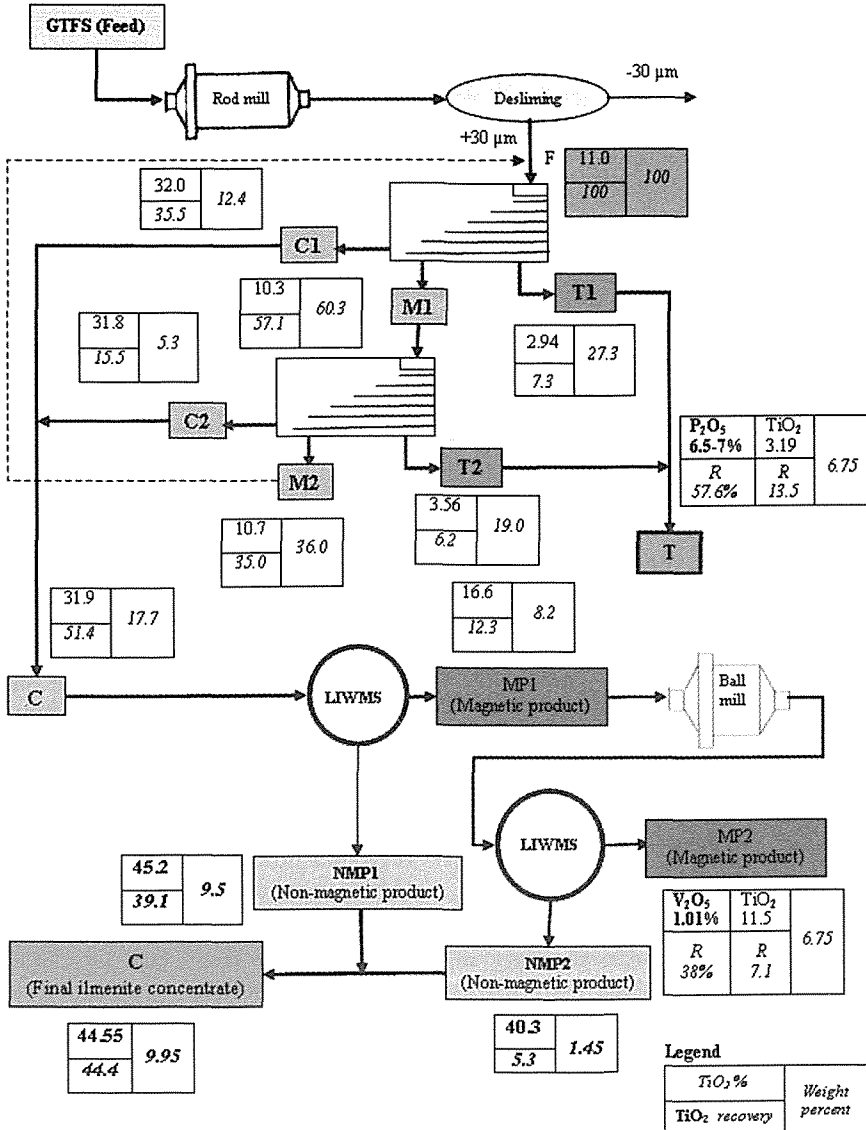


Figure 12. Schematic diagram of of shaking table - LIWMS combination test.

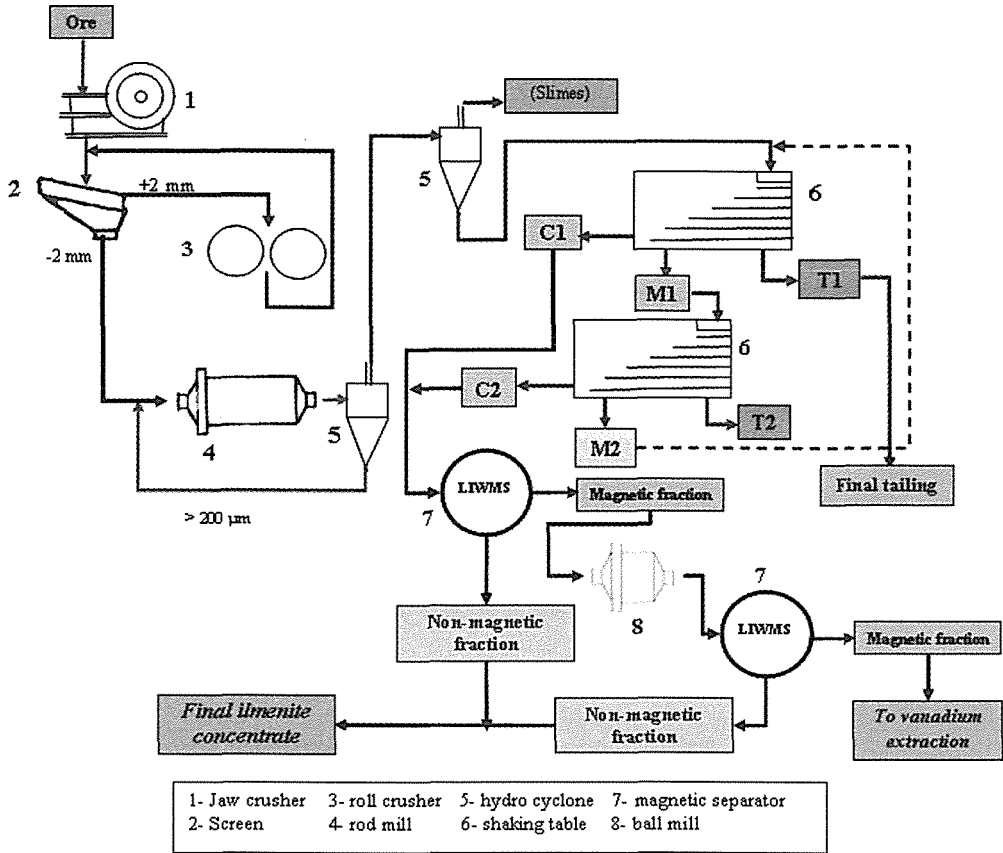


Figure 13. Flowsheet proposed for concentration of the Qara-aghaj titanium ore.

REFERENCES

Chernet, T., (1999); "Mineralogical and textural Constraints on mineral processing of the koivusaarenneva ilmenite ore, western Finland". International Journal of Mineral Processing, Vol. 57, PP. 153-165.

Chernet, T., (1999); "Applied mineralogical studies on Australian sand ilmenite concentrate with special reference to its behavior in the sulphate process"; Minerals Engineering, Vol.12, No. 5, PP. 485-495.

Gonzalez, L.M. and Forssberg, K.S.E., (2001); "Utilization of vanadium - containing tittanomagnetite: possibilities of a beneficiation - based approach"; Mineral Processing and Extractive Metallurgy, Vol. 110, pp. 63-72.

Gramatikopoulos, T., Mcken, A. and Hamilton, C.; (2002); "Vanadium-bearing magnetite and ilmenite mineralization and beneficiation from the Sinarsuk V-Ti project, West Greenland"; CIM Bulletin, 95 (1060), 87-95.

Irannajad, M.; (1990); "Pilot plant flowsheet development of the Kahnooj titanium ore deposit. Report of investigation"; Amirkabir University of Technology, Tehran, Iran.

Irannajad M., (1990); "Mineral processing studies on Kahnooj ilmenite samples" MSc Thesis, Amirkabir University of Technology, Tehran, Iran.

Irannajad M. and Mehdilo A.; (2004); "Concentration of Iranian Titanium Ore by Physical Methods"; 2nd International Gravity Concentration Symposium (Gravity 04), Perth, Australia.

- Irannajad M.; (2004); "Mineral processing studies on Iranian titanomagnetite resources: Case study on Qara-aghaj hard rock titanium ore deposit Project"; Research Report, Amirkabir University of Technology, Tehran, Iran.
- Irannajad M.; (1989); "Kahnooj titanium ore processing and Pilot plant flowsheet development"; Amirkabir Scientific- Research Seminar, Tehran, Iran.
- Kärkkäinen, N. and Appelqvist, H.; (1999); "Genesis of a low-grade apatite – ilmenite–magnetite deposit in the Kauhajärvi gabbro, Western Finland". *Mineralium Deposita*, Vol. 34, PP. 754-769.
- Mehdilo A.; (2003); "Mineral processing studies of Qara-aghaj titanium ore by physical methods", MSc Thesis, Amirkabir University of Technology, Tehran, Iran.
- Mehdilo A. and Irannajad M.; (2005); "Mineral processing of Euromieh Qara-aghaj titanium ore"; Iranian Mining Engineering Conference – 2005 Proceedings Vol. 2, pp. 1247- 1262.
- Nantel, S.; (2001); "The Sept– iles project – A new apatite/ilmenite producer". *CIM Bulletin*, NO.1049, PP. 59-63.
- Panov, S.P., Metson, J.B. and Batchelor, J.J; (2000); "Beneficiation of Newzealand ilmeno–magnetites" *In: The AusIMM Proceedings*.
- Petruk, W.; (2000); "Applied Mineralogy in the Mining Industry"; Elsevier pub.
- Watson, J. L. and Low, H. F.; (1982); "The Role of Titanomagnetite in Gravity Separation of New Zealand Ironsands". *The Metallurgical Society of AIME*; PP. 135-149.
- Weiss, N.L. Editor; (1985); *SME Mineral Processing Handbook*, Vol. 2. SME–AIME; pp. 27-14:27-17.
- Zussman, J.Editor; (1971); *Physical Methods in Determinative Mineralogy*, Academic Press.

Computer-Based Optimization of Air Separators

S. Rashidi

Amirkabir University of Technology, Mining, Metallurgical and Petroleum Engineering Department, Tehran, Iran

M. Irannajad

University of Kashan, Faculty of Engineering, Mining Department, Kashan, Isfahan, Iran

A. Farzanegan

ABSTRACT Air separator devices are commonly used in dry grinding circuits for classification of fine and very fine particles. As performance of air classification affects grinding circuit capacity and energy consumption, different studies have been done to increase performance of air separators through optimizing operational parameters by simulating air classification process. This paper discusses about using models on the basis of performance curve for simulating air classification process by introducing ASSIM implemented in VBTM. Accuracy and validation of obtained results is tested by comparing outputs of ASSIM with measured data.

1 INTRODUCTION

Application of air separators in dry grinding circuits have been increased by increasing demands for finer products. Dry grinding circuit of cement production is the most important application of air separators while cement consumption in 2005 had been 2.3 billion tonnes (GLOBAL CEMENT to 2020) increasing by 1% annually. Grinding circuits use up to 40% of power required to produce one tonne of cement product (Jankovic 2004). This large amount of energy consumption besides increasing demands for finer cement production justifies the need to improve the energy efficiency of grinding process. Higher performance results in increasing circuit capacity and reducing energy consumption. In recent years, considerable efforts have been spent on improving comminution efficiency both in development of machines and in the optimal design of grinding systems.

While manufacturers have gained high efficiency in the 3rd generation of air separators, evidences show that some times overall performance doesn't gain nominal

performance resulting from inefficient classification process that is due to not optimized operational parameters including rotor speed, feed tonnage, air flow rate and percent of fan opening. Mathematical modeling followed by circuit simulation is the best way to describe classification process and to optimize operational parameters by proven functions. In recent years, progresses in computer technologies make it possible to develop available softwares in recent years such as MODSIMTM, JKSimMetTM and COMSIM (Irannajad et al., 2006) which make it simple, easy and rapid in using validated models for describing, simulating and controlling processing devices.

In next sessions whiten equation that its validity has been proved through different case studies and applied for simulating different type of air separators is discussed. Finally, ASSIM is introduced and tested by real data sets.

2 MODELLING

Modeling is a valuable tool for describing different processes by proven mathematical functions. Models make it possible to have better knowledge of variables affecting performance of process and predicting products' characteristics. Final purpose of modeling is to control the device to have the required efficiency with lower energy consumption. In this sections variables and parameters affecting separation process is discussed followed by models used as the basis of software developed by authors of this article.

2.1 Variables and Parameters

Describing separation process by relations of forces acting on discrete particles and resulting to separation of particles into two streams is a useful approach to consider variables affecting separation's efficiency. These forces are centrifugal force resulting from rotor speed and air drag force that results from air transporting feed material (Kolacz 2000). Centrifugal (F_c) and air drag (F_d) forces for a spherical shape are as follow:

$$F_c = M * v^2 / r = V_p * \rho_p * v^2 / r \tag{1}$$

$$F_d = c_x * \rho * A * v_a^2 / 2 \tag{2}$$

Where V_p , ρ_p , A and M are the volume, the density, cross-sectional area and the mass of the particle, respectively, v is the peripheral velocity of the rotor, v_a is air velocity, ρ is gas density and c_x is drag coefficient.

Balance of these two forces across with weight force depends on particle's weight and separates them into fine or coarse streams. There is no doubt that efficient separation depends on good material dispersion, as agglomeration of fine particles together or on the surface of larger particles, make these particles to be classified into coarse stream as they are considered as large particles. In fact, material dispersion is not gained by 100%. So, optimization is a valuable tool in optimizing operating

conditions to have a sharper separation. It should be mentioned that it is impossible to develop simulators on the base of these relations and mostly they are applied to investigate variables affecting separation in order to have a better knowledge of classification process that would be helpful in developing models for simulating air separators.

There are 3 parameters to measure performance of the air separators (Karunakumari 2005) which are cut size (d_{50}), size selectivity (S_d) and separation sharpness (α). Cut size represents the size which 50% of particles are smaller than it and indicates the imaginary boundary size between coarse and fine streams. Size selectivity is defined as the ratio of the percent of particles of size d in the coarse fraction to that in the feed. For efficient classification, S_d should have small value for small particles and vice versa for larger ones. Relations of d_{50} and S_d for an ideal air separator are as follow:

$$\text{For } d > d_{50} \quad S_d = 1 \tag{3}$$

$$\text{For } d < d_{50} \quad S_d = 0 \tag{4}$$

Performance of the most size classification processes is described by a partition or performance curve popular as Tromp curve. It describes the proportion of the mass fractions of different sizes of feed materials which reports to coarse or fine products. The empirical relations to draw actual curves of efficiency for fine and coarse streams respectively are as follow:

$$E_{oa} = 100 \left(\frac{O o_i}{F f_i} \right) \tag{5}$$

$$E_{ua} = 100 \left(\frac{U u_i}{F f_i} \right) \tag{6}$$

Where O , U and F are fine, coarse and feed flow rates, respectively and o_i , u_i and f_i are percent of size "i" in the fine, coarse and feed streams, respectively.

Figure 1 illustrates schematic partition curves drawn according to both streams. It can be seen that there are two phenomena occurring during air classification process

called bypass and fish-hook showed. Bypass phenomenon is due to the fact that very fine particles because of not responding to classification forces enter coarse particle stream and fish-hook phenomenon which is the initial rise of efficiency curves rarely happens and is due to electrostatic forces that results in agglomeration of very fine particles on the surface of the coarse grains. Readers are referred to Nageswararao's article to study about origin, evolution and theory of this phenomenon in detail (Nageswararao 2000).

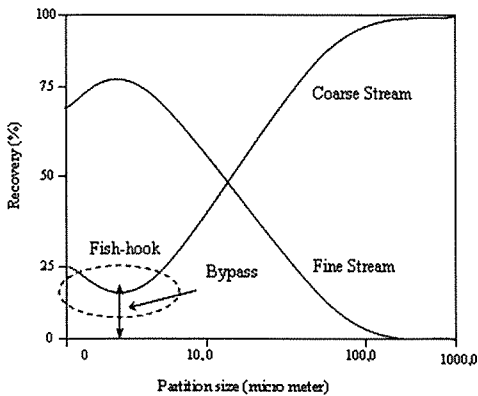


Figure 1. Schematic efficiency curve for fine and coarse streams.

Literatures discuss that the sharper the curve, the smaller the separation sharpness. In other words, sharpness of the separation depends on operating and design conditions. Comparing these curves at different operating and design conditions would be helpful in order to optimize these conditions. Therefore, in order to remove effect of bypass phenomenon and to rely on quantity of α , Kelsall's approaches are applied to obtain normalized or reduced curves (Kelsall 1953). This approach is popular because of its simplicity in calculating. Nageswararao reviewed different approaches in normalizing efficiency curves and proposed a new approach in addition (Nageswararao 1999a). Below relations describe Kelsall's formula as follow:

$$E_{uc} = \frac{E_{ua} - R_f}{1 - R_f} \tag{7}$$

$$E_{oc} = \frac{E_{oa}}{C} \tag{8}$$

Where E_{uc} and E_{oc} are Fraction of feed reporting to coarse and fine stream in reduced curve, respectively, E_{ua} and E_{oa} are fraction of feed reporting to coarse or fine stream in actual curve, respectively, R_f is bypass and C is material that is usually classified (1-bypass).

The best approach in comparing performance of air separators or performance of one air separator under different operating conditions is to use normalized efficiency curves because of removing effect of by-pass phenomenon.

2.2 Models

Many researchers have investigated to present functions capable of fitting efficiency curve in order to have a better knowledge of performance of the classifying device. There are two best known and tested approaches among them that include plitt (Plitt 1971) derived independently on the base of Rosin-Rammler function type and exponential equation derived by Whiten (Napeier-Munn 1999).

Plitt expression is as follow:

$$E_{uc} = 1 - \exp[-\ln 2(d/d_{50c})^m] \tag{9}$$

$$E_{uc} = 1 - \exp[-\ln 2(d/d_{50c})^m] + R_f \left(\frac{d_o - d}{d_o} \right) \tag{10}$$

Where E_{uc} is fraction of feed reporting to underflow (corrected curve), d is particle size, d_{50c} is corrected cut size, m is sharpness of separation parameter, d_o is the size below which entrainment occurs and R_f is percent of by-pass.

Whiten expression is an exponential function defined for the actual efficiency curve of fine stream (Napier-Munn 1999):

$$E_{oa} = C \left(\frac{\exp(\alpha) - 1}{\exp(\alpha X) + \exp(\alpha) - 2} \right) \tag{11}$$

Where E_{oa} is fraction of feed reporting to fine stream (actual curve), C is (1-By-pass), α is sharpness parameter, X is normalized particle size ($d/d50c$), $d50c$ is corrected cut size.

By applying an additional parameter, β , relation (11) would be capable of presenting fish-hook phenomenon (Napier-Munn 1999):

$$E_{oa} = C \left[\frac{(1 + \beta \cdot \beta^* \cdot X)(\exp(\alpha) - 1)}{\exp(\alpha \cdot \beta^* \cdot X) + \exp(\alpha) - 2} \right] \quad (12)$$

Where β is fish-hook parameter and β^* is a parameter that preserve definition of $d50c$ parameter (when $E_{oa}=1/2C$, $d=d50c$).

2.2.1 Comparison of Plitt and Whiten Models

Plitt was whom first proposed the classifiers as mixer models, claimed that his relation is more simple in use though he noted that precision of whiten prediction is much more. Plitt's claim is due to need of applying back calculations method in order to estimate whiten equation's parameters while nowadays, progresses in computer technology by developing statistical or spread-sheet softwares make it so much easy and rapid to fit whiten's model. It should be mentioned though Plitt further reported that sum of squares between the observed and predicted is lower for the Rosin-Rammler function than for the Whiten equation. In contrast with this claim, validity, accuracy and precision of predicted results obtained by whiten equation is tested by different case studies carried out by Benzer and his colleagues (Benzer et al., 2001a; Benzer et al., 2001b; Benzer H., 2004; Lynch et al., 2001) applying whiten equation in simulation air classification for static and dynamic air separators in cement plants. It should be also mentioned that parameters of Whiten equation are independent of operating conditions, so this feature make this function more helpful in optimizing operating conditions.

Nageswararao (1999b) carried out a detailed mathematical analysis of Plitt-Reid and Whiten functions that confirms similar

conclusion for the reduced efficiency curves. Across with Benzer's researches and his success in applying Whiten equation in Hacettepe University and this fact that most popular packages and softwares have used plitt's model in building them, two authors of this research, Farzanegan (1997) and Irannajad (2005), used plitt' model in developing computer program for simulating hydrocyclones. Besides all these softwares, it should be also mentioned that Conway (1985) developed a computer program based on Plitt's model. Therefore, authors of this article decided to develop a simulator focusing on air classification using capabilities of Whiten equation (Rashidi 2006).

3 ASSIM DEVELOPMENT

This air separator simulator (ASSIM) is implemented in VBTM. This software provides a user friendly environment in WindowTM. Model used in developing this software is Whiten equation that was discussed in previous section. Values of Whiten equation is unique for any air separator, so one set of sampling from three streams of feed, fine and coarse around one separator is enough to estimate parameters of the model. All data sets need to be mass balance before using in ASSIM that provides accurate results.

3.1 ASSIM Introduction

ASSIM has 2 steps including Model calibration and Process simulation. After running executive file of ASSIM, user have two options choosing between these two steps. User is able to enter simulation step directly if parameters of Whiten model is provided by using statistical softwares, if not calibrating step can be applied to fit the model. For calibrating, user is required to sample all three streams around the air separator and to enter number of size fractions and flow rates of the three streams in tph in text boxes available for this purpose plus with size fractions in micron and size distributions of the three streams in percent of mass remained in each fractions in table

(Fig. 3). ASSIM provides analysing results by clicking “View” menu in tables and curves including recovery and cumulative size distributions plus with values of Whiten model’s parameters.

By clicking “Run” menu, user can enter simulation process after fitting the model and

obtaining parameters’ values. In this step, feed characteristics including number of size fractions, size fractions in micron, flow rate in tph and size distributions in percent of mass remained of feed are required (Fig. 4).

Figure 4 shows worksheet of simulation data entry.

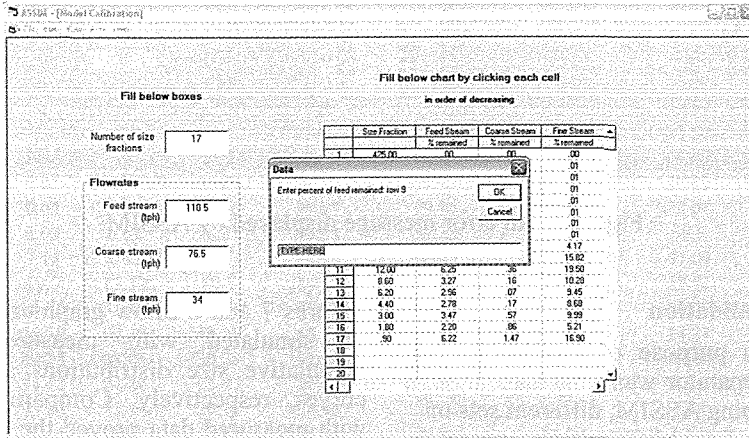


Figure 3. Worksheet of calibration data entry.

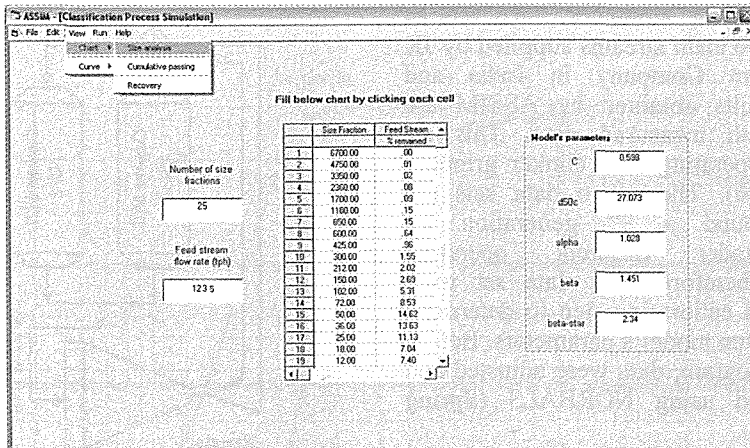


Figure 4. Worksheet of simulation data entry.

User is able to see the predictions in percent of mass remained and flow rates of fine and coarse streams plus with simulator analyze in different curves and tables of recovery and size distributions of products

streams. ASSIM is capable of checking input data for any errors and a message is shown to correct data before going through another step (Fig. 5).

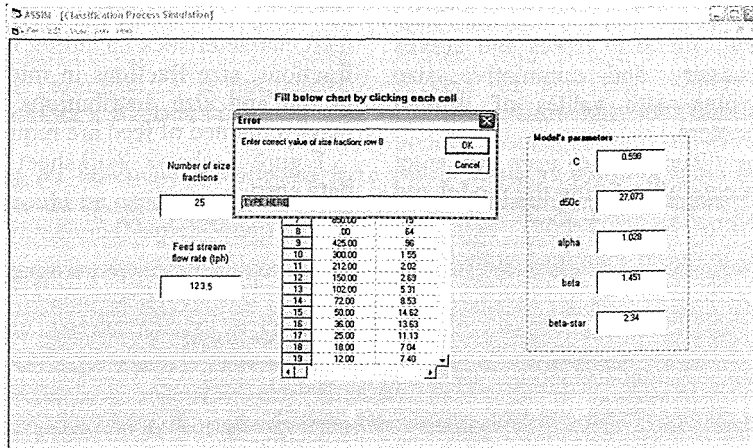


Figure 5. An error message displayed by ASSIM.

3.2 ASSIM Validation

For validation purpose of ASSIM, a real dynamic air separator was simulated, though during developing ASSIM, different sets of data collected from different air separators operating in cement plants were used to test calculations and logic of the program in order to verify the simulator. Two sets of data from three main streams supplied by JK White Cement Company in India and predicted results obtained by ASSIM are compared with measured data. This air separator is operating in a clinker grinding circuit (Fig. 6). These two data sets are collected around a 3rd generation air separator under different operating conditions. Therefore, first data set were used in model calibration step to determine values of Whiten model's parameters. Before starting the program, data were adjusted and mass balanced using NORBAL3 (Spring 1992).

Second set of data collected under different operating conditions is used independently to evaluate obtained results by ASSIM by using characteristics of feed stream and predicting size distributions and flow rates of coarse and fine stream. Table 1 shows comparisons of cumulative particle size distributions and recovery data of fine and coarse streams with measured data.

Figures 7 and 8 Show graphical comparison of simulated with measured data of cumulative size distributions and recovery curves, respectively. Comparing simulated with measured data proved the accuracy and precision of ASSIM in simulating air separators.

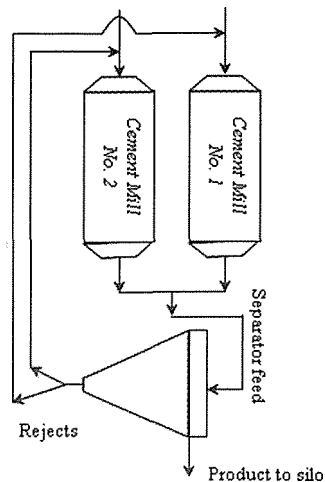


Figure 6. JK White clinker grinding circuit flowsheet.

Table 1. Comparison of fine and coarse streams simulated vs. measured, JK White Cement Company (Size distribution and recovery).

Particle size (micron)	Recovery				Size distribution			
	Obs.	ASSIM	Obs.	ASSIM	Obs.	ASSIM	Obs.	ASSIM
	Fine	Fine	Coarse	Coarse	Fine	Fine	Coarse	Coarse
6700	0	0	100	100	100	100.00	100.00	100.00
4750	0	0	100	100	100	100.00	100.00	99.80
3350	0	0	100	100	100	100.00	99.00	99.50
2360	0	0	100	100	100	100.00	98.50	98.20
1700	0	0	100	100	100	100.00	98.00	97.87
1180	0	0	100	100	100	100.00	97.60	97.30
850	0	0	100	100	100	100.00	97.20	97.00
600	0	0	100	100	100	100.00	96.00	96.30
425	0	0	100	100	100	100.00	94.00	94.45
300	0	0	100	100	99.99	100.00	92.50	92.76
212	0	0	100	100	99.98	100.00	90.89	90.20
150	0.05	0	99.95	100	99.97	99.99	87.80	87.46
102	0.04	0.03	99.96	99.97	99.96	99.97	82.01	81.30
72	3.03	0.62	96.97	99.38	99.23	99.20	68.5	68.02
50	7.15	4.42	92.85	95.58	96.49	96.50	47.00	46.73
36	19.9	15.39	80.1	84.61	89.25	89.00	29.43	29.50
25	26.35	33.73	73.65	66.27	76.90	76.87	18.39	18.62
18	56.79	53.27	43.21	46.73	64.67	64.70	14.21	14.30
12	69.25	68.06	30.75	31.94	49.53	49.50	10.46	10.48
8.6	74.13	74.86	25.87	25.14	38.43	38.50	8.70	8.53
6.2	75.88	75.94	24.12	24.06	30.32	30.30	7.33	7.00
4.4	75.11	74.47	24.89	25.53	24.01	24.00	6.51	6.10
3	71.47	71.81	28.53	28.19	18.21	18.17	5.02	4.90
1.8	67.48	68.48	32.52	31.52	11.19	10.80	3.59	3.72
PAN	64.94	65.01	35.06	34.99				

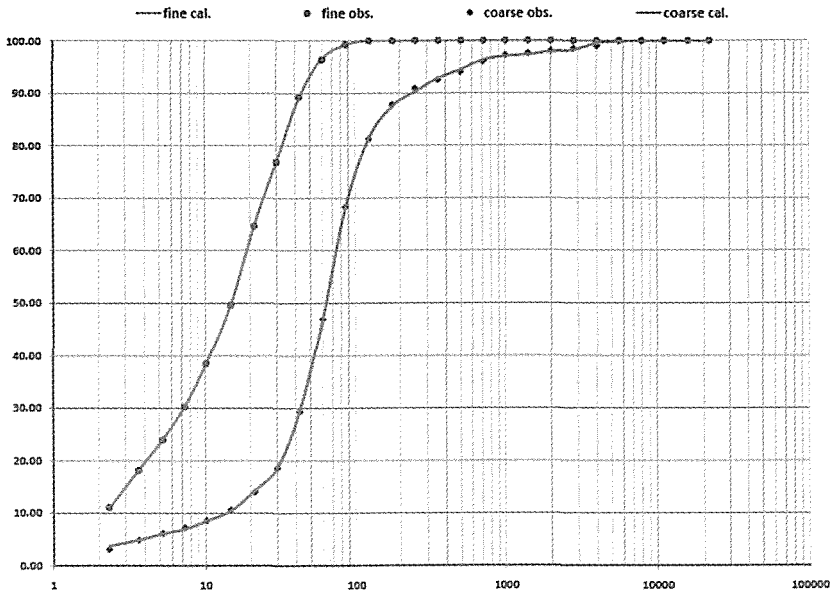


Figure 7. Size distributions curves of feed and simulated vs. measured products.

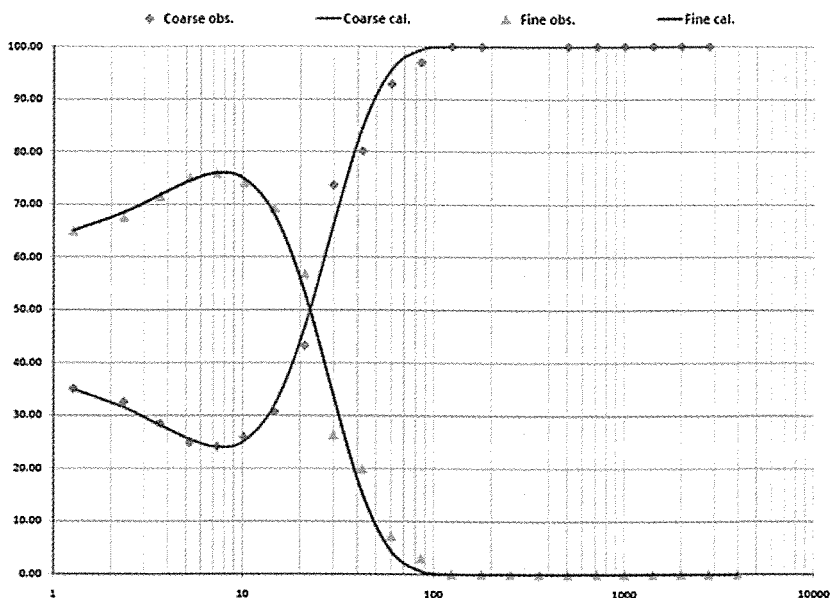


Figure 8. Recovery curves of simulated vs. measured fine and coarse streams.

4 CNCLUSIONS

ASSIM is an easy-to-use simulator and can be used in simulation of any type of air separators especially for managers of cement plants considering growing demands for finer cement products. It is easy to go back to initial window for entering another set of data taken under different operating conditions in simulation process or entering another set of data collected from different air separators by clicking "Run" in any steps and any windows. This is helpful in comparing simulation results for different operating conditions for one separator in order to optimizing or comparing different air separators as ASSIM is capable of analyzing data in both steps of calibration and simulation by drawing efficiency curves. Capability of printing or saving data is another useful tool in analyzing and comparing data easily. ASSIM provide a help file which make it simple for every process manager to understand the logic and routines of it. The new version of this simulator would simulate multi-chamber mills using validated models and its functionality would be expanded, too.

ACKNOWLEDGEMENT

Authors would like to thank Professor Benzer and Okay Altun in Hacettepe University for their helpful guidance and JK White Cement Company in India for supplying data.

RFERERENCES

- Benzer H. et al., 2001a. Simulation of Open Circuit Clinker Grinding, *Minerals Engineering*, Vol. 14, pp. 701-710.
- Benzer H. et al., 2001b. Modeling Cement Grinding Circuit, *Minerals Engineering*, Vol. 14, pp. 1469-1482.
- Benzer H., 2004. Modeling and Simulation of a Fully Air Swept Ball Mill in a Raw Material Grinding Circuit, *Power Technology*, Vol. 150, pp. 145-154.
- Conway, T.M., 1985. A Computer Program for the Prediction of Hydrocyclone Performance, Parameters and Product Size Distributions, MINTEK, Ore Dressing Division, Randburg, South Africa, Report No. 233.
- Farzanegan A., Laplante A.R. & Lowther D.A., 1997. A Knowledge-based System for an Off-line Optimization of Ball Milling Circuits, *Proceedings of 29th CMP Conference*, Ottawa, pp. 165-185.

- GLOBAL CEMENT to 2020, 2005.
<http://www.OSCLimited.com>, Ocean Shipping Consultants Ltd.
- Irannajad M., Farzanegan A. & Razavian S.M., 2005. Steady-state Simulation of Hydrocyclones in Excel Spreadsheet, *Proceeding of Iranian Mining Engineering Conference-2005*, Tehran, Iran, pp. 811-821.
- Irannajad M., Farzanegan A. & Razavian S.M., 2006. Spreadsheet-based Simulation of Closed Ball Milling circuits, *Minerals Engineering*, Vol. 19, pp. 1495-1504.
- Jankovic A., 2004. Cement Grinding Optimization, *Minerals Engineering*, vol. 17, pp. 1075-1081.
- Karunakumari L. et al., 2005. Experimental and Numerical Study of a Rotating Wheel Air Classifier, *AIChE Journal*, Vol. 5, pp. 776-790.
- Kelsall, D.F., 1953. A Further Study of the Hydraulic Cyclone, *Chemicals Engagemet Science*, Vol. 2, pp. 254 - 273.
- Kolacz J., 2000. Improving the Air Classification Process by Optimal Operating Parameters, *XXI International Mineral Processing Congress*, Rome, pp. A431-A437.
- Lynch et al., 2001. Simulation of Closed Circuit Clinker Grinding, *Zement Kalk Gips (English Translation)*, Vol. 53, pp. 560-567.
- Nageswararao K., 1999a. Normalization of the Efficiency Curves of Hydrocyclone Classifiers, *Minerals Engineering*, Vol. 12, pp. 107-118.
- Nageswararao K., 1999b. Reduced Efficiency curves of Industrials Hydrocyclone-An Analysis for Plant Practice, *Minerals Engineering*, Vol. 12, pp. 517-544.
- Nageswararao K., 2000. A Critical Analysis of the Fish-hook Effect in Hydrocyclone Classifiers, *Chemicals Engineering Journal*, Vol. 12, pp. 107-118.
- Napier-Munn T.J. et al., 1999. Mineral Comminution Circuits: Their Operation and Optimization, *JKMRC*, 413p.
- Plitt L.R., 1971. The Analysis of Solid - solid Separations in Classifiers, *CIM Bulletin*, Vol. 64, pp. 42-47.
- Rashidi S. Farzanegan A. & Irannajad M., 2006. Development of a New Software for Optimization of Air Separators in Cement Plants, *4th Asian Cement Conference*, 11-14 June, Tehran, Iran.
- Spring R., 1992. NORBAL 3: Software for Material Balance Reconciliation, *Center de Recherche Noranda*, Point-Claire, Quebec.

Floatability of Barite

R. Albuquerque

CDTN/CNEN, Belo Horizonte, Brazil

R. Papini

EEUFMG, Belo Horizonte, Brazil

A. Peres

EEUFMG, Belo Horizonte, Brazil

ABSTRACT This study investigates the floatability of barite, involving zeta potential determinations, microflotation, and bench scale flotation, aiming at its depression in systems where the mineral is associated with apatite. The IEP was determined at pH=3.0. NaOH and H₂SO₄ rendered the surface charge negative in the full pH range investigated. The depressing action on barite of corn starch, amylose, amylopectin, quebracho, lignin sulfonate, gluten, zein, and potassium dichromate was studied via microflotation in a modified Hallimond tube. Amylose was the most effective depressant, for either coarse (+43 μm) or fine (-43 μm) barite, followed by corn starch and lignin sulfonate. The action of depressants was more effective on fine barite than on coarse barite. In the plant, significant levels of depression of fine barite were reached in the presence of corn starch, at pH=12. Even at this high pH value, corn starch was not effective in the depression of coarse barite.

1 INTRODUCTION

Sparingly soluble minerals, such as phosphates, carbonates, sulfates, tungstates, among other, are characterized by presenting lower solubility than halite (NaCl) and silvite (KCl), but higher solubility than most oxides and silicates. Among them apatite Ca₁₀(PO₄)₆·(OH,Cl,F)₂, barite BaSO₄, and magnesite MgCO₃ (Dana & Hurlbut, 1971), deserve special attention due to their economical relevance.

The selective separation of minerals belonging to this class via flotation is relevant regarding either theoretical or practical aspects. The separation is, in general, extremely complex and hard to be achieved in plant practice. The similarity of the flotation behavior of these minerals arises from the resemblance in surface characteristics, the high surface activity of the collectors used in these systems, and especially from the interaction of dissolved ions from the minerals with other minerals or

even with collector species (Somasundaran et al, 1991).

The solubility of minerals plays a relevant role in flotation systems for it determines the chemical composition of the aqueous phase and the surface charge of the mineral particles. Most sparingly soluble minerals present solubility constants (K_{so}) of approximately 10⁻¹⁰. The solubility of the minerals is also affected by the presence of impurities, either in the mineral lattice or in the flotation pulp.

Hanna & Somasundaran (1976) pointed out the relevance of the knowledge of the sparingly soluble minerals structure, stressing that substitutions in the lattice may cause significant changes in the flotation behavior. The surface properties of the minerals are strongly affected by the pH and also by the temperature.

The selective depression of one or more mineral species is vaguely suggested in the literature (Aplan et al, 1991), but references

on organic or inorganic depressants effective for specific systems are scarce (Gerdel & Smith, 1988; Iskra et al, 1973).

The present investigation addresses the sparingly soluble mineral barite aiming at its depression in flotation systems where barite is associated with apatite.

2 MATERIALS AND METHODS

The barite sample was supplied by Bunge *Fertilizantes, Araxá, MG, Brazil*. Chemical analysis indicated BaSO_4 content >99%. The sample was ground 100% minus 106 μm and then wet screened at 43 μm yielding the coarse and fine barite samples.

Zeta potential determinations were performed in a Rank Brothers II microelectrophoretic cell, in the presence of KCl (1×10^{-3} M) as supporting electrolyte. The pH was adjusted with NaOH and HCl or H_2SO_4 . The Smoluchowski equation (Leja, 1982) was used to convert electrophoretic mobility to zeta potential.

Microflotation tests were performed in a modified Hallimond tube. In the tests with fine barite (<43 μm), a 30 cm long extension was inserted between the top and bottom parts of the tube. Saponified rice bran oil was the collector used in all tests. The tube was operated under the conditions: collector dosage 10 mg/L, collector conditioning time 3 min, flotation time 1 min; nitrogen flowrate 60 mL/min; pH 10. The depressants selected for the investigation were: conventional non-modified corn starch, corn amylose, corn amylopectin, corn zein, gluten, quebracho, sodium lignosulfonate, and potassium dicromate. The depressant dosage was varied between 10 mg/L to 400 mg/L.

The phosphate ore sample used in the bench scale flotation tests was also supplied by Bunge and was collected at the feed of the barite flotation section. The chemical analysis of this sample indicates: P_2O_5 19.60%; CaO 24.19%; Fe_2O_3 18.68%; SiO_2 9.27%; MgO 0.46%; BaSO_4 10.23%. A Denver laboratory machine (model 533000) was used in this stage of the investigation, operated under the conditions: pH 10 and 12, percent solids 20%, collector conditioning

time 3 min, collector dosage from 150 g/t to 500 g/t; depressant conditioning time 10 min, depressant dosage 200 g/t to 400 g/t, froth collecting time until the froth was barren, weight of solids 600 g; rotor speed 1200 rpm.

3 RESULTS

Figure 1 illustrates curves of zeta potential of barite as a function of pH. The zero charge condition was achieved at $\text{pH}=3$ when the pH was modified with NaOH and HCl . This pH is not strictly an isoelectric point (IEP), as defined by the IUPAC (Parks, 1975), but is usually referred as such in the literature. When HCl was replaced by H_2SO_4 as pH modifier, it was impossible to reach a condition of zero charge. Barite was solubilized by the acid at pH levels lower than 3.5 and it was impossible to determine the zeta potential below this limit.

Enhanced depressing action was observed for the reagents corn starch, corn amylose, and sodium lignosulfonate. Barite (coarse and fine fractions) floatability curves as a function of the depressant dosage are illustrated in Figures 2, 3, and 4, respectively for non modified conventional corn starch, corn amylose, and sodium lignosulfonate.

Figure 2 shows that corn starch is an effective depressant for either coarse or fine barite, the effect being clearly more pronounced for fine barite. Corn amylose is a stronger barite depressant. Both fractions, fine and coarse, are equally depressed by this reagent, as illustrated in Figure 3. Sodium lignosulfonate is mildly effective in the depression of barite. In contradiction with the trend observed for corn starch, the action is more pronounced with respect to the coarse fraction, as shown in Figure 4.

The next step was performing bench scale flotation tests with the feed of the concentrator (barite circuit) using the depressants selected from microflotation experiments. A summary of the results is presented in Table 1. Despite the promising results from microflotation, no selectivity was observed at bench scale.

The company started a long sequence of tests aiming at replacing mechanical flotation cells by flotation columns. A search for corn starches with higher contents of amylose failed. The cost of a variety of white corn with 50% amylose content makes its use as flotation reagent unfeasible. Nevertheless, the depression of fine barite with corn starch, in pilot scale columns, was successfully achieved since flotation was performed at pH=12.

Bunge's concentrator was refurbished, flotation columns substituting for mechanical cells. Barite pre-flotation was kept in the coarse particles circuit, but this stage was eliminated in the fine particles circuit. Barite was depressed by corn starch together with other gangue minerals. This procedure has the advantage of eliminating one column in the concentrator but represents a large consumption of caustic soda, an expensive reagent that presents large price fluctuations.

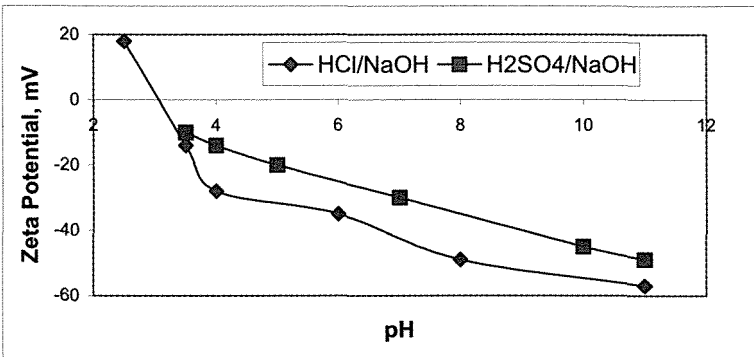


Figure 1. Zeta potential of barite as a function of pH.

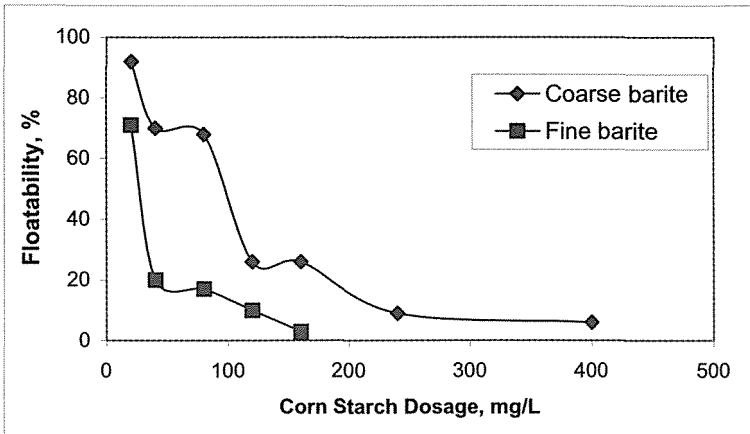


Figure 2. Floatability of barite as a function of corn starch dosage.

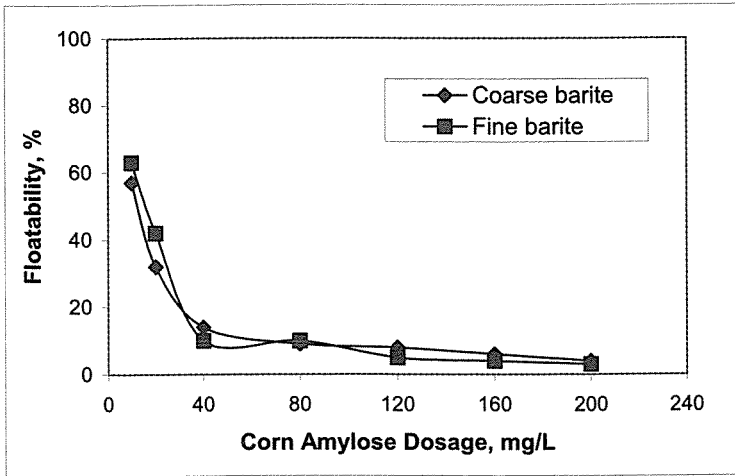


Figure 3. Floatability of barite as a function of corn amylose dosage.

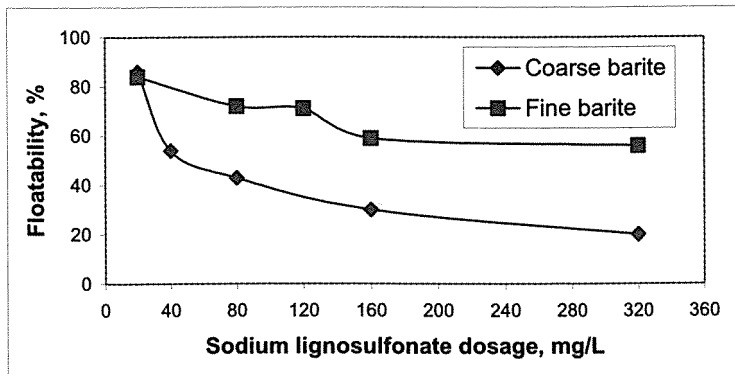


Figure 4. Floatability of barite as a function of lignosulfonate dosage.

Table 1. Summary of bench scale barite flotation in the presence of different depressants.

Test no	Depressant/ dosage (g/t)	Rice bran oil dosage (g/t)	pH	P ₂ O ₅ (%)	BaSO ₄ (%)
1	corn starch 400	500	10	22.72	11.17
2	corn starch 300	500	12	20.41	11.14
3	corn amylose 400	150	10	22.53	13.30
4	corn amylose 400	250	12	22.29	12.78
5	sodium lignosulfonate 400	500	10	20.70	10.28
6	sodium lignosulfonate 200	250	12	20.72	12.25

4 CONCLUSIONS

The zero charge condition of barite was determined at pH = 3.0 for pH modulation with NaOH and HCl. For pH modulation with H₂SO₄ the reversal of the surface charge of barite to positive values was not achieved, confirming that sulfate is a potential determining ion for barite.

In microflotation tests, corn amylose was the most effective depressant for barite, either coarse (>43µm) or fine (<43µm). Corn starch was also effective, especially in the depression of fine barite (<43µm). Among other depressants investigated, it is worth mentioning sodium lignosulfonate, but its performance was by far inferior than that of the starch products.

In bench scale flotation tests with a barite bearing apatite ore, selectivity was not achieved with any of the above mentioned depressants.

In pilot scale column flotation tests, adequate depression of fine barite was possible with corn starch for operation under highly alkaline conditions (pH = 12).

A Brazilian concentrator uses this plant practice, despite the high cost of NaOH.

REFERENCES

- Aplan, F.F.; Castillo, M.; Harris, C.L. & Parekh, B.K., 1991. Surface properties and selective flotation of the slightly soluble minerals. *XVII International Mineral Processing Congress*, vol. II, pp.45-58.
- Dana, J.D. & Hurlbut, C.S., 1971. *Manual of Mineralogy*, John Wiley & Sons, New York, 642 p.
- Gerdel, M.A. & Smith, R.W., 1988. The role of lignin sulfonate in flotation of bastnaesite from barite. In: Bautista, R.G. & Wong, M.M. eds. *Rare earth, extraction, preparation and application*. The Minerals, Metals & Materials Society, New York, pp. 35-44.
- Hanna, H.S. & Somasundaran, P., Fuerstenau, M.C. ed., 1976. *Flotation A, M. Gaudin Memorial Volume*, pp. 197-272.
- Iskra, J.; Gutierrez, C. & Kitchener, J.A., 1973. Influence of quebracho on flotation of fluorite, calcite, hematite and quartz with oleate as collector, *Transactions Institution of Mining and Metallurgy Section C*, vol. 82, pp.73-78.
- Leja, J., 1982. *Surface Chemistry of Froth Flotation*, Plenum Press, New York, 758 p.
- Parks, G.A., 1975. Adsorption in the Marine Environment. In: Riley, J.P. & Skirrow, G. eds *Chemical Oceanography*, pp. 241-308.
- Somasundaran, P.; Xiao, L. & Vasudvan, T.V., 1991. Separation of salt-type minerals by flotation using a structurally modified collector. *XVII International Mineral Processing Congress*, vol. II, pp.379-391.

Drilling and Blasting

Effect of Blasted Rock Particle Size on Excavation Machine Loading Performance

M. Sari

Aksaray University, Department of Mining Engineering, 68100 Aksaray, Turkey

P.J.A. Lever

The University of Arizona, Department of Mining and Geological Engineering, Tucson, Arizona, USA

ABSTRACT Earthmoving (i.e. excavation, loading and transportation of material) makes up a major portion of surface mining operations. Today, there is a wide array of equipment used to perform excavation and loading tasks in open pit mines. However, the performance of these machines is often not fully optimized since the excavated material characteristics have not been thoroughly investigated. In this study, results of some parts of a research project that is undertaken to quantify the factors effective on excavation machines' loading performance are presented. The research project originally consisted of performing mine site visits and collecting video camera images from typical front-end loader, cable shovel, and hydraulic shovel applications. In the study, the video images were carefully scanned to obtain machine loading cycle times and amount of hourly production whilst video images of the material being loaded were successively captured, scaled and processed to obtain rock fragmentation size distributions of muckpile in the vicinity of blasted benches. Regression analysis on site-specific data was statistically performed in order to investigate, if exists, possible linear relationships between machine performance parameters and particle size of blasted rock. The results suggested that there was little to be gained by attempting to match the performance of loading machines (loading cycle time and maximum production) with only size features (maximum and 63% passing) of excavated material.

1 INTRODUCTION

A major activity in many mining operations is the earthmoving (i.e. overburden removal and ore production). Fragmentation, loading and transportation form the integral parts of this process. Presently, there are many different types of equipment on the market to perform loading and excavation tasks in surface mines. They basically include cable shovels, hydraulic front shovels, draglines and wheel loaders. Higher ownership and operating costs dictate that these machines should be utilized in the most efficient and productive manner. Besides the efficiency of the loading equipment has a significant effect on the overall economy and productivity of mining operations.

The productivity and efficiency of a loading machine is affected by several aspects including: muckpile characteristics, loading geometry and practice, operating conditions and loader design (Singh and Narendrula, 2006). Excavation is a complex operation, which is influenced by many parameters such as excavator type, size, operator experience, material and site characteristics, machine operating conditions, blasting and formation properties including intact rock properties and rock mass conditions (Ceylanoglu et al., 1994).

The performance of the loading machines is often not fully optimized since the relationships between the properties of the material being loaded and machine

performance parameters have not been carefully investigated. In order to achieve maximum loading performance, it is needed to match the digging capabilities of loading equipment with the characteristics of excavated material. While it is widely accepted that muckpile characteristics have a pivotal effect on loading operations, little quantitative information is available upon which parameters are the most relevant. The objective of this study is, therefore, to characterize the relationship between rock fragmentation characteristics (maximum and 63% passing size) and production performance (loading cycle time and maximum production) of the loading equipments employed in the open pit mines.

2 PRIOR STUDIES

The effect of fragmentation and muckpile characteristics on loader performance has not received adequate attention. The followings are some of the relevant studies that have been performed.

Neilson (1987) conducted model studies of loading equipment as a function of rock fragmentation and observed fairly good linear correlation between 50%, 80% and 90% passing size and bucket fill factor.

Chung et al. (1991) studied shovel digging time to obtain data on the effects of explosive energy consumption on shovel productivity. It was observed that explosive energy is not the only factor affecting fragmentation but rock mass structure with respect to the blast direction also has influence.

Paşamehmetoğlu et al. (1992) assessed the performance of hydraulic and cable shovels with regard to ease of diggability, degree of bucket filling, cycle times, observed and computed net production. They have based their investigation on the collection of information from 284 locations of some 40 surface lignite mines of the Turkish Coal Enterprises (TKI).

McGill and Freadrich (1994) conducted loader productivity studies in limestone and sandstone mines. The time study of loader cycle time was compared with the

fragmentation of the muckpile in two different rocks. It was concluded that the cycle time is directly related to the fragmentation size.

Hanspal et al. (1995) reviewed the physical, chemical and mechanical features of muckpile and reported the field studies of muckpile and loading system performance. The field analysis showed the control exerted by the size distribution and compaction on loading machine performance.

Frimpong et al. (1996) investigated the effect of powder factor on dragline productivity. It was observed that increasing powder factor enhances fragmentation and hence dragline productivity, but increasing energy output beyond an optimum region results in reduced bucket fill factor.

Michaud and Blanchet (1996) presented a case study to quantify the effect of fragmentation on mine productivity. A linear relationship between the mass of fragmented rock and the fragmentation index was observed. It was concluded that smaller fragmentation affects mine productivity by increased tonnage of individual dipper and hauler per cycle.

Singh and Yalçın (2002) studied scooping operations with a scaled model of a loader on muckpile samples with different size distributions. Using a simulation program the effect of size distribution on scooping operations was examined. The results indicated that the larger the particle size and narrower the size span of the material, the higher was the penetration force and the lower the fill factor.

Singh et al. (2003) investigated the significance of size distribution in mucking operations by determining different scooping parameters. According to their study both the mean particle size and index of uniformity play a significant role in muck scooping operations. Higher scooping rates and lower energy consumptions were observed in muckpile with a smaller mean particle size and flatter size distribution curve.

Singh and Narendrula (2006) conducted a study to examine the effects of the looseness, angle of repose, size distribution and moisture content of the blasted material on

the production rate of a wheel loader. They have found that looseness in the muck increases with the increase in the value of the mean particle size and index of uniformity of the fragmented rock. It was concluded that the bucket fill factor and rate of production decreased with increasing values of mean particle size and index of uniformity.

3 METHODOLOGY

Data for predicting the production capabilities of loading machines in different conditions are needed for effective loading equipment selection and operation. Since the earthmoving activity in mining applications is complex and affected by many factors, the raw information should be as complete as possible. For this purpose, considerable data were gathered from a variety of different mining sites (13 open-pit copper and gold mines and 3 quarries with a total of 67 individual sites) located in the western United States. The observational data contains representative video camera images of material being loaded and video of loading cycles with emphasis on the bucket loading for each machine, and also includes images of the final bench faces of the unblasted rock mass in the vicinity. The field notes consist of information about type, make, model and dimensions of mining equipment operated at the sites and also include drilling and blasting data. All of the excavation machines studied for this research were operated to load large off-highway mine haul trucks.

For the analysis, loading machine movements were observed on the video cassette and machine cycle times and hourly production numbers were simply determined by timing the number of passes necessary for loading a truck of known capacity. Cycle times including load, swing, dump and return times are basically used to characterize machine production while waiting segments were excluded from the calculations since they are not at all related to material fragmentation effects. The machine productivity defined on a per truck basis as:

$$P = 3600 * C_i / T_i \quad (1)$$

where,

P: machine production (tons/hr)

C_i: rated truck capacity (tons)

T_i: truck load time (sec), defined over the total number of passes “n” required to serve the truck.

The digital video camera images of the material being loaded were successively captured, scaled and delineated with SPLIT (Wu and Kemeny, 1992), a digital image processing software developed to compute size distribution of rock fragments from digital images. The procedure used by SPLIT system can be outlined as in the following steps:

- First, an image of the muckpile containing the rock fragments is captured together with an object of known dimension (i.e. rim diameter) to permit determination of image scale,
- Second, a subsequent zoomed image of the muckpile close to the bucket tip is captured and the scale of this image is determined by cross-reference with an object in the previously captured one,
- Third, the final image is delineated into discrete fragments and the program fits an ellipse into each delineated fragment,
- Finally, shape data for the fragments is filtered through a statistical filtering function to determine the physical screen size of the fragment and a cumulative particle size distribution is produced for a user specified screen size increment.

The major pieces of surface loading equipment currently available and employed in discontinuous mining systems are wheel loaders, electric cable shovels and hydraulic shovels. They can be conveniently classified as excavator-loaders (Martin et al., 1982). Each type of excavator has distinctly digging characteristics and capabilities. Loading equipment size is generally defined by bucket capacity and all machines in the database have bucket sizes greater than 10 cu yd. A comparative analysis of three machines is illustrated in Figure 1 and 2, respectively. Average values for three types of loading

machines in database are presented in terms of their size and load cycle time in Figure 1. It shows that cable shovels have the largest bucket size with 29.3 cu yd while wheel loaders are the smallest capacity with 15.4 cu yd. An opposite trend is observed when bucket widths are considered only. Although, wheel loaders have the smallest bucket size, they have the widest buckets of 16.7 ft. In contrast to bucket capacity, cable shovels have the narrowest of buckets width of 11.4 ft. In both cases, the bucket dimensions of hydraulic shovels take place between these two types. It can be concluded from the above comparison that each machine type has a different bucket configuration; therefore, the way the bucket penetrates into the excavated material might be affected differently. Average load cycle times for each machine type are presented in Figure 1, and it is surprisingly found that all machines have similar loading cycle periods that is approximately 12 sec.

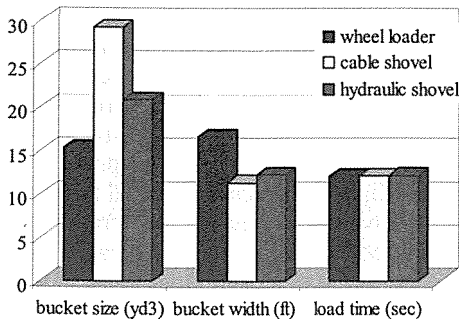


Figure 1. Comparison of machines in the database.

Using the time-study information, a projection of the maximum production capabilities of the loaders is presented in Figure 2. Maximum production is defined as the hourly rate at which material can be loaded when both wait and delay times are excluded. While cable shovels have the highest loading rate (4651 tons/hr), wheel loaders are the lowest one (2335 tons/hr) and hydraulic shovels are between these two machines (3192 ton/hr). The variation in production is evidently due to the differences

in bucket and machine sizes. Subsequently, it is necessary to normalize the production figure by dividing it to cubic yard capacity. More consistent values are obtained for each machine as shown in Figure 2. All excavators in the database almost have a production rate of 150 tons/hr for their each bucket capacity.

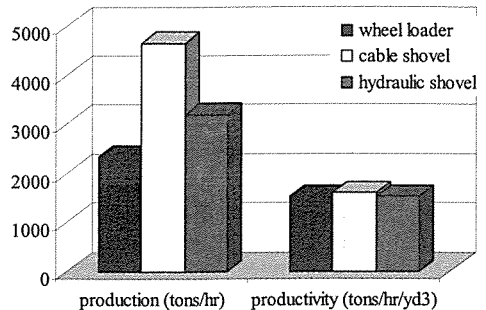


Figure 2. Production figures of machines in the database.

4 RESULTS

In this study, it is aimed that particle size will be analyzed statistically as one predictor of loading machine productivity. The particle size distribution at each site is represented with a single value, either the particle size at the 63rd percentile or at maximum size (100th percentile) in the plots. Actually, the 63rd percentile size, in most cases, corresponds to the mean size of the fragments in a specific image. The basic cycle time of an excavating machine employed in loading trucks can be categorized into four periods; load, swing, dump and return and only the loading cycle is sensitive to the variations in the properties of material at a muckpile. The others are mostly related to machine type, positioning of loader and truck, and operator skill.

The effect of particle size on machine performance is compared between machine types as scatter plots and degree of relation is shown by correlation coefficient on each graph. Each point in the scatter plots represents a site average value. The site average production value defined on a per truck basis does not account for variations in the bucket fullness and truck fullness.

Proficiency of the machine operators cannot be included easily in the calculations. Also, the tractive conditions of loading surface and climatic conditions during operation of machines are not completely considered. Another factor not accounted for calculation of site production value is the mechanical condition of the excavation machines.

Data for all three machines are illustrated together on the same graphs in the following figures. Maximum production vs. 63rd percentile particle size plot is presented for three machines in Figure 3. It can be seen that there are no any significant correlations. The highest correlation coefficient of - 0.36 is obtained for wheel loaders and it shows that as particle size increases the production decreases. Unfortunately, this is not true for hydraulic shovels where raise in the particle size results in increase in production ($r = 0.15$). For cable shovels, it is hard to detect any effect of particle size on machine production with a negligible correlation ($r = - 0.04$).

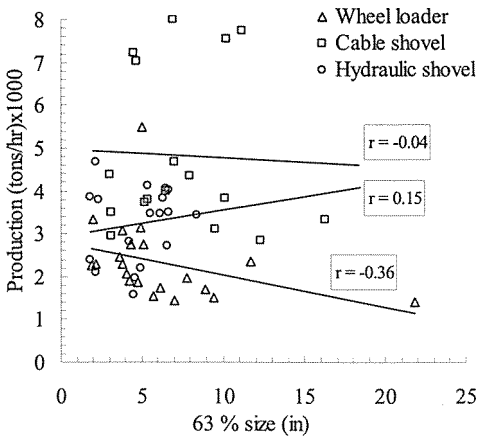


Figure 3. Maximum production vs. 63rd percentile particle size.

In Figure 4, instead of 63rd percentile size, maximum particle size was plotted against the loading cycle time. A coefficient of correlation of 0.26 is calculated for hydraulic shovels indicating a low positive linear relation between maximum size of material being loaded and loading cycle. However, an

opposite trend was observed for cable shovels with a negative value of $r = - 0.38$, which means that increase in maximum particle size leads to decrease in loading cycle that seems not realistic. For wheel loaders, a value of -0.07 indicates that there is a lack of association between two parameters.

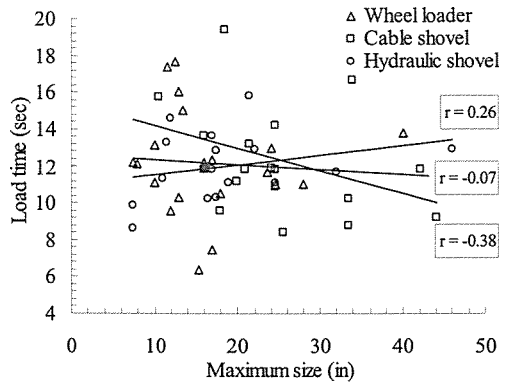


Figure 4. Loading cycle vs. maximum size.

5 CONCLUDING REMARKS

This study was mainly based on the observational data collected from different open pit mines. In this type of data, all the possible excavation factors can not be controlled separately and the results are a combination of all their influences. To learn the effects, if any, of material size on machine productivity, we would have to separate their effects from that of these other influences. When the results of regression analysis are considered, there is little to be gained by attempting to match the performance of loading machines (loading cycle time and maximum production) with only size features (maximum and 63% passing) of excavated material. Usually, weak relationships indicated by very low correlation coefficients were observed between dependent variables and independent variables. Only a moderate relationship ($r = - 0.38$) was detected between bucket load time of wheel loaders and maximum size of blasted fragments. It is concluded that since the size of fragments

produced by blasting is very narrow in range when compared with the bucket size of excavators, therefore, influence of fragment is negligible on the performance of those huge machines commonly employed in the surface mines. However, it does not mean that mines should set rock fragmentation factors solely on the performance of loading equipment. Here, the major concern with reduction of size of material produced by blasting is of interest because of their pronounced effects on downstream operations such as crushing, grinding and leaching processes.

REFERENCES

- Ceylanoğlu, A., Karpuz, C., Paşamehmetoğlu, A.G., 1994. Specific digging energy as a measure of diggability. *Mine Planning and Equipment Selection '94*, pp.489-494.
- Chung, S.H., Lee, N.H., Hunter, C.J., 1991. A blast design analysis for optimizing productivity at INCO Ltd's Thompson Open Pit. *Proc. of 17th Conf. On Explosives and Blasting Techniques*, pp.119-127.
- Frimpong, M., Kabongo, K., Davies, C., 1996. Diggability in a measure of dragline effectiveness and productivity. *Proc. of 22nd Annual Conf. On Explosives and Blasting Techniques*, pp.95-104.
- Hanspal, S., Scoble, M., Lizotte, Y., 1995. Anatomy of a blast muckpile and its influence on loading machine performance. *Proc. of 21st Conf. on Explosives and Blasting Techniques*, pp.57-67.
- Martin, J.W., Martin, I.J., Bennett, T.P., Martin, K.M., 1982. *Surface Mining Equipment*, 1st ed., Martin Consultants, Inc., Golden, Colorado.
- McGill, M. and Freadrich, J. 1994. The effect of fragmentation on loader productivity. *Proc. of 5th State of the Art Seminar on Blasting Technology, Instrumentation and Explosives Application*, pp.713-724.
- Michaud, P.R. and Blanchet, J.Y., 1996. Establishing a quantitative relation between post blast fragmentation and mine productivity: a case study. *Proc. of 5th Int. Symp. on Rock Fragmentation by Blasting*, pp.386-396.
- Neilson, K., 1987. Model studies of loading capacity as a function of fragmentation from blasting. *Proc. of 3rd Mini-Symp. on Explosives and Blasting Research*, pp.71-80.
- Paşamehmetoğlu, A.G., Karpuz, C., Müftüoğlu, Y., 1992. Performance assessment of hydraulic and cable shovels. *Int. J. Surface Mining and Reclamation*, 6:73-80.
- Singh, S.P. and Yalçın, T., 2002. Effects of muck size distribution on scooping operations. *Proc. of 28th Annual Conf. on Explosives and Blasting Techniques*, pp.315-325.
- Singh, S.P., Yalçın, T., Glogger, M., Narendrula, R., 2003. Interaction between the size distribution of the muck and the loading equipment. *Proc. of 4th Int. Conf. on Computer Applications in Mineral Industries*, pp.1-13.
- Singh, S.P. and Narendrula, R., 2006. Factors affecting the productivity of loaders in surface mines. *Int. J. of Mining, Reclamation and Environment*, 20 (1):20-32.
- Wu, X. and Kemeny, J.M., 1992. A segmentation method for multiconnected particle delineation. *Proc. of the IEEE Workshop on Applications of Computer Vision*, pp.240-247.

Two-Component Bulk Emulsions: A Revolution in the Explosives Manufacturing

M. Cardu

*Politecnico di Torino, Land, Environment and Geo-Engineering Department, Torino, Italy
CNR-IGAG, Torino, Italy*

ABSTRACT Two-components emulsions fall within an optimisation process aimed to support an improvement of the safety and of the environmental quality in the explosives use; these products, conceived in USA at the beginning of 70's, add to the advantages of cartridge emulsions all benefits rising from a product that, from the production to the charging into the blastholes, doesn't have explosive properties: they result from a chemical reaction taking place between the precursors, that are not explosives, immediately after charging. Explosive properties vanish rapidly, and therefore, in case of unsuccessful blast or misfire, no residual risk is foreseen. An immediate advantage of that is the exclusion of risks caused by manufacture, transport and use of explosives.

The in-situ mixing technique, together with the loading of a bulk product, involves an improvement of the performances of the blast: in fact, it becomes possible to modify both the blasting pattern, being the choice of the drilling diameter independent from the diameter of cartridges, and the explosive composition. Thanks to the excellent coupling between the charge and the blasthole, the specific drilling can be reduced, being the same the powder factor; moreover, the reduced charging times allows for many advantages, not only on the safety point of view, but also for the economic aspects.

The emission of dangerous gases is limited, and this allows, in underground excavations, a quick access to the stope after the blast, with a further reduction of costs.

The needs of qualified personnel and of sophisticate equipment, together with a rapid decay of the explosive properties of the mixed product, don't permit its use for illegal purposes: that is a big advantage also from the public Security point of view.

1 FOREWORD

Explosive was born as a weapon, evolved in a powerful, general purpose, destruction device, and lastly entered, first, the specialization stage, and then the optimization one. The two component emulsions are probably the most advanced explosives available for mining and civil rock excavation purposes: a safe and useful means to induce in the rock the desired level of impulsive pressure.

Let us briefly analyze the path that led to the present "last generation" products. The

points dealt with are: oxidizer and fuel; micro-structure; sensitization; efficiency; safety and security aspects. Lastly, an appraisal will be provided of the success attained, based on recent example.

2 OXIDIZER AND FUEL

Any chemical explosive basically consists of an oxidizer and a fuel and, presently, the commonplace oxidizer is Ammonium Nitrate NH_4NO_3 . At the beginning of the "Ammonium Nitrate era" (mid 1900), AN, a low cost chemical being mass produced for a

variety of uses, had to fight against other low cost competitors, chlorates and perchlorates (by-products of the caustic soda production); the battle was easily won, thanks mainly to the superior stability of the nitrate, and chlorate based explosives are, presently, a rarity.

AN is a salt, with specific gravity 1,725; 1 gram of salt can provide 0,2 grams of oxygen, 1 cc of salt can provide 0,345 grams of oxygen. At the beginning of the NA era, the salt in the solid state gained the place of standard oxidizer for civil explosives; standard fuel, in the first half of 1900, was TNT, an oxygen deficient explosive available at low cost from ordnance disposal, acting both as a fuel and as a sensitizer, then finely ground coal, and lastly fuel oil, giving rise to the commonplace AN-FO explosives, or other kinds of liquid fuel. NA is very soluble. At room temperature, 100 cc of water can dissolve, roughly, as much as its weight of salt, hot water can dissolve 8 times more salt than its weight. Even at room temperature, a saturated solution with specific gravity around of 1,3 is an excellent oxidizer: 1 gram of solution can provide

more than 0,12 grams of oxygen, and 1 cc of solution around of 0,16 grams of oxygen. Moreover, undissolved nitrates can be added, producing oxidizing pulps providing, by weight, roughly the same amount of oxygen as the dry salt.

A liquid oxidizer shows a number of advantages on a granular, namely higher density and resistance to groundwater, being not porous, more perfect contact between oxidizer and fuel, more complete filling of the hole by the resulting explosive mix, that were promptly exploited, giving rise to the "slurries". Fuels were initially in the solid state (TNT, aluminum, finely ground coal), replaced, later, by liquid fuels, which started the present era of the "explosive emulsions" (an emulsion is a dispersion of a liquid in another liquid, being the two not miscible). To stabilize the mixtures, gelatinizing agents were added, giving rise to the popular "water gel" explosives, suitable to cartridgeing. Emulsions, however, evolved along a separate path. Figure 1 shows the microscopic particle size of a typical emulsion, compared to a typical water gel explosive.

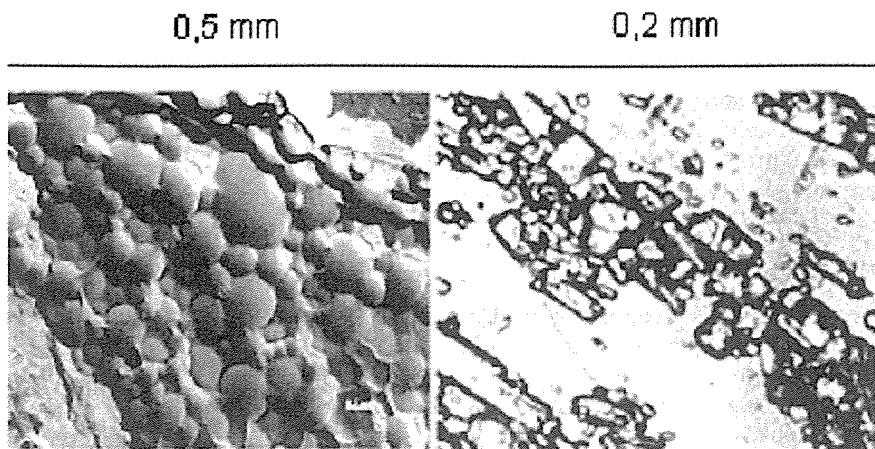


Figure 1. Left: Typical emulsion; light circular areas are the oxidizer droplets surrounded by a thin coating of fuel. The intimate particle-to-particle contact can easily be seen. Right: Typical water gel. Light areas are the water solution and the rectangular particles are oxidizer crystals. Notice their large size and seemingly random distribution; this causes a large separation between the oxidizer and fuel, with less intimate contact, thereby degrading the efficiency during detonation (from Atlas Powder Company, 1987, modified).

3 MICRO-STRUCTURE

For quite obvious reasons, in all AN based explosives the volume of the oxidizer greatly exceeds the volume of fuel; primitive solid oxidizer/solid fuel mixtures (Amatols, Akremites and so on) consisted simply of a small amount of very finely ground fuel dispersed in a large amount of coarser oxidizer, which means oxidizer grains coated by fine fuel powder. In this way, a very large oxidizer-fuel contact surface, mainly dictated by the fineness of the fuel component, was assured. As solid oxidizer/liquid fuels came of age (AN-FO), the most obvious way to assure a large oxidizer-fuel contact surface was to have the fuel absorbed by the oxidizer's fine porosity.

Oxidizer porosity, rather than grain size, became the critical factor. In the primitive, liquid oxidizer/solid fuel slurries, a large oxidizer-fuel contact surface (and a satisfactory stability against segregation) can be only assured by a large specific surface (or grinding fineness) of the fuel. Gelatinizing agents can improve the stability and change the mechanical properties of the mixture, but leave unchanged the structure.

With liquid oxidizer/liquid fuel mixtures (broadly speaking, emulsions) we have two possible structures, which can be easily explained with an example.

An air-water mixture can assume the form of a fog (water droplets suspended in air) or of a foam (an assembly of polyhedral bubbles of water filled with air); neither fog nor foam are indefinitely stable: droplets tend to coalesce, foam tends to minimize the inter-facial free surface energy, but foam lasts longer than fog. Air-water contact surface depends, inversely, on the droplet diameter in the case of fog, on the bubble wall thickness in the case of foam. Modern emulsions are of the latter type, apart from the fact that the liquid oxidizer takes the place of air. Bubble wall thickness can reduce to a few molecular radii, giving rise to an enormous contact surface; the inter-facial free surface energy, on which the stability of the system depends, can be steered by minute additions of surface active agents.

4 SENSITIZATION

Ancient "blasting agents" were, simply, not sensitive: they failed to detonate under the action of a standard cap, and required booster charges to be used. The most obvious way to sensitize the mixtures is by adding some kind of sensitive explosive, and this is commonly done: sensitive explosive particles are dispersed in the mixture. But, another sensitization method soon emerged, allowing to dispose of the sensitive explosive particles, much in the same way a diesel engine can dispose of the spark plug, the typical ignition device of gasoline engines: actually, in diesel engines, the ignition of the air-fuel mixture is caused by the heating of the air due to the adiabatic compression in the cylinder. In liquid oxidizer based explosives, minute cavities can be dispersed in the liquid, whose collapse under the impulsive pressure generated by the cap produces "hot spots" acting as ignition points. Glass micro-balloons (minute hollow spheres) became popular as sensitizing agents, and are widely used, solving the problem of producing a sensitive explosive lacking of explosive components. They represent, however, a still perfectible solution. Indeed, a static, or a dynamic, pressure (not so strong to cause detonation) could crush the micro-balloons, thus abolishing the sensitivity of the mixture; moreover, the dispersion of the sensitizing micro-balloons in the mixture necessarily takes place before charging, hence the substance handled during charging is a sensitive explosive. Gaseous micro-bubbles dispersed in the liquid can replace the micro-balloons to the same effect, and avoid the above quoted mechanical strength problems; lastly, the generation of the bubbles can be induced by a non explosive reagent (gassing agent) added to the mixture during charging, which reacts in the hole after charging (see Fig. 2). That represents the last achievement: non sensitive substances are introduced in the hole, and give rise to a sensitive explosive in the hole. Present day components of the emulsions currently attain this level of sophistication.

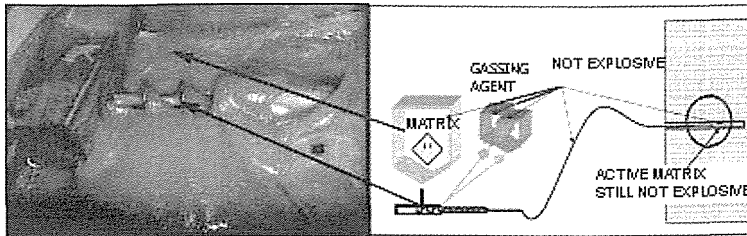


Figure 2. Explosive emulsions are “blasting agents” composed by an oxidizer matrix (concentrated NH_4NO_3 in water solution emulsified in a fuel) and by a gazing agent. The two components are produced separately, then transported and kept apart in the work site. The reagent is added to the mixture during charging and the reaction takes place in the hole only after charging.

A problem still remains, up to now impossible to solve: the volume of the charge is somewhat larger than the volume of the substances introduced in the hole; consequences of the volume increase are to be taken into account in the design of the blast.

5 EFFICIENCY ASPECTS

Cartridged charging has its own preferential application fields, but undeniably is scarcely efficient in exploiting the hole’s volume. In some cases, decoupled charging, implying low filling efficiency, is desired but, usually, the objective is the full exploitation of the available volume and, to this aim, cartridged charging is at the lowest level, bulk charging with granular mixtures in an intermediate position and bulk charging with a fluid mixture at the top position (Fig. 3).

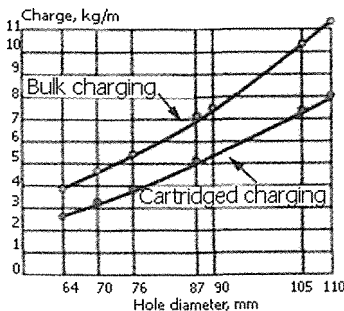


Figure 3. Comparison between bulk and cartridged explosives: dependence of the linear charge (kg/m of hole) from the hole’s diameter (mm) in the two cases.

Also another aspect of efficiency (efficiency in releasing the calculated chemical reaction energy; roughly speaking, the combustion efficiency) shows an improvement when the most advanced explosives (of the emulsion type) are compared to explosives of less refined micro-structure (Fig. 4).

That is due to the larger and more evenly distributed fuel-oxidizer contact surface.

A more complete combustion means also better fumes, which represents an important additional advantage.

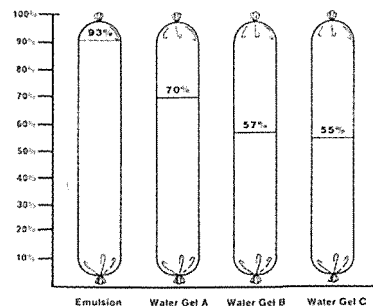


Figure 4. Total efficiency comparing calculated thermochemical energy to measured energy by the underwater bubble test. These studies have shown that the emulsions release 93% of the calculated thermochemical energy and are significantly more efficient than water gels which, with varying particle size, achieve only 55-70% of their calculated thermochemical energy (Atlas Powder Company, 1987).

A further gain in efficiency comes from the possibility of modifying, through components proportioning variations, the explosive performances, adapting them to the rock features.

6 SAFETY AND SECURITY ASPECTS

Safety (against accidents) and security (against possible criminal uses) are important subjects, when dealing with explosives; both took profit from the development of the advanced two-components (emulsion-gassing agent) civil explosives.

A system where non explosive substances are carried to the working place, handled in the non explosive state, and become explosives upon charging, in the hole, is obviously safer than the conventional system.

The only explosive substances present in the working place are represented by the ignition system. Moreover, the sensitizing action of the gas bubbles is not permanent, but vanishes upon a known time lapse, which makes safer the handling of misfires, if any.

Obviously, a system by itself safe can not be used if not officially recognized as safe. On this subject, Table 1 shows the official labelling of the precursors of a two-components emulsion.

To warrant security, a compromise, generally speaking, must be reached: a system should be simple enough to not cause

discomfort to the legal user, but complicated enough to discourage possible illegal users, and the two-components system (including the substances, the means to use them, and the training of the authorized users) fulfils these conditions.

Table 1. Precursors of the two-component emulsions, with the relevant classes of risk, according to the ONU/ADR (Medex S.r.l.).

Substance	Risk class ONU/ADR	Classification
Matrix	5.1	Oxidizer (comburent)
Gassing agent	6.1	Toxic for ingestion
Acidity control	-	It is not a dangerous product

7 AN EXAMPLE

The case presented to show the advantages obtained from two-component emulsions use refers to a tunnel driving operation. Advantages came mainly from time savings, due to the possibility of re-designing the working time cycle, and from the reduction of the transport and storage costs, thanks to the non explosive nature of the precursors..

The case examined is a railway tunnelling work, for the connection between Austria and Italy (Verona city); the excavated cross section is of about 120 m² (Fig. 5).

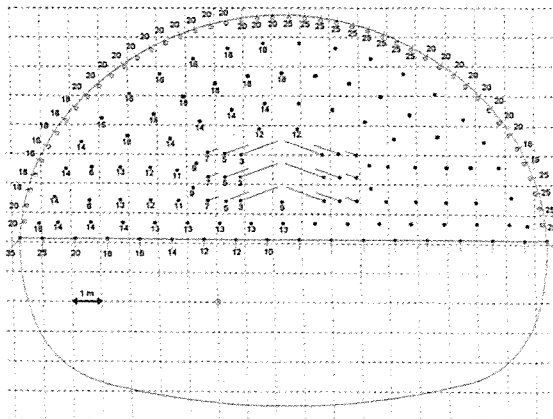


Figure 5. Scheme of the round. Numbers represent the delays of the detonators.

Drilling machinery used consists of 4 booms hydraulic automatic jumbo (3 drills + 1 charging platform). Explosive used was a two-component emulsion named "Emulgir RT-P", with a 2600 m/s V.O.D., 1.15 g/cm³ S.G. and 4.4 MJ/kg Specific Energy. Firing was by Nonel detonators, with a 20 cm piece of 50 g/m detonating cord, acting as booster, in each hole; drilling diameter was 51 mm.

Explosive was mixed and sensitized at the workplace thanks to a Tunnel 01 module, mounted on a truck (Fig. 6). Overall data of the round are given in Table 2.

The most interesting feature of the operation is the celerity of the working cycle, made possible by the bulk charging and by drilling – charging partial superposition, as shown in Figure 7.



Figure 6. Tunnel 01 module, mounted on a truck.

Table 2. Main data of the blasting round.

Design pull	2.5 m
Actual pull	2.2 mm
Drilling efficiency η	88%
Blasted volume	229 m ³
Specific drilling	1.75 m/m ³
Total amount of explosive	280 kg
Number of detonators	159
Powder Factor	1.22 kg/m ³
Specific Consumption of detonators	0.7 pieces/m ³
Volume to be removed (B.F. = 1.4)	322 m ³

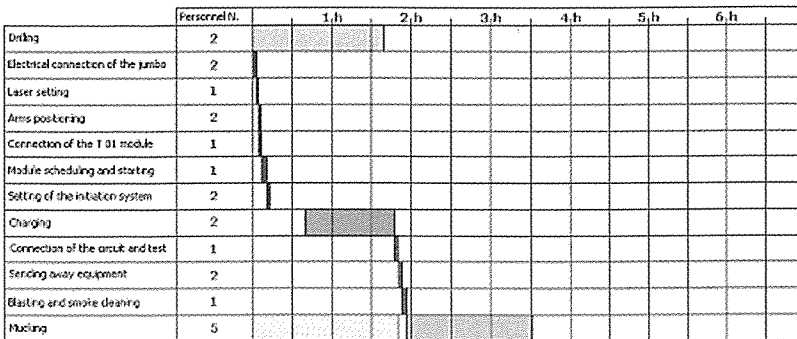


Figure 7. Representation of the working cycle.

The cycle is completed in 3 hours. To be noticed, 280 kg of explosive have been charged in 159 holes in less than 1.5 hours

by 2 persons, where conventional cartridge charging should have required either twice the personnel, or twice the time.

REFERENCES

- Atlas Powder Company, 1987. *Explosives and rock blasting*, Dallas, USA.
- Bauer, A., Glynn, G., Heater, R., Katsabanis, P., 1984. A laboratory comparative study of slurries, emulsions, and heavy Anfo explosives. *Proc. of the 10th Conf. on explosives and Blasting Technique, ISEE, Lake Buona Vista, Florida*.
- Dick, A.R., Fletcher, L.R., D'Andrea, D.V., (Aba Publishing Company, P.O. BOX 758,) 1986. *Explosives and blasting procedures*. Westport, Washington, USA, 105 pp.
- Ehnes, H., Friesen, G., Pichl, W., (ed. Balkema Pub., Rotterdam) 2000. Explosive accident in the Federal Republic of Germany, an analysis of the accident rate and conclusions for the body of regulations. *Explosives and Blasting Technique*.
- Folchi, R., 2001. Rapporto di sicurezza ex D.Lgs. 334/99: Quantificazione delle aree di egual-danno per gli effetti indotti da un'esplosione confinata. *AMBIENTE E SICUREZZA*, n. 19.
- Folchi, R., (ed. R. Holmberg Ed., Balkema Pub.) 2003. Explosion and fire hazard assessment for explosives, ammunition and fertilizing agents facilities after EU directive 96/82/EC Seveso II". *E.F.E.E. 2nd World Conference on Explosive and Blasting Technique, Prague*, pp 15-20.
- Folchi, R., 2004. Tunnel 01 (RP-T Tunnel) per la composizione ed il caricamento nei fori da mina di emulsioni esplosive sciolte. *Relazione Tecnica, Medex S.r.L., Sirmione*.
- Folchi, R., 2004. Tunnel 01 (RP-T Tunnel) per la composizione ed il caricamento nei fori da mina di emulsioni esplosive sciolte, contesto legislativo. *Relazione tecnica Medex S.r.L., Sirmione*.
- Folchi, R., 2004. Il mercato degli esplosivi in Italia. *COSTRUZIONI macchine mezzi d'opera e attrezzature*, n. 5.
- Giorgio, G., Polselli, S., (Pei Ed.) 1999. Le emulsioni: esplosivi non scoperti...ma progettati. *Atti convegno Attualità e problematiche degli scavi in galleria in Italia, Verona, Samoter*, pp 75-80.
- Harrington, T.B., Lydon, M.L., Sudweeks, W. B., 1989. Repumpable emulsions/anfo blends: the best of both worlds. *Proc. of the 15th Conference on Explosives and Blasting Technique, ISEE, New Orleans, USA*.
- Johansson, C., Svard, J., (Balkema, Pub. Rotterdam) 2000. How environmental and transport regulations will affect blasting. *Proc. Int. Congr. On Explosives and Blasting Technique*, (ISBN 90 5809 168 6).
- Mayer, A.A., (Balkema Pub., Rotterdam) 2000. Evaluation of the kind of hazards and risks encountered with explosives when blasting in quarries, a simple concept. *Explosives and Blasting Technique* (ISBN 90 5809 168 6).
- Murrey, F.M., Hueer, B., 2003. EU Directives affecting the explosives industry. *Proceedings of EFEE Second World Conference on Explosives and Blasting Technique, Prague; Czech Republic*, pp 5-14.
- Polselli, S., (Pei Ed) 2003. Sperimentazione delle emulsioni in galleria. *Quarry and Construction*, pp. 51-57.
- Retacchi, F., (Pei Ed) 2002. La normativa italiana e comunitaria nel settore degli esplosivi civili. *Quarry and Construction*, n. 9.
- Roberti, E., 2004. Utilizzo delle emulsioni esplosive sciolte ri-pompabili per l'ottimizzazione della sicurezza e dell'efficienza dei lavori nell'industria estrattiva e delle costruzioni. *Grad. Thesis, Politecnico di Torino, Italy*, 168 pp.
- Yan, S., Wang, Y., Liu, Y., 2002. Research on the relationship between water-based explosive desensitization and delay time under dynamic. *Proc. Fragblast -7, Rock fragmentation by blasting, Metallurgic Industry Press, Beijing*, pp 88-89.
- U.S. Department of Transportation, Federal Highway Administration, 1991. Rock blasting and overbreak control. *National highway Institute* (Publication No. FHWA-HI-92-001).
- Wetzig, V., 2003. Influence of different types of explosives on economical and working hygienic aspects in tunnel. *Proceedings of EFEE, 2nd World Conference on explosives and blasting technique, Prague; Czech Republic*.
- Wang, X., et al. 2002. Study on powdered emulsified explosive. *Proc. Fragblast 7, Rock fragmentation by blasting, Metallurgic Industry Press, Beijing*, pp 47-49.
- Xuguang, W., Jinquan, S., Baofu, D., 2002. Experimental study on shock sensitivity of emulsion explosives. *Proc. Fragblast 7, Rock fragmentation by blasting, Metallurgic Industry Press, Beijing*, pp 84-87.

Geostatistics

A Geostatistical Approach for Estimation of the Permeability and Groundwater Path in Rocks

A. Majdi

School of Mining Eng., University College of Eng. University of Tehran, Tehran, Iran

Y. Pourrahimian & B. Kushavand

Faculty of Mining Eng., Sahand University of Technology, Tabriz, Iran

ABSTRACT Groundwater flow path in a complex rock formations, based on field data via geostatistical approach, were estimated. Lugeon water-pressure tests were carried out in boreholes drilled into the base-rocks. Then permeabilities of the rocks were obtained in terms of Lugeon values (Lu). By employing geostatistical approach, distribution of the Lugeon numbers were estimated. The results demonstrated that the estimated high and low permeable zones overlapped each other on a horizontal plane. Finally, the preliminary estimation of major groundwater flow paths based on geostatistical analysis were used for determination of the strategy of detailed field hydro-geological surveys and measurements of the area.

1 INTRODUCTION

Proper evaluation of in-situ rock masses, in particular, for dam foundations and the corresponding abutments are the most significant part of rock characterization in dam engineering. Sufficient knowledge of foundation rocks permeability is essential if water seepage control grouting is required. Permeability data is helpful in other forms of grouting as well. It is obvious that an accurate estimation of the ground water flow path based on a limited data obtained from the field measurements is cumbersome. Hence, geostatistical estimation of spatial distribution of permeable zones in a complex rock formations based on scattered in-situ permeability data is an advantageous. Therefore, effort is made to investigate the in-situ permeability of the rock masses in order to estimate spatial distribution of permeable zones. For this purpose the Kriging approach which is one of the most reliable method for geostatistical estimation in the hydroscience has been implemented. (Delhomme 1978, Delhomme 1979, Clifton

& Neuman 1982, Ahmed & Marsily 1987, Issaks & Srivastava 1989).

The dam site area is located in northwestern of Iran and a dam has been planned to be constructed. Single-hole permeability measurements (Lugeon water-pressure test) were carried out for 20 boreholes to a depth of about 150 meters below the foundation level in base-rocks.

2 GEOLOGY

Geological investigation for the site selection was made within an area of about 3 square kilometers. The width of the V-shaped valley with similarly sloping flanks, at an elevation of 1185m with respect to sea level is 38m and at an elevation of 1310m, is 467m. Due to the existing meandering river, at an elevation of 1180m, the existence of fine particle metamorphic rocks was a major consideration in finalizing the choice of the dam site. Two systems of faults with mechanisms of shearing and tensile had the most significant effect on the regional geology of the area. The right bank of the site dipping at an angle of 28 degrees was

highly affected by the shearing mechanism; while the left bank dipping at a uniform angle of about 30 degrees was structurally controlled by tensile mechanism. The bedrocks consist of two types of low temperature metamorphic rocks, namely, slates and phyllites(Majdi *et al.*, 2005).

2.1 Engineering geological investigation of Dam site

In order to obtain engineering geological information from the dam site, the area has been divided into two sections. 20 boreholes, with depth ranging from 40m to 150m were drilled for core recovery and performing permeability tests. From the 20 boreholes drilled only 14 boreholes were used for permeability tests purposes among which eight boreholes are located at the right bank and the six of them are located at the left bank of the dam site (Fig. 1). Finally, the data obtained from the 14 boreholes were used for the permeability and groundwater flow path investigations.

3 DATA SET

Water pressure tests (WPT) were carried out for determination of the dam site permeability. WPT is an effective and widely used method for determination of rock mass

permeability for which 789 data set were produced. Lugeon (Lugeon, 1933) invented this method in 1933, since then it has become an excellent tool for evaluation of grout needs as well as the degree of grout requirement of a project, and finally it is used as a means of grout quality control as well (Majdi *et al.*, 2004). The Lugeon value, which is also known as the Lugeon Number (N_{Lu}) is defined as follows:

$$N_{Lu} = \text{Water take (litres/meter/min)} \times [10 \text{ (bars)/actual test pressure (bars)}]$$

The Lugeon unit is not a coefficient of permeability, but to get a sense of proportion, it might be related such that: $1 \text{ Lugeon} = 1.3 \times 10^{-5} \text{ Cm/s}$.

In practice, the Lugeon test is used before and after grouting to quantitatively determine the volume of water take per unit of time, then we can calculate the Lugeon number. The Lugeon number may go above 100; however, the scale has no upper limit. Above 100 lugeons it is meaningless to distinguish further (Houlsby, 1990). Since, in practice, the maximum meaningful Lugeon is considered as 100. In-Situ permeability test results as a general assessments of the boreholes at left and right banks are shown in Table 1 that the lugeon values are divided into five parts; $Lu \leq 1$, $1 < Lu \leq 3$, $3 < Lu \leq 10$, $10 < Lu \leq 30$, $Lu > 30$.

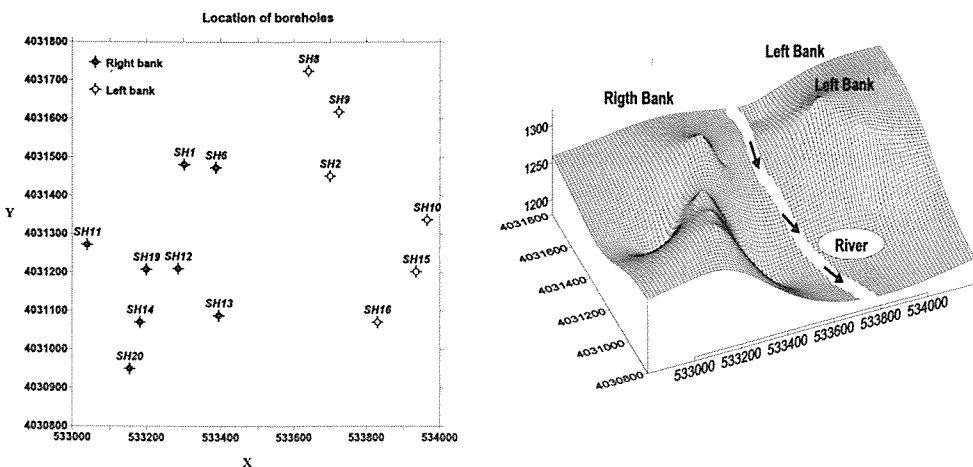


Figure 1. Boreholes locations at dam site area.

Table 1. In-Situ borehole permeability test results.

B.H.No	Lugeon Value				
	Lu<1	1<Lu<3	3<Lu<10	10<Lu<30	Lu>30
SH1	44%	44%	12%	----	----
SH2	84%	5%	----	----	11%
SH6	78.5%	10.7%	3.6%	3.6%	3.6%
SH8	69.2%	15.4%	15.4%	----	----
SH9	85.7%	----	----	----	14.3%
SH10	65.5%	10.3%	3.5%	6.9%	13.8%
SH11	44.5%	----	11.5%	22%	22%
SH12	73.4%	6.6%	----	----	20%
SH13	75%	12.5%	----	----	12.5%
SH14	84.6%	3.8%	7.8%	----	8.8%
SH15	37.5%	25%	12.5%	12.5%	12.5%
SH16	62.5%	25%	----	----	12.5%
SH19	54.5%	4.5%	27.3%	----	13.6%
SH20	55.6%	----	22.2%	22.2%	----

3 GEOSTATISTICAL ESTIMATION OF PERMEABILITY

Block ordinary kriging which is one of the commonly used geostatistical methods, has been applied to lugeon water test values. In ordinary kriging the following equation is solved for each of unsampled location to estimate a variable, V_i , by finding λ_i weights for each of sampled point, V_j , around the target block, B.

$$\sum_{j=1}^n \lambda_j \gamma(h_{ij}) + \mu_i = \gamma(h_{iB}) \quad i = 1, 2, 3, \dots, n \quad (1)$$

$$\sum_{j=1}^n \lambda_j = 1$$

Where; $\gamma(h_{ij})$ is semi-variogram value between points i, j and $\gamma(h_{iB})$ is semi-variogram value between block B and point I and μ_i is Lagrange parameter.

Experimental variogram is calculated for measured values as below:

$$\gamma(h_{ij}) = \frac{1}{2n(h)} \sum_{i=1}^{n(h)} (V_i - V_j)^2 \quad (2)$$

Where; $n(h)$ is the number of pair points, which have h distance from each other? Figure 2 shows the histogram of measured

lugeon water test values. Since histogram, shows a lognormal distribution, all values have been transformed by log function and zero lugeon values assumed as miss data, which has been, eliminate from data file.

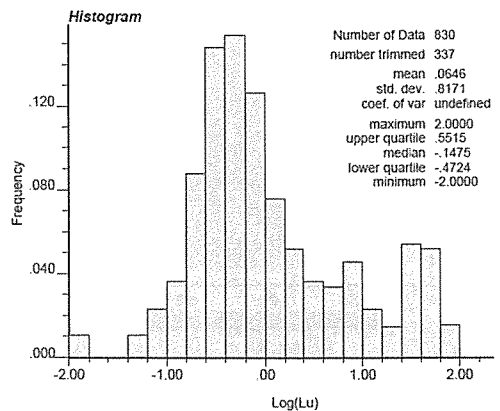


Figure 2. Histogram of measured Lugeon water-pressure test values.

The experimental semi-variogram of $\text{Log}(\text{Lu})$ has been calculated at horizontal and vertical direction to detecting the anisotropic semi-variogram model then the suitable theoretical model has been fitted to each of then by WINWAM software (Kushavand *et al.*, 2004).

Figure 3 shows experimental semi-variogram (dash line) and fitted spherical

model (solid line) with the range of 100m at vertical direction. Figure 4 shows horizontal semi-variogram (dash line) and its spherical fitted model (solid line) with the range of 600m.

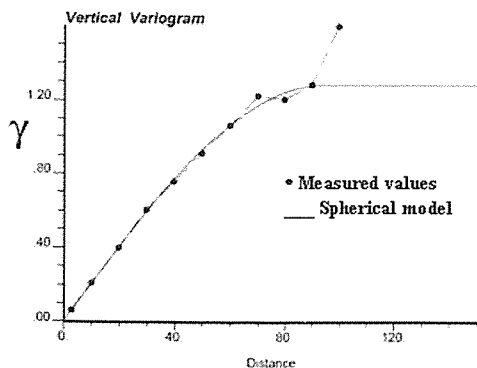


Figure 3. Semi-variogram of Ln (Lu) for vertical direction.

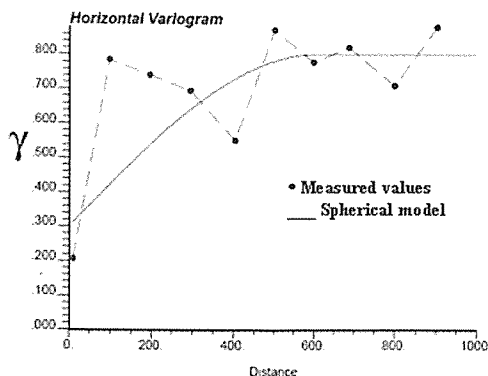


Figure 4. Semi-variogram of Ln (Lu) for horizontal direction.

KB3D program from GSLIB (Deutsch, 1997) has been applied to estimate the regular grid with the block size of 30*30 m2 and height of 5 m because the injection interval of lugeon water test is 5 m in length along a borehole.

4 ESTIMATION OF LUGEON DISTRIBUTION

A successful grouting is achieved if the field permeability due to grouting can be lowered

to a desired level. Hence, measuring the field permeability distribution before and after grouting must be taken into consideration in order to fulfill the needs for quality control purposes. Otherwise a reliable method must be employed for proper estimation of Lugeon numbers distribution at each required elevation through out the borehole depth. Due to this, according to the geostatistical methods, Lugeon values estimated at different elevations can be used for the analysis. The distribution of Lu values on some elevations represented on Figure 5. In this analysis each elevation is limited to an area of 30*30 square meters. The results indicate that high permeable zones appear in left bank more than that of in right bank.

5 ESTIMATION OF GROUND WATER FLOW PATH

Determination of groundwater flow path due to complex parameters involved is a difficult task. In order to detect the major ground water flow path, one can use the following procedures:

- 1) Picking out the square areas where two or more squares have the lower lugeon values on the every plane between elevations that we need.
- 2) Picking out the square areas where two or more squares have the higher lugeon values on the every plane between elevations that we need.
- 3) Picking out the square areas where the squares searched in the procedures 1 & 2 overlap each other then connecting the centroid of present squares together.

In the other method to detect the major ground water flow path, one can use the results that obtained from the Lugeon distribution at different elevations to plot the Iso-lugeon contours, or Iso-Lugeon wireframe for every elevation (Figure 6). Then, the Iso-Lugeon curves can be plotted with respect to depth. These curves represent the distribution of Lugeon numbers with depth. The water flow path can be estimated by connecting the points where they have higher lugeon values.

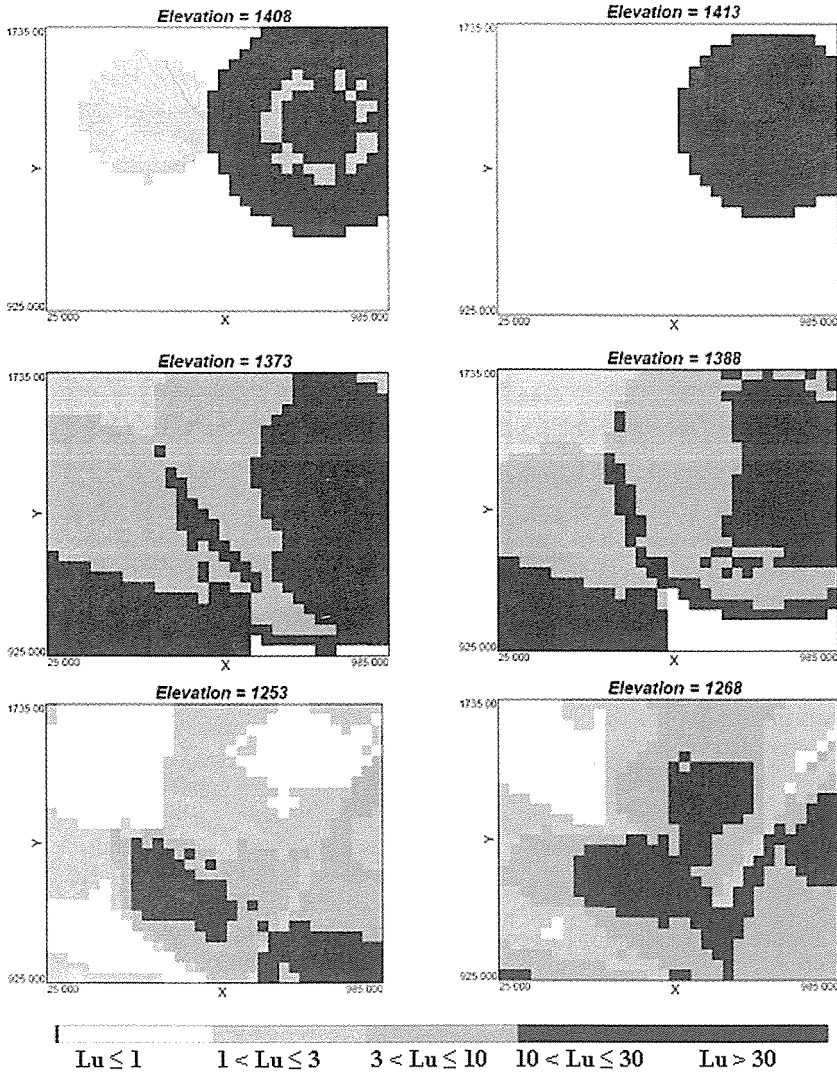


Figure 5. Lugeon distribution of representative elevations.

6 CONCLUSIONS

In this research the geostatistical kriging method was applied to measured Lugeon water-pressure values in base rocks of a proposed dam site located in northwestern province of Iran. By analyzing the results, the three-dimensional hydro-geological sub-structure was estimated and presented. The

following concluding remarks also can be drawn:

1. The three-dimensional hydrological sub-structure estimated by kriging is concordant with observed subsurface flow in complex rock formations.
2. The Iso-lugeon contours with depth help to estimate the ground water flow path.

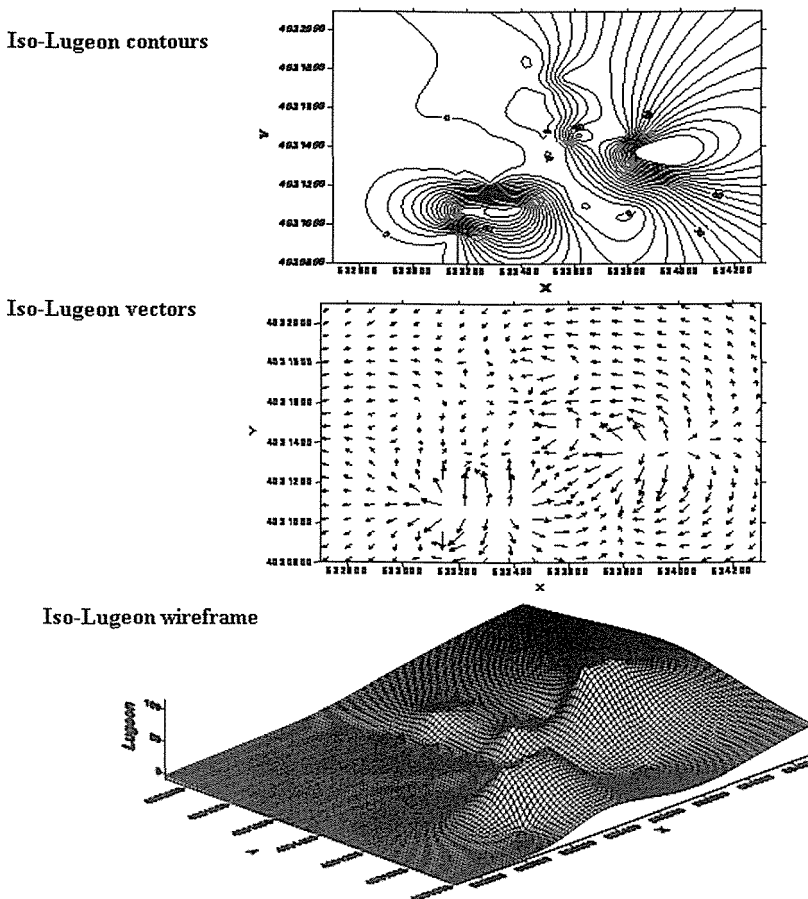


Figure 6. Variation of Lugeon values in local coordinates at elevation 1163

REFERENCES

Ahmed, S & G Demarsily, 1987, Comparison of geostatistical method for estimating transmissivity using data on transmissivity and specific capacity, *Water Resour.Res.* 23, Pp.1717-1737.

Clifton, P.M., & S.P.Neuman, 1982, Effect of kriging and inverse modeling on conditional simulation of the avra valley aquifer in southern Arizona, *Water Resour.Res.*, 18(4), pp.1215-1234.

Delhomme, J.P., 1979, Spacial variability and uncertainly in ground water flow parameters-A Geostatistical approach, *Water Resour.Res.*, 15(2), pp.269-280.

Deutsch, C.V. & A.G. Journal, 1998, *GSLIB: Geostatistical software library and user's guide*, Oxford University Press, New York, NY, p.369.

Issaks, Edward H., & Srivatava, R. Mohan, 1989, *Applied geostatistics*, Oxford University Press, p.561.

Houlsby A. C., 1990, *Construction and design of cement grouting - A guide to grouting in rock foundation*, John Wiley & Sons, New York, p.442.

Kushavand, B., Aghababaei, H., Mohammadzadeh, M.J., Alizadeh, B., 2005, *Semivariogram fitting with a simple optimizing algorithm*, *Jour. Of Applied science*, Vol.7. 4, pp.1405-1407.

Majdi, A. Pourrahimian, Y. & Bagheri, H, 2004, Theoretical prediction of grout- take in jointed rock masses, *5th International Conference on Ground Improvement Techniques*, Malaysia, pp.237-244.

Majdi, A., Pourrahimian, Y., & Bagheri, H.,2005, Study of Groutability of Shivashan Earth dam foundation and the corresponding abutments, *6th International Conference on Ground Improvement Techniques*. Portugal, pp.415-421.

Mining Method Selection of Charar Gonbad Deposit Based on Fuzzy Decision Making (FDM)

K. Shahriar, F.Samimi namin

Faculty of Mining and Metallurgical Engineer, Amirkabir University, Tehran, Iran.

H. Dehghan jan abadi

Faculty of Engineering, Tarbiat Modares University, Tehran, Iran.

ABSTRACT The main task in exploitation of mines is to select a method with the best consistence to deposit specific features (Geometric, Geomechanical, Geological and etc) and observing the safety limitations raise the least cost and the most profit. Research to develop numerical methods based on ranking is based on parameters indicating mineral deposits status and in analytic approaches decision making principles in management science is enjoyed. Fuzzy decision making softwares have been prepared considering effective norms, and the influence of qualitative parameters and in a situation that the decision maker do not access the precise information. Among these softwares is FDM (Fuzzy Decision Making). In this paper, the mineral function of this software in selecting mineral deposit extraction method is examined. Application of this software, considering the inclusion of various indexes (Deterministic, Linguistic and Fuzzy) required selecting the method of extracting a mineral deposit, doing not that the disadvantages existing in numerical methods and other analytic methods, and its results comparing with other methods are more consistent to reality.

1 INTRODUCTION

Various approach have been offered by researchers such as Bashkof (1973), Labscher (1981), Nicholas (1981), its modifying in (1993), Hartman (1987), Miller (1995) to select the mining method. Researchers' attempts led to the development of numerical methods to select the method of extracting mineral deposits. Numerical ranking methods are based on ranking to the indexes of a deposit such as depth, thickness, strength and etc. which explain the mineral deposit status.

In these methods in addition to the limitation of indexes number and choices, ambiguity and simultaneous influence of parameters has been neglected in decision making process. Considering these limitations and disadvantages, efforts have recently been done in order to develop decision making methods about selection of

extraction method. Among these efforts are studies of researchers such as Garadoghan (2001) and Goray (2003).

Although the disadvantages existing in numerical ranking methods have been removed in the decision making methods offered, these methods have their own disadvantages. In the present paper the problems with numerical and analytic methods are discussed and the results of applying Fuzzy Decision Making software in the process of selecting the extraction method for Chahar Gonbad deposit are offered.

2 DISADVANTAGES & LIMITATIONS OF SELECTION MINING METHODS

Numerical methods, such as UBC, or the method offered by Nicholas (1993), are based on ranking to parameters explaining the mineral deposit status which have some

disadvantages. Among these are limitation in number of parameters, and selection Alternatives. In the method offered by Nicholas, geometric parameters such as general shape, thickness, dip, and grade distribution manner, are considered. Although in this method, deposit depth is considered as an effective parameter in selecting the method of deposit extraction, no points is considered for its influence. In this method, the geomechanical indexes of joint frequency RQD (Rock Quality Designation), ratio of compressive strength to overburden pressure, and shear strength factor of joints in ore deposit and its surrounding rocks are considered. Of a great importance is the fact that geometric and geomechanical indexes affecting selection of extraction method are much more than the considered parameters. In UBC method, although the depth and RMR point are added, this limitation is still binding. Indexes such as overburden height, deposit dimensions, thickness changes manner, or its uniformity, accessing expert personnel in extraction, recovery in any extraction method, subsidence effect or gas leak effect, underground water status etc. which are effective in the extraction method and their number is not low, which have considerable number are neglected in both methods. This limitation is also existent in the choices and alternatives of selection. In numerical approach, ten mining methods are considered for selection. These methods on the order of increasing operational costs are: Open pit mining, Block caving, Sublevel stoping, Sublevel caving, Longwall, Room and pillar, Shrinkage, Cut and fill, Top slicing, Square-set. Although the mining traditional methods are divided to eighteen extraction methods, each of which may include several executively different alternatives (Hartman, 1987). Among the methods not included in the above methods one can refer to stope and pillar mining, Vertical Crater Retreat mining (VCR), strip mining and new extraction methods such as hydraulic mining and bore hole mining, moreover, underground methods such as Longwall can be done retreat or advance or ground control be

performed by caving or filling. Therefore choices in extraction method selection process are much more various than the ten considered methods.

Considering the fact that parameters affecting on selection of mine extraction method, are divided to three classes of Deterministic, Linguistic and fuzzy parameters, Deterministic explanation by numerical ranking and analytic methods, can be mentioned as the most important disadvantage, because in the method offered by Nicholas and the UBC method, parameters are explained deterministic, while most of the statements introducing the mineral deposit are linguistic statements. For example about the dip of an ore body, usually low dip (Flat), moderate dip (Intermediate), high dip (Steep) term are used and about the deposit hanging wall cavability, the terms appropriate cavability, moderate cavability, or inappropriate cavability are used. Also for ranking namely conversion of Linguistic statements about deposit to numerical rates, parameters introducing a mineral deposit are divided into classes which have no exact definition in boundary status and have some ambiguities. In numerical ranking methods, the influence of each parameter is verified separately and their mutual effects are ignored. For example, dip, thickness and depth parameters are simultaneously effective on determination of open pit method. In numerical methods, as the ore bodies dip increases, the probability of choosing open pit method decreases. But with the increase in the thickness, the rate decreasing trend should not be involved, because maybe for an inclined and thick deposit, the open pit method is preferred to other underground extraction methods. Also in these methods, all the parameters have equal effect on decision making, while considering the status of each deposit such thinking is out of reality. Also in analytic methods which are based on multi-criteria decision making, although there is no limitation in the number of indexes and choices, but we face with time consuming calculations.

3 TOPSIS & FUZZY THEORY

Fuzzy Theory is a modern theory which was proposed by Zade (1965). Classic sets logic saw the events as two values: To be or not to be, to exist or not to exist, black or white and one or zero. In this logic, also named Aristotle logic, the answer to a question is true or false. Values corresponding to these answers are one or zero, respectively, and there is no moderate status. But Fuzzy logic in answer to the events, considers a consistent spectrum between to exist and not to exist, and see the world phenomena as gray-neither black nor white. After Zade proposed such theory, by now this branch of mathematics have found many applications in controlling the systems and in decision making and improvements in industries.

TOPSIS method is a popular approach to Multiple Criteria Decision Making (MCDM) and has been widely used in the literature (Abo-Sinna & Amer, 2005; Agrawal, Kohli & Gupta, 1991; Cheng, Chan & Huang, 2003; Deng, Yeh & Willis, 2000; Feng & Wang, 2000, 2001; Hwang & Yoon, 1981; Jee & Kang, 2000; Kim, Park & Yoon, 1997; Lai, Liu & Hwang, 1994; Liao, 2003; Olson, 2004; Opricovic & Tzeng, 2004; Parkan & Wu, 1997, 1999; Tong & Su, 1997; Tzeng, Lin & Opricovic, 2005; Zanakis, Solomon, Wishart & Dublsh, 1998). The method has also been extended to deal with fuzzy MCDM problems. For example, Tsaur, Chang and Yen (2002) first convert a fuzzy MCDM problem into a crisp one via centroid defuzzification and then solve the nonfuzzy MCDM problem using the method. Chen and Tzeng (2004) transform a fuzzy MCDM problem into a nonfuzzy MCDM using fuzzy integral. Instead of using distance, they employ grey relation grade to define the relative closeness of each alternative. Chu (2002a; 2002b) and Chu and Lin (2003) also change a fuzzy MCDM problem into a crisp one and solve the crisp MCDM problem using the method. Differing from the others, they first derive the membership functions of all the weighted rankings in a weighted normalization decision matrix using interval arithmetics of fuzzy numbers and then defuzzify them into crisp values using the

ranking method of mean of removals (Kaufmann & Gupta, 1991). Chen (2000) extends the method to fuzzy group decision making situations by defining a crisp Euclidean distance between any two fuzzy numbers. Triantaphyllou and Lin (1996) develop a fuzzy version of the method based on fuzzy arithmetic operations, which leads to a fuzzy relative closeness for each alternative (Ying-Ming Wang and Taha M.S. Elhag 2005).

TOPSIS method is a Technique for Order Preference by Similarity to Ideal Solution and proposed by Hwang and Yoon (1981). The ideal solution (also called positive ideal solution) is a solution that maximizes the benefit criteria/attributes and minimizes the cost criteria/attributes, whereas the negative ideal solution (also called anti-ideal solution) maximizes the cost criteria/attributes and minimizes the benefit criteria/attributes. The so-called benefit criteria/attributes are those for maximization, while the cost criteria/attributes are those for minimization. The best alternative is the one, which is closest to the ideal solution and farthest from the negative ideal solution.

4 FUZZY DECISION MAKING SOFTWARE

Fuzzy Decision Making (FDM) Software has been prepared to make decisions considering specific criteria and effect of qualitative parameters and in the situation where the decision maker do not have access to precise information. In this paper it is tried to unwind the defects in numerical methods by using this software and applying that systematically (Meamareiani, 2003).

The most important advantage of applying this software in selecting the ore deposits mining method is diversity of the data. This software can receive three types of information including deterministic, linguistic, and fuzzy information. These three types of data can indeed be parameters affecting decision making for selection of mining method. But in numerical methods only the Deterministic parameters constitute the decision making process input. In

Table.1, the variety of the data which can be explained in extraction method selection has been offered.

Regarding fuzzy numbers related to the mine costs mentioned in the last line of Table.1, it should be added that the mentioned costs are related to block caving method, and it is meant that the mine costs in block caving method is about 12.5\$ per ton and a and b values are left and right tolerances, respectively. Moreover there is no limitation in the number of choices and alternatives sin this software.

Table 1. Data Input to FDM Software.

Data type	example	value
Deterministic variable	Annum Production	300000 (ton per year)
Linguistic Variable	Deposit thickness	intermediate
Fuzzy variable	Mine costs	(m=12.5,a=5,b=20)

FDM software has been designed based on Fuzzy Decision Making Method. In fuzzy decision making, the point for each alternative of fuzzy decision making process is Deterministic variables fuzzification. In this stage, definite and Linguistic variables are converted to fuzzy variables. This stage is called fuzzification because fuzzy sets are used to convert Deterministic variables to fuzzy variables.

The second stage is fuzzy extrapolation. In this stage, system behavior is defined by {If, Then} rules. The result of this extrapolation will be a linguistic value for the above linguistic variables. In the third stage, (defuzzification), linguistic values are converted to deterministic numbers. Decision making process in fuzzy environment is the same as decision making process in human brain, because everyday, human analyze many inaccurate information (fuzzy) and then make decisions. In this software, before any calculation qualitative terms are converted to fuzzy numbers with appropriate criteria. Selection of appropriate criterion for conversion of data to fuzzy numbers, are done by the software for user convenience

and the user has any role here. This action is done for all numbers including parameters' weights and decision table information. Then, in order to remove dimension, parameters are normalized and parameters indexes are exerted in the relevant vector. The next action is to find negative ideal answers and positive ideal answers. After finding the ideal answers, distance of each choice is obtained in an n-dimension space (n, is the number of parameters affecting decision making). Final scores of each parameter, is its approximation to positive ideal. After extrapolation in fuzzy environment, obtained fuzzy scores are defuzzed for any of the alternatives and are converted to real numbers. These processes are done by the software itself and the user only enters the input information such as parameters affecting selection, effective weight of each of them and selection choices.

5 VALIDITY MEASUREMENT

In order to investigate the competence of this software, Chahar Gonbad deposit was choosing as sample. This Copper ore deposit is located in 50 km of North of Sirjan between 20°56'E longitude and 30°29'N latitude. Chahar Gonbad deposit is located under a relatively flat field. Geometric specifications and some of Geomechanical specifications of this deposit are represented in Table.2.

In order to select the method to extract this deposit, 11 methods are considered for comparison and competition. Examined extraction methods include: Open pit mining, Block caving, Sublevel stoping, Sublevel caving, Longwall, Room and pillar, Shrinkage, Cut and fill, Top slicing, Square-set, Stope and pillar. These methods are entered to the software as alternative. Parameters involved in this selection include suitability of deposit shape, grade distribution, deposit dip, Deposit thickness, deposit depth, hanging wall RMR, deposit RMR, Hanging wall RSS (overburden pressure/UCS), deposit RSS, footwall RSS, extraction method recovery, access to expert force, Production ability, hanging wall RQD,

shear strength of deposit joint, hanging wall joint shear resistance, mine costs. These parameters are entered as attribute. The first step is to gather input information for the software. Data matrix for Chahar Gonbad was entered the FDM according to Figure 1. In this decision making index type or in the other word its effect on mine cost index decision making is entered as cost and for other parameters it is entered as profit. Decision making index weight is according to the situation and priority shown in Figs.1 Simplicity of changing these weights and studying different decision making situations are some advantages of this software.

Figure 2 shows the points obtained by each extraction method in Fuzzy decision making, after the data processed by FDM software.

As you see Open pit mining with 78.90 points is the first and Square-set method with 28.03 points is at the bottom of this ranking.

6 COMPARISON OF THE RESULT WITH NUMERICAL METHODS RESULTS

Selection of extraction method for Chahar Gonbad deposit was performed by Nicholas and UBC methods. Results of these calculations are presented in Table 3. Considering Table 3, Open pit mining in Nicholas method has obtained the best score while we did not achieve such a result with the other methods.

This fact is not so surprising considering the fact that in UBC and MMS, scoring has been done with refer to Canada mining and giving priority to stope extraction methods such as sublevel stoping.

Table 2. Specifications of Chahar Gonbad Deposit.

	Parameters	Description
Ore zone	General deposit shape	Seamy
	Ore thickness	2-15meters (Average 8.5meters)
	Ore dip	70 degree
	Grade distribution	Irregular
	Depth	Low depth (<100meters)
	Uniaxial Compressive Strength (UCS)	128.3 MPa
	RQD	75%
	Rock Substance Strength (RSS)	8.7
	Rock Mass Rating (RMR)	Good (60-80)
	Ore reserve estimation, by air born magnetometry	700 million tons
Joint condition	Filled with talk strength less than rock substance strength	
Hanging wall	Uniaxial Compressive Strength (UCS)	92 MPa
	RQD	38%
	Rock Substance Strength (RSS)	15.63
	Rock Mass Rating (RMR)	Good (60-80)
	Joint condition	Clean joint with a smooth surface
Foot wall	Uniaxial Compressive Strength (UCS)	50 MPa
	RQD	15%
	Rock Substance Strength (RSS)	9.1
	Rock Mass Rating (RMR)	Average (40-60)
	Joint condition	Clean joint with a rough surface

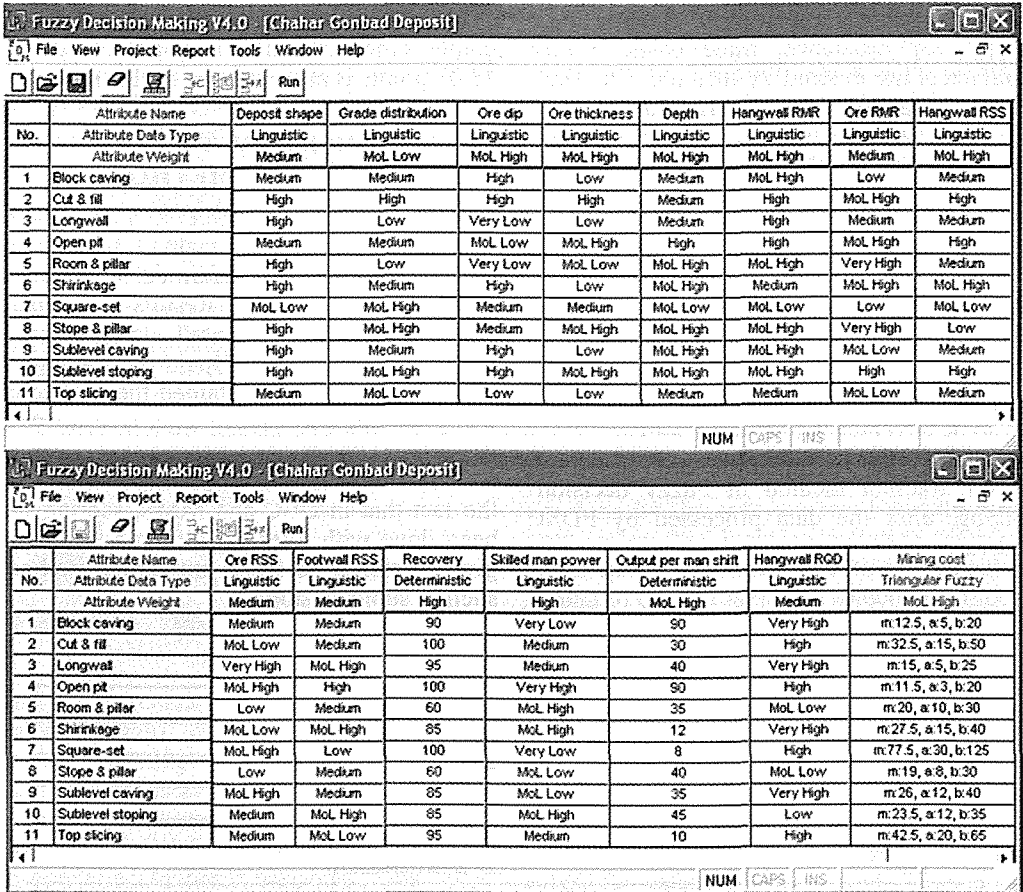


Figure 1. Geometrical and geomechanical input data of Chahar Gonbad deposit.

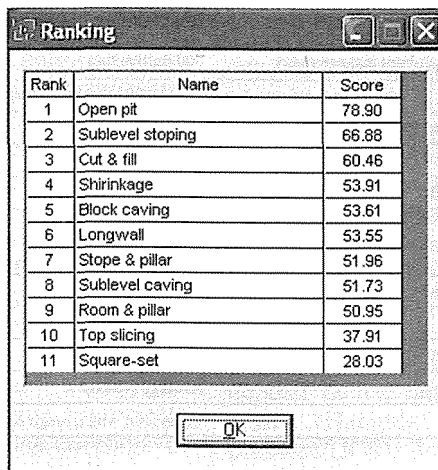


Figure 2. The points obtained by each extraction method in Fuzzy Decision Making (FDM).

Table 3. Scores of different mining methods according to the methods prevalent in Chahar Gonbad deposit.

	Open pit	Cut and fill	Shrinkage	Sublevel stoping	Top slicing	Square-set	Block caving	Sublevel caving
Nicholas	32	30	25	21	negative	25	negative	negative
UBC	33	34	34	32	13	15	negative	negative
MMS	24.7	28.5	23	25.3	10.8	12.5	negative	negative

7 CONCLUSION

With application of FDM based on fuzzy logic a strategy was offered to extract mineral deposits. This strategy has advantages in comparison with previous numerical ranking methods such as Nicholas and UBC, including: Having strong theoretic bases based on fuzzy theory, possibility of user continuous reconsideration in input attributes and changing that in order to achieve more convenient results, No need to change Linguistic variables to numerical quantities, infiniteness of the examined alternatives parameters affecting the selection of extraction method, and possibility of defining the problem according to local requirements, high speed in achieving the result and most important of all the possibility to consider the mutual effects of different parameters in selection process.

FDM software can be a good means to select the extraction method. The process for selection of Chahar Gonbad deposit extraction method was examined by this method. At the end of this examination, open pit mining was assigned as the best extraction method for this deposit.

REFERENCES

- Abo-Sinna, M. A., & Amer, A. H. (2005). Extensions of for multi-objective large-scale nonlinear programming problems. *Applied Mathematics and Computation*, 162, 243–256.
- Agrawal, V. P., Kohli, V., & Gupta, S. (1991). Computer aided robot selection: The multiple attribute decision making approach. *International Journal of Production Research*, 29, 1629–1644.
- Chen, C. T. (2000). Extension of the for group decision-making under fuzzy environment. *Fuzzy Sets and Systems*, 114, 1–9.
- Chen, M. F., & Tzeng, G. H. (2004). Combining grey relation and concepts for selecting an expatriate host country. *Mathematical and Computer Modelling*, 40, 1473–1490.
- Cheng, S, Chan, C. W., & Huang, G. H. (2003). An integrated multi-criteria decision analysis and inexact mixed integer linear programming approach for solid waste management. *Engineering Applications of Artificial Intelligence*, 16, 543–554.
- Claton .C, Pakalnis .R, Meech .J,(2002). A knowledge .A-based system for selecting a mining method, IPPM conference.
- Deng, H., Yeh, C. H., & Willis, R. J. (2000). Inter-company omparison using modified with objective weights. *Computers and Operations Research*, 27, 963–973.
- Feng, C. M., & Wang, R. T. (2000). Performance evaluation for airlines including the consideration of financial ratios. *Journal of Air Transport Management*, 6, 133–142.
- Feng, C. M., & Wang, R. T. (2001). Considering the financial ratios on the performance evaluation of highway bus industry. *Transport Reviews*, 21, 449–467.
- Hartman, H.L. (2002), *Introductory mining engineering*, Second edition, John Wiley & sons, Inc, P.570
- Hwang, C. L., & Yoon, K. (1981). *Multiple attribute decision making: Methods and applications*. Berlin: Springer.
- Jee, D. H., & Kang, K. J. (2000). A method for optimal material selection aided with decision making theory. *Materials and Design*, 21, 199–206.
- Kim, G., Park, C. S., & Yoon, K. P. (1997). Identifying investment opportunities for advanced manufacturing systems with comparative integrated performance measurement. *International Journal of Production Economics*, 50, 23–33.
- Lai, Y. J., Liu, T. Y., & Hwang, C. L. (1994). for MODM. *European Journal of Operational Research*, 76, 486–500.

- Liao, H. C. (2003). Using PCR- to optimize Taguchi's multi-response problem. *The International Journal of Advanced Manufacturing Technology*, 22, 649–655.
- Meamariani, A. (2003). FDM software (Fuzzy Decision Meaking). Tarbiat Modares University. Tehran, Iran
- Miller .L, Pakalnis .R, Poulin .R,(1995). UBC mining method selection university of British columbia, vancouver, Canada.
- Nicholas,(1993). selection variables, Hartman, Mining engineering hand book.
- Olson, D. L. (2004). Comparison of weights in models. *Mathematical and Computer Modelling*, 40, 721–727.
- Opricovic, S., & Tzeng, G. H. (2004). Compromise solution by MCDM methods: A comparative analysis of VIKOR and . *European Journal of Operational Research*, 156, 445–455.
- Parkan, C., & Wu, M. L. (1997). On the equivalence of operational performance measurement and multiple attribute decision making.*International Journal of Production Research*, 35, 2963–2988.
- Parkan, C., & Wu, M. L. (1999). Decision-making and performance measurement models with applications to robot selection. *Computers and Industrial Engineering*, 36, 503–523.
- Tong, L. I., & Su, C. T. (1997). Optimizing multi-response problems in the Taguchi method by fuzzy multiple attribute decision making. *Quality and Reliability Engineering International*, 13, 25–34.
- Triantaphyllou, E., & Lin, C. T. (1996). Development and evaluation of five fuzzy multiattribute decision-making methods. *International Journal of Approximate Reasoning*, 14, 281–310.
- Tzeng, G. H., Lin, C. W., & Opricovic, S. (2005). Multi-criteria analysis of alternative-fuel buses for public transportation. *Energy Policy*, 33, 1373–1383.
- Ying-Ming Wang and Taha M.S. Elhag. (2005). Fuzzy method based on alpha level sets with an application to bridge risk assessment. *Expert systems with applications*, 1-11
- Zanakis, S. H., Solomon, A., Wishart, N., & Dublish, S. (1998). Multi-attribute decision making: A simulation comparison of select methods. *European Journal of Operational Research*, 107, 507–529.

Lignite Thickness Estimation via Adaptive Fuzzy-Neural Network

B. Tütmez

Inonu University, Department of Mining Engineering, Malatya, Turkey

A. Dağ

Cukurova University, Department of Mining Engineering, Adana, Turkey

A.E. Tercan

Hacettepe University, Department of Mining Engineering, Ankara, Turkey

U. Kaymak

Erasmus University Rotterdam, Econometric Institute, Rotterdam, The Netherlands

ABSTRACT Thickness estimation is an important step in reserve estimation. In this study, lignite thickness is estimated using fuzzy-neural network. For this purpose, the lignite thickness data derived from Afşin-Elbistan lignite deposit were employed and the estimation has been conducted by the Adaptive Network Based Fuzzy Inference System (ANFIS). The method estimates thickness based on a data-driven model structure which is constructed from the adaptation of artificial neural networks to fuzzy modelling algorithm. Modelling process consists of data clustering, inference and learning mechanisms. The results have been compared with kriging estimations and it is seen that performance of the model is high.

1 INTRODUCTION

Reserve estimation is of paramount importance for mineral exploration and mining investments, for their financial investors and shareholders (Bardossy and Fodor, 2004). Many methods were developed for purpose of reserve (grade, thickness) estimation. Geometrical methods depends on geometrical relationships between sample points while geostatistical methods (Journel and Huijbregts, 1981; Goovaerts, 1997) are based on random functions and consider spatial relationship of the sample data. Limitations of these approaches were presented in detail by different authors (Diehl, 1997; Bardossy and Fodor, 2001).

Recently, applicability of soft methods in geological estimations has been discussed (Bardossy and Fodor, 2001; Bardossy and Fodor, 2004). One of these soft methods, fuzzy set theory has been applied in reserve estimation (Tutmez et al., 2007). By this paper, use of neuro-fuzzy adaptive modelling in reserve estimation is investigated. The lignite thickness data collected from Afşin-

Elbistan lignite deposit are used and the estimations are conducted by the Adaptive Network Based Fuzzy Inference System (ANFIS).

2 THICKNESS ESTIMATION

The reserve of a mineral deposit is estimated using the available data in the feasibility stage. If reserve estimation includes estimating grade and thickness of an entire deposit such estimates are called global estimates. Reserve estimation should be discussed as not only a mathematical problem but also a reliable deposit modelling (Tutmez, 2007). In mineral inventory estimation, models are used as a means of focussing on particular characteristics; the aim should be to determine to what degree a "deposit-to-be-estimated" fits a model (Sinclair and Blackwell, 2002).

The thickness estimation is an important step in reserve estimation and it can be stated as follows: one measures the actual thickness in certain locations and one wants to estimate the thickness of the whole deposit. The natural solution is thus, knowing a few

values t_1, t_2, \dots, t_n to manipulate these values in order to come out with a combination of these thicknesses which will be considered as the real thickness of the site under study.

3 NEURO-FUZZY COMPUTING

Fuzzy-neural synergism is a judicious integration of the merits of neural and fuzzy approaches. This incorporates the generic advantages of artificial neural networks like massive parallelism, robustness, and learning in data-rich environments into the system (Habibagahi, 2002).

The computing technique employed in this paper is based on adaptive neuro-fuzzy inference system (ANFIS). The ANFIS is a fuzzy inference mechanism implemented in framework of adaptive neural networks and it consists of two steps: (1) Structure identification, (2) Parameter learning and tuning (Jang et al., 1997).

3.1 Structure Identification

In order to determine network structure and the number of rules, fuzzy c-means clustering (FCM) (Bezdek et al., 1984) is applied. FCM employs fuzzy partitioning such that a given data point can belong to several groups with the belonging degree specified by membership grades between 0 and 1.

The algorithm minimizes the following objective function based on distance measures between cluster centers and data points.

$$J(X, U, V) = \sum_{i=1}^c \sum_{k=1}^N (\mu_{ik})^m \|x_k - v_i\|_A^2 \quad (1)$$

where U is a partition matrix of data X , and V is a vector of cluster centers

$$V = [v_1, v_2, \dots, v_c] \quad v_i \in R^n.$$

In addition to clustering, the selection of convenient inference system is another stage of structure identification. Among various fuzzy inference systems, Takagi-Sugeno systems (Takagi and Sugeno, 1985) have been applied successfully for data-driven

based fuzzy modelling. The Takagi-Sugeno (TS) model consists of a set of local input-output relations that describe the overall system. The rules in a first-order TS model have the following structure.

$$R_i : (\text{if } x_1 \text{ is } A_{i1} \text{ and } \dots \text{ and } x_n \text{ is } A_{in}) \text{ then } y_i = a_i^T x + b_i, \quad i = 1, 2, \dots, K,$$

where R_i is the i -th rule in the rule base, $x = [x_1, \dots, x_n]^T$ is the input (antecedent) vector, and A_{i1}, \dots, A_{in} are the fuzzy sets defined for the respective antecedent variables. The rule consequent y_i is an affine combination of the inputs with parameters a_i and b_i (Sousa and Kaymak, 2002).

Let the inputs of the fuzzy system be x and y , and let the output be f . We consider a TS system with first order consequents (Takagi&Sugeno, 1983) and two rules:

Rule 1:

If x is A_1 and y is B_1 , then $f_1 = p_1 x + q_1 y + r_1$,

Rule 2:

If x is A_2 and y is B_2 , then $f_2 = p_2 x + q_2 y + r_2$,

Figure 1 shows the network structure ANFIS. In order to establish the adaptive system, five layers are employed. Each layer involves several nodes described by a node function. The circles in the network represent nodes that possess no variable parameters, while the squares represent nodes that possess adaptive parameters to be determined by the network during training.

Layer 1: The fuzzification layer represents the fuzzy sets in the antecedents of the fuzzy rules. Each node in this layer is an adaptive layer. It has parameters that control the shape and the location of the centre of each fuzzy set. For this study, we choose $\mu_{A_i}(x)$ to be Gaussian with height equal to 1. The membership function is given by

$$\mu_{A_i}(x) = e^{-\frac{(x-c_i)^2}{2\sigma_i^2}} \quad (2)$$

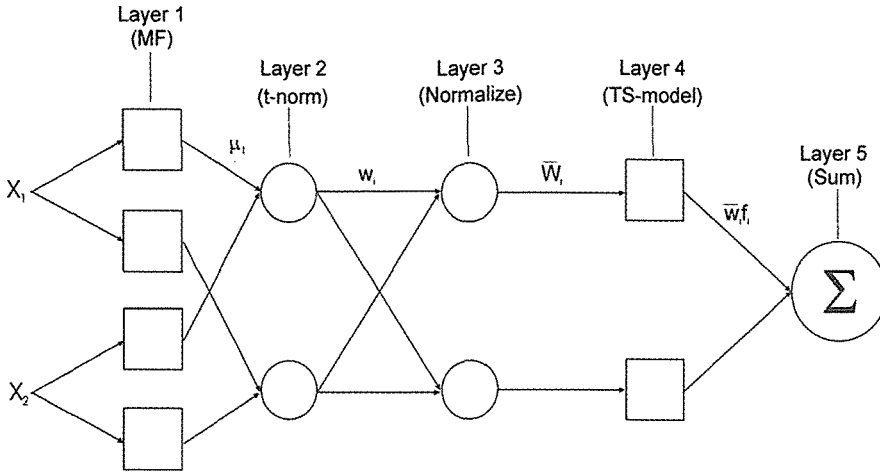


Figure 1. ANFIS architecture (from Tutmez et al., 2006).

where c_i represents the centre of the Gaussian function, and σ_i represents the spread of the membership function. The outputs of this layer are the values of the antecedent membership functions corresponding to the fuzzified inputs of the system.

Layer 2: The purpose of this layer is to compute the degrees of activation (firing strength) of particular fuzzy rules (Gorzalczany, 2001). Every node in this layer computes the product of its inputs. The output of the layer is given by

$$w_i = \mu_{A_i}(x) * \mu_{B_i}(y), \quad i = 1, 2, \quad (3)$$

where μ_{A_i} and μ_{B_i} are the fuzzy sets defined for the variables x and y respectively.

Layer 3: The nodes in this layer normalize the firing strength of the rules by calculating the ratio of the i -th rule's firing strength to the sum of all rules firing strengths.

$$w_i^* = \frac{w_i}{w_1 + w_2}, \quad i = 1, 2. \quad (4)$$

Layer 4: This layer denotes the then part (i.e., the consequent) of the fuzzy rule. Nodes in this layer are adaptive where each node function represents a first order model with the consequent parameters. Thus, the output from this layer is expressed by

$$O_i^4 = w_i^* f_i = w_i^* (p_i x + q_i y + r_i) \quad (5)$$

where w_i^* is the output of layer 3, and $\{p_i, q_i, r_i\}$ is the parameter set.

Layer 5: This is the aggregation layer where each node is fixed. The single node labelled Σ computes the overall output as the summation of all the inputs from the previous layer, i.e.,

$$O_i^5 = \sum_i w_i^* f_i = \frac{\sum_i w_i f_i}{w_i} \quad (6)$$

3.2 Training And Learning

In order to determine the parameters of an ANFIS, a hybrid algorithm has been presented by Jang (1993). A hybrid learning algorithm combines gradient descent and the least square techniques for optimizing the network parameters. In this method, the output of the system, f is written as

$$\begin{aligned} f &= \frac{w_1}{w_1 + w_2} f_1 + \frac{w_2}{w_1 + w_2} f_2 = w_1^* f_1 + w_2^* f_2 \\ &= (w_1^* x) p_1 + (w_2^* y) q_1 + (w_1^* r_1) + (w_2^* x) p_2 \\ &\quad + (w_2^* y) q_2 + (w_2^* r_2) \end{aligned} \quad (7)$$

where $(p_1, q_1, r_1, p_2, q_2, r_2)$ are the consequent parameters of the linear sub-systems. If the objective function to minimize is chosen to be the minimization of the squared prediction errors, the objective function is linear in the consequent parameters. Assuming that the parameters of Layer 1 are fixed, then they can be determined by least squares estimation. Afterwards, the parameters of Layer 4 can be fixed, and a backpropagation approach is used to adapt the premise parameters in Layer 1. Iterating between optimizing the Layer 1 parameters and Layer 4 parameters, the optimal values for all free parameters are computed (Jang et al., 1997).

4 CASE STUDY

4.1 Data Preparation

The Afsin-Elbistan lignite deposit, covers an area of 900 km² and 3.4 billion metric tons of reserves, is the biggest lignite basin and one of the most important resources for electrical energy production with power plant in Turkey (Tutmez and Dag, 2007). The Collolar field is one of the three fields of the lignite basin and the Collolar open-cast mine is currently planned for feeding coal to a power plant.

The data employed were come from the boreholes achieved by General Directorate of Mineral Research and Exploration of Turkey (MTA) between 1966 and 1980. For the case studies, 70 holes in an irregular pattern were taken into consideration. Firstly, the data set was divided into two subsets randomly: the training set (60%: 42 records) and the validation set (40%: 28 records), respectively. In practice, data conditioning is necessary. In the present study, scaling was carried out between 14.2 and 56.2 (max and min thickness values) by using a linear transformation (Fig.2).

4.2 Fuzzy Clustering

Clustering applications were carried out using the FCM clustering method. For different number of clusters, data set were trained and various cluster centers and

partition matrix alternatives have been taken from these operations.

For this study, optimal number of clusters was determined experimentally using the index method presented by Tutmez et al. (2007). The adopted method aims the reproducing STS variability of the sample data in STS of cluster centers with minimum number of clusters. As a result of this optimization, the appropriate number of clusters are defined to be five (Fig.3).

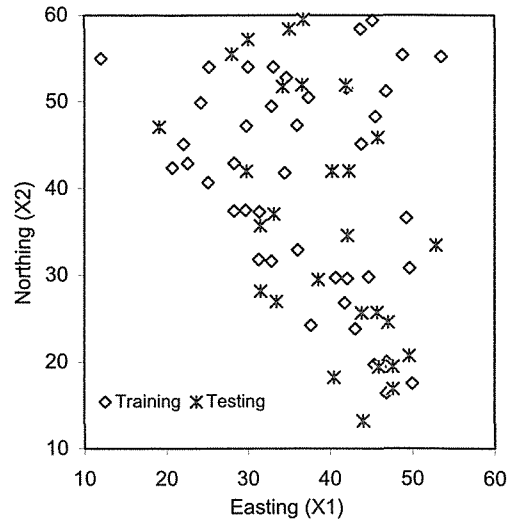


Figure 2. Data sets.

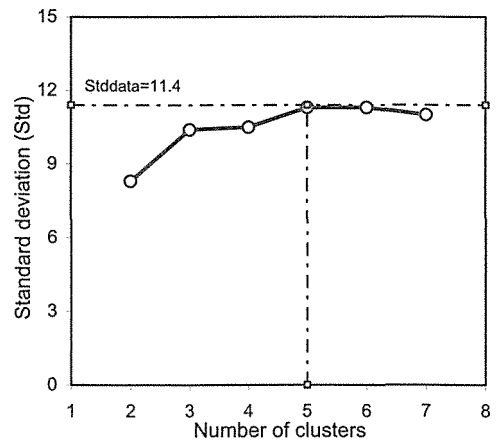


Figure 3. Cluster validity index.

4.3 Initial Inference System

Gaussian type membership functions are used in the rules. Gaussian membership functions are more common in fuzzy systems literature, as they provide both simplicity and flexibility (Tutmez et al., 2007). The function centers were selected same as the cluster center values. The rule consequents were determined from local least squares regressions, leaving it up to ANFIS to optimize the consequent parameters. Hence, all the rules in the rule base initially had the different consequents determined by the least square estimation. Rule consequents and clusters centers are indicated in Table 1.

Table 1. Initial centers and rule consequents.

No	X1	X2	Constant	Center X1	Center X2
1	0.10	-0.58	61.80	37.68	31.94
2	-0.19	-0.69	91.06	32.41	49.54
3	-1.07	-0.68	79.65	25.36	42.03
4	-1.15	0.33	56.89	47.47	55.25
5	0.05	0.11	21.26	45.26	23.38

4.4 Learning and estimation

After the initialization, the ANFIS system was trained by using a hybrid training algorithm. Figures 4-7 show the initial and the final membership functions for the two inputs that have been determined by training. The rule consequents and cluster centers optimized are shown in Table 2.

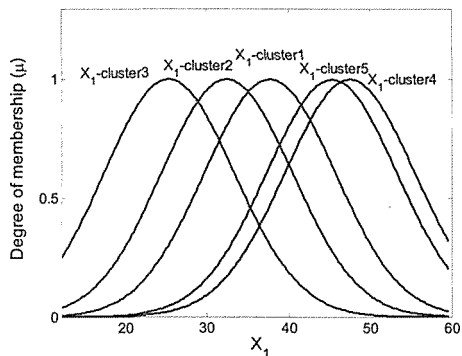


Figure 4. Initial input memberships for X1.

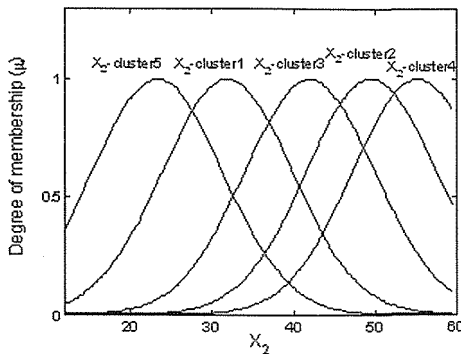


Figure 5. Initial input memberships for X2.

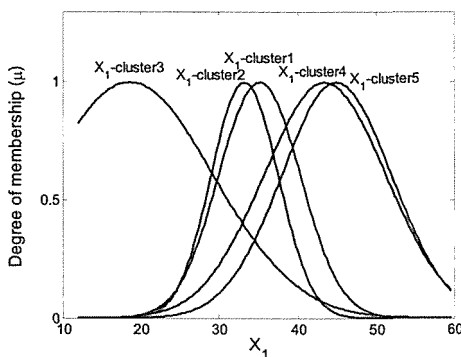


Figure 6. Optimized memberships for X1.

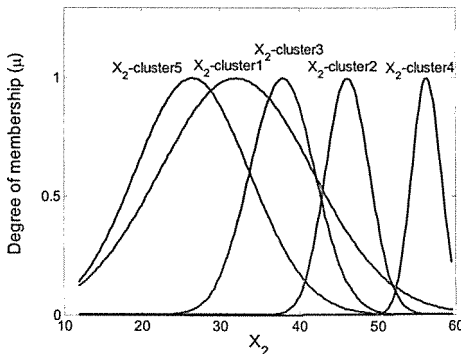


Figure 7. Optimized memberships for X2.

Table 2. Final centers and consequents.

No	X1	X2	Constant	Center X1	Center X2
1	-6.29	5.86	67.82	35.12	32.04
2	-0.20	-14.07	698.80	33.21	46.22
3	-12.19	-5.31	521.00	18.60	37.90
4	0.61	4.18	-248.10	43.45	56.26
5	-4.85	1.06	244.70	44.93	26.42

5 PERFORMANCE EVALUATION

In order to appraise the performance of the neuro-fuzzy method, the results have been compared with geostatistical (kriging) estimation. Kriging is a well-known strong estimator which is based on the spatial autocorrelation of the variables (Webster and Oliver, 2001). Spherical variogram model parameters were determined from the training data and the kriging estimations were carried out on testing data using XVOK2D from GSLIB (Deutsch and Journel, 1998).

Performance comparisons have been carried out based on four effective indicators: standard deviation (Std), coefficient of correlation (r), Variance Account For (VAF) and Root Mean Square Error (RMSE). Figures 8-9 show the results with their standard deviations. Std, VAF and RMSE values are summarized in Table 3. It has been observed that the fuzzy model outperforms more kriging modeling.

5 CONCLUSION

This paper has presented a soft hybrid methodology based on fuzzy-neural modelling in reserve estimation. The methodology is applied to estimation of lignite thickness of the Collolar field. The case study has shown that the method is applicable to reserve estimation and in fact estimates produced by this method are comparable to the estimates obtained by kriging.

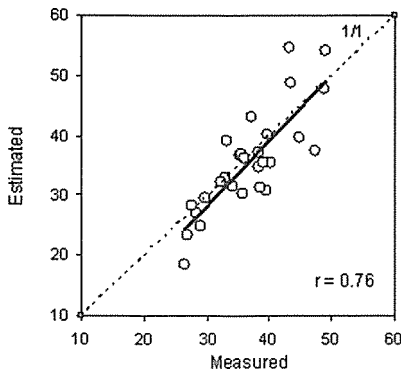


Figure 8. Testing plot of the ANFIS.

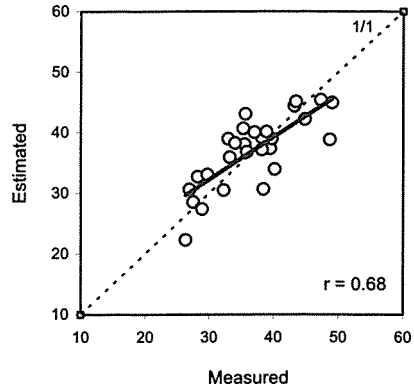


Figure 9. Testing plot of kriging model.

Table 3. Performance measures.

Model	Std	VAF	RMSE
Measured (Testing)	6.47	-	-
Fuzzy-Neural Training	-	86.84	4.08
Fuzzy-Neural Testing	7.87	62.23	4.42
Kriging Testing	4.92	51.01	4.61

REFERENCES

Bardossy, Gy., Fodor, J., 2001. Traditional and new ways to handle uncertainty in geology, *Natural Resources Research* 10(3), 169-187.

Bardossy, Gy., Fodor, J., 2004. *Evaluation of Uncertainties and Risks in Geology*, Springer-Verlag, Heidelberg, 221pp.

Bezdek, J.C., Ehrlich, R., Full, W., 1984. FCM: the fuzzy c-means clustering algorithm, *Computers&Geosciences* 10(2-3), 191-203.

Deutsch, C.V., Journel A.G., 1998. *GSLIB: Geostatistical Software Library*, Oxford Press.

Diehl, P., 1997. Quantification of the term geological assurance in coal classification using geostatistical methods, *Schriftenreihe der GDMB* 79, 187-203.

Habibagahi, G., 2002. Post-construction settlement of rockfill dams analyzed via adaptive network based fuzzy inference systems, *Computers and Geotechnics* 29, 211-233.

Goovaerts, P., 1997. *Geostatistics for Natural Resources Evaluation*, Oxford University Press, New York, 483pp.

Gorzalczany, M.B., 2001. *Computational Intelligence Systems and Applications*, Physica-Verlag, Heidelberg, 362 pp.

Jang, J-S.,R., 1993. ANFIS: Adaptive network-based fuzzy inference systems, *IEEE Trans. on Systems, Man, and Cybernetics* 23(3), 665-685.

Jang, J-S.,R., Sun, C.T., Mizutani, E., 1997. *Neuro-Fuzzy and Soft Computing: A Computational Approach to Learning and Machine Intelligence*, Prentice Hall International (UK) Limited, London, 614pp.

- Journel A.G., Huijbregts Ch.J., 1981. *Mining Geostatistics*, Academic Press, London, 600pp.
- Sinclair, A.J., Blackwell, G.H., 2002. *Applied Mineral Inventory Estimation*, Cambridge University Press, Cambridge, 381pp.
- Sousa, J.M.C., Kaymak, U., 2002. *Fuzzy decision making in modeling and control*, World Scientific.
- Takagi, H., Sugeno, M., 1983. Derivation of fuzzy control rules from human operator's control actions, *Proceedings of IFAC Symposium on Fuzzy Information, Knowledge Representation and Decision Analysis*, 55-60.
- Takagi, H, Sugeno, M., 1985. Fuzzy identification of systems and its applications to modeling and control, *IEEE Trans. On Systems, Man, and Cybernetics* 15, 116-132.
- Tutmez, B., Hatipoglu, Z., Kaymak, U., 2006. Modelling electrical conductivity of groundwater using an adaptive neuro-fuzzy inference system. *Computers&Geosciences* 32, 421-433.
- Tutmez, B., 2007. An uncertainty oriented fuzzy methodology for grade estimation, *Computers&Geosciences* 33(2), 280-288.
- Tutmez, B., Dag, A., 2007. Use of fuzzy logic in lignite reserve estimation, *Energy Sources Part B* 2, 93-103.
- Tutmez, B., Tercan, A.E., Kaymak, U., 2007. Fuzzy modelling for reserve estimation based on spatial variability, *Mathematical Geology* 39(1).
- Webster, R., Oliver, M., 2004. *Geostatistics for Environmental Scientists*, Wiley&Sons, 255pp.

Cuttability

Full-Scale Linear Cutting Tests towards Performance Prediction of Chain Saw Machines

H. Çopur, C. Balcı, N. Bilgin, D. Tumaç & İ. Düzyol

Istanbul Technical University, Mining Engineering Dept., 34469 Maslak, İstanbul, Turkey

ABSTRACT Preliminary results of a project supported by The Scientific and Technological Research Council of Turkey (TÜBİTAK) are presented in this study. Chain saw machines used for extraction of natural stones as blocks are introduced and parameters affecting chain saw performance are summarized. A set of full-scale linear rock cutting tests using chain saw cutting tools and some physical and mechanical property determination tests are performed on a block of white marble sample obtained from a quarry on Turkey in the laboratories of Mining Engineering Department of Istanbul Technical University. Using the full-scale linear rock cutting tests, tool forces and specific energy to cut a unit volume of rock can be found and optimum cutting conditions and tool pattern can be defined for a certain stone type.

1 INTRODUCTION

Natural stone industry has been growing gradually in all over the world. The related technology has also been developing in accordance. As for today, it is not a problem to produce soft stones such as travertines. However, there are still problems in producing high strength and abrasive natural stones such as marbles and granites. The problems mainly arise as low production rates, high cutting tool consumption rates, and thus, high costs.

Chain saw machines are used for cutting low to medium abrasive and soft to medium strength natural stones, such as travertine and marble, in both underground and surface quarrying operations, as well as in squaring purposes. They are able to cut slots vertically or horizontally. The productivity is higher when chain saw and diamond wire machines are used in combination. Adding only one chain saw to the equipment fleet, in addition to diamond wire cutting machines, improves the overall performance of a quarry about 20%, (Copur et al., 2006).

The basic advantages of using chain saw machines can be summarized as follows:

- They eliminate time losses and labor for drilling boreholes for wire insertion when using with diamond wire cutting machines, especially in high benches more than 6 to 7 m. In other words, they eliminate collimation problems.
- They reduce production and time losses to enter a new bench front, due to their ability of sumping horizontally or vertically to a new bench or bench front, by eliminating triangular plug removal.
- They result in directly saleable material.
- They create regular and planar surfaces, which make excellent working environment for quarrying operations.

The miners usually use standard chain saw machines for cutting every type of natural stones. However, it is very well known in rock cutting mechanics that as the rock properties change, the optimum cutting conditions change, as well. Therefore, the design of lacing pattern of the cutting tools (cutters, bits, teeth, segments, sectors) should

be different for different stones to improve performance. Any improvement of cutting rates of these machines, cutting harder stones and/or longer arm lengths would also increase the profitability.

Literature on performance of chain saws was rather limited in the past. Mellor (1976) analyzed kinematically the working principles and design parameters of continuous belt machines such as coal cutters, trenchers, chain saws. Mancini et al. (1992, 1994) analyzed the parameters affecting the performance of different chain saws, and simulated geostatistically the chain cutting; the results were compared with the field performances of different chain saws working in different conditions. Mancini et al. (2001) analyzed in-situ chain saw applications in terms of cutting performance, tool wear and stone parameters affecting these issues.

Full-scale laboratory linear rock cutting tests make possible to deterministically simulate the cutting action of a chain saw machine, as well as other mechanical miners. Full-scale testing minimizes uncertainties of scaling and any unusual stone cutting behavior not reflected in its physical and mechanical properties. These tests result in tool forces and specific energy to cut a unit volume of rock. The force data may be used as input for selection and design of an excavator, selection of cutting tool, definition of optimum cutting geometry and prediction of performance and cost for a certain stone type by optimizing torque and thrust requirement of the machine, thus maximizing the machine performance.

This study summarizes the preliminary results of a research project supported by Turkish National Science and Technology Foundation (TÜBİTAK). Characteristics of cutting by chain saws are experimentally investigated by applying laboratory full-scale linear cutting tests on a block of white marble obtained from a quarry in Turkey. The tests are performed at different cutting conditions (sideways angles of the cutting tools, depth of cut, tool spacing, etc) to find out sample cuttability (cutter forces, specific energy, optimum cutting geometry).

2 PARAMETERS AFFECTING PERFORMANCE OF CHAIN SAWS

Cutting performance of a chain saw depends on geological-geotechnical conditions of the quarry, chain saw (mechanical) features, and operational parameters.

Geological and geotechnical parameters include rock mass properties such as joint set number and frequency, dip and direction of the deposit, bedding and foliation; and intact rock properties such as cuttability, strength, elasticity, abrasivity, petrographic and texture properties.

Mechanical parameters include torque-power-thrust capacities, arm (boom) length and thickness, lacing design and metallurgical and geometrical properties of the cutting tools.

Operational parameters include arm cutting depth and angle, cutting length, chain rotation speed, cutting dry or water feeding, cutting vertical or horizontal, greasing, quality of labor, and material availability.

3 CHAIN SAW MACHINES

Chain saw machines have been in use for more than 70 years, starting with coal mining applications. In the natural stone industry, they have been in use for nearly 30 years with some modifications to coal cutters (Fig. 1).

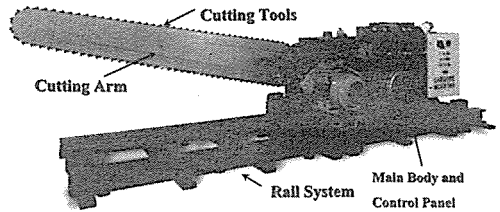


Figure 1. Garrone MRCH 340 chain saw.

These electro-hydraulic machines usually work together with diamond wire cutting machines, as well as can work, rarely, alone. Chain rotation and progress of the machine are controlled by two different hydraulic motor, which are powered by one electric motor. They move along a rail system. Their arm lengths vary up to around 7 m. The arm

thicknesses are usually either 38 mm or 42 mm, depending on the manufacturer.

Cutting tools are placed on; usually bolted to, tool holders which are mounted on sockets. The sockets are connected to each other making an endless chain (continuous belt), which slides over the arm edge after giving a pretension. The grease is used to ease sliding to reduce the torque requirement of the machine.

There are different cutting tool designs in terms of geometry (rectangular prism, cubic prism, star-shaped, etc.), composition (widia, polycrystalline diamond) and metallurgical features (Fig. 2 and 3). Four edges (with 0° of rake angle and a clearance angle of β) or eight edges (with usually negative rake angle) of the rectangular prism tools, which are the most widely used tools, are just rotated after a certain amount of wearing to get a sharp edge on operation. The entire tools should be rotated at the same time to get a better performance out of the machine, excluding prematurely broken tools.

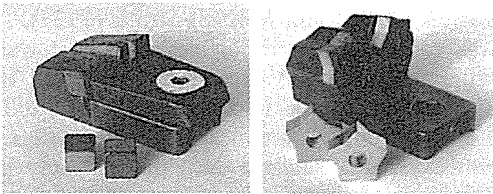


Figure 2. Cubic (left) and star-shape (right) tool geometries (Fantini Catalogues).

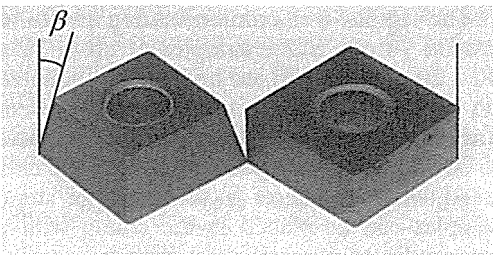


Figure 3. Rectangular prism tools: 4-edge tool (left) and 8-edge tool (right).

Analysis of a batch of worn 4-edge tools indicated four general groups of wear types: major breakage (around half or quarter of the tool is broken down and lost), minor

breakage (small pieces of the tool is broken down and lost as small chips), major abrasive wear (half or quarter edge width and corners of the tool is worn out) and minor abrasive wear (only corners of the tool is worn out), (Fig. 4). The type, shape and amount of wearing of a tool mostly depend on cutting profile, layout / lacing design of the tools in a sequence, its metallurgical features, and abrasivity of the stone.

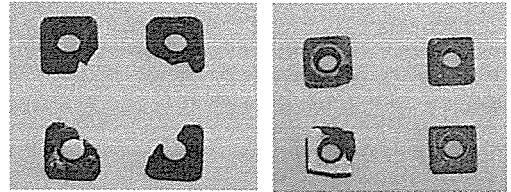


Figure 4. Major (left) and minor (right) breakage of the tools (Copur et al., 2006).

There are different designs of cutting sequences depending on the manufacturers. A cutting sequence can be composed of different numbers of tool holders and/or sockets, usually 8 to 10, depending on cutting conditions. Usually two to three of the tool holders located at the end of sequence include two tools and the others only one tool. Tools on a sequence is usually and should be located symmetrically to counterbalance the sideways forces coming from the tools for avoiding an uneven wear on the tools and arm plate.

Cutting action of a sequence, and thus the tools, is repeated by the following sequences. Total number of sequence on a chain depends on the arm and/or chain length. A picture of a cutting sequence is presented in Figure 5. An example of a tool lacing (layout) design is presented in Figure 6. An example of a cutting profile is presented in Figure 7.

Tool (line) spacing along the cutting profile varies; usually smaller at the edges and larger around the center (Fig. 8). However, the tool spacing along the cutting trajectory (mesh length) is constant and depends on the socket length; for example it is 90 mm in Figure 6.

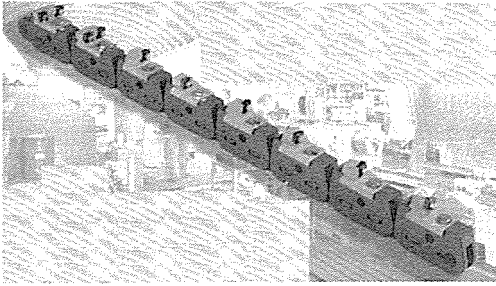


Figure 5. A picture of a “tool lacing design” in a sequence (Garrone Catalogues)

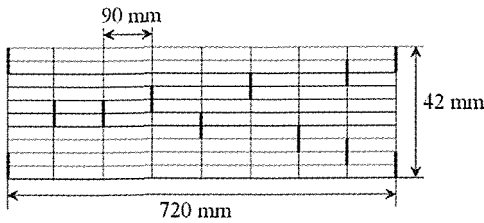


Figure 6. An example of “tool lacing design” in a sequence (Copur et al., 2006).

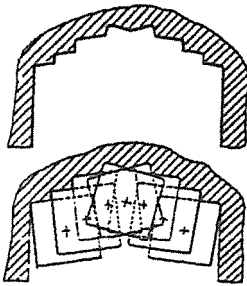


Figure 7. An example of “cutting profile” (Fantini, Catalogues).

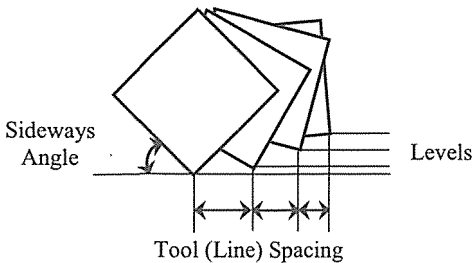


Figure 8. Variable tool (line) spacing, sideways angles and levels.

Angular positions of each tool (sideways angle) vary usually along the profile of a sequence (Fig. 8). Sideways angle is usually between 45° and -5° , being at maximum on the center and getting gradually smaller at the sides of the profile. Levels of strike points of each tool also vary in a sequence.

Any design or operational condition away from the optimum solution would result in higher tool wear rates and lower production rates. To get the best performance out of a chain saw for certain type of stone includes a complex optimization problem including all the parameters mentioned above; the solution of which should be looked for in the science of rock cutting mechanics.

4 FULL-SCALE LINEAR CUTTING EXPERIMENTS

4.1 Experimental Equipment, Procedures and Parameters

The rig used in the linear cutting experiments is a shaping machine (Fig. 9), which is similar to the one originally developed by Fowell (1976) and McFeat-Smith (1977). It was called “core cutting rig”, since it was originally designed to cut core samples in diameter of 76 mm by a standard chisel tool for predicting roadheader performance. However, the machine used in this study is named as “full-scale linear cutting rig” since block samples and real life cutters similar to the ones used in chain saws are used in this study.

The rig has a maximum cutting stroke of around 70 cm. Stone samples of up to 30 x 30 x 20 cm can be fixed on a clamp mounted on the machine table, which can be raised, lowered and laterally traversed with respect to cutting tool; line spacing between the cuts is adjusted by lateral traversing. The stone samples can be placed in the clamp with a certain dip angle or parallel or perpendicular to the bedding planes in order to simulate the actual cutting conditions of the deposit.

The cutting tool is fixed with a tool holder directly to a 5 ton capacity steel load cell (dynamometer), equipped with strain gauge bridges, used for recording the forces acting on the tool. Tool-holder-dynamometer

assembly can be raised or lowered with a mechanical device to adjust cutting depth. The tool has to be calibrated with the dynamometer prior to testing by applying different loads with a hydraulic jack.

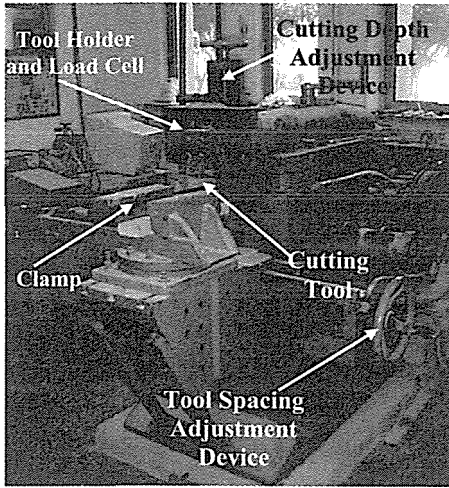


Figure 9. Full-scale linear cutting test rig of the Istanbul Technical University, Mining Engineering Department.

An electric motor actuator forces the tool-holder-dynamometer assembly, which are located in front of a slipway, through the fixed/clamped stone sample at a preset cutting depth, line spacing and constant velocity. During the cut, the dynamometer measures the normal, cutting and sideways forces acting on the tool. After each cut, the clamped stone sample is moved sideways by a preset line spacing to duplicate the action of the multiple tools on a miner.

Data acquisition system includes a dynamometer, amplifier and personal computer. The data is recorded at required gain and sampling rate by a commercial software. The data acquisition card includes eight independent channels and monitors and collects data from the dynamometer. Excitation voltage of amplifier is 10 V. Data sampling rate is adjustable up to 50000 Hz. The recorded data is evaluated using a spreadsheet program.

The attack, skew and tilt angles can also be simulated in linear cutting experiments.

Sieve analysis is performed to measure the size gradation of the muck samples.

The three orthogonal forces (cutting, normal and sideways forces) acting on a tool is presented in Figure 10. The cutting (drag) force, acting parallel to the surface being cut, is directly related to the torque requirement of a mechanical excavator, and used to calculate the specific energy. The normal force, acting perpendicular to the surface being cut, is used to calculate the required effective mass and thrust of the excavator. The side force, acting perpendicular to the tool travel direction and the direction of normal force, may be used along with normal and cutting forces to balance the tool lacing.

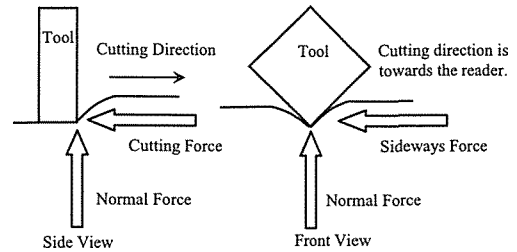


Figure 10. Forces acting on a tool

Specific energy is one of the most important factors in determining the efficiency of cutting systems and defined as the amount of energy required to excavate a unit volume of rock. Using the specific energy (MJ/m^3), achievable production rates can be calculated for a machine with a known cutting power. Lower specific energy means that a given machine will produce more material, or that a smaller / less expensive machine may be used to produce the required amount of material. The effect of line spacing and depth of cut on cutting efficiency is explained in Figure 11.

If the line spacing is too close (a), the cutting is not efficient because the rock is over-crushed; tool wear is also high in this region due to the high friction between tool and rock. If the line spacing is too wide (c), the cutting is not efficient since the cuts cannot generate relieved cuts (tensile fractures from adjacent cuts cannot reach to form a chip), creating a ridge or a groove-

deepening situation which creates shock loads causing gross failures in cutting tools. The minimum specific energy is obtained with an optimum spacing to depth of cut ratio (b), which indicates the most efficient cutting condition and the largest chips.

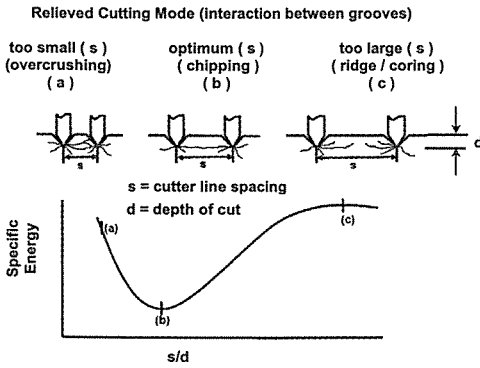


Figure 11. Effect of line spacing and depth of cut on specific energy.

The linear cutting tests mentioned in this study are performed on a homogeneous and massive white marble sample. Using only one block helped to avoid a block confounding problem. The experiments are carried out with specially shaped widia (tungsten carbide) tools to be easily mounted on the tool holder. All of the tools have the same width of 12.7 mm. However, their tips are arranged to simulate the different sideways angles on a cutting profile. Sideways angles of 0°, 15°, 30° and 45° are tested in the study. The tip angles of all the tools are 90°. Pointed and sharp tips are located at the center of the tool (Fig. 12).

The tests are performed in unrelieved cutting mode; in other words, there is no interaction between the tools. The values of depth of cut are varied as 1, 2, 3 and 4 mm.

The constant parameters throughout the testing are rake angle of (-5°), clearance angle of (5°), cutting speed of 40 cm/s and data sampling rate of 1000 Hz. Average tool forces (cutting and normal) and yield are recorded in each cut. Specific energy is obtained by dividing average cutting force to

yield. Yield is defined as the volume of rock obtained per unit length of cutting.

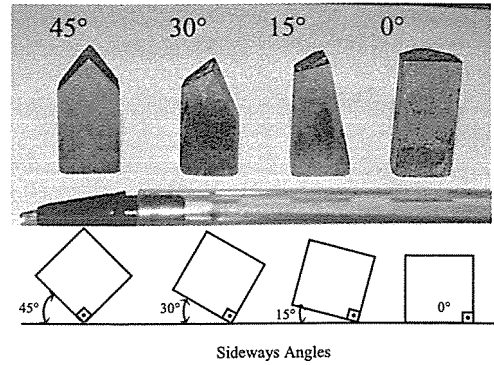


Figure 12. Tools used in the tests.

The surface of stone block, before each set of cut, is trimmed with a standard chisel tool (0° tool) to have a flat surface and dyed by a spray paint to see easily the breakout pattern. Each cut is replicated at least 3 times.

4.2 Results and Discussion

The physical and mechanical properties of the white marble are summarized in Table-1. Picture of the white marble sample after linear cutting testing is presented in Figure 13. The average normal and cutting forces of unrelieved cutting tests with all the tools are summarized in Figure 14 for different depth of cut values, and also summarized in Figures 15 and 16. The average specific energy values of unrelieved cutting tests with all the tools are summarized in Figure 17 for different depth of cut values.

Table 1. Some physical and mechanical properties of white marble used in the tests.

Natural unit weight	2.70 g/cm ³
Uniaxial compressive strength	35.8 MPa
Brazilian tensile strength	5.0 MPa
Cerchar abrasivity index	1.5
Static elasticity modulus	12.21 GPa
Static Poisson's ratio	0.21
Dynamic elasticity modulus	143 GPa
Dynamic Poisson's ratio	0.38
Cone indenter hardness	1.36

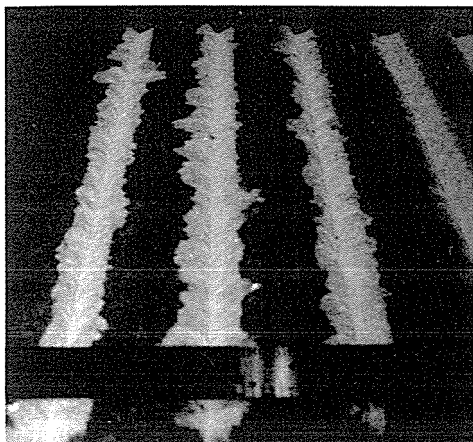


Figure 13. Picture of the grooves on white marble after testing by linear cutting test rig.

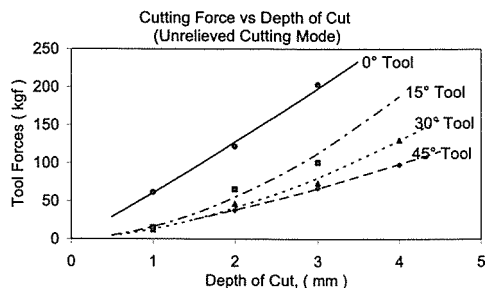


Figure 15. Cutting forces for different sideways angles versus depth of cut.

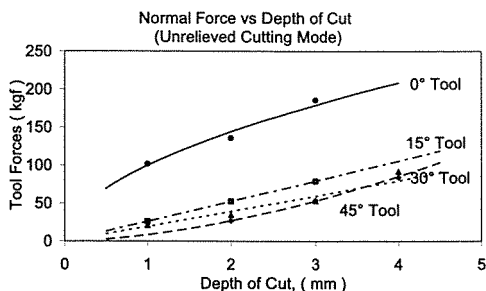


Figure 16. Normal forces for different sideways angles versus depth of cut.

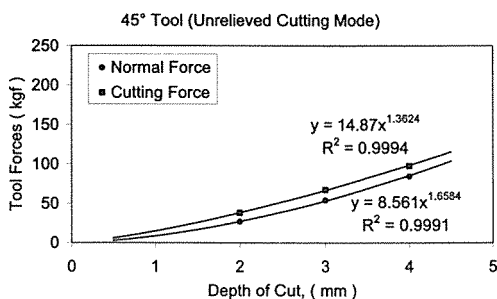
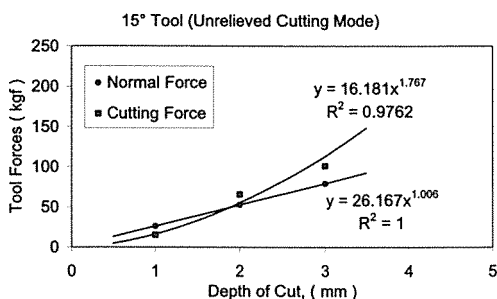
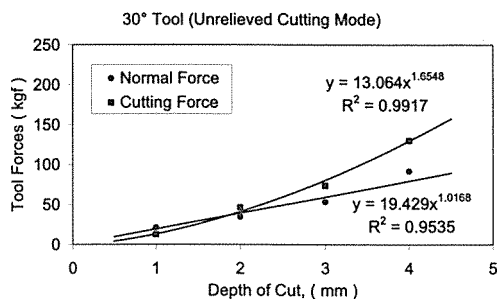
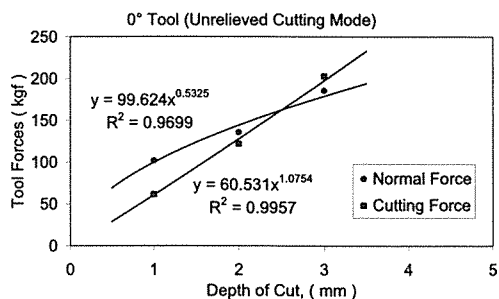


Figure 14. Cutting and normal tool forces for different sideways angles versus depth of cut in unrelieved cutting mode.

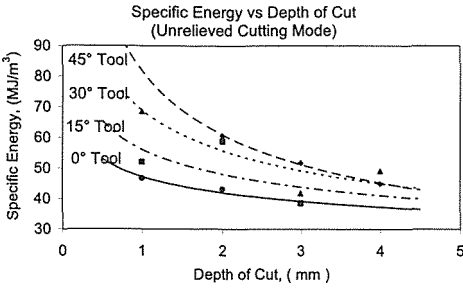


Figure 17. Specific energy for different sideways angles versus depth of cut.

The cutting and normal forces acting on the tools with different sideways angles yield relationships in power function of the depth of cut, as it is seen in Figures 14, 15 and 16. The tool forces from the lowest to the highest are obtained by 45°, 30°, 15° and 0°, respectively. It should be noted that, in reality, the tools with 0° or close to 0° of sideways angles do not cut in so large cutting width of 12.7 mm. They usually cut the stone with a few or several millimeters of width. Therefore, the results of 0°-sideway-tool should be linearly corrected for real cutting width, depending on the lacing design.

The specific energy plots of the different sideways angles for different depth of cut values (Fig. 17) indicates that the specific energy values from the lowest to the highest are 0°, 15°, 30° and 45°, respectively. The relationships follow a decreasing trend with increasing depth of cut. The trend gets asymptotic with increasing depth of cut. This is an expected result according to rock cutting mechanics. Specific energy decreases with increasing sweeping area.

Usually for the mechanical miners using conical tools and disc tools such as roadheaders and tunnel boring machines, the optimum depth of cut value is obtained when this plot approaches to almost horizontal. Above this depth of cut value, the efficiency of excavation can not be improved much. The chain saw machines usually work with the depth of cut values of fractions of a millimeter in marbles, may be around 1 to 2 mm for soft stones such as travertines. It can be said that these depth of cut values are not

optimum in terms of cutting mechanics. However, when considering the optimum cutting conditions for a certain type of tool, the line spacing should also be taken into account as seen in Figure 11.

The force and specific energy trends obtained in this study are as expected, since the forces, especially cutting force, are generally functions of theoretical swept area for chisel tools. Theoretical swept area depends on the depth of cut and the geometry of the tool (Fig. 18). Theoretical swept areas for the tools used in this study are plotted against depth of cut in Figure 19. As it is seen, the experimental tool forces and theoretical swept areas follow the similar trends. This also indicates the predictive power of the full-scale linear cutting experiments. If it is necessary, it is possible to predict the forces for the fractions of millimeters of depth of cut values, at which it is really difficult to do testing with any of such a rig, by extrapolation out of the predictive equations.

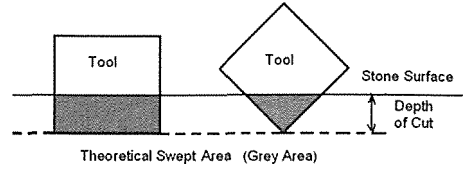


Figure 18. Theoretical swept area.

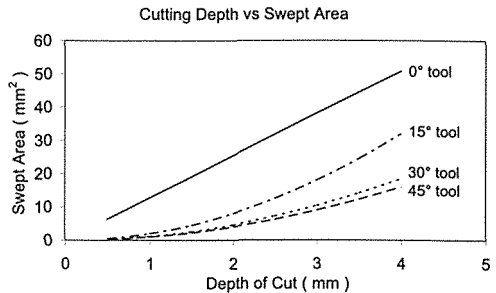


Figure 19. Theoretical swept area for different sideways angles versus depth of cut.

It should be kept in mind that these results are for unrelieved cutting modes. In reality, the tools work together in accordance with each other by generating relieved cuts (Fig. 11). There is an interaction between the tools in relieved cutting mode.

These results show that it is possible to deterministically simulate the cutting action of a chain saw machine based on full-scale linear cutting tests. Using this test rig, it is also possible to better understand the cutting characteristics of chain saws, to develop optimum lacing designs for a given stone type and to predict machine performance.

5 CONCLUSIONS

The full-scale linear cutting tests indicate that the cutting and normal forces acting on the tools with different sideways angles yield relationships in power function of the depth of cut for unrelieved cutting mode. The tool forces from the lowest to the highest are obtained by 45°, 30°, 15° and 0°, respectively. The relationships follow an increasing trend with increasing depth of cut.

The specific energy values of the tools from the lowest to the highest are 0°, 15°, 30° and 45°, respectively. The relationships follow a decreasing trend with increasing depth of cut.

The study sets the first step and preliminary results of a research project. As a future work, including unrelieved and relieved cutting modes, an extended set of full-scale linear rock cutting tests will be performed for different stone samples using chain saw cutting tools in order to find out cutting characteristics of chain saws, to develop optimum lacing designs and cutting conditions for a given stone type for maximum production rates and to predict machine performance by deterministic simulation. Studies will be in accordance with field analysis of the chain saw machines in terms of tool consumption and cutting rates.

ACKNOWLEDGEMENTS

The Scientific and Technological Research Council of Turkey (TÜBİTAK) is appreciated for their support on the Project 105M017. The authors would also like to thank to Adnan Saraçoğlu, President of SET Makine Ltd. Sti., for his valuable contributions and help on this study.

REFERENCES

- Copur, H., Balci, C., Bilgin, N., Tumac, D., Feridunoglu, C., Dincer, T. and Serter, A., 2006. Cutting performance of chain saws in quarries and laboratory. *Proc. 15th Int. Symp. on Mine Planning and Equipment Selection*, Torino-Italy, Sep.20-22. Editors: M. Cardu, R. Ciccu, E. Lovera, and E. Michelotti, pp. 1324-1329
- Fantini, *Product Catalogues*
- Fowell, R. J. and McFeat-Smith, I., 1976. Factors influencing the cutting performance of a selective tunnelling machine. *Int. Tunnelling '76 Symp.*, London, 1-5 Mar., pp. 301-318.
- Garrone, *Product Catalogues*
- Mancini, R., Cardu, M., Fornaro, M. and Toma, C.M., 2001. The current status of marble chain cutting. *Proc. Mine Planning and Equipment Selection*, pp. 151-158
- Mancini, R., Cardu, M., Fornaro, M., Linares, M. and Peila, D., 1992. Analysis and simulation of stone cutting with microtools. *Proc. III Geoengineering Congress, Rock Excavation: The Future and Beyond*, 1-2 Dec., Torino-Italy, pp. 227-236
- Mancini, R., Linares, M., Cardu, M., Fornaro, M. and Bobbio, M., 1994. Simulation of the operation of a rock chain cutter on statistical models of inhomogenous rocks. *Proc. Mine Planning and Equipment Selection*, Eds. Pasamehmetoglu et al., pp. 461-468
- McFeat-Smith, I. and Fowell, R.J., 1977. Correlation of rock properties and the cutting performance of tunnelling machines. *Conference on Rock Engineering*, UK, organized jointly by the British Geotechnical Society and Department of Mining Engineering, The University of Newcastle Upon Tyne, pp. 581-602
- Mellor, M., 1976, *Mechanics of cutting and boring, Part 3: Kinematics of continuous belt machines*. CRREL (US Army, Cold Regions Research and Engineering Laboratory, Hanover, New Hampshire), Special Report, No: 76-17

Predicting the Cuttability of Rocks using Artificial Neural Networks and Regression Trees

B. Tiryaki

Hacettepe University, Department of Mining Engineering, Beytepe, Ankara, Turkey

ABSTRACT This paper is concerned with the applications of artificial neural networks (ANN) and regression trees along with the multivariate statistical tools for predicting specific cutting energy (SE) of rocks from their intact properties. For that purpose, data obtained from three rock cutting projects have been subjected to statistical analyses using MATLAB software. Principal components and factor analyses have shown that uniaxial compressive strength (UCS), Brazilian tensile strength (BTS), static modulus of elasticity (Elasticity), and cone indenter hardness (CI) seemed to be the most influential independent variables in the data set. Hierarchical cluster tree analysis has divided the variables into three different natural clusters.

Three predictive models for SE were developed using multiple nonlinear regression, ANN, and regression trees methods. Regression tree model has been understood to fit the data better than the other two models. ANN model also produced a high correlation coefficient, indicating its significance in predicting rock cuttability.

1 INTRODUCTION

One of the difficulties inherent in building predictive models in different areas of mining and rock engineering is the problem of summarizing the data set that has many variables. In data sets with many variables, groups of variables often move together. One reason for this is that more than one variable may be measuring the same rock property governing the behavior of the rock in a given engineering application. Multivariate statistical tools are known to help overcome this difficulty by reducing the total number of variables, detecting the outlying data points, and finding the possible natural clusters in the data set (MATLAB, 2006). However, such multivariate statistical tools have not yet been widely employed in building predictive models for SE.

Traditionally, statistical methods such as bivariate and multiple linear or nonlinear

regression techniques are employed to develop predictive models for SE. In multiple nonlinear regression, the form of the relationship between the response and the predictors is supposed to be known before building a predictive model. If the relationship between the response and the predictor (s) is unknown and is assumed to be not well approximated by a linear model as in SE prediction, it is needed a more nonparametric type of regression fitting approach. One such approach is based on the regression trees (MATLAB, 2006). However, this technique has not been employed in predicting SE.

Fuzzy logic and ANN have been used in building predictive models for the prediction of rock strength parameters in mining and tunneling applications in the last few years (Sonmez et al., 2004; Gokceoglu, 2002; Singh et al., 2001; Finol et al., 2001; Alvarez

Grima and Babuska, 1999; Meulenkamp and Alvarez Grima, 1999). However, ANN has not yet been utilized for predicting SE.

This paper is concerned with establishing prediction models for rock cuttability using ANN and regression trees using intact rock properties. For that purpose, data obtained from three different rock cutting projects were considered in this study. All the data were firstly evaluated using the multivariate statistical tools. Original data set, after removing the outliers, was then subjected to bivariate correlation, regression, and curve fitting analyses. Results of all above analyses were employed to develop predictive models for SE using multiple nonlinear regression, ANN, and regression trees methods. Development of the new prediction models was given and outputs of these models were discussed in this paper.

2 CUTTING ROCKS WITH DRAG TOOLS

Cuttability of rocks is one of the most significant decision-making parameters in mechanical excavation. Being not an intrinsic rock property, it is determined in linear rock cutting tests where the core or block samples of proper dimensions are cut by using standard chisel picks on a rig. This test has been developed to determine the cuttability characteristics of rocks, which is usually expressed by the specific energy consumed during rock cutting. SE is closely related to intact rock properties and the performance of mechanical excavators (Tiryaki and Dikmen, 2006; Fowell and Johnson, 1982; Fowell and Pycroft, 1980).

3 DATA ANALYSIS

Statistical analyses on the relationships between SE and intact rock properties have been carried out based on the data obtained from three different projects undertaken by McFeat-Smith and Fowell (1977), Roxborough and Philips (1981), and Tiryaki and Dikmen (2006). SE, quartz content (Quartz), effective porosity (Porosity), BTS, UCS, Elasticity, CI, and Shore hardness (Shore) were measured for the samples of 45 different rocks in those studies. Mean values of the above parameters were subjected to statistical analyses using MATLAB.

3.1 Principal Components Analysis

A principal components analysis has been applied on the data set of independent variables. The coefficients for eight principal components are given in Table 1. The columns are in order of decreasing component variance. The absolute largest coefficients in the first principal component are UCS, BTS, Elasticity, and CI. The second principal component is weighted on Quartz and Porosity whereas the third component is weighted on Shore (Table 1).

The percent variability explained by each principal component has been given in Table 2 that reveals that the most of the variance (83%) in data set can be explained by only three principal components with the first principal component account for the highest percent of total variance (52%).

Table 1. Coefficients for the principal components.

Variables	Principal Components							
	1st	2nd	3rd	4th	5th	6th	7th	8th
Quartz (%)	-0.23	0.59	-0.42	0.02	-0.36	0.22	0.43	0.24
Density (gr/cm ³)	0.35	0.01	0.16	0.88	-0.19	-0.07	0.18	-0.02
Porosity (%)	-0.19	0.69	0.25	0.13	0.09	-0.31	-0.55	-0.03
UCS (MPa)	0.42	0.26	0.14	-0.31	-0.31	-0.02	0.17	-0.71
BTS (MPa)	0.45	0.13	0.01	-0.03	0.01	0.75	-0.42	0.21
Elasticity (GPa)	0.44	0.00	0.20	-0.31	-0.35	-0.43	0.02	0.60
Shore	0.27	-0.08	-0.81	0.08	-0.07	-0.31	-0.37	-0.12
CI	0.38	0.29	-0.11	-0.04	0.78	-0.12	0.36	0.09

Table 2. Variances explained by principal components.

Principal Components	Variances	% of variance explained
1	4.15	51.90
2	1.51	18.90
3	0.99	12.31
4	0.59	7.32
5	0.37	4.67
6	0.19	2.37
7	0.14	1.71
8	0.07	0.82

Scatterplot of the second principal component versus the first one shows the original data projected onto the first two principal components in Figure 1. It can be seen from Figure 1 that there are six outlying points in the lower left portion of the plot, a single outlier on the upper right corner, and another one in the upper left corner. Those outlying data points in the lower left corner of the plot belong to all six non-sandstone coal measures rocks in the data set, which were taken from McFeat-Smith and Fowell (1977). It has been understood that those rocks behave differently from the others because they are argillaceous rocks with high bulk density and very low porosity, and are the finest-grained rocks in the data set of McFeat-Smith and Fowell (1977).

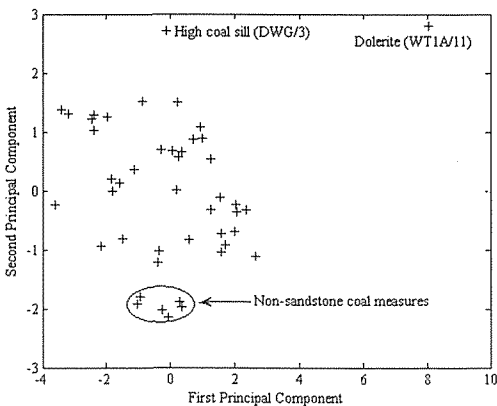


Figure 1. Scatterplot of second principal component against the first one.

Dolerite is behaving differently from other rocks, since it is the only very high strength rock in the data set. A separate outlier analysis was also carried out on the data set including SE by taking the observations greater than three times the standard deviations for each variable as outliers.

This outlier analysis showed that dolerite had outliers for Density, UCS, BTS, and CI whereas Nattrass gill hazle (WT2/12) had an outlier for SE. Outlier analysis has not identified any outlier for High coal sill.

3.2 Factor Analysis

A factor analysis has been applied on the data set of independent variables. The estimated loadings and the estimates of specific variances are given in Table 3. It can be seen from Table 3 that each variable depends primarily on only one factor, and it is possible to describe each factor in terms of the variables that it affects.

Table 3. Factor loadings and estimated specific variances.

Variables	Factors			Specific variance
	1	2	3	
Quartz	-0.05	1.05	0.25	0.01
Density	0.46	-0.20	0.06	0.65
Porosity	0.21	0.65	-0.39	0.36
UCS	1.06	0.13	-0.09	0.02
BTS	0.80	-0.03	0.11	0.24
Elasticity	0.87	-0.20	-0.07	0.13
Shore	-0.02	0.17	1.06	0.01
CI	0.68	0.10	0.19	0.44

Factor1 is mainly weighted on the independent variables of UCS, BTS, Elasticity, and CI with the highest four loading values. Factor2 is mainly weighted on Quartz and Porosity with the highest two loading values. Factor3 is weighted only on Shore. These findings indicate that the results of the factor analysis are in line with those of the principal components analysis. SE was not included in principal components and factor analyses to find out the most influential independent variables in the data set. However, the results of above analyses

on original data set when SE was included were similar to those given in here.

3.3 Hierarchical Cluster Analysis

Hierarchical clustering is a way to investigate grouping in the data set, simultaneously over a variety of scales, by creating a cluster tree. The tree is not a single set of clusters, but rather a multilevel hierarchy, where clusters at one level are joined as clusters at the next higher level (MATLAB, 2006).

Original data set has been subjected to a hierarchical cluster analysis. The hierarchical binary cluster tree (dendrogram display) created by MATLAB for the original data set is given in Figure 2 where the links between variables are represented as upside-down U-shaped lines. Hierarchical cluster analysis has shown that SE and CI fall into one category as representing the cuttability characteristics of rocks whereas UCS, BTS, and Elasticity being the mechanical rock properties constitute another category. The third cluster is comprised of Quartz and Porosity, being mineralogical-physical rock properties.

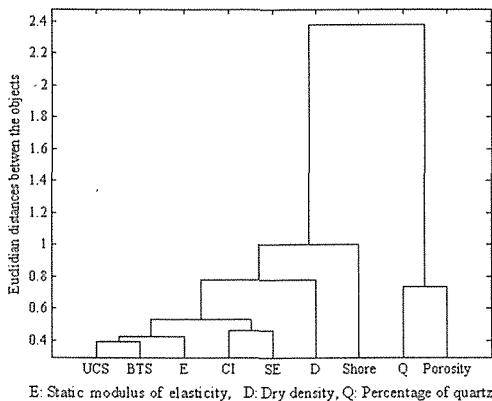


Figure 2. Dendrogram display for the original data set.

Calculated cophenetic correlation coefficient for this hierarchical cluster tree is 0.99, which shows that the clustering solution reflects the data set very accurately.

4 BUILDING PREDICTIVE MODELS

A new data set (regression data set) has been employed for the model development studies in this section, which has been formed by removing six non-sandstone coal measures, dolerite, and Natrass gill hazle from the original data set.

4.1 Correlation Analysis

A correlation matrix was produced applying bivariate correlation technique to the regression data set to test the data in order to define the degree of linear relationships between the variables. Pearson's correlation coefficients (r -values) between all variables are given in Table 4. Correlation matrix of the regression data set exhibited close linear relationships between Density, UCS, BTS, Elasticity, Shore, CI, and SE. This result is consistent with those of the previous studies. Powell (1970) stated that Shore hardness could be used to asses the cuttability of rocks by mechanical tools. Cone indenter hardness is known correlated well with SE and roadheader performance (NCB, 1977). Strong correlations have been found between UCS and SE for coal measures rocks (Rostami et al., 1993). It is also very well known that as BTS increases SE also increases for the most of the rocks. Brittle rocks were reported to show tensile failure, whilst tougher rocks fail in shear mode. However, the failure cracks in a rock forced by a pick are tensile in nature free from rock type (Roxborough, 1973; Nishimatsu, 1979).

4.2 Bivariate Linear Regression and Curve Fitting

Rock properties that were found to be in statistically significant correlations with SE were subjected to bivariate linear regression and curve fitting analyses. All the nonlinear models along with the linear model were tried to fit the data to establish bivariate regression models for SE. Best models summarizing the relationships between the independent variables and SE are given in Table 5. Sum of squares due to error (SSE), root mean squared error (RMSE), the

coefficient of determination (R^2), and the adjusted R^2 were used as the numerical measures of the goodness of the fit (Table 5). According to these values, UCS, BTS, Elasticity, and CI have appeared as the best predictors for SE, being in line with the results of the multivariate statistical analyses.

Regression models including UCS, BTS, Elasticity, and CI as predictors are also illustrated in Figure 3, respectively. The prediction bounds for each model indicate that new observations can be predicted accurately throughout the entire data range.

Table 4. Full correlation matrix for the regression data set.

	Quartz	Density	Porosity	UCS	BTS	Elasticity	Shore	CI	SE
Quartz	1	-0.34*	0.63*	-0.18	-0.3*	-0.45*	-0.01	-0.14	-0.04
Density	-0.34*	1	-0.17	0.5*	0.62*	0.53*	0.3	0.47*	0.36*
Porosity	0.63*	-0.17	1	-0.07	-0.23	-0.31*	-0.44*	-0.03	-0.08
UCS	-0.18	0.5*	-0.07	1	0.83*	0.87*	0.31*	0.7*	0.67*
BTS	-0.3*	0.62*	-0.23	0.83*	1	0.77*	0.45*	0.74*	0.57*
Elasticity	-0.45*	0.53*	-0.31*	0.87*	0.77*	1	0.33*	0.6*	0.63*
Shore	-0.01	0.3	-0.44*	0.31*	0.45*	0.33*	1	0.44*	0.48*
CI	-0.14	0.47*	-0.03	0.7*	0.74*	0.6*	0.44*	1	0.72*
SE	-0.04	0.36*	-0.08	0.67*	0.57*	0.63*	0.48*	0.72*	1

*: Correlation coefficient is significant at 0.05 level.

Table 5. Best bivariate regression models for SE.

Predictors	SSE	R ²	Adj R ²	RMSE	Regression Model
Elasticity	543.86	0.79	0.78	4.00	SE = -71.69*Elasticity ^{0.27} +51.67
UCS	670.42	0.74	0.73	4.38	SE= 2.04* UCS ^{0.52}
BTS	861.44	0.67	0.66	4.96	SE = 7.05*BTS ^{0.61}
CI	840.25	0.67	0.65	4.97	SE = -65.11*CI ^{0.29} +62.53
Shore	1725.40	0.33	0.29	7.12	SE = -0.03*Shore ² + 3*Shore-43.82
Density	1772.00	0.31	0.29	7.12	SE = 49.12*Density -107.6
Porosity	1935.00	0.25	0.23	7.44	SE = -0.9*Porosity +28.93

4.3 Multiple Nonlinear Regression

The twin-logarithmic model has been used in multiple nonlinear regression for predicting SE. UCS, BTS, Elasticity, and CI were participated as the predictors in regression analysis that resulted in the following model:

$$SE = 3.33 \times UCS^{0.05} \times BTS^{0.09} \times Elasticity^{0.17} \times CI^{0.5} \quad (1)$$

The F-statistic of 25.26 and its p -value of zero indicate that it is highly unlikely that all of the regression coefficients in this model are zero.

Contribution of each independent variable to the explanation of variation in SE seems reasonable as this model proposes increases in SE values as UCS, BTS, Elasticity, and CI

values increase. Scatterplot of the fitted SE values against the observed SE values for the multiple nonlinear model of SE is given in Figure 4. The correlation coefficient between observed and predicted SE values for the model (R-value) is 0.89 that is statistically significant at 95% level. Sum of squares due to error value for this model is 549.31.

With the scatterplot of predicted values of the dependent variable from any regression model against those observed, data points are expected to be evenly distributed over, above, and below the regression line without any outlying data points to reason that the prediction model fits the data well.

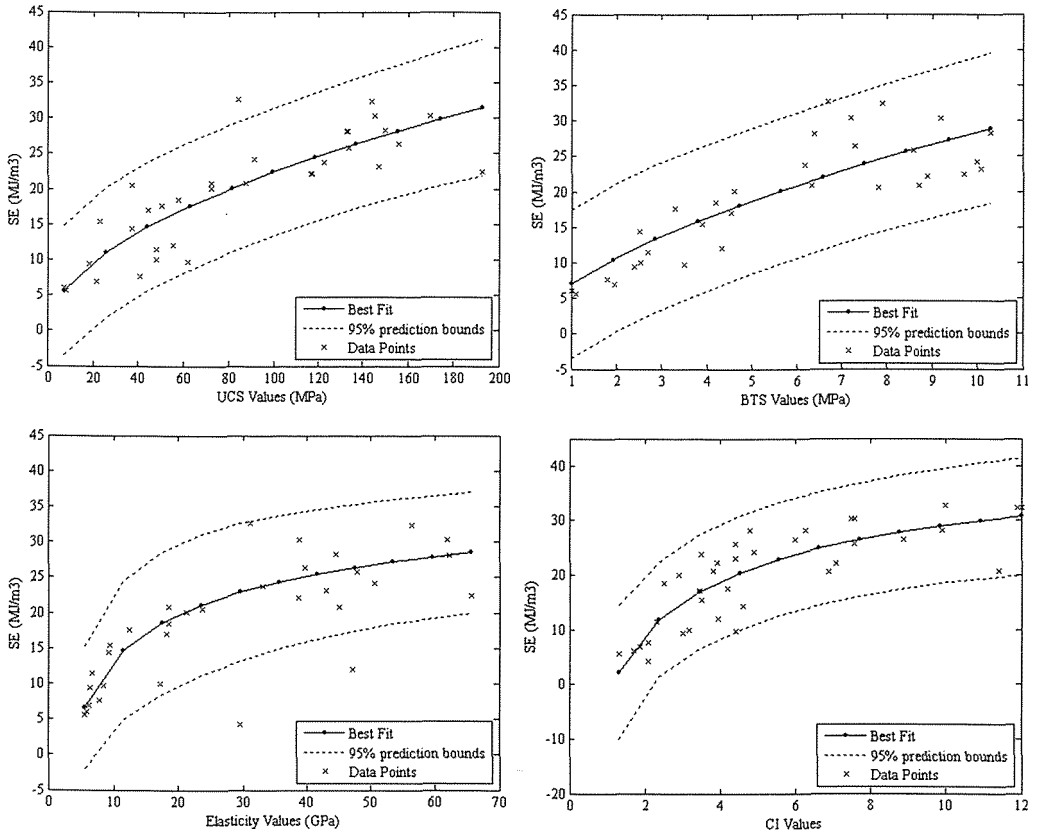


Figure 3. Best fits summarizing the relationships between the predictors and SE.

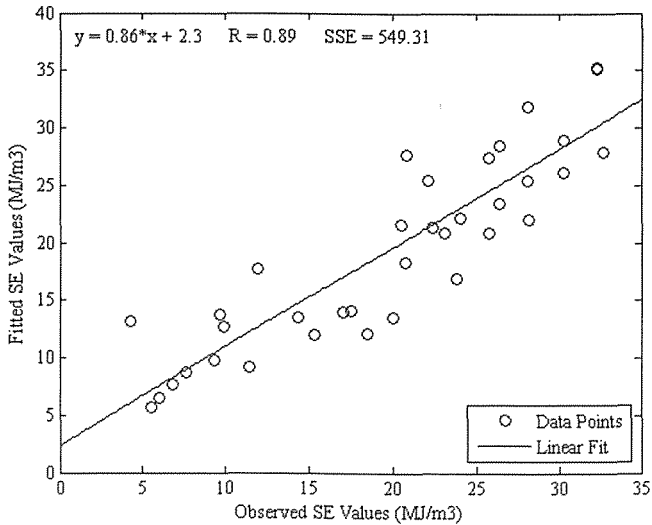


Figure 4. Scatterplot of SE values predicted by nonlinear model versus those observed.

Scatterplot in Figure 4 indicates that nonlinear regression model of SE fits the data well and is a good choice to predict SE values from the observed values of UCS, BTS, Elasticity, and CI.

4.4 Artificial Neural Networks

Artificial neural networks (ANN) are simplified models of the biological structure found in human brain. A neural network is a massively parallel-distributed processor that

has a natural propensity for storing experiential knowledge and making it available for use.

A typical architecture (standard multilayer perceptron) of neural network is shown in Figure 5, which consists of one input layer, one or more hidden layers, and one output layer. A fully connected ANN as in Figure 5 with one output and one hidden layer of units can compute the following function (Bishop, 1995):

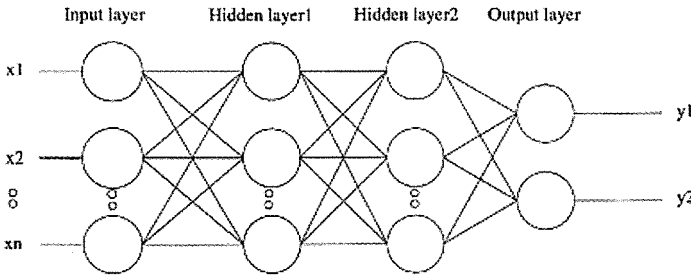


Figure 5. Artificial neural network.

$$f(x) = \varphi_0 \left(\sum_{i=1}^{N_h} \lambda_i \varphi_i(w_i, x, b_i) + b_0 \right) \quad (2)$$

Where, $\lambda_i, b_i, b_0 \in R, x, w_i \in R^N$ and N_h is the number of units in the hidden layer.

The most widely used activation functions, $\varphi_i(w, x, b)$, in the hidden units are sigmoidal for multilayer perceptron, although many other functions may be used. Output activation functions, $\varphi_0(u)$, can be sigmoidal or linear.

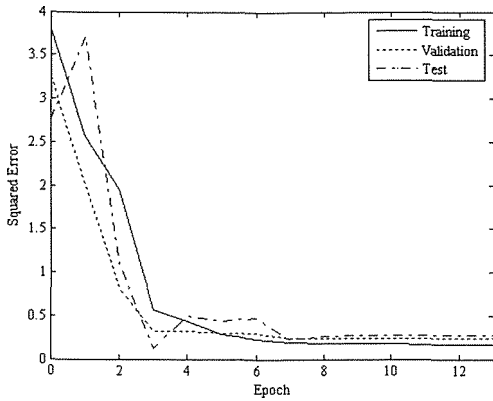
Because ANN offers many useful properties and capabilities, such as nonlinearity, input-output mapping, and fault tolerance, neural network model have its greatest potential in areas such as speech and image analysis, pattern recognition, system control and prediction (Haykin, 1994).

Neural network system has been used in the prediction of aggregate quality, the rock indentation depth, and UCS, optimization of a soft rock replacement scheme, predicting the advance rates of tunnel boring machines, and the sawability prediction of rocks (Kahraman et al., 2006; Benardos and Kaliampakos, 2004; Feng and An, 2004;

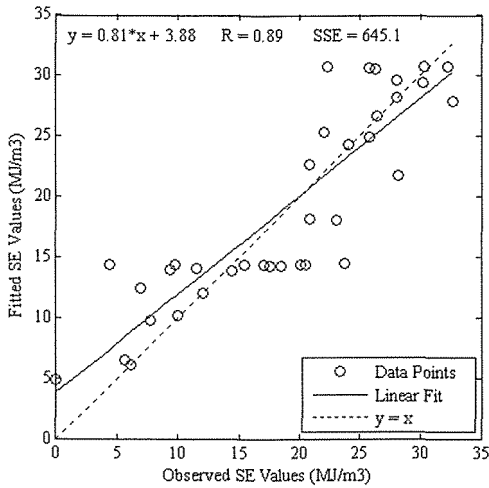
Meulenkamp and Alvarez Grima, 1999; Huang and Wanstedt, 1998).

Feed-forward back propagation network was chosen to build the ANN model for SE in this study, which is two-layered. The input layer has four neurons correspond to four independent variables (UCS, BTS, Elasticity, and CI) in the prediction model. The hidden layer has tangent sigmoid transfer function neurons while the output layer has one pure linear neuron corresponding to SE. Neuron numbers for hidden layers is selected as three for this study. The ANN was trained and implemented by using the MATLAB R14 neural network toolbox using back propagation with Levenberg–Marquardt algorithm on the regression data set.

It is a useful diagnostic tool to plot the training, validation, and test errors to check the progress of training. The result is shown for the ANN model of SE in Figure 6a, which is reasonable, since the test set errors and the validation set errors have similar characteristics, and it does not appear that any significant overfitting has occurred.



(a)



(b)

Figure 6. Network errors (a) and the predicted values for SE (b) using neural network.

The network responses were also analyzed for the ANN model of SE. After unnormalizing the network outputs, the entire regression data set was put through the network (training, validation, and test) and bivariate linear regression was performed between the network outputs and the corresponding targets for the network (Figure 6b).

It can be understood from Figures 6b that ANN model of SE has given predicted values very close the measured ones. This indicates that ANN model is a good choice to predict SE values, as almost all of the data points are

quite close to the regression line without exhibiting any pattern and/or outliers. R-value for the ANN model of SE is 0.89, which is equal to that was found for the nonlinear regression model of SE.

However, the correlation coefficient values for the relation between observed and predicted values do not necessarily identify the most appropriate model. The sum of squares due to error statistics (SSE) is better statistics in deciding which model fits the same data set better than the others do. The sum of squares due to error for the ANN model is greater than that of the nonlinear regression model, indicating that nonlinear model is more accurate for predicting SE than the ANN model.

4.5 Regression Tree

Regression tree technique for building predictive models approximates a regression relationship using a decision tree. Such a tree partitions the data set into regions, using values of the predictor variables, so that the response variables are roughly constant in each region.

A regression tree is a sequence of questions that can be answered as ‘yes’ or ‘no’, plus a set of fitted response values. Each question asks whether a predictor satisfies a given condition. Predictors can be continuous or discrete. Depending on the answers to one question, it either is proceeded to another question or is arrived at a fitted response value. If the answer is ‘yes’ to a particular question, the left branch is taken to proceed. Mathematical foundations of this technique can be found elsewhere (MATLAB, 2006; Breiman, et al., 1984).

Regression tree given in Figure 7 was generated for the regression data set by MATLAB using UCS, BTS, Elasticity, and CI as predictors. Rational expressions that are associated with the triangles in Figure 7 correspond to the questions that must be answered for the target rock to estimate its SE depending on rock properties. Regression tree in Figure 7 starts with questioning Elasticity value of the rock. If it is less than 30.4 GPa, the left branch of the regression

tree is taken to answer the question about if CI value of the target rock is less than 2.2. If it is less than 2.2, the terminal node that is indicated by a black circle is arrived, which is associated with a number 6.1144. This means that SE value of the target rock is 6.1144 MJ/m³. If CI value is higher than 2.2, SE can be either 12.5693 MJ/m³ or 19.398 MJ/m³ depending on BTS value of rock.

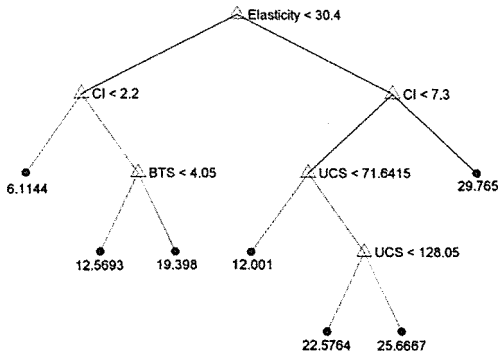


Figure 7. Regression tree chart for predicting SE.

Scatterplot of the fitted SE values against the observed SE values for the regression tree model in Figure 7 is given in Figure 8. The correlation coefficient between observed and predicted SE values based on the regression tree model is 0.97. This value is greater than that for both the multiple nonlinear regression and ANN models of SE.

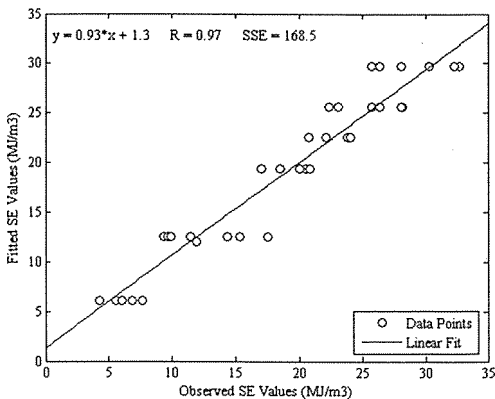


Figure 8. Scatterplot of fitted values against those observed for the regression tree.

SSE value for this model is 168.5 that is smaller than that for both the multiple nonlinear regression and ANN models of SE. Scatterplot in Figure 8 indicates that the regression tree model is a good choice to predict SE values, as almost all of the data points are very close the regression line without exhibiting any pattern and/or outliers. These results indicate that regression tree model predicts the data set better than the multiple nonlinear regression and ANN models do.

5 CONCLUSIONS

The following conclusions can be drawn from the current study of building predictive models for SE using intact rock properties:

1. Results of the principal components analysis have shown that the most of the variance in the data set of independent variables can be explained by three principal components. The first principal component is mainly weighted on UCS, BTS, Elasticity, and CI. It has also been found that all the non-sandstone coal measures from McFeat-Smith and Fowell (1977) and dolerite from Roxborough and Philips (1981) were standing out of the main group of the data points in Figure 1. Those rocks acted differently from the rest of the rocks in principal components analysis due to their geological and geotechnical properties.
2. Factor analysis showed that three common factors seemed to summarize the data set of independent variables instead of eight variables, being in line with the results of the principal components analysis.
3. The hierarchical cluster tree that has been developed has successfully divided the original data set into separate natural clusters indicating that SE and CI fall into one category representing the cuttability characteristics of rocks, UCS, BTS, and Elasticity being the mechanical rock properties, and Quartz and Porosity being mineralogical-physical rock properties.
4. Bivariate correlation, regression, and curve fitting analyses revealed that UCS, BTS, Elasticity, and CI could be used as

individual predictors in estimating SE, confirming the results of the multivariate statistical analyses.

5. Three predictive models of SE were developed by using multiple nonlinear regression, ANN, and regression trees approach. UCS, BTS, Elasticity, and CI have been employed as predictors for building those models. Subsequent statistical analyses revealed that regression tree model fit the data better than the other two models. ANN model has also been understood useful to estimate SE.

Rock cutting process is mainly a process of fragmenting the rock by mechanical tools, in which elastic properties of rock materials play a very important role. Therefore, especially fracture toughness, being an intrinsic rock property, has a great potential in estimating SE for a wide range of rocks. However, fracture toughness is more difficult to obtain than other parameters such as UCS, BTS, Elasticity, and CI.

Until an easy-to-use field test is developed for fracture toughness, model built by the regression tree method can be used to estimate SE value of a target rock in the field. When changes in rock conditions were observed in a roadway development or civil tunneling operation, the mean values of UCS, BTS, Elasticity, and CI can easily be determined from the samples of the new ground. Then the regression tree chart developed in this study can be used to predict SE in the field. Coupling that value with the cutting performance charts and graphs proposed in previous studies by McFeat-Smith and Fowell (1977) and Fowell and Pycroft (1980), mining and rock engineers can see whether the new ground is suitable for mechanical excavation and, if it is, estimate the likely drivage rate.

REFERENCES

- Alvarez Grima, M. and Babuska, R., 1999. Fuzzy model for the prediction of unconfined compressive strength of rock samples. *Int. J. of Rock Mech. Min. Sci.*, 36, pp. 339–349.
- Benardos, A.G. and Kaliampakos, D.C., 2004. Modelling TBM performance with artificial neural networks, *Int. J. of Rock Mech. and Min. Sci.*, 19, pp. 597–605.
- Bishop, C., 1995. *M. Neural Networks for Pattern Recognition*, Oxford University Press Inc., NY.
- Breiman, L., Friedman, J. H., Olshen, R. A., Stone, C. J., 1984. *Classification and regression trees*. Chapman and Hall/CRC New York.
- Feng, X. and An, H., 2004. Hybrid intelligent method optimization of a soft rock replacement scheme for a large cavern excavated in alternate hard and soft rock strata. *Int. J. of Rock Mech. and Min. Sci.*, 41, pp. 655–667.
- Finol, J., Guo, Y.K., Jing, X.D., 2001. A rule based fuzzy model for the prediction of petrophysical rock parameters. *J Petrol Sci Eng*, 29, pp. 97–113.
- Fowell, R.J. and Johnson, S.T., 1982. Rock classification and assessment for rapid excavation. *Proceedings of the Symposium on Strata Mechanics*, The University of Newcastle Upon Tyne, April 5-7, pp. 241-244.
- Fowell, R.J. and Pycroft, A.S., 1980. Rock machinability studies for the assessment of selective tunnelling machine performance. *21st National Rock Mech. Symp. USA*. pp. 149-158.
- Fowell, R.J., 1970. Assessing the machineability of rocks. *Tunnels and Tunnelling*, July, pp. 251-253.
- Gokceoglu C., 2002. A fuzzy triangular chart to predict the uniaxial compressive strength of the Ankara Agglomerates from their petrographic composition, *Eng Geo.*, 66, pp. 39–51.
- Haykin, S., 1994. *Neural networks*. MacMillan College Publishing Company.
- Huang, Y. and Wanstedt, S., 1998. The introduction of neural network system and its applications in rock engineering, *Eng. Geo.*, 49, pp. 253-260.
- Kahraman, S., Altun, H., Tezekici, B.S., Fener, M., 2006. Sawability prediction of carbonate rocks from shear strength parameters using artificial neural networks, *Int. J. of Rock Mech. and Min. Sci.*, 43, pp.157-164.
- MATLAB, 2006. *Statistics Toolbox for use with MATLAB, User's Guide Version 5*. The MathWorks, Inc
- McFeat-Smith, I. and Fowell, R.J., 1977. Correlation of rock properties and the cutting performance of tunnelling machines. *Proceedings of a conference on rock engineering*, Newcastle Upon Tyne, England, pp. 581-602.

- Meulenkamp, F. and Alvarez Grima, M., 1999. Application of neural networks for the prediction of the unconfined compressive strength (UCS) from Equotip hardness, *Int. J. of Rock Mech. and Min. Sci.*, 36, pp. 29-39.
- NCB, 1977. NCB cone indenter, MRDE Handbook No. 5, National Coal Board, England.
- Nishimatsu, Y., 1979. On the effect of tool velocity in the rock cutting. *Proc. of Int. Conf. on Mining and Machinery*, Brisbane, July, pp. 314-319.
- Rostami, J., Neil, D.M., Ozdemir, L., 1993. Roadheader application for the Yucca Mountain experimental study facility, Colorado School of Mines. 122 p.
- Roxborough, F.F., 1973. Cutting rock with picks. *The Mining Engineer*, June, pp. 445-455.
- Roxborough, F.F. and Philips, H.R., 1981. Applied rock and coal cutting mechanics. Workshop course 156/81. Australian Mineral Foundation, Adelaide, May 11-15.
- Singh, V.K., Singh, D., Singh, T.N., 2001. Prediction of strength properties of some schistose rocks from petrographic properties using artificial neural networks, *Int. J. of Rock Mech. & Min. Sci.*, 38, pp. 269-284.
- Sonmez, H., Tuncay, E., Gokceoglu, C., 2004. Models to predict the uniaxial compressive strength and the modulus of elasticity for Ankara Agglomerate, *Int. J. of Rock Mech. and Min. Sci.*, 41, pp. 717-729.
- Tiryaki, B. and Dikmen, A.C., 2006. Effects of rock properties on specific cutting energy in linear cutting of sandstones by picks, *Rock Mech. and Rock Engng.*, 39 (2), pp. 89-120.

Mining and Environment

Sources of Mining Effluents and Suitable Treatment Options

N. Kuyucak

Golder Associates Ltd., Ottawa, Ontario, Canada

ABSTRACT Mining and metallurgical processes may generate effluents such as tailings water, acid mine drainage (AMD), seepage and process acid streams. AMD is characterized as a low pH, high acidity effluent containing heavy metals and sulphate. If generation of AMD cannot be controlled, AMD needs to be collected and treated for neutralization of acidity and reduction of metals and TSS to meet regulated water quality standards.

Lime neutralization and precipitation is the most common method used in the mining industry to treat AMD. Other viable options include the use of a high density sludge process (HDS), the use of other chemical reagents, waste or by-products from other industries, biological sulphate reduction methods etc. Recently, several passive treatment systems have been designed and successfully operated. This paper will discuss available options and provide insights for selecting a suitable method for a given situation using case studies over the last decade.

1 MINE EFFLUENT SOURCES: FROM EXPLORATION TO AFTER CLOSURE

1.1 Acid Mine (or Rock) Drainage (AMD or ARD)

Acid generation occurs when sulphite minerals (predominantly pyrite, (FeS_2) , and pyrrhotite, (FeS)) contained in the waste material are exposed to oxygen and water (Kuyucak, 2001a, b; Kuyucak, 2002). If sufficient alkaline or buffering minerals (e.g., calcite) are not present, the leach water from the waste pile or dump becomes acidic, resulting in high dissolved concentrations of metal ions such as iron (Fe), manganese (Mn), aluminium (Al), zinc (Zn), copper (Cu), nickel (Ni), lead (Pb), cadmium (Cd), arsenic (As), etc. This water is known as acid rock drainage (ARD) or acid mine drainage (AMD). (Kuyucak *et al.*, 1990).

1.2 Mine Dewatering - Ammonium and Nitrate

Explosives made of ammonia and nitrate compounds are in general use wherever blasting is required for extraction of the ore. As a result, water produced from mine dewatering may contain ammonia ($\text{NH}_4\text{-N}$) and nitrate (NO_3) in elevated concentrations (Kuyucak, 1998).

1.3 Process Waters – Cyanide and Acids

Chemicals such as cyanide, sulphuric acid, and hydrochloric acid are used for processing of ores and recovery of metals. Cyanide (CN) is widely used for extraction of precious metals (i.e. gold, silver, and platinum) as well as for conditioning of mineral processes to improve recovery of base metals such as Cu, Pb, and Zn (Kuyucak, 1998).

1.4 Mineral Processing and Tailings Reclaim Water - Thiosalts

Grinding and flotation (milling) of complex sulphite ores in an alkaline media produces a series of sulphur oxyanions called 'thiosalts', including thiosulphates, polythionates, sulphide, and sulphate. They represent a delayed acid-generating capacity in mill effluents that results in a drop in pH and, subsequently, an increase in metal and TSS concentrations.

2 TREATMENT OBJECTIVES AND APPROPRIATE PROCESS SELECTION

Treatment objectives are set based on the local regulated standards, which influence the selection and design of an appropriate treatment process for a given site.

2.1 Regulatory Standards

Each country sets standards to regulate the quality of water entering the environment. Regulatory water quality standards in Canada are set by both the federal and the provincial or territorial levels of government which will involve monitoring of waters for certain parameters. For instance, in the 1990s, the Ontario government launched the Municipal Industrial Strategy for Abatement (MISA) program for the management of industrial discharges of potentially toxic substances into Ontario's waterways. MISA sets daily and monthly maximum concentrations for certain parameters and also requires that the effluent must not be toxic to aquatic organisms. (Specifically, Rainbow trout fry and water fleas (i.e., *Daphnia magna*) Mining sites located in the Province of Quebec must meet the water quality standards described by MENVIQ Directive 019. Alternatively, site specific standards (e.g., Policy 2: No more than background value) can be set by Quebec authorities for a site.

The World Bank and the World Health Organization also set standards for waters resulting from mining activities; their standards are particularly applicable for the

projects, in developing countries, or which depend on World Bank or IFC financing.

2.2 Sustainability Considerations

Treatment processes can be designed to produce an effluent and sludge of adequate quality to be recycled and reused for other purposes, including mining processes, agricultural water for irrigation and livestock, recreational water, hydro-electric generation, and process water for industries in the vicinity of the mining site.

A pilot study performed at the Kingsmill Tunnel site in Peru involved treatment of AMD using high density sludge (HDS) process. The results of physical, chemical, biological, and toxicological tests were compared to both the Peruvian Drinking Water Quality Standards and the U.S. EPA standards. The treated AMD was found to be acceptable as a supplement to the primary drinking water resources for the City of Lima. The process could also be economically viable because of the revenue generated from the sale of the treated AMD (Kuyucak et al., 2004). A HDS process was implemented at the Apirsa site in Spain to be able to obtain a water quality that could be recycled back to the mining/mill processes, thereby reducing the need for fresh water use (Kuyucak et al., 1999). Metal laden wastes can potentially be sent to smelters or metal manufacturing processes as a secondary feed material (Rao et al., 1994; Zinck, 2006). In addition, the use of sludge as a back fill material has been put into practice.

3 TREATMENT OPTIONS FOR ACIDITY, METALS AND SULPHIDE

Heavy metals found in acid mine waters react with a chemical agent to form a metal complex and precipitate in solution at a certain pH level. (Kuyucak, 2001d). Factors governing this process include: the type of chemical reagent used, the pH of the water, oxidation/reduction and hydrolysis reactions, the presence of biotic and abiotic catalysts, and the retention time of the water. A selection of various AMD treatment processes is described below.

3.1 Active methods – Neutralization and Precipitation Processes

Neutralization and precipitation processes are often performed in a treatment plant consisting of pumps, mixing (aerating) reactors and/or a clarifier/thickener.

Lime neutralization is efficient for the treatment of common heavy metals (Cu, Zn, Cd, Mn, Pb, Fe²⁺) as their solubility is low at a pH greater than 9 and they precipitate readily. The relationship between metal solubility and pH is illustrated in Figure 1.

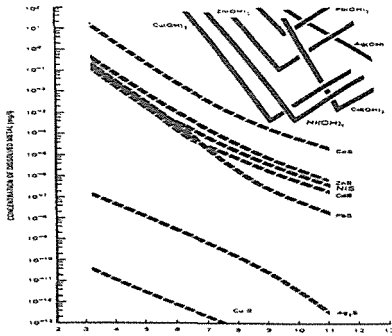


Figure 1. Comparison of solubility of metal hydroxides and sulphides as a function of pH.

Neutralization/precipitation processes can achieve reduction of concentrations of selected metals to certain levels as summarized in Table 1.

Table 1. Removal of metal ions by Neutralization/precipitation

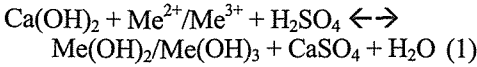
Metal	pH	Concentration Achievable	Comment
Cr	7-8	<0.5 µg/L	reduction of Cr ⁶⁺ to Cr ³⁺
Cu & Zn	9-10	<0.1 mg/L	
Pb & Fe ³⁺	9-10	µg/L range	
Cd & Ni	>10	< 1mg/L	hindered by high Fe concentrations
Mn	>10	<1 mg/L	strong oxidation required

In some cases, pH adjustment is not quite effective. Addition of other precipitation reagents such as S²⁻ compounds and/or emerging technologies (ion exchange, membrane separation, solvent extraction, etc.) for metal removal can be considered.

Contaminants such as As, Sb, Mo and Se usually require the use of additional chemicals (e.g. H₂O₂, FeCl₃ or Fe₂(SO₄)₃, Na₂S, CO₂) as adjuncts to the lime neutralization processes. As an example Na₂S (e.g. 5 mg/L) was added in lime neutralization at pH 10.5 to lower Cd to less than 0.01 mg/L in the treated tailings water of the Samatosum treatment plant in Kamloops, British Columbia. At this site Dynasand filters were also installed to separate solids to produce a final effluent quality with low turbidity and a final concentration of each metal below 0.1 mg/L (i.e. Zn, Pb, Mn, Cd). A common method for removing Hg is by sulphide precipitation to 10-20 µg Hg /L in a treated effluent. Co-precipitation with iron can lower Mo to <0.5 mg/L. Ion exchange (IX) appears to be an alternative method to achieve low Hg and Mo levels, in the ranges of 1 to 5 µg/L and 2 mg/L, respectively. Recently selective IX resins are available on the market for removal of metal ions such as Cu, Zn, As, Se, and NO₃. Oxidation of As³⁺ to As⁵⁺ is necessary to remove As from the effluent prior to lime addition and ferric iron precipitation. Cr⁶⁺ needs to be reduced to Cr³⁺ before being neutralized for its removal as Cr(OH)₃.

3.2 Lime Neutralization Processes, High Density Sludge (HDS) Method and Critical Process Parameters

The use of lime, either as quick lime (CaO) or hydrated lime (Ca(OH)₂), is often preferred over other alkaline reagents, particularly for treating acidic effluents (i.e., ARD) in large quantities, due to its high reactivity and its wide availability (Kuyucak, 2001 a, d). Acid is neutralized and the metals (Me) are precipitated in the form of metal hydroxides. The resulting mixture of CaSO₄ (gypsum) and metal hydroxides is called "sludge." The principal reaction in lime neutralization can be expressed as follows (Eq. 1):



Aeration is used to oxidize the ferrous (Fe^{2+}) iron to ferric iron (Fe^{3+}) during precipitation because ferric iron sludges are chemically more stable. Other oxidation methods include chemical (e.g., hydrogen peroxide) and biological (e.g., iron and/or

sulphur oxidizing bacteria *Thiobacillus sp.*) methods (Rao et al., 1995).

Lime neutralization facilities range from the simple addition of lime to the tailings pipe lines to a constructed plant consisting of reactors, clarifiers, and sludge dewatering equipment as depicted in Figure 2.

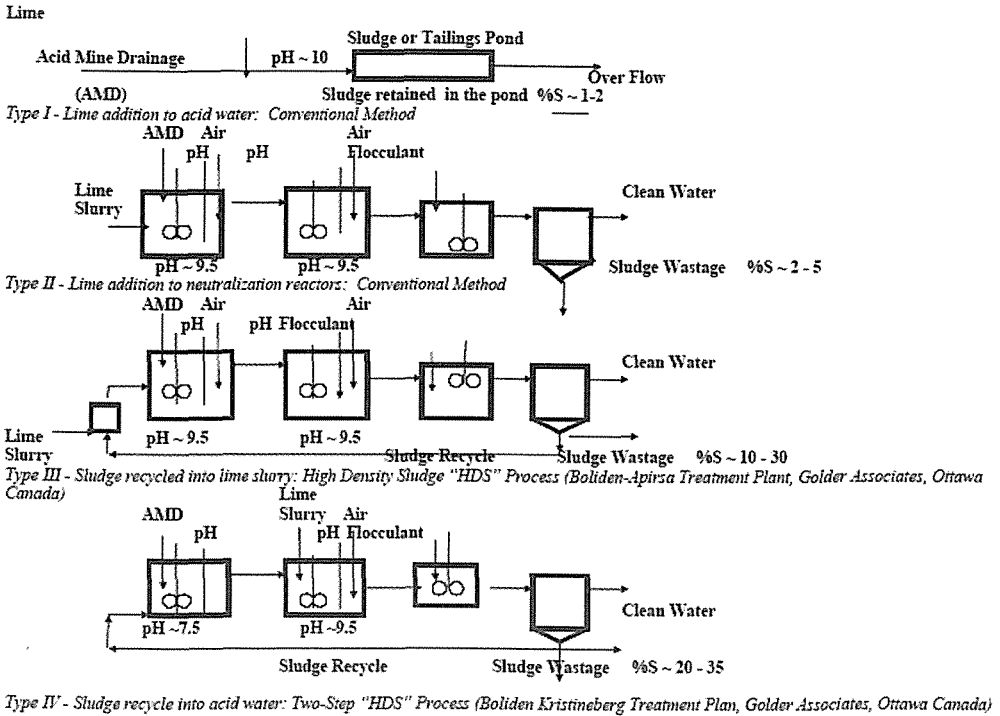


Figure 2. Types of lime neutralization processes and resulting sludge densities.

The current state-of-the-art lime neutralization process for treating AMD and other acidic waters is called the "High Density Sludge (HDS)" process that is capable of producing more compacted sludges than traditional methods of lime addition processes (Kuyucak et al., 2001a, d). In the HDS process, more than one reactor is used to perform the neutralization (Fig.2). The solids content in the resulting sludge is significantly higher (e.g. 10-30%) as opposed to process not involving sludge recycling. Sludge recycling can be facilitated by either using the sludge alone to

partially neutralize AMD or after mixing with lime.

A two-step lime neutralization process developed by Kuyucak and Sheremata (1995) is illustrated in Figure 2 (e.g. Type IV treatment). In this process, the pH of the influent is raised to an intermediate level with recycled sludge in the first reactor and, in the second reactor, the pH is adjusted to an optimum pH using lime sufficient to precipitate the metals of concern. Aeration is provided to the reactors for oxidation of Fe to produce a more chemically stable sludge.

Based on pilot tests conducted for HDS processes, including conventional and multiple step neutralization methods (Kuyucak et al., 2003; Kuyucak et al., 2004; Kuyucak et al., 2005). It was found that almost all HDS systems reduce the SO₄ content in the acid water to levels lower than the theoretical solubility limit of gypsum (i.e., 2000 mg/L CaSO₄). At two sites, the sludge from the clarifier underflow was further dewatered using a drum "vacuum" filter (Fig. 3). In these cases, the sludge solids content has been increased to more than 50%. At the Kristineberg site in Sweden, the dewatered sludge is backfilled to the mine for storage and ultimate disposal after being mixed with mine tailings. The quality of the effluent generated in these facilities often surpasses the permitted effluent quality objectives. The HDS increases the quantity of the recovered water and the scaling in the process is significantly reduced. The process control is well automated requiring less maintenance and labour.

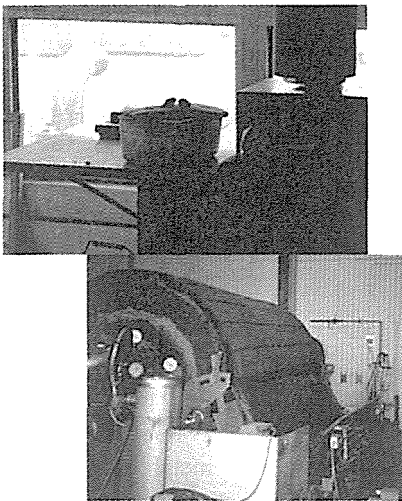


Figure 3. Drum vacuum filter dewatering metal hydroxide sludge from HDS processes at Falun site, Sweden.

3.3 In-Line Lime Treatment

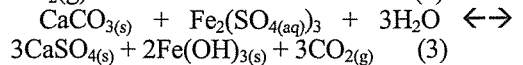
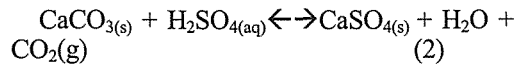
Neutralization and aeration can be combined into a single step by injecting the caustic

reagent into the port of a jet pump. The overall cost of this process was found to be much lower than the conventional mechanical aerators (Kuyucak, 1995). The in-line method has been recommended to neutralize low strength AMD containing Zn, Cu, Pb, Mg and Fe²⁺ (38, 0.96, 0.4, 17 and <200 mg/L, respectively).

3.4 Alternative Neutralizers

3.4.1 Limestone (CaCO₃) neutralization

Under controlled conditions, higher density sludges can be obtained from neutralization of AMD using CaCO₃, as shown below:



The released CO₂ gas forms a carbonate ion which acts as a buffer and sets an upper limit on pH (max pH 6.5) and also affects the rate and amount of lime consumption. A treatment process involving the sequential addition of limestone and lime, has been suggested for removal of a wide range of metal ions (Kuyucak, 1995).

3.4.2 Magnesium hydroxide (Mg(OH)₂)

The addition of Mg(OH)₂ can result in a lower volume of more dense metal hydroxide sludge when properly applied in the neutralization system. Mg(OH)₂ can also remove metals through surface adsorption. However, the rate of neutralization is slow and the buffering capability of Mg(OH)₂ prevents the pH from exceeding 9. Depending on the pH requirements, it can be used in conjunction with NaOH. Mg(OH)₂ is employed in treatment plants where the disposal cost of the sludges generated is high, such as Canadian Copper Refinery (CCR) in Montreal east, in order to reduce sludge disposal costs (Kuyucak et al., 1990).

3.4.3 Sulphides

Na₂S, FeS, (NH₄)₂S, BaS or H₂S can be used as reagents. The use of sulphide precipitation results in better metal removal in effluents

which contain phosphate, ammonia, organics, surfactants, chelators and Cr^{6+} . Metal sulphite complexes are less voluminous than hydroxide precipitates. They are also less susceptible to changes in pH when stored in anaerobic conditions. In addition to the noxious H_2S gas production from the system, the settling and separation of fine and colloidal metal precipitates from the treated water may require a filtering system. It also bears a higher cost than the lime neutralization. Biologically generated sulphide precipitation processes have been investigated as an alternative treatment method (Kuyucak, 2000).

3.4.4 Sodium hydroxide (NaOH)

Sodium hydroxide is highly reactive and results in less voluminous sludge. However, sodium hydroxide is expensive and the resulting sludge does not settle well, and requires filtering in most cases.

3.4.5 Ammonia (NH_3)

Ammonia use is preferred by coal mining industries due to its high solubility and ability to produce less sludge. Ammonia is usually injected near the bottom of ponds or inlet water as gaseous anhydrous ammonia (Kuyucak, 2000). Some hazards are associated with the handling of ammonia, and there is some uncertainty concerning potential biological reactions.

3.4.6 Others

Some industrial wastes or by-products such as: fly ash, kiln dust, paper pulp, and red mud (bauxite residue), from power plants, crude oil combustion gasification processes, paper production, and aluminium extraction, have the potential to be a lime substitute for the treatment of AMD. However, potential metal contaminants present in these compounds may raise some concerns. In addition, their neutralization potential and reaction rates may be low and slow as compared to lime (Kuyucak, 2000; Zinck and Griffith, 2006).

3.5 Coagulation/Flocculation for Better TSS Removal (Solid/Liquid Separation)

Coagulants such as inorganic Al^{3+} or Fe^{3+} salts help to discharge the electronegative colloids, and then flocculants (i.e., organic "polymers") bridge the neutral particles. The following parameters are critical for design: the type of polymer and dosages, the temperature of the system, the viscosity and chemical characteristics of the pulp, and external stirring (Kuyucak, 2000). Since fish gills are negatively charged, the use of cationic polymers (or their residual quantities in water) may result in some concerns.

3.6 pH Adjustment for Meeting Final Effluent Quality Requirements

Following the neutralization process, depending on the required treatment, the pH of the final effluent may need to be decreased to an acceptable range by adding either sulphuric acid or CO_2 . The use of CO_2 may be more beneficial since it raises the alkalinity and buffering capacity of waters. Sulphuric acid is sometimes selected due to its low cost, or if an increase in SO_4 levels is not of a concern or not required.

3.7 Sludge Dewatering Options

Dewatering via filters has not been widely practised in the mining industries, except for very site-specific applications. It is found that the technique of freeze/thaw dewatering of sludge can be an efficient alternative to dewatering via filters and a single freeze/thaw cycle could reduce the volume of sludge by 90%.

3.8 Sludge Stability and Fixation

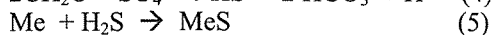
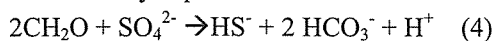
The possibility of metal mobilization is determined by a "leaching test" (e.g. EPA Toxicity Characterisation of Leaching Protocol "TCLP", Synthetic Precipitation Leaching Protocol "SPLP", etc.). Depending on sludge characteristics and site specific requirements, sludge is sometimes stabilized by mixing it with cement and/or lime prior to its disposal (Kuyucak, 1995; MacDonald and Webb, 2005; Zinck, 2006).

3.9 Biological and Passive Processes

The most common passive treatment systems are sulphate reducing bacteria based processes, anoxic limestone drains, constructed anaerobic and aerobic wetlands, and biosorption. Experience has demonstrated that the influent flow rate, contaminant concentrations, pH and alkalinity (or acidity) are all important to the system performance. In addition, the capacity of a biological treatment system is significantly affected by ambient temperatures and changes in the pH.

3.10 Sulphate Reducing Bacteria "SRB" Based Processes

Under reducing and anaerobic conditions, and in the presence of organic carbon nutrient sources, sulphate reducing bacteria (SRB) convert AMD sulphate to sulphide, as illustrated by Equations 4 and 5.



The use of SRB in engineered lagoons, in open pits and flooded mines have been investigated world wide and have received greater attention (Kuyucak and Germain, 1995; Kuyucak 2002). Their use in a controlled reactor was implemented by Budelco (in The Netherlands) at full scale to remove metals and SO_4 from underground mine water in the early 1990s. Recently several new developments are underway to be either pilot tested or implemented at mining sites to treat AMD and recover metal values for sale or use (Bratty et al., 2006). Sometimes, limestone and soil are also added into the nutrient mixture to increase alkalinity and, subsequently, enhance the activity of the SRB.

Alkalinity can be generated by the dissolution of limestone or other carbonates rocks, Bacterial sulphate reduction generates sulphite to precipitate/remove metals, too.

Base metal ions including Pb^{2+} , Zn^{2+} , Fe^{2+} etc. in net-acidic AMD can be removed with the help of anaerobic sulphide reducing bacteria. Removal of aluminum (Al) occurs by precipitation which is dependent on pH

and alkalinity levels in the treatment media. Ferric iron (Fe^{3+}) can undergo hydrolysis and iron hydroxide precipitation occurs in solutions where pH levels are > 4.5 . In passive treatment systems, reduction in manganese (Mn) levels is usually marginal (Kuyucak, 2002; Kuyucak *et al.*, 2006).

A recent project to a decommissioned mining site in Val d'Or in Quebec, Canada in 2004 proved that passive systems can be a cost-effective alternative to active systems. The water quality produced is in compliance with the provincial government regulations. The site-specific passive treatment facility included: a seepage collection system; anaerobic and aerobic cells; and a limestone filter. Parameters critical for successful operation of the system included: nutrients and organic substrate biodegradation; anaerobic/reducing conditions; hydraulic loading and metal loading rate changes; storm water impact; hydraulic design of the system (i.e. to avoid short-circuiting and channelling); gas lock-up; and temperature (Kuyucak, 2006). It has been revealed that passive systems should be started at relatively high ambient temperatures for optimal performance. The SRB-hosting organic substrate should be protected against freezing conditions by covering it with a thick soil layer (i.e. > 0.6 m). Burying the organic substrate containing the bacteria to conserve heat and prevent freezing was an approach used by several system designers and operators (Kuyucak *et al.*, 2006).

3.11 Wetlands

A wetland can remove organic/inorganic compounds and suspended solids. It is usually composed of Oxidation Zone, which contains aquatic plants, and Reducing Zone, which is the sedimentation zone rich in SRB, denitrifying and Mn reducing bacteria. Plants play a filter role, taking up metals and helping oxidation processes to occur, while bacteria act as catalyzers for chemical reactions.

3.12 Anoxic Limestone Drains (ALD)

An ALD system generally consists of an excavated seepage interception trench

backfilled with crushed limestone and covered with plastic and clay-soil to keep air out. ALD provides an increase in alkalinity, oxidation of Fe^{2+} and formation of ferric oxyhydroxides. Designs of ALD are reported to be site-specific. Usually, an ALD system is followed by a wetland for oxidation and precipitation of iron and other contaminants.

3.13 Open Limestone Trenches

Trenches are typically most effective for polishing/conditioning of AMD with relatively low strength and acidity. A trench contains a layer of limestone where alkalinity and buffering capacity in the acid water are increased. A process consisting of aeration, mixing and open limestone trenches that was designed and operated at a decommissioned Barrick Gold site in Val d'Or, Quebec has been operated successfully year round since 1997. The system generates an effluent quality that meets Menviq standards, especially for parameters including pH, Ni, Cu and Fe.

3.14 Biosorbents

A bed of biosorbents such as sawdust, sphagnum moss or algae can be placed where the seepage occurs. When it is saturated by metal ions, the saturated biosorbent materials can either be disposed of with tailings or recycled to a smelter, or washed with an appropriate eluate for recovery of metals (Kuyucak, 1990; Kuyucak and Volesky 1990; Kuyucak 2002; Volesky and Kuyucak, 1988; Gusek, et al., 2006).

4 REMOVALS OF THIOSALTS, SULPHATE(SO_4^{2-}), TDS, CYNIDE(CN), AMMONIA(NH_3) AND NITRATE(NO_3)

4.1 Thiosalts in Mill 'Tailings Reclaim' Water

Majority of thiosalts treatment methods are usually based on the degradation principle.

Many of the methods have been evaluated only in laboratory scale tests and a few of them have been pilot tested or applied at full-scale. The treatment options include: Chemical oxidation using hydrogen peroxide

(H_2O_2), chlorine (Cl_2) and ozone (O_3); electro-oxidation; Air oxidation including alkaline oxidation, Cu-catalysed air oxidation and SO_2 -air oxidation; Biological oxidation including the use of biological contactors, activated sludge and packed columns where degradation of thiosalts and the oxidation of sulphite to sulphate occurs with the help of sulphur oxidising bacteria such as *Thiobacillus ferrooxidans* and *Thiobacillus thiooxidans*; and other methods such as anaerobic sulphide reduction processes and reduction by metals. A carbonate-based method may function satisfactorily for low thiosalts concentrations (e.g. < 100 mg/L). Deep sea disposal has practiced for the management of thiosalt rich-mining effluents at some sites. In recent years, membrane and electrochemical processes including reverse osmosis (RO), electro dialysis (ED) have been considered as viable alternatives to conventional treatment options.

An effective method was designed and evaluated to address thiosalts at the Boliden Apirsa (Spain) site. It was determined that the addition of H_2O_2 to only a portion of the treated effluent coming from a HDS lime neutralization process before its discharge to the environment was the most cost-effective method due to the low capital cost of the process. In addition it offers a very short delivery and construction time to meet the short deadline for when the treatment needed to be in operation. A direct relationship between the chemical oxygen demand (COD) levels and thiosalts concentrations was found in the treated final effluent. The analysis of COD is relatively simple and rapid compared to the analysis of thiosalts. To be able to meet the regulated COD limit of 30 mg/L in the final effluent during the studies at the Boliden Apirsa site, the concentration of thiosalts had to be less than 52 mg/L.

At another site in Canada, a combination of lime and soda ash (Na_2CO_3) was applied to add buffering capacity while neutralizing the water. This replaced the old practice of increasing the pH to 11 and dropping it to pH < 9 with CO_2 . This buffering capacity

method resulted in significant savings in the lime consumption and, subsequently, overall treatment costs.

4.2 Removal of Sulphate (SO₄)

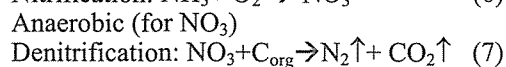
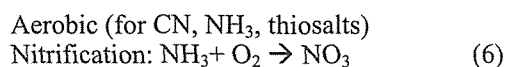
There exist several methods for removal/reduction of SO₄ from waters. These methods include: precipitation with barium (Ba); ion exchange (IX); biological sulphate reduction (SRB process) and aluminium hydroxide (Al(OH)₃) precipitation (Kuyucak et al., 2003; Kuyucak et al., 2004). Despite their technical feasibility, their application may not be economically feasible for large volume flows. When required, treatment of a small fraction of the water that will be discharged to the environment can be considered.

4.3 Removal of Total Dissolved Salts(TDS)

The expected concentration range for total dissolved salts (TDS) is generally in the order of 100 mg/L to 30 000 mg/L. These levels can lead to a reduction in the quality of potable surface and ground water supplies and therefore these compounds require removal/reduction from the ARD before it reaches the natural environment or water resources. Recently, RO been considered to reduce TDS.

4.4 Removal of Cyanide Ammonia and Nitrate

Since free ammonia can form soluble amine complexes with heavy metals such as copper, zinc, silver and nickel, the presence of ammonia may inhibit precipitation of these metals at pH values above 9 which is known to be an effective range for the precipitation of metal hydroxides (Kuyucak, 1998; Kuyucak, 2002). Nitrate is the end-product of the cyanide oxidation process and forms as a result of the chemical or biological oxidation of ammonia. Reactions are presented with Equations 6 and 7.



The widely used method for removal of cyanides and ammonia is through natural degradation in holding ponds where cyanide is converted to ammonia and then to non-toxic by products (carbon dioxide and nitrogen compounds). These natural reactions have been utilised by the mining industry as the most common means of attenuating cyanide. However, the rate of natural degradation is largely dependent on environmental conditions and the environmental regulations have become more and more stringent with respect to cyanide in the recent years. The removal is enhanced by increasing the pond surface area, increasing the pH and by allowing for more contact with air. A biological process unique to Homestake Mining in South Dakota decomposes the metal-cyanide complexes and efficiently oxidises cyanides to ammonia which is further oxidised by bacteria to nitrate (Eq. 6).

The potential processes for removal of nitrates and nitrites include: biological denitrification where nitrates/nitrites are reduced to nitrogen gas (Eq. 7), ion exchange and reverse osmosis where nitrates/nitrites are removed from the water and are obtained in a very concentrated form requiring further disposal methods. As wetland filtration has a limited use, anaerobic passive systems containing organic materials such as woodchips and denitrifying bacteria have been practiced for denitrification of nitrates. The Hemlo/Golden Giant uses copper and iron sulphate precipitation process. The Inco SO₂/Air Process has been receiving worldwide attention. The application of hydrogen peroxide to address cyanide has also been increasing. Investigations for the development of new processes have been ongoing. In arid climates, evaporation has been used to obtain zero discharge flow.

Installation of a continuous on-line monitoring device is very useful. The process should not produce undesirable by-products and should be able to destroy harmful by-products of the cyanide destruction. The effluent treatment process should be appropriate to site-specific climatic conditions, solution chemistry and

discharge requirements. The capital and operational costs should suit the mining production conditions such as production rate and life expectancy.

5 CONSIDERATIONS FOR DESIGN AND IMPLEMENTATION OF AN APPROPRIATE TREATMENT PROCESS

5.1 Process Selection (i.e. Lime Precipitation, Active, Passive, etc)

An appropriate treatment process for a given site is selected based on the quality and quantity of the mining water, type of parameters that require removal/reduction, acidity, treated water quality objectives and capital and operational costs. Availability of space at the site is as important as the quality and quantity of the water to be treated.

5.2 Conducting Tests and Evaluating Treatability

Desktop evaluations are usually followed by bench-scale treatability tests where treated water can be produced and its quality can be evaluated. The optimal pH range and the quantity of the chemical reagent required for treating per unit volume of the water being treated are determined. The optimal retention time for reactions and the need for the use of auxiliary processes such as oxidation with air or chemicals can also be investigated.

Pilot tests aim to simulate the selected process at a large scale to obtain treated water and sludge. The quality of the treated water and sludge generated are examined and the overall treatment efficiency is evaluated. Parameters required for scaling up and design is defined. In addition to construction requirements, specifications of process units and equipment are identified. Conducting a pilot-scale test may be particularly beneficial when the use of a new 'emerging' technology is considered or the water quality is a typical or the quality of the treated water requires evaluations for its use and toxicity. Pilot studies such as Boliden Apirsa (Spain), Kristineberg (Sweden), and Kingsmill Tunnel (Peru) were conducted using an automated system as shown in Figure 4.

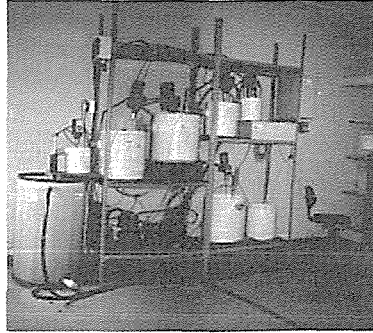


Figure 4. Pilot HDS treatment unit.

5.3 Design and Implementation

Design should consider flexibilities for construction, operation and maintenance.

Equipment with a critical role in the process should be duplicated (e.g. ARD influent pumps, sludge recycling and disposal pumps, etc.) and selected from robust/durable materials. The system should be equipped with proper alarms/devices to stop operation when required. The use or adaptation of equipment currently available at the site should be considered to reduce capital costs where possible. Rake in the clarifier or thickeners serving a HDS process should be designed properly to handle heavy mass.

6 CONCLUSIONS

Treatment costs are site specific since the quality of water to be treated, cost of reagent and degree of treatment requirements may vary from site to site. Some processes may require up front high capital costs and may provide lower operational costs (e.g., reagent cost, energy and maintenance requirements), while some processes can be implemented to a site with small capital costs, but requiring high operational cost. During the project planning stage, a cost-benefit analysis should be conducted for potential alternative treatment methods to determine the most appropriate process for the given site. Conducting treatability studies using bench and pilot scale tests are useful to determine

critical process, design and scale up parameters.

ACKNOWLEDGEMENT

The author likes to thank Ms. Tian Gou and Mr. Paul Smolkin, Principle of Golder Associates Ltd., for assisting in preparation and reviewing this paper, respectively.

REFERENCES

- Bratty, M., R. Lawrence, D. Kratochvil, and B. Marchant, 2006. Applications of Biological H₂S Production from Elemental Sulphur In The Treatment of Heavy Metal Pollution Including Acid Rock Drainage. 7th ICARD "Leadership: Gateway to the Future", St. Louis, Missouri, USA, March 27-30, 2006.
- Gusek, J. 2004. Scaling Up Design Challenges for Large Scale Sulphate Reducing Bioreactors. Presented and Published at the *National Meeting of the American Society of Mining and Reclamation the 25th West Virginia Surface Mine Drainage Task Force*, April 18-24, 2004. pp. 752-765. pp. 1-9.
- Gusek, J.J., T. R. Wildeman, K.W. Conroy, 2006. Conceptual Methods For Recovering Metal Resources From Passive Treatment Systems. 7th ICARD "Leadership: Gateway to the Future", St. Louis, Missouri, USA, March 27-30, 2006.
- Kuyucak, N., F. Chabot, and J. Martschuk, 2006. Successful Implementation and Operation of a Passive Treatment System in Extremely Cold Northern Quebec, Canada. 7th ICARD "Leadership: Gateway to the Future", St. Louis, Missouri, USA, March 27-30, 2006.
- Kuyucak, N., E. Mattsson, and H. Bringsaas, 2005. Implementation of a Site-Specific High Density Sludge Process for Treating High Strength Acid Mine Drainage at Falu Mine Site, Falun, Sweden. *Proceedings of Securing Future, Mining and the Environment Conference*, Skelefta, Sweden, June 27-July 1, 2005.
- Kuyucak, N., J. Chávez, J. R. del Castillo, and J. Ruiz, 2004. Potential use of treated Acid Mine Drainage at Kingsmill Tunnel, Peru - Technical and economic feasibility studies. 5th Int'l Symposium on Waste Processing and Recycling in Mineral and Metallurgical Industries, (CIM Conference), August, Hamilton ON Canada
- Kuyucak, N., 2002c. Microorganisms in Mining: Generation of Acid Rock Drainage, Its Mitigation and Treatment, EJMP & EP, V.2, No.3.
- Kuyucak, N., 2002b. Acid Mine Drainage (AMD) – Prevention and Control Methods. CIM Bulletin, April 2002.
- Kuyucak, N., 2001a. AMD Prevention and Control Options. *Mining Environment Management Journal*, January 2001, pp: 12-15.
- Kuyucak, N., 2001d. Acid Mine Drainage (AMD) - Treatment Options for Mining Effluents. *Mining Environment Management Journal*, March 2001.
- Kuyucak, N., M. Lindvall, T. Sundqvist and H. Sturk., 2001. Implementation of a High Density Sludge "HDS" Treatment Process At the Kristineberg Mine Site. *Securing the Future 2001, Mining and the Environment Conference proceedings*. June 2001.
- Kuyucak, N., 2000. Microorganisms, Biotechnology and Acid Rock Drainage, *Int. Minerals and Metallurgical Processing*, May 2000.
- Kuyucak, N., 1998a. *Mineral Processing and Extractive Metallurgy Review*, Gordon and Breach Science Publisher.19(1-4), pp: 1-408, Guest Editor.
- Kuyucak, N., 1998b. *Mining, the Environment and the Treatment of Mine Effluents*. Int. J.Environmental and Pollution, Vol.10, Nos 2/3, 1998
- Kuyucak, N. and T. Sheremata, 1995. Lime Neutralization Process for Treating Acid Waters. U.S. Patent: 5,427,691.
- Kuyucak, N. and B. Volesky (1990). Biosorption by Algal Biomass. In *Biosorption of Heavy Metals*, Ed. B. Volesky, CRC Press.
- Kuyucak, N., 1995b. Discussion: Effect of pH on Metal Solubilization from Sewage Sludge. *Canadian J. of Civil Eng.*, August 1995.
- Kuyucak, N., (1990). Feasibility of biosorbent applications. In *Biosorption of Heavy Metals*, Ed. B. Volesky, CRC Press.
- McDonald, D., and J. Webb, 2005. Comparison of the Chemical Stability of ARD Treatment Sludges Precipitated Using Conventional Lime Neutralization and the High Density Sludge Process. *Proceedings of Securing Future, Mining and the Environment Conference*, Skelefta, Sweden, June 27-July 1, 2005.
- Rao, R., N. Kuyucak, T. Sheremata, and J. Finch, 1994. Prospect of recovery/recycle from acid mine drainage. *Int. Land Reclamation and Mine Drainage Conf. and 3rd Int.Conf. on Abatement of Acid Drainage*. Pittsburgh, PA, April 26-29, 1994.

- Rao, S.R., J.A. Finch and N. Kuyucak, 1995. Ferrous-Ferric Oxidation in Acidic Mineral Process Effluents. *Minerals Eng.*, Vol. 8, No. 8, pp. 905-911.
- Volesky, B. and N. Kuyucak (1988). Biosorbent for Gold. U.S. Patent: 4.769.223.
- Zinck, J., 2006. Disposal, Reprocessing and Reuse Options For Acidic Drainage Treatment Sludge. 7th ICARD "*Leadership: Gateway to the Future*", St. Louis, Missouri, USA, March 27-30, 2006.
- Zinck, J., and W. Griffith, 2006. Utilizing Industrial Wastes And Alternative Reagents to Treat Acidic Drainage. 7th ICARD "*Leadership: Gateway to the Future*", St. Louis, Missouri, USA, March 27-30, 2006

Economic and Environmental Constraints Relevant to Building Aggregates Beneficiation plants

V. Badino, G.A. Blengini, E. Garbarino & K. Zavaglia

Politecnico di Torino - Land, Environment and Geo-Engineering Department, Torino, Italy

ABSTRACT In order to meet the specific requirements of the construction industry, an appropriate beneficiation process aimed at enhancing technical characteristics of building aggregates is often required. As it usually occurs, natural raw materials undergo a primary abatement process by means of drilling and blasting or mechanical excavation, followed by one or more size reduction stages and finally wet or dry separation in order to remove unwanted materials. As the beneficiation process is carried on, the technical performances of building aggregates improve, but, on the other hand, production costs and energetic-environmental burdens increase, as well. The paper will analyse the main economic and energetic-environmental constraints which characterise the building aggregates production streamline, by paying attention to the contribution of the different beneficiation steps and making use of the LCA (Life Cycle Assessment) methodology. In the second part, the paper will deal with alternative low grade sources of building materials, namely secondary materials from building demolition and rubble recycling, as well as rock excavation waste, which could partially replace traditional building aggregates. Also in this case, an energetic-environmental profile of recycled aggregates will be outlined.

1 TECHNICAL, ECONOMIC AND ENVIRONMENTAL ASPECTS OF BUILDING AGGREGATES

The importance of building aggregates for the construction industry – sand, gravel, crushed stones and tout-venant – is often underestimated.

They should, in fact, be considered amongst the most important mineral commodities, both in terms of produced quantities and market value.

According to the statistics (Wellmer F.W., 2002) building aggregates steadily rank in the first position in terms of production quantity: roughly 18 billion tons in the year 2000, that accounts for 58% of the world total mining production.

Moreover, building aggregates hold the fourth position in the world rank in terms of

market value: 92 billion euro, which is lower than the market value of energy mineral commodities (oil, natural gas and coal), but higher than gold (24 billion euro) and ornamental stones (23 billion euro).

Based on the analysis of these parameters, it becomes therefore clear that building aggregates hold an important role in the overall economy at both local and global scale.

However, their most salient economic significance stems from their essential contribution to the construction industry.

It is in fact the final use of mineral commodities the ultimate reason that stands at the very beginning of the mining production.

Thus, because of their role of input raw materials, they represent the first step of the

construction industry streamline, whose products are aimed at satisfying some of the most important needs of mankind.

For these reasons, the availability of building aggregates must be considered strategic for the overall economic system.

Even though it is a common understanding to consider building aggregates as "third class" raw materials whose supply and availability can always and easily be met, it must be recognised that, according to the different fields of employment, well defined technical performances are required.

In order to meet the specific technical requirements which characterise the different construction sectors, appropriate beneficiation processes aimed at enhancing technical characteristics of building aggregates are often required.

As it usually occurs, natural raw materials undergo a primary abatement process by means of drilling and blasting or mechanical excavation, followed by one or more size reduction stages and finally wet or dry separation in order to remove unwanted materials.

As the beneficiation process is carried on, the technical performances of building aggregates improve, but, on the other hand, production costs and energetic-environmental burdens increase, as well.

Therefore, because of the environmental impacts that are always induced by virtually any industrial activity, it becomes of the utmost importance to find a reasonable balance between exploitation of natural resources and their proper management, in order to meet sustainable environmental protection requirements.

However, the point is not whether exploiting or not exploiting mineral resources, but it is more a question of evaluating what should be the correct quantity of mineral commodities to be produced and what is the most suitable production process.

Undoubtedly, building aggregates are essential and valuable resources for the economic and social development of mankind, but they must be produced

according to economic and environmental sustainability principles.

1.1 Environmental and Energetic Profiles of Building Aggregates

Quarrying activities for the production of building materials, which can be considered the first step of the construction industry streamline, are often claimed to be responsible of a number of harmful environmental impacts.

The common negative perception which is often associated to mining/quarrying by the general public, presently more and more concerned about environmental issues, can be interpreted in terms of a generalized increase of "environmental quality demand".

However, in a densely populated country like Italy, for instance, rich in natural beauties, as well as industrialised, not surprisingly the environmental protection requirements often conflict against the market demand for raw materials.

Among the most strongly opposed environmental interventions connected to the extractive industry, it is possible to quote local scale effects such as visual impact and land quality degradation, but the analysis should also be extended to wider scale issues by encompassing, for instance, depletion of non renewable resources, with and without energy content, for the production of consumer goods that necessarily begins in a mining/quarrying site.

From the local to the global scale, the extractive industry can therefore be associated to the environmental effects summarised in Table 1.

The analysis of the relationship between the extractive industry and such environmental effects contributes to outline the environmental-energetic profiles of building aggregates.

Although all the environmental effects quoted in Table 1 deserve interest and should therefore be avoided or relieved, it must be recognised that their relative importance is mostly a matter of subjective evaluation.

Moreover, when dealing with extractive activities, even though the general opinion

and several public administrations consider local scale burdens the most important, it must be noticed that such environmental effects are the most difficult to quantify, while for the regional and global scale it is possible to make use of well known and objective assessment tools (Badino et al.1998).

Table 1. Environmental effects ascribable to the extractive industry and their scale of influence.

ENVIRONMENTAL EFFECT	SCALE OF INFLUENCE
Resources depletion	Global
Global warming	Global
Ozone depletion	Global
Acidification	Regional
Eutrophication	Regional/local
Photochemical smog	Regional
Human toxicity	Regional/local
Eco-toxicity	Regional/local
Waste generation	Regional/local
Visual impact	Local
Surface water pollution	Local
Land use	Local
Water resources use	Local
Dust emissions	Local
Noise / vibrations	Local
Traffic	Local

In this paper, while for the local scale environmental effects the analysis is limited to the list quoted in Table 1, as far as the regional and global scale are concerned, the results of some investigations run by Politecnico di Torino research staff (Badino et al. 2005) are here presented and discussed.

Beyond the fact that environmental impacts ascribable to the extractive industry are numerous and difficult to quantify, they are also deeply inter-connected and influence each other.

Therefore, when facing such issues one at a time, by means of a separate approach, without taking into account the scale of influence, the analysis can lead to contradictory results. Not surprisingly, the solution of a single environmental problem may cause further environmental consequences, sometimes worse than the

previous one, or the problem is simply transferred elsewhere.

Because of the different environmental interventions that can be associated to the mining-construction production streamline, and because of the existence of direct and indirect issues to be taken into account, Life Cycle Assessment (LCA) methodology, standardized according to ISO14040 (ISO 1997), is being more and more used as a tool for quantifying natural resources consumption and pollutant emissions with reference to the whole life cycle of mineral raw materials.

This is a methodological approach similar to the one adopted in the previous paragraphs in order to emphasize the economic significance of building aggregates. In fact, as for the market value that should be extended to the added value of the construction industry, the energetic and environmental performances of building aggregates should be assessed by encompassing their production, use and end-of-life.

With this in mind, in order to assist LCA practitioners when developing their Life Cycle Assessment models, it is of the utmost importance to make available the energetic-environmental profiles of building materials, describing and analysing their production processes, from quarry to delivery: the so called eco-profiles. Eco-profiles represent therefore the starting point and the first part of a full Life Cycle Assessment. They summarize, in fact, the energetic-environmental background of building materials, from their very beginning, in the earth's crust, until the time in which they enter the building worksite.

2 NATURAL AGGREGATES PRODUCTION IN EUROPE/ITALY

The European industry for the production of building aggregates accounted, in the year 2004, for around 25000 quarries which correspond to an estimated annual supply of 2.8 billion tons: 7 t per capita (source UEPG, 2005).

As far as Italy is concerned, the Italian central statistics agency ISTAT estimates the national production of building aggregates around 288 million tons in the year 2004.

The Italian production of building aggregates steadily increased at a annual growth rate of 1.7% during the last two decades, the country total supply being 193 million tons in the year 1980. Therefore, according to the official statistics, per capita production of building aggregates is about 5 t in 2004.

However, ISTAT statistics sensibly differs in comparison with other sources, as well as Italian per capita supply differs from other industrialised countries.

According to a research recently carried out by DITAG of Politecnico di Torino (Badino et al. 2006b) the Italian average annual requirement of building aggregates in the period 2000-2010 can be estimated in 6.5 t per capita.

In any case, for comparison, it is worth noticing that according to UEPG (European Aggregates Association) per capita yearly production of building aggregates is 6.5 t in Europe in 2004, the maximum per capita supply being 20 t in Ireland and the minimum being 1.4 t in the Netherlands.

For comparison, per capita production of building aggregates in the USA was 8.7 t at the end of the 1990's (source USGS).

2.1 Case study: Ceretto quarry

In the following case study, which is framed within a wider life cycle assessment investigation relevant to concrete run by DITAG of Politecnico di Torino in the year 2004 (Martaspina, 2004), the main parameters relevant to the eco-profiles of natural aggregates, excavated from an alluvial deposit, will be summarised.

The LCA model that has been developed in order to outline the eco-profile of natural aggregates, has considered all the physical exchanges, including use of natural resources, air, water and soil emissions, as well as generated waste *from-cradle-to-delivery* of the final product to the building worksite.

The production worksite under analysis is a quarry where building aggregates are excavated from an alluvial deposit, under the water table, by means of a grab dredge (Ridinger) equipment.

Ceretto quarry is located in the southern surroundings of Torino, along the left side of the Po river. The production of gravel and sand was around 500000 t in the year 2003 (Fig.1).

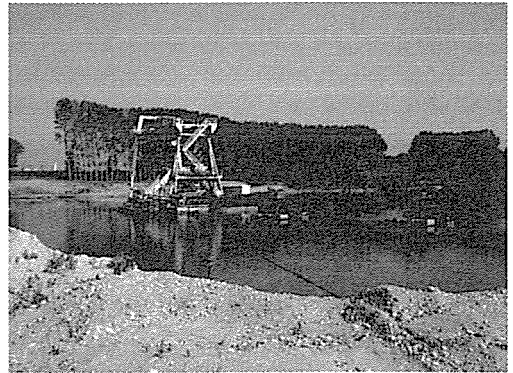


Figure 1. View of Ceretto quarry (Torino).

The scheme in Figure 2 supplies an overview of the main industrial processes which characterise Ceretto quarry unit, with emphasis on main excavation, transportation and mineral treatment equipment, as well as some technical data.

The software applications SimaPro6 and Boustead5 have been used, as supporting tools, in order to set up the LCA model, allowing inventorying of energetic and environmental intervention relevant to the production under study.

Beyond the processes aimed at quarrying, crushing, sieving and piling the final products, for which energy consumption, as well as materials use, emissions and waste have been accounted, also the transportation to the final user, by means of a truck, for a distance of 15 km, has been included in the model.

Figure 3 can be useful in order to understand how the LCA model has been developed.

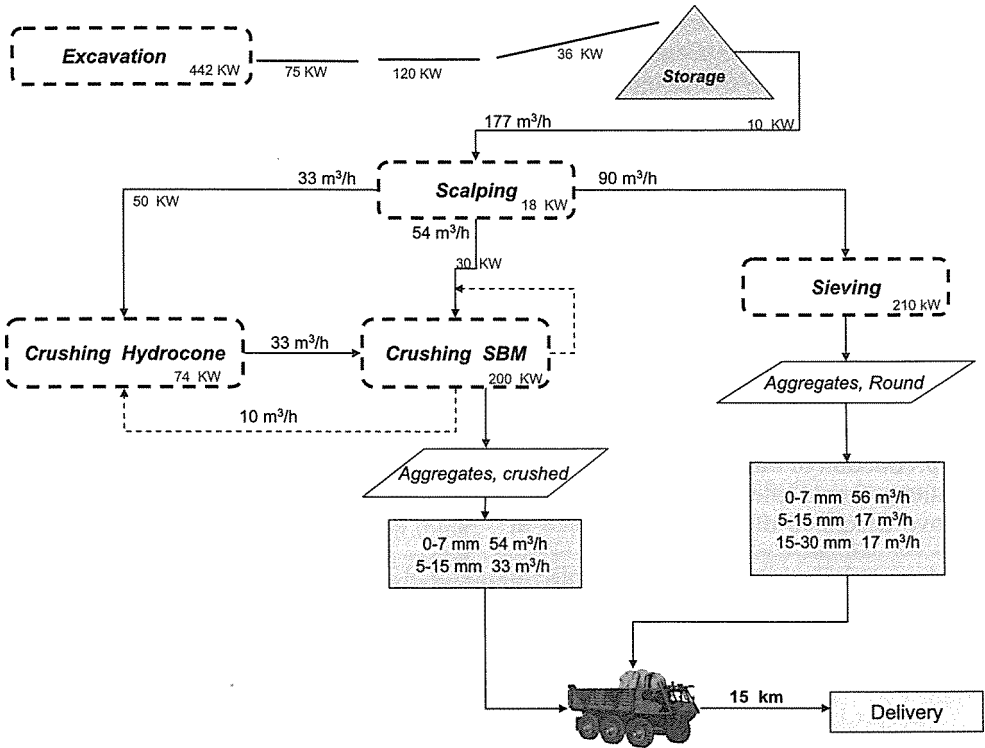


Figure 2. Main processes for the production of natural aggregates at Ceretto quarry.

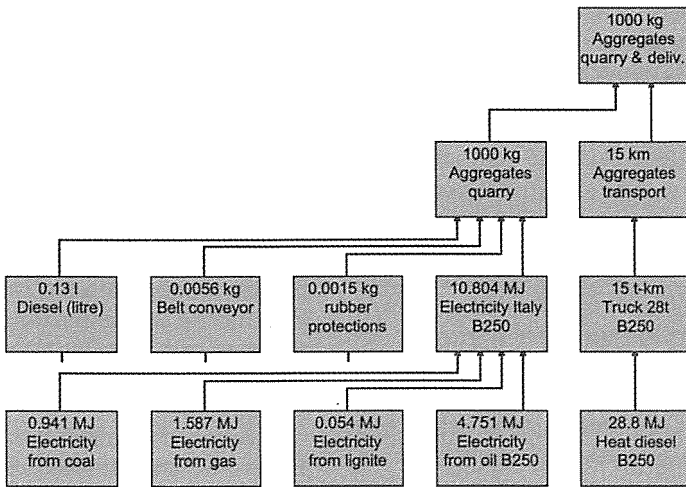


Figure 3. LCA model relevant to production and transportation of building aggregates at Ceretto quarry.

According to the flow chart shown in Figure 3, the eco-profile model is built up by exploding the production process, starting

from the outlet gate, going backwards along the production streamline.

Each box represents a unit process or, in other words, an elemental industrial operation, which is connected up and downwards to other units. For each box, systematic information is collected, relevant to physical input and output from and to upstream and downstream operations.

For each elemental industrial operation within the eco-profile model, a comprehensive physical ecobalance must be made available (Badino et al., 1998).

Each box in Figure 3 calls up physical input/output from upstream operations, so that the top box carries on the cumulative environmental-energetic interventions of the whole production of building aggregates.

Results gathered after the interpretation of the above described model, are presented in

the next paragraph, jointly with the eco-profiles of sand and gravel that are available in different databases.

2.2 Eco-profiles of natural aggregates

From-cradle-to-gate LCA models, carried out in compliance with ISO 14040 recommendations, relevant to several building materials, including building aggregates, can be found in different databases.

Table 2 summarizes some of the typical environmental impact indicators (eco-indicators), as gathered after the Impact Assessment step (ISO 1997), which can be regarded as representative of natural building aggregates eco-profiles.

Table 2. Main potential impact indicators representative of natural building aggregates eco-profiles, according to different sources.

From-cradle-to-gate Potential Environmental Impacts (data per 1 ton)	Unit	Gravel		Gravel	Gravel,	Gravel	Gravel	Gravel	Gravel
		Gravel	Sand	& sand	crushed	& sand,	& sand,	& sand,	& sand,
		ETH-ESU	ETH-ESU	IDEMAT	Ecoinvent	Ecoinvent	Boustead	Boustead	DITAG
Energy resources, GER	MJ	162.6	152.0	114.2	135.0	57.8	107.1	75.7	67.7
Global warming, GWP CO ₂ eq	kg	10.4	10.0	8.7	4.2	2.3	6.7	5.7	4.6
Acidification, mol H ⁺ eq	mol	1.69	1.59	2.97	0.88	0.57	2.18	2.43	1.70
Eutrophication, O ₂ eq	kg	0.28	0.28	0.62	0.19	0.13	0.43	0.61	0.32
Photochemical smog, C ₂ H ₄ eq	g	0.54	0.53	0.16	0.35	0.12	0.13	0.08	0.06
Waste generation	kg	x	x	0.48	x	x	x	x	0.03

The first seven columns are relevant to sand and gravel LCA models included in different databases, while the last column refers to the building aggregates produced at Ceretto quarry. Energetic and environmental indicators given in Table 2 are typical of a LCA analysis (Badino et al., 1998).

As far as energy use is concerned, in the case of GER (Gross Energy Requirement) indicator, the term "gross" indicates the cradle-to-gate energy and includes energy consumption from all ancillary operations, tracking all operations back to the extraction of raw materials from the earth crust.

GWP (Global Warming Potential) as parameter relevant to greenhouse effect, AP (Acidification Potential) as parameter

relevant to acid rain phenomenon, EP (Eutrophication Potential) as parameter relevant to surface water Eutrophication, POCP (Photochemical Ozone Creation Potential) as indicator of photo-smog creation and, finally, waste generation are calculated by means of a similar cradle-to-gate approach.

An analysis limited to the first two rows of Table 2 shows that the total energy requirement for the production, delivery and average transportation of 1 ton of building aggregates ranges from a minimum of 58 MJ to a maximum of 163 MJ. Similarly, the production of greenhouse gases ranges from a minimum of 2.3 kg CO₂ to a maximum of 10.4 kg.

3 RECYCLED AGGREGATES PRESENT SITUATION AND FUTURE PERSPECTIVES

Among “new” building materials that could replace the traditional ones, secondary materials from demolition and rubble recycling deserve more than some interest.

The challenge is to deeply understand what destiny deserve construction and demolition (C&D) waste, whose quantities are becoming higher and higher, and to understand whether, and until what extent, such demolition materials can replace virgin building materials.

In fact, from a certain point of view, the future aggregate quarries could be the old buildings to be demolished, but this must not be generalized. In fact, it is not fair to think that such new secondary “quarries” might completely displace the traditional ones. Quality requirements for commodities used in many industrial processes do not allow recycled materials use and, moreover, there are objective and insurmountable limits to recycling, which can be ascribed to decay of quality, loss of mass and energy as well as pollution caused during recycling processes.

The solution probably stands in a fair equilibrium between traditional and secondary mines/quarries. It would be unwise to underestimate the ones or the others.

In any case, this is a topic of great interest within the political debate about natural resources conservation on which, too often, some misconceptions are quite common

The point to be faced is the correct evaluation of what can be the effective contribution, in qualitative and quantitative terms, that recycled aggregates can supply in order to satisfy the requirement for building aggregates.

A careful evaluation, based on economic and environmental criteria, must be done relevant to the industrial process of recycling construction and demolition waste, in order to compare the two ways of producing building aggregates from virgin or recycled materials.

In fact, only when it will be proved that the recycling process is both economically

and environmentally sustainable, in comparison with the production of natural aggregates, the contribution of recycled aggregates could be considered positive.

During the last years, excavation, construction and demolition waste (C&DW) management activities have faced a remarkable growth. In fact, their contribution, in terms of secondary raw material supply, as well as in terms of employment, presently represents a meaningful input resource to the manufacturing industry.

According to the UE official data (Symonds et al. 1999), in the EU-15 the C&DW production was about 180 million tons at the end of the 1990's, corresponding to about 500 kg per capita.

An interesting remark is that relevant to the flows of C&D waste, which grew by 50% in Italy in the period 1999-2005 (APAT, 2005) and are nowadays comparable with the quantity of municipal solid waste.

The future perspectives of recycled aggregates strictly rely on the quality level requested for the different final uses. For example, organic and lightweight materials have to be absent in those recycled aggregates produced for concrete manufacturing and this condition implies remarkable technologic costs for the product valorisation, through dry or wet separation. On the contrary, for road construction, the lower required quality level may allow the presence of limited quantities of lightweight materials.

As far as Italy is concerned, official data says that the production of C&D waste has doubled during the last five years. In fact, per capita yearly C&D waste arose from 380 kg in 1998, to 740 kg in 2003.

The Italian Association of Recycled Aggregates Producers (ANPAR) has estimated a total production of C&D waste around 40 million tons all over Italy in the year 2004.

Based on C&D waste data relevant to Italy, as shown in Table 3, and considering the yearly requirement of building aggregates, according to the different

sources, it is possible to make the following remarks.

Table 3. C&D waste production in Italy (adapted from APAT, 2005).

Year	C&D waste (Mt)	C&D waste per capita (t)
1998	21.3	0.38
1999	23.9	0.43
2000	27.3	0.49
2001	31.0	0.55
2002	37.3	0.62
2003	42.5	0.74

As far as the Italian per capita requirement of building aggregates is comprised between 6 and 11 tons (Badino et al., 2006b), the production of recycled aggregates represents a maximum potential contribution of about 10%, even in the theoretical case of a C&D waste recovery rate nearly 100%.

For this reason, it is possible to state that recycled aggregates market cannot be considered as a potential substitute of natural aggregates.

The two typologies of aggregates must therefore not be considered as competitors but, on the contrary, their jointly use must be considered strategic.

In fact, the construction industry could easily absorb the whole production of recycled building aggregates and use them as a mix of recycled and natural commodities in compliance with the different specific requirement of the final uses.

3.1 Case study: the CAVIT stationary rubble processing plant

The CAVIT plant is targeted to the C&D waste recycling, with a yearly average production of 150000 t, and performs a dry treatment on raw building rubble (Fig. 4).

The presently operating dry process is shown in Figure 5 and is characterized by:

- a feeding and scalping unit (1);

- a single stage crushing unit (2), setting up through an impact crusher and an overband separator, that removes the steel and reinforced re-bars;
- a silty rubble treatment unit (3), setting up through an overband separator and a screen, that separates the granulometric class lower than 10 mm from the 10-40 mm class carrying on the process;
- a building rubble screening unit (4), in which the 0-8 mm, 8-40 mm and 40-100 mm classes are divided;
- an air separation unit (5), that beneficiates only the 8-40 mm and 40-100 mm classes through the organic lightweight materials removal;
- a handling unit for piling up the final products (6);

At the end of the recycling process, aggregates are delivered within a distance of about 15 km by means of trucks.

Figure 6, which refers to the LCA model relevant to the production of 0/40 mm class recycled aggregates at Cavit plant, can be useful in order to understand how the LCA methodology has been applied to the processes shown in Figure 5.

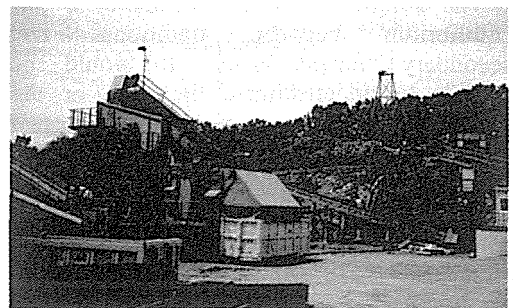


Figure 4. CAVIT rubble processing plant, La Loggia (Torino).

3.2 Eco-Profiles of Recycled Aggregates

When dealing with recycling processes, the from-cradle-to-gate philosophy must be turned into from-grave-to-cradle.

In fact, as far as recycling operations are concerned, the raw materials are represented by scraps or waste otherwise addressed to landfill, which re-enter a further life cycle in substitution of virgin materials.

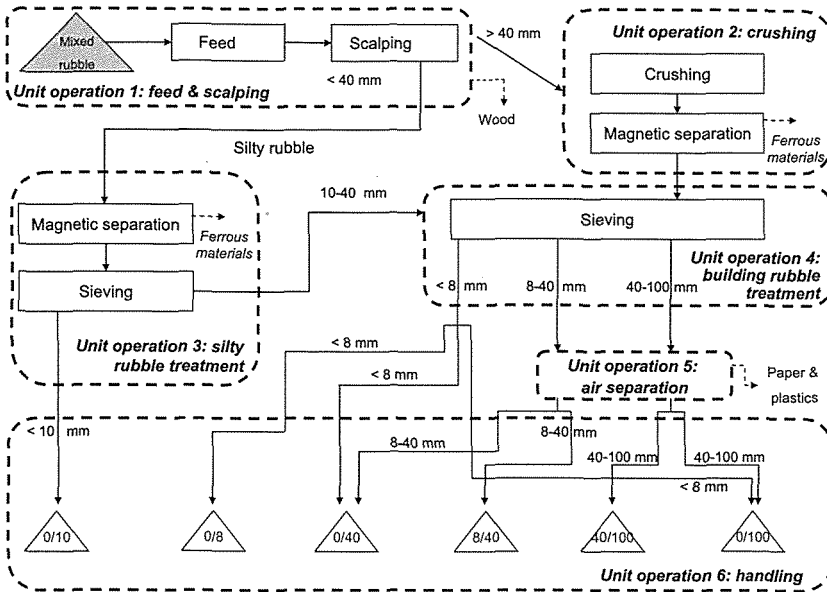


Figure 5. Main processes for the production of recycled aggregates at CAVIT plant.

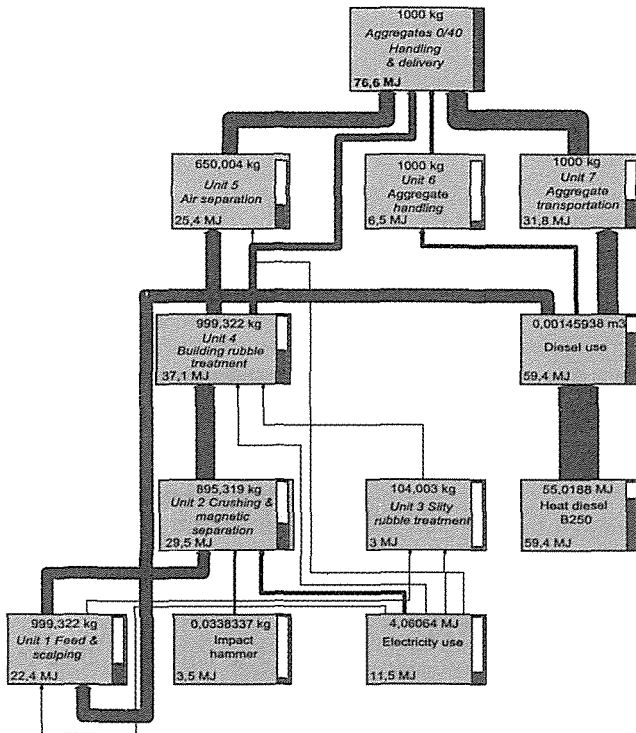


Figure 6. LCA model relevant to production and transportation of 0/40mm recycled aggregates at CAVIT processing plant.

The eco-profiles of recycled building aggregates, some example of which are dealt with in Table 4, represent therefore the cumulative energetic and environmental interventions, from waste collection to the delivery of valuable secondary materials.

On this point, it is worth noticing that among LCA practitioners it is a common understanding that scraps or waste do not hold any past energetic-environmental burdens when entering a recycling process.

In other terms, waste materials do not take part in the allocation of environmental burdens relevant to the process that generated them.

With that in mind, the system that has generated the waste is credited of the waste that otherwise had to be disposed and the

system that receives the waste is credited of the avoided virgin raw materials, but is charged with energy and ancillary materials used within the recycling process.

Moreover, the system that makes use of recycled materials is credited by the energetic-environmental interventions that characterise the virgin building materials that are displaced.

In other terms, with reference to Table 2 and Table 4, the eco-profiles of recycled building aggregates tells us what are the energetic-environmental impacts associated with the recycling operations, while the eco-profiles of virgin aggregates tell us what are the gross benefits that can be achieved by recycling building aggregates.

Table 4. Main potential impact indicators representative of recycled building aggregates eco-profiles, CAVIT 2002.

From-cradle-to-gate Potential Environmental Impacts (data per 1 ton)	Unit	0/10	0/8	0/40	8/40	40/100	0/100	Average Cavit 2002	Average Cavit 2002	
		mm	mm	mm	mm	mm	mm			
		Processing + handling + delivery 15km							(no transport)	
Energy Resources, GER	MJ	66.9	75.4	76.6	77.3	77.3	76.8	76.3	44.5	
Global warming, GWP CO ₂ eq	kg	5.0	5.5	5.5	5.6	5.6	5.5	5.5	3.1	
Acidification, mol H ⁺ eq	mol	2.01	2.33	2.35	2.36	2.36	2.35	2.34	1.32	
Eutrophication, O ₂ eq	kg	0.48	0.49	0.49	0.49	0.49	0.49	0.49	0.23	
Photochemical smog, C ₂ H ₄ eq	g	0.07	0.08	0.08	0.08	0.08	0.08	0.08	0.04	
Waste generation	kg	0.60	0.54	1.08	1.37	1.37	1.16	1.08	1.08	

The difference between parameters relevant to virgin and recycled aggregates, also considering the mass yield of rubble processing, represents the net achievable benefit.

As it can be remarked by analysing Table 4, the production of 1 ton recycled aggregates, including all industrial processes starting from the feeding of rubble into the Cavit plant until the delivery of the final products to the customers, roughly corresponds to 67-77 MJ/t of Gross Energy Requirement and entails to an emission of 5-5.6 kg CO₂/t.

Moreover, Table 4 contains figures relevant to other impact indicators which

characterize the different secondary raw materials.

Average AP Acidification Potential is 2.34 mol H⁺ equivalent, average EP Eutrophication Potential is 0.49 kg O₂ equivalent and the average Photochemical Smog Creation Potential is 0.08 g C₂H₄ equivalent.

Moreover, the production of recycled aggregates corresponds to about 1 kg/t of waste.

Some more remarks can be done by analysing Figure 7 in which the contributions of recycling processing, bulk handling and transportation are emphasised.

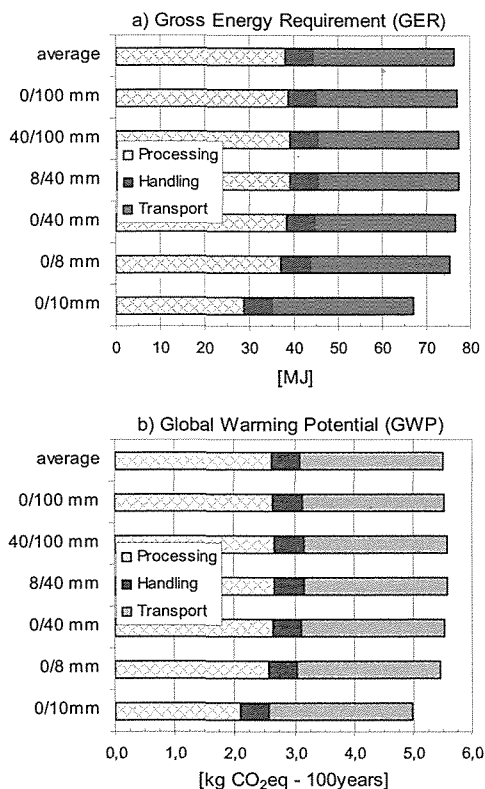


Figure 7. Contribution of processing, handling and transportation to the eco-profile of recycled aggregates.

As far as energy use is concerned, recycling processing is responsible for 50% of the total energy consumption relevant to the production of average secondary aggregates, while handling and delivery are responsible for 8% and 42%, respectively.

In case of greenhouse gas emissions, recycling processing is responsible for 47%, while handling and delivery are responsible for 9% and 44%, respectively.

4 CONCLUSIONS

As far as the present research is concerned, the eco-profiles relevant to virgin aggregates and those relevant to recycled aggregates have shown that in both cases most of typical environmental and energy indicators have a comparable magnitude.

The average GER relevant to natural aggregates is 109 MJ/t while recycled aggregates corresponds to 76 MJ/t.

The average GWP relevant to natural aggregates is 6.6 kgCO₂eq/t, while recycled aggregates corresponds to 5.5 kgCO₂eq/t.

On the contrary, AP, EP and POCP indicators relevant to natural aggregates are lower than those relevant to recycled aggregates.

On the average, production of natural aggregates corresponds to a waste generation of 0.3 kg/t, while recycled aggregates produce 1.1 kg/t waste subsequently to recycling operations.

However, recycling 1 ton of secondary aggregates avoid the landfill of about 1 ton of inert waste and its subsequent impacts.

One more important consideration is that relevant to the remarkable contribution of transportation to the final energetic and environmental impacts: almost 45%.

All this considered, it is worth to emphasise once more that when comparing natural and recycled aggregates, it must be proved that the recycling process is both economically and environmentally sustainable, in comparison with the production of natural aggregates.

The results of the present research have confirmed that natural aggregates and recycled aggregates must not be considered as competitors but, on the contrary, their jointly use must be considered strategic in different sectors of the construction industry.

REFERENCES

- APAT, 2005. I rifiuti da C&D. available on line at <http://www.apat.it>
- Badino, V., Blengini, G.A., Zavaglia, K., 2006 a. Analisi tecnico-economico-ambientale degli aggregati per l'industria delle costruzioni in Italia. Parte 1^a - I prodotti e l'offerta di mercato. *GEAM*, n. 117, Anno XLIII n.1-2, pp.5-14.
- Badino, V., Blengini, G.A., Zavaglia, K., 2006 b. Analisi tecnico-economico-ambientale degli aggregati per l'industria delle costruzioni in Italia. Parte 2^a - La stima dei fabbisogni. *GEAM*, n. 118, Anno XLIII n.3, pp.5-16.

- Badino, V., Blengini, G.A., Zavaglia, K., (Singhal, Fytas, Chiwetelu ed.), 2005. Demolition and rubble recycling as a new source of building materials. *Proc. XIV International Symposium on Mine Planning and Equipment Selection (MPES 2005)*. Banff, Canada, (ISSN 1712-3208), pp 64-82.
- Badino, V., Baldo, G., (Esculapio Ed.), 1998. *LCA Istruzioni per l'Uso*. Bologna: Progetto Leonardo.
- Blengini, G.A., Garbarino, E., (ed. Cardu, Ciccu, Lovera & Michelotti), 2006. Sustainable constructions: eco-profiles of primary and recycled building materials, *MPES 2006, XV International Symposium on Mine Planning and Equipment Selection, Torino, Italy* (ISBN 88-901342-4-0) volume 2, pp. 765-770.
- Derks, J.W., Moskala, R., Scheider-Kuhn, U., 1997. Wet processing of demolition rubble with pulsator jigs, *Aufbereitungs Technik*, volume 38, n. 3, pp. 139-143.
- ENEA, 2004. *Rapporto Energia e Ambiente 2004*. Rome
- Garbarino, E., Mancini, R., (ed. Cardu, Ciccu, Lovera & Michelotti), 2006b. Unconventional feed source and products for a quarrying and processing plant system, *MPES 2006, XV International Symposium on Mine Planning and Equipment Selection, Torino, Italy* (ISBN 88-901342-4-0) volume 2, pp. 836-841.
- Garbarino, E., 2005. Stato dell'arte e risultati di una ricerca sperimentale inerente la valorizzazione e l'impiego nella produzione di calcestruzzo di aggregati riciclati derivanti da rifiuti da costruzione e demolizione. *PhD thesis*. Politecnico di Torino.
- ISO International Standard 14040, 1997. *Environmental management – Life cycle assessment – Principles and framework*. Geneva: International Organisation for Standardisation (ISO).
- ISTAT, 2005. *Annuario statistico italiano 2005*. Rome.
- Marta Spina, C., 2004. Sostenibilità della produzione di materiali per l'industria delle costruzioni: LCA del calcestruzzo. *Master Degree thesis*. Politecnico di Torino.
- Pruwasser, J., 2001. New processing plant sets new standards, *Aufbereitungs Technik*, volume 42, n. 12, pp. 580-584.
- SYMONDS, ARGUS, COWI & PRC BOUNCENTRUM, 1999. Construction and demolition waste management practices and their economic impacts. *Report DGXI European Commission "C&DW"*, Brussels http://ec.europa.eu/environment/waste/studies/cdw/cdw_report.htm.
- UEPG, 2005. *Annual Report 2004*. European Aggregates Association, Brussels.
- Wellmer, F.W., 2002. Aspects for formulating mineral resources management policies. *Proc. Conf. Sustainable Resource Policy for Europe, Brussels*.

Online Information Management on Coal and Gas Outburst

N. Aziz, R. Caladine, L. Tome & D. Vyas

University of Wollongong, Wollongong, NSW, Australia,

ABSTRACT A Website on coal and gas Outbursts in the Australian environment www.uow.edu.au/eng/outburst has been developed by The University of Wollongong with funding received from the Australian Coal Association Research Program (ACARP) in 2005. The primary objective of the Website is to provide the coal mining industry with information on the occurrence, mechanisms and means of treating Outburst phenomena. The Website provides access to the experience, knowledge and information acquired by the coal mining industry, research organisations and educational institutions in a quality-controlled environment. Although the Website is specific to the Australian scene, it contains information and issues from other countries. The Website is the work of an interdisciplinary team of professionals from across the university. The site draws on expertise from specialists in the mining, electronic communications and information professions. The information on the Website includes reports on the latest operational and research activities from field studies, as presented at various seminars, conferences, and in other publications.

1 INTRODUCTION

In February 2003, an ACARP Outburst Research Needs Workshop, at the University of Wollongong, identified the need for the establishment of a Website on coal and gas Outbursts. This need was later reflected in the ACARP Sponsored Scoping Study Project (ACARP project C10012). One of the recommendations of the scoping study was the establishment of an online information management system in the form of a Website on Outbursts of gas and coal in underground coal mines. As a consequence ACARP funded a project (C 14015) to support the development of the Outburst Website by personnel at the University of Wollongong. The funding came into effect in May 2005 and a dedicated Website developer was recruited for the project. The Website is currently in the second year of development.

The primary objectives of this project are:

- a) To develop a quality Website on Outbursts. To disseminate information, knowledge and experience on Outbursts as from the Australian coal mining industry and research organizations.
- b) To consolidate information that presently exists in conference proceedings, Websites and the experience and knowledge of people working in the mining industry or in research.
- c) To provide resources that have been filtered, selected, evaluated and organized for the Websites primary audience: researchers, students and mining practitioners. Quality controls will ensure a selective yet comprehensive collection of resources.

- d) To provide a collated body of knowledge and reference point that represents a 'critical mass' of information on this topic. The information will be used to create new knowledge.
- e) To provide practitioners with a discussion forum to openly communicate issues and concerns and network across geographical boundaries via an online forum.

2 PROJECT DEVELOPMENT

Planning and construction of the Website involved the expertise of a team of professionals from across the University including a PhD student. Each team member contributed from their area of expertise in terms of content, design and the legal aspects of the Website. The Website provides the coal mining industry with information necessary for the control and management of coal mine Outburst phenomena. In addition it will also serve as a virtual forum for the exchange of ideas and information between mine operators, mining engineers, geologists, consultants and researchers in the field. To meet the aim of making the Website technically credible and to reflect the current status of Outburst management and control, specifically on Australian conditions, the Website is continually being developed. Planned organization of information is essential if users are to navigate the Website in an efficient way. Accordingly, the structure of the Website has the following sections:

- a) Site map
- b) Definition of Outbursts
- c) Factors that contribute to the occurrence of Outbursts
- d) Management of Outbursts: prediction, prevention and control
- e) ACARP research reports and presentations from various meetings and seminars including case studies of occurrence of Outbursts in Australia and world-wide

- f) Links to other relevant and useful Websites
- g) Glossary of Outbursts related terms
- h) Contact details of the development team
- i) Home page

3 WEBSITE CONTENT AND NAVIGATION

The content of the Website comprises technical papers, ACARP reports, journals, presentations by mining industry personnel *and an Outburst scoping study*, predominantly the work of Lama and Bodziony, (ACARP Project No C 4034, 1996). These items are supplemented with technical material from industry personnel as well as specialist mining consultants. Mining personnel and expert industry consultants have supplied the reported case studies and will provide future ones. Although the Website is linked to various national and international Websites it will not be used to actively promote any company, product or the like. The Website's primary function is to disseminate knowledge in the mining literature and to share industry's experiences. The discussion function will provide users with the opportunity to maintain networks within the industry, share knowledge and experiences and seek assistance from peers.

Assessment and feedback components will be included to optimise the usefulness and to guide future directions of the site. Positive feedback has been received from the mining industry in various forums such as ACARP meetings and Outburst seminars.

The Website has been constructed using the standard Web format (Hyper Text Markup Language, HTML). Access to the site is by standard Web browsers, for example, Netscape Navigator, Firefox or Internet Explorer. The address of the site is <http://www.uow.edu.au/eng/outburst>. A standard design template has been developed and incorporated onto each page of the site to maintain consistency and ease of use. The home page of the website is shown in Figure1. Complex Websites require efficient

and universal navigation systems to ensure that users can find what they are looking for, return to previously viewed pages and bypass the non-germane in an efficient manner. The system employed in the Outburst Website

consists of a horizontal menu directly below the banner on each page. Hovering the mouse over an item on the menu reveals a drop down menu with links to various pages on the site.

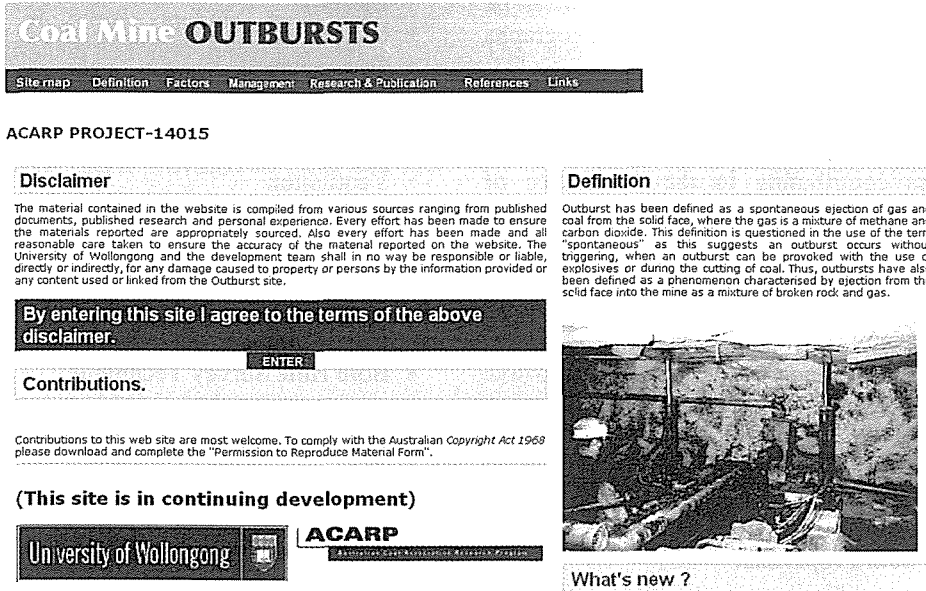


Figure 1 University of Wollongong/ACARP outburst website.

When users first access the site the home page, as shown in Figure 1 is displayed. A banner and horizontal menu is a disclaimer. Agreeing to its terms can further access the site. Below the disclaimer is the “Enter” Website. The second page starts with the “Aim and Objectives” of the Website. On the bottom of the page a link has been provided to the “copyright form”. All contributions to the Website are welcome, however as per the “Australian Copyright Act 1968” permission is required before materials can be uploaded to the Website. The copyright form can be downloaded and signed by the author of the material to be uploaded. This form can be faxed or scanned and sent by e-mail to the Research Training Librarian, University of Wollongong. The topics in the horizontal menu are, Site Map, Definition, Factors,

Management, Research and Publications, References and Links. These topics are also modules of the Website and an overview of each of them follows banner, “Mine Outbursts”, is incorporated at the top of the index page. Beneath the button allowing entry to the rest of the site.

3.1 Site Map

This module provides an overview of the contents of the Website and contains links to each topic in the Website. Note that some areas are still under construction.

3.2 Definition

Definitions provide an excellent introduction to Outburst phenomena. As well as defining Outbursts, links are provided to definitions

of related topics, Outburst size and Outburst caverns. The topic explains how an Outburst occurs, the composition of an Outburst and where it occurs. "Outburst Size" assists users through definition and classification of Outbursts based on size. "Outburst Cavern" is defined as different types of cavern can be formed as a result of Outbursts. Photographs accompany the definitions.

3.3 Factors

Factors contributing to the occurrence of Outbursts are:

3.3.1 Geological Conditions:

- Depth of Mining
- Faults and Folds
- Seam Thickness
- Gas Environment
- Gas Content
- Mining Induced Stresses

3.3.2 Coal Properties:

- Strength of Coal Seam
- Rank of Coal Seam
- Coal Permeability
- Volumetric Change
- Cleats and Joints

3.4 Management

Mining of seams prone to Outbursts requires the development of specific procedures to ensure that the risk to miners and equipment is eliminated or reduced. The purpose of management systems is to ensure that the procedures are in place and are precisely followed so that the mining activities are performed as per the management plan. The Management module includes:

3.4.1 Prediction:

- Geology
- Prediction Indices
- Monitoring

- Geophysical
- Seismic
- Electromagnetic
- Radar
- Radiometric
- Gas environment
- Gas type
- Gas pressure
- Gas content

3.4.2 Prevention:

- Ventilation
- Gas Threshold Value
- Gas Drainage
- Pre-Drainage
- Inseam Drainage
- Post Drainage
- Bore Hole Survey Technique

3.4.3 Control:

- Ground De-Stressing
- Gas Drainage
- Bore Hole Survey Technique
- Hydro Facing
- Pulse Infusion Shot Firing
- Blasting and Borehole Simulation
- Outburst Hazard Control
- Outburst Management Plan

3.5 Research and Publications

This section includes reports of ACARP on the subject. They include:

- ACARP Gas and Outburst Workshop: 28th August 2004
- Gas and Outburst Workshop: 22nd November 2003
- Outburst Scoping Study- John Hanes
- Real Time Return Gas Monitoring for Outburst and Gas Drainage Assessment.
- Outburst Scoping Study- March 1996 (Lama & Bodziony)
- Outburst Symposium-March 1995

As well, various presentations on the latest developments on mine Outbursts and the practices being followed at mine sites as

reported at the Outburst committee meetings, have been uploaded and this is an ongoing activity.

3.6 References

An exhaustive list of relevant references, some of which include links to other Websites can be found in this module.

3.7 Links

Links have been provided to other relevant national and international mining Websites as a source of information on coal and gas Outbursts. They are not intended to actively promote any company, product or the like.

4 FUTURE ISSUES

Future issues addressed include:

- Feedback form
- A forum for two way communication and active discussions
- Uploading information on prediction, prevention and control of Outbursts
- Modification of the template
- International history and further case studies to be uploaded

5 CONCLUSION

This web site through information dissemination will provide:

- Increased awareness of Outburst issues, practices and strategies
- Remote access to information
- Public awareness of issues related to Outbursts, coal mining and green gas effect
- Increased awareness of safety issues. Including prevention and management of outbursts

The Website has been placed in the public domain to assist in the upgrading and training of mining industry personnel as well as raising awareness of mining operations for the general public. The Website is a valuable

and useful resource for those concerned with Outbursts in remote regions and rural areas of Australia and also throughout the world. The Website represents a dynamic body of knowledge in this field.

ACKNOWLEDGEMENTS

The authors accord their appreciation to ACARP for funding this project. Various mining companies, mining consultants, government organizations have and continue to provide material for the Website. Significant materials uploaded to the Website are Power Point presentations compiled by John Hanes. Thanks are also extended to Illawarra Gas Outburst Committee for providing the opportunity allowing regular presentations on the progress of the work on the web site.

Geotechnical Engineering

Effect of Confining Stress on Rock Mass Deformation Modulus in Javeh Dam Site

H. Aliasghari & R. Berry

Moshanir Power Engineering Consultants, Tehran, Iran

ABSTRACT The engineering behavior of the specific rock mass is significantly affected by deformation modulus of the rock mass. This parameter also has a direct effect on designing the underground and surface structures. The mentioned modulus also varied with confining pressure for a same rock with similar geological aspects. In this paper the effect of confining pressure on a same rock mass with same geological specifications is measured by insitu dilatometer tests which have been carried out in the Javeh Dam Site in Iran (Earth fill dam with 110m height). Based on the obtained results, a criterion for determination of the relation between confining pressure (Tests in different depths) and modulus of deformation is suggested.

1 INTRODUCTION

Designing the structures is significantly affected by modulus of elasticity. In most of cases, this parameter only affected by lithological and geological specifications of the rock mass. For a specific rock with a same geological and lithological aspects, the unique value of deformation modulus is considered for all of the surface and subsurface structures designations, but owing to the significant variation of this parameter with depth especially for the underground structures the destination of the temporary supports or permanent lining could be optimized by considering the mentioned variation.

For determining the effect of depth and confining pressure on the rock mass deformation modulus, one of the best methods is using a Dilatometer insitu rock mechanic tests. In this paper with using of the obtained results of the Dilatometer tests which have been carried out in Javeh Dam Site, the effect of the confining stress on the rock mass deformation parameter is

presented by suggestion of a criteria. The high numbers of these tests give the opportunity to us to determine the mentioned effect, precisely.

2 JAVEH DAM SITE CHARACTERIZATIONS

Javeh earth fill Dam site is located on the western part of the Iran, near to the Sanandaj city. The rock mass of the foundation and abutments of the dam consists of Metamorphic rock (Slate) of the third geological era.

Three joint systems with spacing equal to 1-2 meters exist in the site. The lithology and geological conditions of the dam site don't change significantly in different parts of the dam site.

2.1 Exploratory excavations

In order to geological observations and achievement of the insitu rock mechanical tests, three galleries were excavated in dam axis. The specifications of the galleries are shown in Table 1.

Table 1. Exploratory galleries specifications.

Name	Length (m)	Location	Overburden (m)
A	90	Right Abutment	75
B	60	Left Abutment	40
C	80	Left Abutment	20

2.2 In Situ Rock Mechanical Tests

In the exploratory galleries, Plate Load and Dilatometer tests were carried out. Due to the few numbers of the Plate Load Tests, in comparison with Dilatometer tests, the results of the plate load tests were not considered. In Figure 1 the approximate location of the galleries and tests in the dam axis is shown. The dilatometer tests were carried out according to ISRM (1987). The equipment used was an Interfels IF096 (Interfels, 2002).

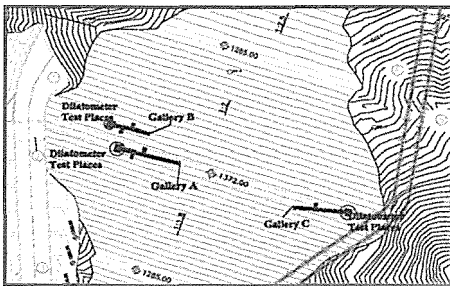


Figure 1. Location of the exploratory galleries and dilatometer tests in the Javeh Dam Site.

3 Basic Assumption of the Investigation

In this research to determine the effect of confining stress on the rock mass modulus of deformation, the following assumptions are considered:

- According to the important effect of anisotropy on rock mass deformations, only the results of tests which schistosity direction is perpendicular with load axis were considered. Under this circumstance the effect of anisotropy of the rock mass would be the same for all tests and can be ignored.

- In this investigation only the obtained results of the tests which were carried out in the horizontal bore holes is considered.
- The coefficient of horizontal to vertical stress ratio (K) was considered equal to 0.5.
- By using dilatometer borehole tests logs, only the results were considered that they have the same geological conditions (RQD, lithology, joint spacing and directions, weathering). In this condition the effect of geological situation on the rock mass specifications could be ignored.

4 Data Analysis

Totally, 38 dilatometer tests were carried out in the different parts of the drilled bore holes in galleries. The boreholes detail specifications are shown in Table 2.

As mentioned before, because of the required assumption in this research some of the obtained results was eliminated. The location and other specification of the tests which are used in this investigation are presented in the Table 3.

Table 2. Specification of the dilatometer test boreholes.

Location	Name	Depth (m)	Angle to horizon (deg)	Number of tests
Gallery A	AD1	50	0	6
	AD2	50	60	6
Gallery B	BD1	48	70	7
	BD2	47	30	7
Gallery C	CD1	48	20	6
	CDV	50	90	6
	CDH	50	0	4

5 Estimation of Confining Stress for Each Test

For determining the confining stress in each test, the equation (1) is used:

$$\text{Confining Stress} = K \times \gamma \times h \tag{1}$$

K : Horizontal to vertical stress ratio = 0.5

H : Depth of the test location (m)

γ : Density of rock mass = 2.7 g/cm³

Table 3. Specifications of the tests location in the bore holes.

No	Gallery Name	Bore Hole Name	Rock Type	RQD (%)	Burden (m)
1	Gallery A	AD1	Slate	75	75
2		AD1	Slate	78	76
3		AD1	Slate	80	75
4		AD2	Slate	95	91
5		AD2	Slate	90	106
6		AD2	Slate	75	115
7		AD2	Slate	95	80
8		AD2	Slate	90	85
9		AD2	Slate	75	92
10	Gallery B	BD1	Slate	87	53
11		BD1	Slate	90	60
12		BD1	Slate	81	47
13		BD2	Slate	98	44
14		BD2	Slate	79	58
15	BD2	Slate	75	56	
16	Gallery C	CDI	Slate	78	27
17		CDI	Slate	78	30
18		CDI	Slate	80	32
19		CDV	Slate	75	57
20		CDV	Slate	83	62
21	CDV	Slate	75	69	

Table 4. Dilatometer test results in holes.

No	Measured deformation modulus (GPa)	Overburden height (m)	Confining stress (MPa)
1	4.5	75	1.012
2	4.8	76	1.012
3	4.2	75	1.012
4	7.0	91	1.230
5	7.0	106	1.420
6	7.8	115	1.550
7	5.8	80	1.080
8	6.0	85	1.140
9	6.5	92	1.240
10	3.0	53	0.715
11	3.5	60	0.807
12	3.2	47	0.630
13	2.8	44	0.599
14	4.5	58	0.780
15	4.0	56	0.755
16	1.0	27	0.360
17	1.5	30	0.404
18	1.8	32	0.436
19	4.2	57	0.760
20	4.0	62	0.830
21	4.5	69	0.920

6 OBTAINED RESULTS

With regard to all of the mentioned assumptions and relationships, the obtained results from dilatometer tests and their confining stresses are presented in Table 4.

7 DISCUSSION

Based on the results that have obtained from Javeh Dam site dilatometer tests, effect of confining stress on modulus of deformation was studied and a criterion is suggested. The results are shown in Figures 2-3. The relationship between modulus of deformation and confining stress is presented in Figure 2 and the relationship between modulus of deformation and overburden height is presented in Figure 3.

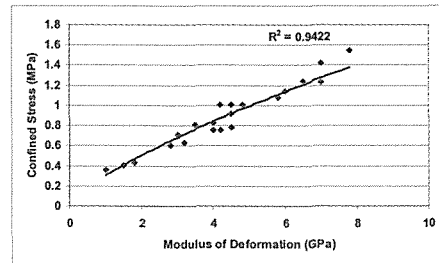


Figure 2. Relationship between modulus of deformation and confining stress.

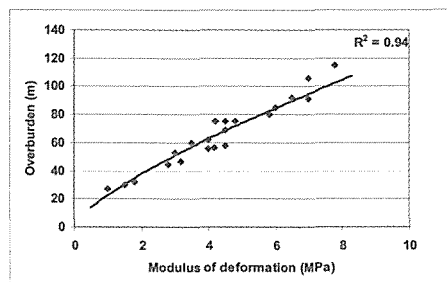


Figure 3. Relationship between modulus of deformation and overburden height.

By acceptable R^2 (=0.9422) of the trend line in Figure 2, the equation 2 is suggested for determining the relationship between confining stress and modulus of deformation in Javeh dam site.

$$\text{Modulus of deformation (GPa)} = 5.0378 \times (\text{Confining stress (MPa)})^{1.385} \quad (2)$$

For checking the suggested formula, the values of modulus of deformation which are predicted with Equation 2 are compared with obtained results from dilatometer tests and the results of them are presented in Table 5.

Table 5. Comparison between measured and predicted modulus of deformation.

Measured deformation modulus (GPa)	Confining stress (MPa)	Predicted deformation modulus (GPa)	Error (%)
4.50	1.012	5.123	12.169
4.80	1.012	5.123	6.314
4.21	1.012	5.123	17.829
7.00	1.229	6.672	4.671
7.00	1.428	8.178	14.405
7.80	1.556	9.184	15.071
5.80	1.080	5.592	3.704
6.00	1.147	6.072	1.197
6.50	1.242	6.761	3.870
3.00	0.715	3.195	6.107
3.50	0.807	3.769	7.159
3.20	0.630	2.694	15.805
2.80	0.599	2.516	10.142
4.50	0.779	3.895	13.432
4.00	0.755	3.441	16.228
1.00	0.363	1.276	21.683
1.50	0.404	1.471	1.906
1.80	0.436	1.632	9.285
4.20	0.764	3.785	9.870
4.00	0.837	3.954	1.101
4.50	0.927	4.548	1.055

The comparison of results, between measured and prediction modulus are shown in Figure 4.

As it is obviously observed in Figure 4 the value of measured and predicted modulus of deformation have a close relationship with each other but in the confining stress more than 7 MPa, they are approximately divided.

As a result, the uncertainty of the suggested criteria increases in high range of confining pressure.

Therefore the usage of suggested criterion should be limited to confining stress less than 7 MPa.

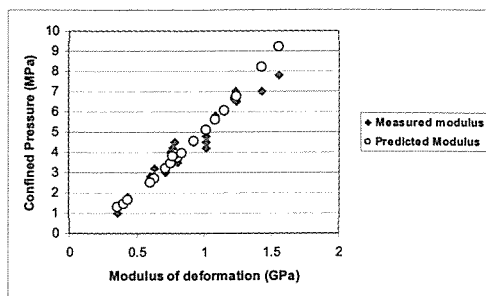


Figure 4. Comparison between measured and predicted modulus.

8 CONCLUSION

According to the mentioned results, it can be seen that increasing the overburden on underground structures and consequence increasing of the confining stresses, can cause severe increasing in the elasticity and deformation modulus.

In fact, increasing the elasticity and deformation modulus indicates increasing in the rock strength. With regard to this point, it is possible to consider the realistic amount of this modulus for excavation of the openings in different depths of the region.

By using the equation of this paper, deformation modulus in different depths of the Javeh dam site can be obtained. By considering that result, we can decrease the operational cost of the stability measurements for underground structures.

REFERENCES

Interfels, 2002. "Dilatometer System", Boart Longyear Interfels GmbH, available at <http://www.Interfels.com>.
 ISRM, 1987. "Suggested methods for deformability determination using a flexible dilatometer", Int. J. Rock Mech. Min. Sci, Vol. 24, No 2, pp 123-134.

Technique on Optimization of Geomechanical Monitoring in an Underground Construction

A.V. Man'ko

Moscow State University of Civil Engineering, Moscow, Russia

ABSTRACT The basic idea of scientific work consists in creation of a technique of rational accommodation of the equipment for geomechanical monitoring with use thus of modern computer technologies. New information technologies in a mode of geographical information systems allow forming models of underground constructions in real geological conditions. At the decision of tasks of optimum accommodation of systems of geomechanical monitoring underground constructions, the great value has numerical modeling of an underground construction. Joint application of these technologies, at a sufficient methodical and scientific substantiation, will allow carrying out long geomechanical forecasts of behavior of object, and for stages of construction and operation for a design stage to serve as the control standard of behavior of object that will provide acceptance of necessary engineering decisions in real time.

1 INTRODUCTION

It is necessary to make a complex of works for all underground constructions on monitoring a mass of rocks containing an underground construction during the various periods of existence of object.

In this connection there are no precise recommendations on rational accommodation of the equipment for monitoring in underground constructions. Arrangement of the equipment is made, more often, proceeding from experience of builders. Such approach to the organization of system of monitoring behind work of an underground construction is not comprehensible at the present stage. It is necessary to prove and confirm scientifically with results of the lead modeling necessity of statement for the given place of the research equipment.

In given article results of the scientific work continued of seven years, on development of a technique on optimization

of system of geomechanical monitoring in underground constructions are resulted on the basis of joint application of modern methods of numerical modeling and Geographical Information Systems (GIS) in rock mass.

On the basis of the developed technique, optimization of system of monitoring is carried out by the example of the project of a complex of underground constructions located in a rock mass.

2 COMPUTER MAINTENANCE OF GEOMECHANICAL MONITORING

Process of interaction of system developing in time «underground construction - rock mass» cannot be submitted by a series of independent calculations, consecutive reflection of all events from geological formation of a rock mass and its intense condition up to last stage of existence of considered object here is necessary. In these

conditions the choice of the software for the decision of a task in view has basic value.

The finite element method is widely used in calculations of chamber developments and now is the basic at designing practically all large underground constructions. High universality of finite element method demands creation of professional software products.

In the geomechanical world among leaders there is program "Z_SOIL.PC", delivered by the Swiss firm ZACE Ltd, realizing a finite element method. This program allows taking into account all geological conditions of a rock or soil mass, a stage of development and erection of an underground construction. It was the basic at a choice of the software for carrying out of numerical modeling in this work.

Geographical information system is a modern computer technology for creation of maps and the analysis of objects of the real world, and also occurring events.

Rough distribution of GIS technologies has led to that today in the market of this technologies operates already more than 150 organizations and the firms developing and distributing software GIS. There are among them large and finer firms. By technical opportunities GIS of large firms much more win against fine firms. As optimization of systems of monitoring needs all spectrums of capacities of GIS it is necessary to take advantage of software product of a large firm. As software GIS as the most suitable to operating conditions the product of ESRI (Canada) "ArcMAP" has been chosen from all variety GIS.

3 STAGES AND STEPS OF GEOMECHANICAL MONITORING

Monitoring in this work is understood as all complex of research and the control of a rock mass over a design stage, constructions and operation of a complex of underground constructions. All geomechanical monitoring can be divided into four stages.

The first stage of monitoring includes the researches spent for a rock mass at a stage of geological researches. The second stage of

monitoring begins on a design stage of an underground construction. The third stage of monitoring carries out at construction of an underground construction. The fourth stage of monitoring begins from the moment of the ending of construction of an underground construction and input of a construction in operation.

Each stage of monitoring shares on the certain steps.

Steps in the first stage:

1) Revealing block structure of a mass, an arrangement, capacity and feature of a structure of layers of the geological blocks; revealing of active zones of explosive infringements; an establishment of all laws of deformation of a mass in view of a geological structure.

2) An estimation of an intense condition and deformations in a mass and in zones of tectonic infringements and their changes in time; definition of dangerous sites of a mass, which infringement of balance is possible at the given mode of deformation.

3) The forecast of the future motions of blocks, formation new and display of already available infringements in a mass under action of natural and artificial factors.

Steps in the second stage:

1) Specification of block structure of a mass; arrangements, capacities and features of a structure of layers of the geological blocks; detailed consideration of active zones of explosive infringements.

2) Modeling is intense - deformed conditions of a mass and work of a underground construction in a surrounding mass at constant updating the information.

3) The forecast of motions of blocks, formation new and display of already available infringements in a mass under action of natural and artificial factors by means of mathematical modeling.

Steps in the third stage:

1) Specification of characteristics of cracks by their detailed research; revealing of errors in the previous researches in an estimation of quality of breeds by visual supervision, a radar and seismic tomography, drilling of chinks;

2) Measurements of pressure in a mass consistently methods of unloading and indemnification of pressure, on distance from a contour - a method "Doorstopper"; installation, on the same directions, multidot rock extensometer for the control of displacement of a contour of the chamber over development of the chamber; measurement of size of the module of deformation and factor Poisson of breed - as on cores, and is direct in a mass; hydrodynamic researches; the control of seismic activity of a rock mass.

In the fourth stage of precise steps does not exist because this stage consists in the constant control over a condition of a surrounding mass and a construction. This stage of monitoring lasts all period of existence of a construction.

Simultaneously with the beginning of the first stage of monitoring the project in GIS with a database where at each stage the corresponding information will be worn out is created.

4 TECHNIQUE ON OPTIMIZATION OF GEOMECHANICAL MONITORING

In Figure 1 the flowsheet of the developed technique of optimization is submitted.

At the beginning of each construction, studying geological features of a place of prospective construction serves. At this time spend numerous researches geological maps of a site and also spend new geological researches of a missing material. On the basis of laboratory researches obtain the geomechanical data on a rock.

All received geological data are displayed in GIS. To each layer GIS there corresponds a layer of rock mass, topography, the rivers, etc. These layers are represented in Figure 2.

After the preliminary engineering analysis of the received geological data, the first representations about an opportunity of construction on this place of an underground construction are formed. Further it is necessary, on the basis of the initial data, to lead preliminary numerical modeling.

First it is necessary to choose model of a schematization of a rock mass. For numerical

experiment as it has been written in §2, the method of final elements was applied. After reception of results lead initial numerical modeling it is necessary to make design decisions for final modeling.

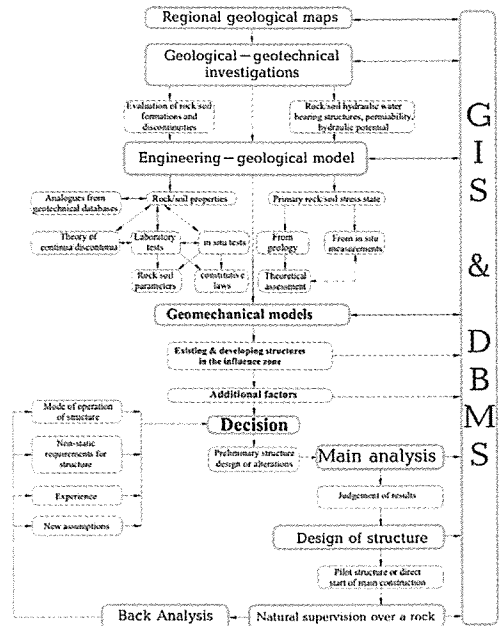


Figure 1. The flowsheet of optimization of geomechanical monitoring.

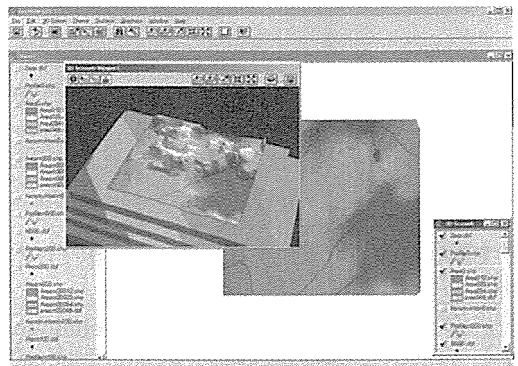


Figure 2. Display of geology and topography layers in GIS.

The main numerical modeling of a underground construction and rock mass is spent in 3D to statement. Underground developments fixed in geographical

coordinates in corresponding layer GIS. After modeling all received results are displayed in GIS on the fixed underground construction.

On the basis of all received data designing and construction of an underground construction begins.

At designing analyze the lead numerical modeling and beforehand fix in project GIS control points arrangement of geomechanical devices. Control points fix those places in a rock mass and an underground construction where the big settlement sizes of displacement and pressure are observed. Other points where sizes of displacement and pressure less dangerous, remain reserve. It means, that devices in these points do not put, and in a case if at construction of a construction the new geomechanical information will appear, it is necessary to pay to these places the most steadfast attention. GIS, in this case, is the tool for visualization of the project and its details.

During construction passes constant supervision over a rock mass in control points, and also various geomechanical experiments. All this information fills up geomechanical databases of project GIS. For the certain accounting period (hours, days, weeks) the information on control points is analyzed and the certain engineering decision makes.

In a case if new geological, geomechanical or other data have appeared is necessary to correct the project and to make new design decisions, a new to lead numerical modeling and to display all received changes in GIS and DBMS. So can take place many times.

5 PRACTICAL APPLICATION OF THE SUGGESTED TECHNIQUE

For an illustration of the suggested technique on optimization of geomechanical monitoring the underground construction consisting of two parallel chambers and a transport tunnel. Chambers and the tunnel have the size of 20x20 meters and length 11 meters.

The choice of model of a schematization of a rock mass and underground construction

has fallen on Hoek-Brown criterion since it is most applicable both for not broken samples of breed, and for cracks rock mass. For not broken breeds this criterion gives a ratio of strength on a stretching and compression within the limits of 1/7-1/25, that more corresponds to the validity.

For this purpose between modules a series of numerical experiments has been lead. The size rock made 5, 10, 20 and 30 meters. By results of modeling the conclusion that the size rock should be 20 meters (figure 3) because displacement in rock has been made have made 2mm. Reduction of the size rock conducts to its deformation (figure 4), displacement in rock have made 15mm, and the subsequent destruction. The increase in the sizes rock is economically inexpedient.

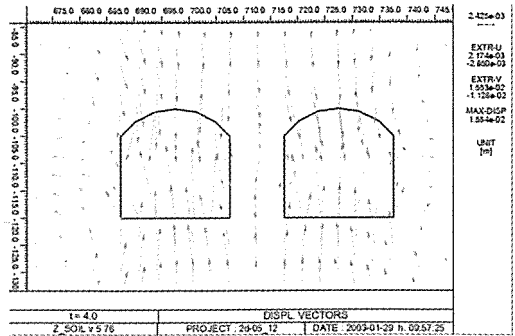


Figure 3. Displacement at the size of a rock 10m.

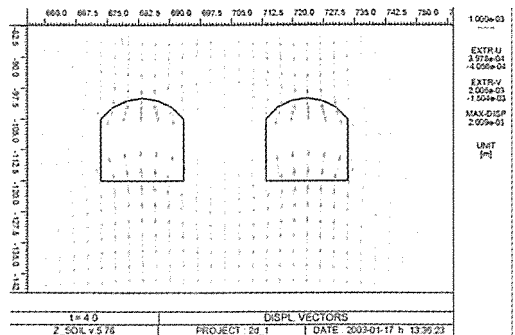


Figure 4. Displacement at the size of a rock 20m.

Further it is necessary to investigate laws of distribution of displacement in a mass at

various combinations of natural pressure and displacement in a rock mass. It is necessary for revealing of the most dangerous, to work of an underground construction, a combination of natural pressure and displacement. In figure 5 the settlement circuit for numerical modeling are represented.

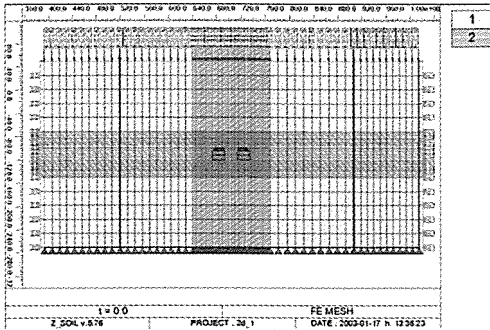


Figure 5. The settlement circuit of numerical modeling of natural pressure and displacement.

For carrying out of numerical experiment in this circuit researched underground chambers, a rock mass with large cracks are reflected and various variants of natural pressure are simulated. Cracks were modeled as a thin strip of final elements with the properties, and natural pressure is replaced with in regular intervals distributed loading. The result of the lead modeling is submitted in Figure 6.

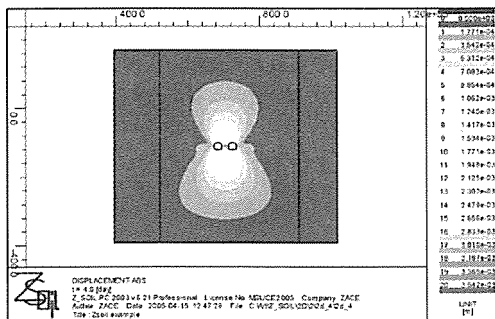


Figure 6. Numerical modeling of the natural intense and deformed condition of a rock mass.

Basing on the received most dangerous distributions of natural displacement and pressure in a rock mass the settlement circuit in 3D statement has been constructed (figure7). Model of a schematization of a rock mass - Hoek-Brown criterion.

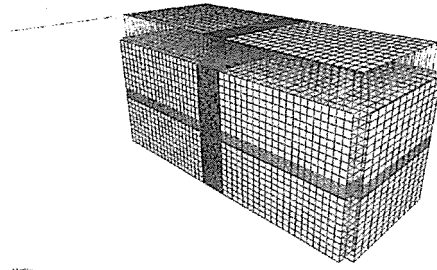


Figure 7. The settlement circuit of numerical modeling of the project of an underground construction in 3D statement.

In parallel with numerical modeling the project in GIS which contained topography and all layers of a rock mass (figure 8) has been made. Also the geographical position of chambers has been fixed.

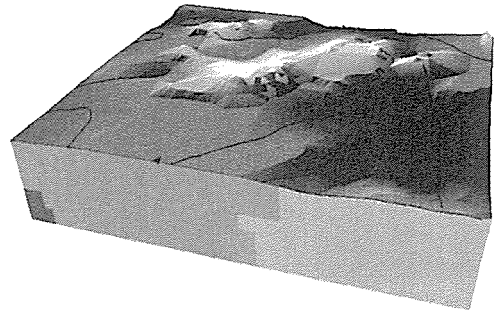
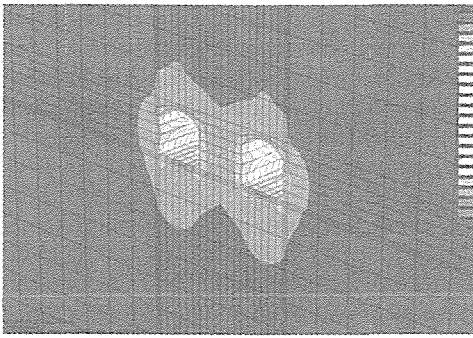
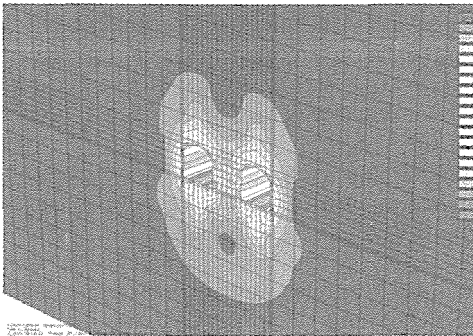


Figure 8. The project in GIS.

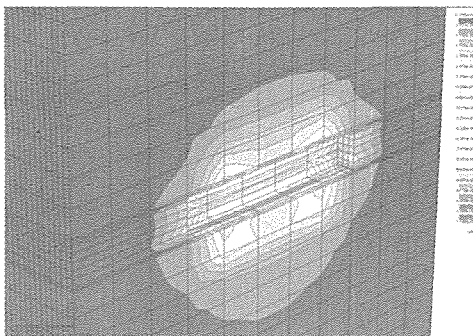
As a result of the lead three-dimensional numerical modeling displacement and pressure in a rock mass have been received. In figure 9 it is shown a part of the received results in various planes. All received results have been fastening in GIS.



a) Displacement to the beginning of chambers



b) Displacement to the middle of chambers



c) Displacement along the middle of chambers

Figure 9. Displacement in the rock mass.

The analysis of results of three-dimensional modeling has shown, that the zone of influence from considered chambers is distributed no more, than to 70 meters on axis Y, on 18-20 meters on an axis X and on axis Z on 15 meters deep into a mass. The maximal displacement in a rock mass are

fixed on distance of 22 meters from each face wall of chambers, thus the maximal zone of influence on a rock mass will be in the middle of chambers. This analysis of results of calculation gives the basis fixing control points of monitoring in project GIS and in corresponding databases. In these control points will be established multidot extensometer optimum length (Figure 10).

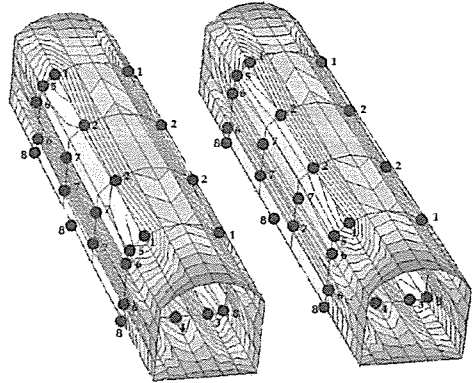


Figure 10. Fastening of results of modeling by control points in project GIS.

The first control point «1» settles down on the arch, on distance 3.33 meters from each of walls chamber and on distance 22 meters from an end face of chambers. Installation extensometers should be made on depth up to 20 meters. The second control point «2» settles down also on the arch, on distance 3.33 meters from each of walls chamber and on distance in section 44 and 66 meters from an end face of chambers. On the same distances, i.e. 3.33 meters from each of walls chamber and on distance in section 22, 44 and 66 meters from an end face of chambers, it is necessary to provide a third control point «3» in a floor chamber and the fourth point «4» in the center of a tray. The fifth control point «5» is at the end of the arch on distance 22 meters from an end face of chambers. The length of researches deep into does not exceed a mass 25 meters. The sixth control point «6» networks of monitoring is located on distance 5 meters downwards from the

end of the arch and 5 m upwards from a floor chamber in section 22 meters from an end face chamber. The seventh control point «7» is located on walls in sections 44 and 66 meters on distance of 5 meters from the center of a rock mass between chambers upwards and downwards. The eighth control point «8» is located at the very bottom of each of walls chamber. On each wall of the chamber is on three points: two distance 22 meters from each end face of the chamber and in the middle of a wall.

In Figure 11 the circuit of optimum arrangement extensometers in control points on length is shown.

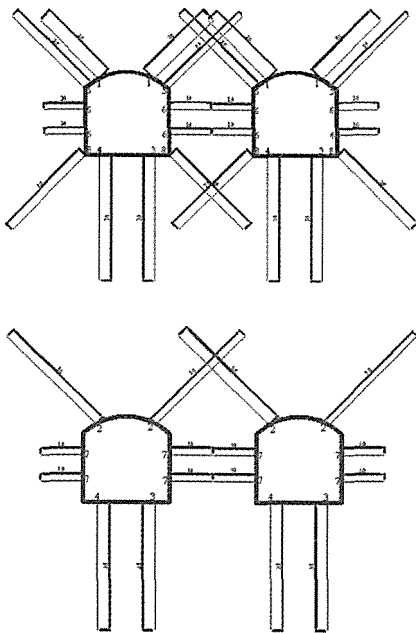


Figure 11. The circuit of optimization of system of geomechanical monitoring.

As has shown the analysis of the lead three-dimensional numerical modeling of underground chambers in a surrounding rock mass in preliminary fastening working control points it is necessary to be limited to these of eight. Other points, where as a result of the lead numerical calculation it is not required arrangements extensometers, should

remain inhibited with the initial data. When during designing or construction of underground object there will be a updating by new geomechanical, geological or other information it is necessary to make new modeling in three-dimensional statement with the updated data and to fill up a databank with this geomechanical information. And on the following step it is necessary to update the data in the project in GIS and in a database.

Further, after the analysis of the received information, it is necessary to lead optimum arrangement extensometers in those points where it is necessary, and fastening of these control points as workers in the event that, till this moment, these points have been inhibited. If these points were workers they and remain workers, but in their database will wear out the new information. And so there is each time when appears, during the designing, the new information. All fastenings of points and arrangement extensometers occur only in the project, but not in a mass. Final arrangement extensometers in a mass and fastening of control points in the combined project in GIS will be made only at the latest stage when the basic manufacture of underground works will be finished.

Further the developed system of monitoring continues to work while in service underground chambers. All geomechanical information received by numerical modeling, serve as the standard. The data with established extensometers periodically act in a database and in case of need make updating system of monitoring.

6 CONCLUSION

Summing up to all work it is necessary to tell that this work is attempt in common to apply modern computer methods (numerical modeling and geographical information systems) to optimization of system of geomechanical monitoring. On the basis of joint application of two computer methods it was necessary to create a technique on an optimum arrangement of the measuring equipment.

If to make short endurance of all written above, essence of the offered technique following. At the available data on geology numerical modeling and creation of the project in GIS is carried out. On the basis of results of the lead modeling arrangement, on a paper, instead of on a ready construction, the measuring equipment is carried out. The project in GIS allows visualizing the project for convenience and speed of work.

At occurrence of new geological or other data new numerical modeling and new arrangement of devices on a paper is carried out. All these data will be worn out in project GIS and on each control point it is possible to learn, that occurred to the given place in a rock mass or a construction from the moment of the first modeling till the moment when in this place it is possible to lead natural supervision. Then, by results of the analysis, it is possible to draw a conclusion on that it is necessary or it is not necessary to put the device in this place. And during all term of operation of a underground construction in project GIS the information on each control point will accumulate, and the initial information will serve reference, that will allow to make in due time the engineering decision and to not admit failure.

But all this technique is fair for an underground construction located in a rock mass. For soil this technique was not checked. It will be continuation of this scientific work.

REFERENCES

- Potapov A.D., Man'ko A.V., 2006. Method of optimization of systems of geomechanical monitoring in underground construction (in Russian), *Building materials, the equipment, technologies of XXI century*, volume 4, pp.78-80.
- Man'ko A.V., MSUCE & SPbSTU (ed.), 2002. Geographical information systems in tasks of geomechanics (in Russian), *The interuniversity collection of proceedings on hydraulic engineering and special construction*, Zertsalov M.G., Alhimenko A.I. (eds.), pp.161-166.
- Postolskaya O.K., Man'ko A.V., Jarosch M., Universität Siegen (ed), 2001. Information system for large projects in rock engineering, *Siegener symposium «Messtechnik im Erd- und Grundbau»*, Herrmann A. (eds.), pp.234-241.

Investigation of Jet Grouting Effect on Slope Stability- A Case Study at the Shahriar Dam, Iran

B. Nikbakhtan, Y. Pourrahimian & H. Aghababaei

Faculty of Mining Engineering, Sahand University of Technology, Tabriz, Iran

ABSTRACT Shahriar dam is a double-curvature concrete arch dam which is under construction near the town of Mianeh in northwest of Iran. The alluvial sediments in the riverbed of the dam are underlain by low-strength clay, and therefore, are likely to cause slope failures. In this paper, an effort has been made to focus on effect of jet grouting to avoid slope failure during excavation and construction of a retaining structure. Finally, the paper concludes with presenting the differences between strength properties of riverbed's clay before and after jet grouting and operation of jet grouting on slope stability.

1 INTRODUCTION

Foundation of the Main Dam requires excavation of the alluvial deposits down to competent bedrock. The average ground elevation of the alluvial plain is about 975 masl. The elevation of the bedrock at its deepest point is about Elev. 920 masl. Hence, about 55 m of alluvium have to be excavated at the deepest section of the valley. Excavation of approximately 55 m deep alluvium is not possible without some strengthening and support measures. The reasons for these measures are the presence of a basal clay layer with relatively low shear strength and the limited space between the upstream cofferdam and the Main Dam requiring relatively steep excavation slopes.

Basically, there are two approaches to ensure the stability of an excavation pit, namely:

1. Strengthening the soil either by mixing it with some material (lime, cement) to increase its shear strength (mainly its cohesion component) or reinforce it with some mechanical device (e.g. net, grid, strips, etc.), mainly to increase the friction angle.

2. Supporting the potentially unstable mass of earth materials by engineered structures, such as retaining walls with or without anchoring.

Often a combination of these two approaches is used to reach the most economic solution.

A value engineering approach was performed on the upstream slope of the Main Dam excavation to compare various alternatives. These were:

1. Constructing a multi-arch diaphragm wall.
2. Reinforcing the soil (both clay and coarse-grained alluvium) by jet grout columns and construction of a low gravity retaining wall.
3. Construction of a buttress-type retaining wall.

Value engineering revealed that soil reinforcement by jet grouting together with a retaining wall at the toe of the excavation slope yields the most economic solution and would also pose the least uncertainties in execution.

Jet grouting is a new method of soil improvement in Iran and there are no data

from local construction. It is, therefore, important that field trials are performed at the Shahriar site before the excavation design is finalized. For the design of the excavation, it is necessary to know the characteristics of the grout columns, mainly their diameter and the strength of the soilcrete. If these data are not known and have to be estimated based on information found in literature, the design will be conservative. If the jet grout columns can be checked and tested, the data obtained will allow an optimization of the layout of the grid and considerable savings in construction cost are possible. Therefore, the jetting parameters and the results achieved from a trial test are described and commented. Design parameters for stability analyses are then derived.

In this paper, after a few principles of jet grouting, the stages of excavation to follow are presented. These stages are the result of optimizing the stabilization needs while ensuring sufficient safety of the slope during the entire excavation process. Stabilization of the excavation slopes is by strengthening the clay stratum by a grid of soilcrete columns and by providing a gravity retaining structure at the foot of the excavation slope. Some strengthening of the coarse-grained alluvium by soilcrete columns is also required.

The methods of analysis used for investigating the stability of the excavation slopes are presented together with the most significant results. The analyses were performed for both two-dimensional and a three-dimensional configurations of instability. This was necessary because of the topographical conditions at the dam site. The narrow gorge has a strong restraining effect on potential sliding bodies. This effect can be realistically modeled only in a three-dimensional configuration. Two-dimensional models yield factors of safety which are too pessimistic.

2 PRINCIPLES OF JET GROUTING

The jet grouting method is frequently used as a mean for ground improvement, especially in shield tunneling, and also in all sorts of

foundation treatment in recent years (Yoshitake et al., 2004).

Jet grouting involves the injection of grout at high pressures into the ground. The high velocity jet erodes the soil and replaces some or all of it with grout.

Jet grouting starts with drilling a borehole, usually 100 to 150 mm in diameter to the required lower end of the section to be treated. After completion of drilling, the jetting pipes (or monitor) are inserted into this hole. The next step consists of applying a jet emitted from a nozzle under very high pressure to erode the soil adjacent to the borehole wall. This process enables the slurry to penetrate the soil adjacent to borehole and mix with it (Fig. 1).

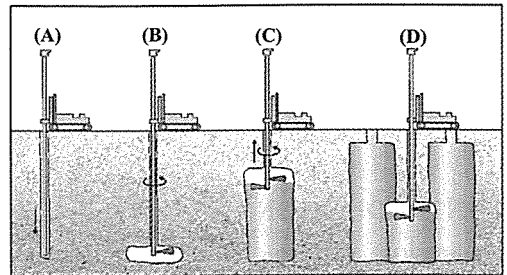


Figure 1. Sequence of jet grouting method: (A) drilling, (B) jetting test, (C) jetting, forming a column, (D): completion.

Jet grouting systems are classified into three types depending on the delivery mechanism (Fig. 2). In a single-rod system, the fluid injected is grout. This system is used mainly for horizontal jet-grouting, for example, in tunnel support systems. In a double-rod system, grout and compressed air are injected. The combined effect of the high-pressure grout and air results in a greater percentage of soil being removed and replaced with grout, and the remaining soil-grout mixture is called soilcrete. In a triple-rod system, grout, air, and water are jetted. This triple combination enables an even higher percentage of soil to be removed, and the system can be used for almost complete replacement of the soil with grout. The triple-rod system offers better control over injection rates and results in better quality of

soilcrete. Although the single- and double-rod systems can be used in loose sandy soils, the triple-rod system can be used in most types of soil (Nonveiller, 1989; Kaushinger et al., 1992a,b; Covil & Skinner, 1992; Bell, 1993; Xanthakos et al., 1994; Bergado et al., 1996; Schalfer, 1997; Poh & Wong, 2001; Warner, 2004).

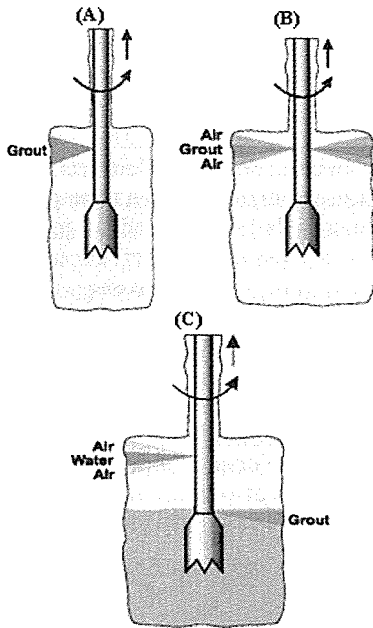


Figure 2. Three basic systems of jet grouting, (A): single fluid, (B): double fluid, (C): triple fluid.

3 EXCAVATION STAGES

The excavation stages at Shahriar dam have been divided into five stages. These stages are as follows.

Stage 1. (Excavation to elevation 955.00 masl): Construction of a soilcrete curtain consisting of two rows of jet-grouted columns. Column spacing is 1.25 m and row spacing is 0.50 m. This curtain is constructed from an elevation of 955.00 masl by drilling first to the top of the clay stratum and then inserting the jet grouting monitor and drill down to bedrock. This second section is then jet grouted by lifting the monitor at the selected withdrawal rate. Grouting is

continued beyond the top of the clay to about elevation 938.00 masl, i.e. about 3 m into the coarse-grained alluvium. In the absence of an artesian pressure, a penetration of about 1 m into the coarse-grained alluvium is sufficient. Subsequently, the clay is jet-grouted as far as row G' with column spacing of 2.5 m (Fig. 3). Starting from row G' jet grouting starts from elevation 952.5 masl in the coarse-grained alluvium. This elevation is reduced continuously to elevation 947 masl when row j' has been reached.

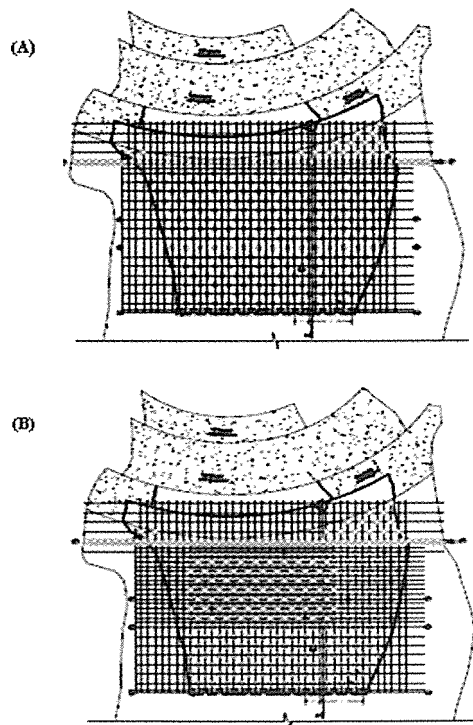


Figure 3. Arrangement of soilcrete columns, (A) in coarse grained alluvium, (B) in basal clay layer.

Stage 2. (Excavation to elevation 947.00 masl): Jet-grouting of coarse grained alluvium and clay continues starting from elevation 947.00 masl and reducing to elevation 942.00 masl when row P' has been reached with column spacing of 2.5 m. Within a 25 m wide and 8.75 m long area in the central part of the grout-treated field the clay is reinforced with a spacing of 1.25 m.

at row P' a second curtain is constructed with a column spacing of 1.25 m and a row spacing of 0.5 m. The tow curtains are designed to reduce the water flow into the excavation and to lower the piezometric head elevation in the toe area of the excavation where the stability is most critical. They are designed to withstand the hydrostatic pressure. This pressure could be substantial if the cutoff wall is not tight. If along the lateral periphery of the area with 1.25 m spacing no clay can be found between the coarse-grained alluvium and the rock, a spacing of the soilcrete columns of 2.5 m is considered sufficient.

Stage 3. (Excavation to elevation 942.00 masl): Construction of the first approximately 5 m wide lamella of a curved retaining wall. First, a trench is excavated in the coarse-grained alluvium to about elevation 934.00 masl (about 1 m below the top of the clay layer) and filled with conventional concrete. Embedded in this concrete are tubes of sufficient diameter with spacing of 1.25 m. After hardening of the concrete, the jet grouting monitor is inserted into these tubes and the clay below the concrete is grouted.

Stage 4. (Excavation to elevation 936.00 masl): Construction of the second 5 m wide lamella of the retaining wall. First a trench adjacent to the first lamella is excavated in the coarse-grained alluvium to about elevation 928.00 masl and filled with concrete. Again tubes with spacing 1.25 m are embedded in this concrete wall that will allow the insertion. In the next step the clay is grouted from the bedrock to elevation 928.00 masl. Finally, in a fourth step formwork is installed for pouring another layer of concrete blocks between elevation 936 to 942 masl.

Stage 5. (Excavation to elevation 930.00 masl): Construction of lamellas 3, 4 and 5, each one about 5 m wide. First, lamella 3 is cast in two steps, namely first from elev. 920 to 930 masl and then from elev. 930 to 938 masl. Lamella 4 is produced in the same way as lamella 3. Finally, lamella 5 concludes the build up of the gravity retaining wall. It is placed between elevations 920 and 930 masl.

The retaining wall is an essential element in the stabilizing system to ensure stability of the slope. Its stabilizing effect is based purely on weight. The design of this wall was governed by the equipment available and the constructability in general.

4 ANALYSIS

4.1 Assessment of design parameters

As pointed out in trial jet-grouting, the assumptions made for the strength of soilcrete were too optimistic and realistic parameters have to be estimated based on the values obtained from the field trial and from an extended literature search. The parameters of the materials not affected by jet grouting treatment are assumed to remain unchanged. For estimating the average strength parameters of the treated basal clay, the following procedure was adopted (Barksdale & Bachus, 1983).

Consider a triangular pattern of soilcrete columns with spacing *S*. The diameter of the columns is *D*. For a triangular unit cell, the area replacement ratio, *a_s*, is defined as Figure 4 and it is calculated from Equation 1.

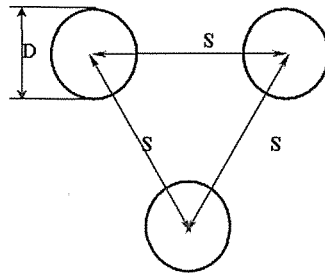


Figure 4. Triangular pattern for soilcrete columns.

$$a_s = \frac{\Pi}{2\sqrt{3}} \left(\frac{D^2}{S^2} \right) = 0.91 \left(\frac{D^2}{S^2} \right) \quad (1)$$

Based on the data obtained at the test site and from the review of published data of jet grouting in soft to stiff clay, the column diameter was assumed as *D* = 1.0 m. Then for a column with spacing 1.25 and 2.5 the

area replacement ratio were 0.58 and 0.15, respectively. The average cohesion, C_{av} , is calculated from Equation 2.

$$C_{av} = \frac{A_C \cdot C_{Cav} + A_S \cdot C_{Soilcrete}}{A_C + A_S} \quad (2)$$

The average friction angle can be obtained from Equation 3.

$$\tan \varphi_{av} = \alpha_S \cdot \tan \varphi_S \quad (3)$$

For the analysis the following values were used. for the soil parameters, based on a weighted average of the meager test data:

$$C_{soilcrete} = 500 \text{ kPa} \ \& \ \varphi_S = 25 \text{ degrees}$$

The untreated clay is assumed to have cohesion of 40 kPa and zero friction angle as assumed in previous stability analyses. It is, however, possible that jet grouting may disturb the clay to some extent. Because the clay is somewhat sensitive, the average strength of the untreated but disturbed clay area may be less than 40 kPa. Table 1 shows the results of calculations for columns with different spacing based on equations 2 and 3.

Table 1. The values of average friction angle and average cohesion for columns with different spacing.

Table 2. Material properties assumed in analyses

Material No.	Material type	Unit Weight (kN/m ³)	Cohesion (kN/m ²)	Friction angle (deg.)	Jet grouting with triangular pattern, spacing
1	Clay core of cofferdam	18	25	25	-----
2	Rock fill of cofferdam shell	22	0	45	-----
3	Coarse-grained alluvium	21	0	35	-----
4	Basal clay	17	40	0	-----
5	Basal crushed layer	17	40	0	-----
6	Treated basal clay 1	16	80	4	S=2.5 m
7	Treated basal crushed layer 1	16	80	4	S=2.5 m
8	Treated coarse-grained alluvium	22	200	35	S=2.5 m
9	Treated basal clay 2	22	300	15	S=1.25 m in central part & S=2.5 m in peripheral parts
10	Treated basal crushed layer 2	22	300	15	S=1.25 m in central part & S=2.5 m in peripheral parts
11	Retaining wall	24	100	40	-----

Spacing	c_{av} (KPa)	φ_{av} (deg.)
1.25	307	15.0
2.5	80.8	4.0

The geological model used for the stability analysis comprised 11 material zones. These are defined in Figure 5. The parameters of the geomaterials of the 11 zones are listed in Table 2. The basal crushed layer below the basal clay is not presents everywhere. The clay can be in direct contact with the fissured rock. For the stability calculations it has been assumed that with high artesian pressures the strength of this material would not be higher than that of the clay.

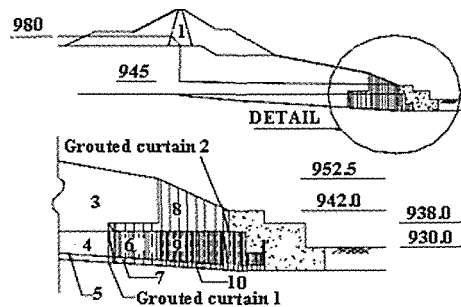


Figure 5. Material zones in the treatment area used in the stability analysis (The numbers refer to Table 2).

Hence Zone 5 was given the same values as the clay although the crushed layer is not likely to have any cohesion. The influence of Zone 5 on the stability of the slope is, however, insignificant.

The groundwater table in the sections analyzed was assumed to be at an elevation of 980 masl upstream of the cutoff wall. It was then postulated that the cutoff wall would be sufficiently efficient to lower the water table to elevation 945 masl.

From that elevation, on the downstream side of the cutoff wall, a linear decrease of the phreatic line to the current elevation of the excavation was assumed.

4.2 METHOD OF ANALYSIS

The computer code CLARA-W was used to analyze the stability of the various stages of excavation (Hungry et al., 1989; Lam & Fredlund, 1993). It is particularly suited for cases involving narrow and irregular slope surfaces, circular slides, and failures situated between lateral constraints. The sliding body is divided into columnar elements, similar to the slices in the 2-D configuration. The solution algorithm for Spencer and Morgenstern-Price assumes that the resultant of the interslice forces on the vertical faces of the columnar elements is parallel to the base of the column. The relationship between the vertical shear forces and the horizontal normal forces is expressed by an interslice force function. When the program operates at its 2-D mode, the equations revert to the well-known Bishop, Janbu, Spencer and Morgenstern-Price methods. In fact, when the axis perpendicular to the movement is extended the factor of safety approaches that of the 2-D failure mode.

For the analysis of the excavation slope of the Shahriar project ellipsoidal surface (this type of surface gave the lowest factor of safety) and simplified Bishop Limit analysis model were selected.

The layout of the area considered for sliding and the locations of the 21 sections used for the 3-D model are shown in Figure 6.

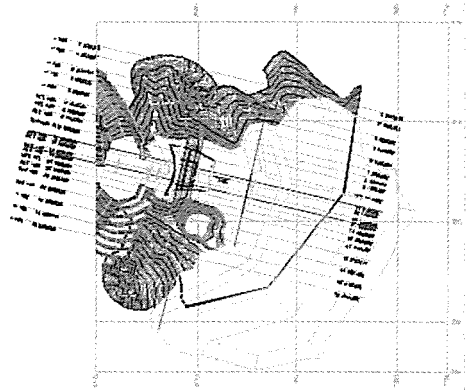


Figure 6. Sections used in the 3-D stability analysis.

4.3 RESULTS OF STABILITY ANALYSES

The results of the stability analyses are summarized in Tables 2 and 3 for the five construction stages. For each stage two failure scenarios were investigated, namely:

1. Failure through the cofferdam
2. Failure through the excavation slope below the cofferdam.

Each failure scenario was then analyzed for the 2-D configuration and for the 3-D case once under static conditions (no earthquake) and once pseudo-statically with seismic coefficients of 0.05 and 0.10 (corresponding to the construction level earthquake).

Hence, altogether 45 different factors of safety (FOS) were calculated. The failure surfaces obtained with the 3-D model are shown in the last column of Table 3. The columns second to the last illustrate the range of failure surfaces considered in the most critical (usually the maximum) section.

Figure 7 shows an enlargement of the last stage, i.e. the operating stage with the failure surface ending at the top of the retaining wall. This is the most critical case with FOS = 2.31. Also visible in this figure are the material zones used for the analysis and listed in Table 2.

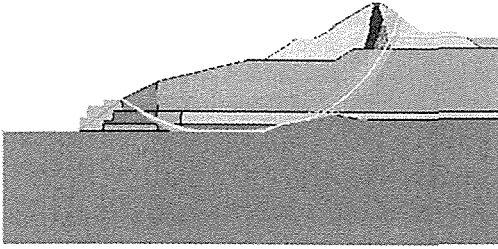


Figure 7. Failure surface from 3-D analysis of operating stage.



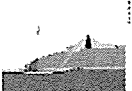



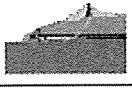

Table 3 shows the factors of safety calculated for the 21 sections used for the 3-D analysis with CLARA-W corresponding to the operating stage. However, these FOS were obtained from a 2-D analysis along each of the 21 sections. These calculations were



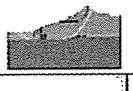



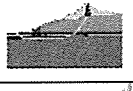

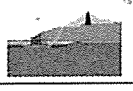

performed to illustrate the variation of the FOS with the position of the section considered. The FOS is also shown in Figure 5. It can be seen that only the central sections are critical, i.e. Sections 11 to 15 with $FOS_{min} = 1.19$ (1.18 in Table 4). In the remaining sections sliding is kinematically impeded by topographical obstructions or constraints. In fact, for some sections at the periphery of the sliding mass considered the program does not even calculate a FOS, e.g. Sections 1 to 5 and 19 to 21. This means that these sections are beyond the limits of any potential sliding body that could develop on the slope. The second and sixth columns of Table 3 give the distance of the section from Section 1. Sections 9 and 10 almost coincide and only one calculation was performed.

Table 3. 2-D factor of safety of each section along the 21 section considered in 3-D analysis with CLARA-W.

SECTION NO.	DISTANCE FROM SECTION 1	SAFETY FACTOR	FAILURE SURFACE	SECTION NO.	DISTANCE FROM SECTION 1	SAFETY FACTOR	FAILURE SURFACE
1	0.0	-		12	101.16	1.19	
2	10.0	-		13	110.0	1.19	
3	25.0	-		14	114.0	1.21	
4	35.0	-		15	120.5	1.48	
5	47.5	-		16	127.75	1.73	
6	60.0	1.56		17	135.0	2.18	
7	67.5	2.26		18	147.5	2.09	
8	75.0	2.35		19	160.0	-	
9&10	85.0	2.41		20	172.5	-	
11	97.0	1.19		21	185.0	-	

Table 4. 3-D failure surfaces and factors of safety obtained for the four construction stages using the CLARA-W program.

Stage no.	Factor of safety not considering earthquake loading		Factor of safety with earthquake loading of			Shape of failure	
	3D	2D	0.05 g	0.1g	0.05 g	Range of failure surface calculated. The most critical failure surface is shown as a thin yellow line.	3D failure surface
						Max Failure surface	
Stage 4	2.08	1.08	1.80	1.59	0.92		
	2.33	1.39	1.99	1.74	1.18		
	2.56	1.26	2.24	1.99	1.12		
Operation Stage	2.31	1.18	2.00	1.76	0.98		

Stage no.	Factor of safety not considering earthquake loading		Factor of safety with earthquake loading of			Shape of failure	
	3D	2D	0.05 g	0.1g	0.05 g	Range of failure surface calculated. The most critical failure surface is shown as a thin yellow line.	3D failure surface
Stage 1	2.59	1.12	2.18	1.87	1.32		
	2.10	1.08	1.80	1.57	0.90		
Stage 2	2.44	1.37	2.03	1.75	1.14		
	2.02	1.04	1.74	1.52	0.88		
Stage 3	2.11	1.33	1.79	1.54	1.12		

5 CONCLUSION

From the stability analyses, the following results can be inferred.

1. The criteria for acceptable stability were to require for the 2-D case a factor of safety of at least 1.05 for static conditions and 0.90 for pseudo-static conditions. The reasons for these criteria are as follow:

a) In the usual 2-D stability analysis the factor of safety for static conditions is usually taken as 1.50. For temporary construction states it may also be lower, for example 1.30. The FOS for pseudo-static conditions should not be less than 0.90.

b) Extending the analysis to a 3-D configuration increases the FOS substantially. This is because the FOS varies for the different sections used in the 3-D model, as demonstrated in Figure 6 and Table 3. The lowest values of FOS are obtained in the central part, whereas in the wing parts of the sliding mass considered the FOS is much higher. Consequently, the

overall 3-D FOS is higher than the 2-D value. The difference between the two values depends on the configuration of the footprint of the sliding mass and on the shape of the sliding surface along a particular section. A hunch in the sliding surface will act as a barrier which the slide has to surpass which is met by increased resisting forces. Also, in the wing parts of the slide the clay layer may no longer be present.

c) Like all mathematical model, the 3-D model used by the CLARA-W will have some deficiencies, i.e. it cannot model all the factors affecting the stability of the potential sliding mass. It will, therefore, not yield an answer completely in agreement with what is going on in the actual case. Engineering judgment may not consider it wise to rely fully on the values obtained from the 3-D model. However, the high values obtained with the 3-D model indicate that the FOS calculated by the 2-D model can safely be increased by a certain percentage, say by

about 30 to 40 percent. In doing so, the values obtained from the 2-D analysis reach the range of acceptable factors of safety, both for static and pseudo-static conditions.

2. The stages shown in Table 3 always present the most critical situation at that particular stage, i.e. the condition after excavation to that particular elevation but without considering the effect of the treatment given from that elevation.

Stage 1 represents the stability when the excavation has reached elevation 955 masl prior to treatment of the clay layer.

Stage 2 represents the stability after excavation has proceeded to elevation 947 masl with the treatment received from elevation 955.

Stage 3 represents the stability after excavation to elevation 942 masl but before constructing the first lamella of retaining wall.

Stage 4 represents the stability after having excavated to elevation 936 masl but before construction of the second lamella.

Stage 5 represents the stability after having excavated to elevation 930 masl but before installing lamellae 3, 4 and 5.

The operation stage, finally, gives the factor of safety after the retaining wall has been completed and the excavation has reached the bedrock at about elevation 920 masl.

It can be seen from Table 3 that the requirements regarding stability in the 2-D configuration are essentially satisfied. The proposed procedure for the excavation of the coarse-grained alluvium and the clay should therefore provide sufficient safety.

REFERENCES

Barksdale, R.D. & Bachus, R.C. 1983. Design and Construction of Stone Columns. *Report No. FHWA/RD-83/026, Natl. Technical Information Service*, Springfield, Virginia.

Bell, F. G. 1993. *Engineering Treatment of Soil*. E & FN Spon.

Bergado, D. T., Anderson, L. K., Miura, N. & Balasubramaniam, A. S. 1996. *Soft Ground Improvement in Lowland and Other Environments*. ASCE Pub.

Covil, C. S. & Skinner A. E. 1992. Jet Grouting-a review of some of the operating parameters that form the basis of the jet grouting process. *Grouting in the Ground, Proc. of Conference Organized by the Institution of Civil Engineering and held in London on 25-26 November*: 605-628.

Hungr, O. Salgado, F.M. & Byrne, P.M. 1989. Evaluation of a three-dimensional method of slope stability analysis. *Canadian Geotechnical Journal*, 26:679-686.

Kaushinger, J. L., Hankour, R. & Perry, E. B. 1992. Method to Estimate Composition of Jet Grout Bodies. *Proc. ASCE Conf., Grouting, Soil Improvement and Geosynthetics*, Feb 25-28, New Orleans Vol. 1: 194-205.

Lam, L. and Fredlund, D.G., 1993. A general limit equilibrium model for 3-D slope stability analysis. *Canadian Geotechnical Journal*, 30:905-919.

Nonveiller, E. 1989. *Grouting in Theory and Practice*. Elsevier Pub.

Poh, T. Y. & Wong, I. H. 2001. A Field Trial of Jet Grouting in Marine Clay. *Canadian Geotech Journal* 38:338-348.

P.Brenner & J.Abed. *Technical Report, Dam Foundation, Alluvial Excavation Stability Analysis, Rep No. R.D.Dam.E1.002.a(j)*

Schalfer, V. R. 1997. *Ground Improvement, Ground Reinforcement, Ground Treatment Development 1987-1997*. Geotechnical Special Pub.69:113-129.

Warner, J.,P.E. 2004. *Practical Handbook of Grouting*. John Wiley & sons, New York.

Xanthakos, P. P., Abramson, L.W. & Bruce, D. A. 1994. *Ground Control and Improvement*. Wiley, New York.

Yoshitake, I., Nakagawa, K., Mitsui, T., Yoshikawa, T. & Ikeda, A. 2004. An evaluation method of ground improvement by jet grouting. *Tunnelling and underground space technology*, 19: 496-497.

Jappelli, R. & Marconi, N. 1997. Recommendations and prejudices in the realm of foundation engineering in Italy: A historical review. In Carlo Viggiani (ed.), *Geotechnical engineering for the preservation of monuments and historical sites; Proc. intern. symp.*, Napoli, 3-4 October 1996. Rotterdam: Balkema

Education

“Miners – Fireman” First Empire at the Beginning of the Ancient Historical Times

H. Sauku

Faculty of Geology and Mining, Tirana, Albania

ABSTRACT Using the language of Symbols and the toponomic data of different lands in Asia, Africa and Europe, are identified human movements and establishing for searching mineral materials such as ores and their probable mining.

It is observed the existing of different phases for such activities since more than 5.000 years ago, when the Anatolian Peninsula had the priority in developments and results.

It is concluded that such oriented a human activity, was a prelude for best results in all Human Civilization. It seams that, by repeating migrations of “fireman” in all the Old World, was formed an inorganizated “Empire” of ancient “Miners”.

In graphical forms, the dispersion of symbols and probable establishing of “firemen” groups are presented.

1 WITH THE LIVING RUINES OF THE FORE - ANCIENTNESS

During the developments in the mining scientific field, it was necessary to penetrate into the ruins of the past for explaining some ambiguities in word-forming and their conception. So, it was selected a way for a better knowledge of the human speaking and conception of human activities and respectively their “actors” in mining at the Old World.

The first results of such an investigation was presented in Sauku (2003a).

As a further continuity, it was the interesting for materials and tools used, in working out and thermal treatment of products (Sauku, 2003b).

In “aric” times (about 8.000 years ago), for such activities and other social communications, began to lead the “fireman” or the “first” man. So, people in migration or in stabilization, had the leader of group, the Father of the fireman, symbolized FRT. To other tribes living near

them, they gave examples for better living conditions.

2 THE STEPS TO THE SYMBOLS LANGUAGE

By informations from actual spoken languages and in combination with the data from the toponomy of the respective lands, in Asiatic and European Countries, it was compiled a paper on the “comperative” possibility to have solution in parallel using of the two sources. It was exposed at the Balkan Symposium on the historical developments of Metallurgy in Southeastern Europe (Sauku, 2004a). There, in a linguistic way, was provided the existing of a common connexion with the symbolic sounds of a pre-aric language. In this way was made clear also that: “The ancient Mining and Metallurgy preceded the Human Civilization.

Lately, the last year, were really fixed simple and composed symbolic sounds (vowels and consonants), which, in ancient past symbolized beings, objects and human

doings from the beginning of human communities, including fireman and fireman activities. That time the evolved and common language of symbols was used. It was the latest presentation at the International Symposium of Tirana in Science of Materials (Sauku, 2006). The paper is gives a vast information on mathematical treatment of the toponomic data with the graphical dispersion of symbols and their frequency in each country. This case may be, also, an evidence of the presence of different human activities and its evolution in time.

3 THE FIREMAN MIGRATIVE MOVEMENTS

3.1 The Central Hearth of the Fireman Groups

Human beings of the Fore-ancientness, with a common symbols language, were in a common establishing territory, as it seems, localized in Central Asia. Who used the fire in his movements, was more hardy and free in his movements around. Perhaps, it was for him, the Mineral World very interesting and he used the fire for breaking rocks, working stones and native metals as copper and gold. The walking near the mountains and the upper run of rivers, was also more attractive and profitable. Thus, for about 2.000 years, the areas in south of the new mountain ranges from Himalaya to the Sub-Caucasian and Anatolian territories in Asia and sub-Alpine terrains in Europe from Balkans to Pyreneys, step by step, were populated by their tribes. However, the hearth of the fireman “Empire” remained the western terrains of Persia, Sub-Caucasian, Anatolia and Balkans.

3.2 The Symbolized Sounds and its Dispersion

The speaking of all the actual people are activated different sounds, vowels and consonants in a proportion V/C under 1. (V/C < 1) The sounds used at ancient times were about 20 where the used vowels were 5. It is verified that all the vowels symbolized

the Sun (God) in his five positions at the sky, as in Figure 1. For working in groups or tribes with a leader (M,T) are symbolized PRM, FRT expressed in association with different vowels. Such combinations maybe isolated in toponomic denominations and also, in the words of the actual speaking. Toponomic data localize their operations in time, and their density in a geographical map, express the density of the operating at the respective territories. In such a way, the problem may be expressed mathematically and represented in graphical forms. The same may be done for all the symbols used in a region or in a country.

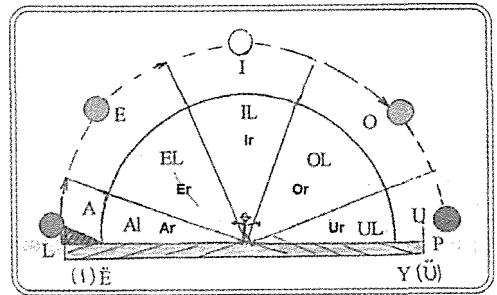


Figure 1. The symbolized vowels of the language of symbols.

3.3 The Experiments with Actual Maps Denominations

For experimenting intensions, we used the toponomic data contained in maps of a normal geographical Atlas (Atlas, 2005). The present denominations were registered at the more detailed maps of different interesting states in Asia, Europe and, partly of Africa. So, by analysing the symbols contained in all the denominations of a state or a region and its dispersion, we compiled graphical representations, expressing their structure of symbols and of combined symbols present at the respective territories. An example of the individual symbols included from the map of Turkey (central and western), is a graphical structure of symbols presented in Figure 2. For a continental global structure we have used the integral of whole the symbols contained within the 60 states of respective continents.

Toponomic Symbols Structure of Turkey

	S	VW	CS	Vowels				CONSONANTS: Simples+Compounded																					
				a	e	i	o	u	M	R	J	B	D	L	N	T	V	P	G	H	K	S	C	Ç	Z	Zh	Nj	Xh	Th
Nr	995	428	561	159	104	89	41	35	32	84	28	33	33	45	57	17	12	19	19	10	73	61	-	15	16	1	-	11	1
%	100	43	57	31.15	24.30	20.79	9.68	8.18	5.84	14.84	4.94	5.82	5.87	7.94	10.05	3.00	2.12	3.95	3.35	1.76	12.87	10.76	-	2.65	2.82	0.18	-	1.94	0.18
VW : CS = 0.75				%				%																					
Symbols				a	e	i	o	u	M	R	J	B	D	L	N	T	V	P	G	H	K	S	C	Ç	Z	Zh	Nj	Xh	Th

Conclusions: Mean symbols: A, R
 Symbols on > 10% : K, S, N
 Symbols on > 8% : L

Figure 2. The structure of symbols from maps of central and western Turkey

4 THE PRESENCE OF THE FIRST “MINERS” EMPIRE

It was an international, global observation. In this case, we observed the presence of symbol combinations FR, PR, FRT, PRM etc., in all EUROASIA and partly Africa. In a global representation with conventional signs, graphically was clear that:

It was a plane dispersion with a prolonged extension on the northern global hemisphere, from the southeast of Asia to the northwestern Europe;

The density of the signs dispersion was higher at the central part of the covered surface in signs, in southern part of Balkan and Anatolian Peninsula, Subcaucasian territories, and Western Persia (Fig.3).

It is a diminution of composed symbols FR, PR at the European western peripheral part, covered by other younger symbol-compositions. Such an evolved dispersion may be explained by the happening of different migrations in waves, in different times, where the younger compositions were as KL, KR, KLT, and KRT.

All that configuration of signs and densities testify the presence of situations evolved in time. Different configurations

connected by the nature of symbol combinations may also be compiled in more detailed maps.

4.1 How the Conceptions in Actual Speaking Bear Witness from the Past.

The priority of “mining” activity development more than 5.000 years ago, is testified by data from “Museum of Ancient Anatolia” (Il Moseo, 1997) An excessively mining and metallurgy is presented as technology and handcraft of metals (copper , bronze, and gold) about 5.000 years ago. The operations with ground and stones and the using of urbanizing criteria in buildings were also brilliantly presented before about 8.000 years ago.

Firemen, as it seems, were the “first” in buildings of “pyramids” in Egypt, migrated there from the Anatolian tribes of Pyram (SE part of actual Turkey). They were “miners” for caves of stones, preparators of rock blocks, designers, constructors and builders of the mountains of PYRAM, that means, the mountain of the Great Mother God of Prys, Miners of that time.

- in Turkish Imperatorluk, where is, also, the radical M P R

In all the denominations; we have the same ancient meaning:

“(Is of the) Great Mother’s Fireman”.

5 WITH ANOTHER SYMBOLISM THAT ARE PRESERVED IN TURKEY

If we refer to the ancient toponymy for “miners” and “mining”, we find three points of orientation which are: a) The above – mentioned PYRAM of about 6.000 years ago;

b) The Turkish denomination of the river “Eufrat”, that is FIRAT = FIR-AT, with the meaning: (It’s) of the “Miners Father”

The fore-existing denomination “FTARA” or PTARA an ancient denomination of the ruins in EUYUK, at the central part of the State of Hatti which, as a toponomic denomination, is used also in a zone of South Albania. I think that it may be also a source of future historical studies and probable linguistic connections. In an allegorical form, by this presence, is published also a book (Sauku, 2004b) titled: “The Fore – Ancientness is speaking.”

A wider interesting may have Turkish denominations connected with the metal “gold”, concepted “altın” which is symbolized by the sounds L, T, N. On the other side, with the symbols L, T, N in Turkey is a great region denominated ANATOLIA and the city named ANTALIA, with the symbol combination NTL. The respective meaning is shortly “Containers of Gold”.

The gold symbolic is really connected with the ancient consideration, that, as metal, it was the blood of God Sun (L- God, T – Father, N – Container of the life).

But human beings had also the “searcher” of the gold (KL), which was in migrative movements about 4.000 years ago at the European Continent. Such people were the Kelts symbolized as KLT. Part of them was also the return back of Phrygians at the quality of “miners” of the gold. As it is known, they were established in “Phrygia” (FRG).

So, wave by waves, human tribes and peoples continued to search their well-being till at our days.

However, at the human actual speaking, we have words as “first”, “premier”, “primo”, “prv”, “par”, which qualify the highest or the best. All their sounds have the same symbols FR and PR. I think also that “birinci”, with the symbols BR, is not so far of them.

6 CONCLUSIONS

The language of Symbols is in the role of “DNA” of the actual used languages and toponomic and hydronomic denominations and other word – forming systems from the past;

The “actors” of Mining and Metallurgy in ancient times were precursors of the Human Civilisation. By ancient peoples and tribes are qualified as the “firsts”.

The ancient “Miners” have realized a great migrative evolution from their antique domicile in Central Asia. The mean directions of their movements were determined by the orientation of the younger mountain ranges Himalaya-Caucasia-Balkanian and European Alps to Pyreneys. A part of later movements was along the mountain – ranges of North Africa;

During 6.000- 4.000 years ago was created the “first Miners Empire” of the Old World with an unorganized dispersion. The Central part of the Empire was in Persian, Subcaucasian, Anatolian and Balkanian territories.

REFERENCES

- SAUKU H., 2003a. The Ancient “Actors” of Mining- Metallurgical Beginning *Proceedings of IMCET 2003*, Ankara, Turkey.
- SAUKU H., 2003b. “Materials and products from the Ancientness of Mining and Metallurgical Beginning” *Proceedings of III Symposium on “Materials and their use”* – University of Prishtina
- SAUKU H., 2004a. “Mining and Metallurgy, precursors of the Human Civilization” *Proceedings of Symposium: Metallurgy in Southeast Europe from Ancient times to the end of XIX Century* “BUM, Bulgaria.

SAUKU H., 2004b. "FLET TEJLASHTESIA" (The Fore – Ancientness is speaking) Ed. "Arian", Tirana.

ATLAS GJEOGRAFIK I BOTES Ed "Albas", Prishtina 2005

IL MUSEO DELLE CIVILTA ANATOLICHE Ankara, Turkey, 1997

SAUKU H., 2006. Symbols Language may accelerate the solutions for determination of Ancient Mining Activity from toponomic denominations. *Proceedings of the International Symposium on "Materials and their use"*, Polytechnic University of Tirana IX.

Virtual Reality - A Toy or a New Way of Training

M. KIZIL

The University of Queensland, School of Engineering, Brisbane, Australia

ABSTRACT Virtual Reality conjures up images of fancy computer games but for the Mining Industry it is quickly becoming a major tool for improving safety and productivity. This technology is increasingly being used to shorten training times and improve its effectiveness, reduce the cost of education, reconstruct mining accident, in production and process simulations and in many hazard awareness applications.

The University of Queensland Mining group has been involved in developing Virtual Reality applications for the minerals industry in the areas of data visualisation, education and training, environmental monitoring application, accident reconstructions, simulation applications and hazard awareness applications. This paper discusses some of the applications developed for the mining industry in the area of education and training.

1 INTRODUCTION

Virtual reality (VR) is a continuously evolving new computer technology, which provides great opportunities for many industries including mining industry. Virtual Reality is described by Aukstakalnis and Blatner (1992) as “*a way for humans to visualise and interact with the artificial 3D environments created using computer graphics*”. VR systems are real-time computer simulations of the real world in which visual realism, object behaviour and user interaction are essential elements (Denby and Schofield, 1999; Filigenzi *et al*, 2000 and Schofield *et al*, 1994).

Recent advances in virtual reality and the constant increase in the power of computers have allowed for the rapid expansion of VR applications. As the power of VR increases so too do its applications. VR has already been shown to be an effective tool in many industries. Surgeons may use VR to plan and map out complex surgeries in 3D, which allows them to view past the skin of the

patient before a knife is even picked up. Real estate agents may use virtual reality to give clients a walkthrough of an estate, from the comfort of their own home.

It is estimated that over 3,600 educational institutions now use VR throughout the world (Teachers, 2002).

1.1 Definition of Virtual Reality

Virtual Reality is the process of human interaction with a simulated (or virtual) world. The term virtual world is a blanket term used to describe a simulated/artificial environment, object or situation. Computers are used to both simulate these virtual worlds and to facilitate the human interaction with them. The human-world interaction is generally achieved through combinations of various techniques, with the following being the most common (Kizil, Kerridge and Hancock, 2004):

- Computer generated visuals (visualisation),

- Aural feedback,
- Haptic and kinetic feedback (sense of touch and motion respectively),
- Operator interaction devices (Input and control mechanisms).

The visualisation aspect of VR is most commonly handled via real-time computer rendered three-dimensional (3D) graphics (polygon based). An example of these types of graphics is shown in Figure 1. The computer graphics can be displayed in a number of different formats, including monitors or screens, head mounted displays, curved projection screens, cave systems, cockpit systems, tabletop systems and augmented reality systems. In addition, stereoscopic vision systems can be used to provide the user with the ability to perceive depth as in the real world – i.e. see in three dimensions.

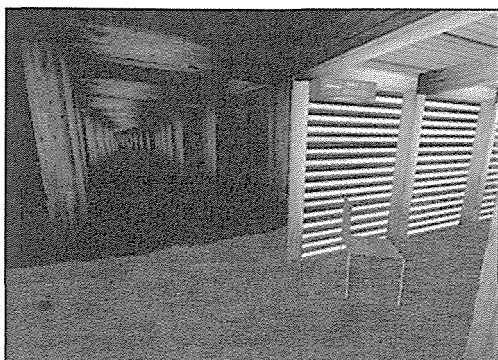


Figure 1. Polygon based three-dimensional computer graphics.

Aural feedback refers to the use of sound to relate the current state of the simulated world or indicate a particular event to the user. An example of this may be the sound of a car engine running or the sound of an alarm in a virtual aeroplane cockpit.

Haptic (tactile) and kinetic (force feedback) devices provide feedback to a user via the senses of touch and the feeling of motion respectively. Louka (1998) describes haptic feedback as providing “...a sense of touch through, typically, vibrating nodules or expanding air bubbles inside a glove or suit”. Kinetic devices use forces induced

mechanically or magnetically to restrict or encourage user movement in some way. According to Louka (1998), these devices are often present in the form of exoskeletons (Figure 2), joysticks, hand controllers and motion platforms.

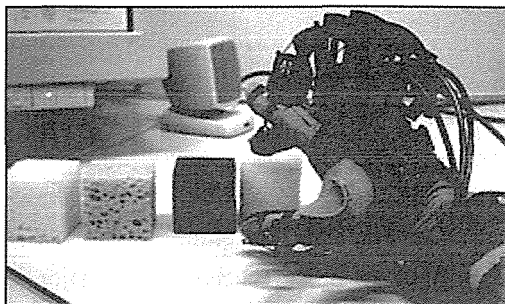


Figure 2. Haptic feedback exoskeleton used to simulate restrictions of movement of users fingers (Maciel, 2004).

Operator (user) control and input in VR systems can be handled in a variety of different ways, depending on the particular simulation. Methods can range from the use of a keyboard, mouse and joystick on desktop systems, to physical mock-ups of cockpits with functioning levers, buttons, wheels and controls sticks as found in vehicle/machinery simulators. The user input and control system used in any VR application should be appropriate to the purpose and audience of the simulation.



Figure 3. Shovel simulator with functioning cockpit used to operate the simulated machine (Immersive Technologies, 2002).

1.2 Types of Virtual Reality Systems

There are three different types of Virtual reality systems; non-immersion, full-immersion and semi-immersion systems. The Advisory Group on Computer Graphics (1995), explains that a non-immersion system, otherwise known as a desktop system, consists of an ordinary desktop computer with standard interaction devices such as keyboards, mice and joysticks.

Full-immersion systems refer to the use of head mounted display hardware while semi-immersion systems refer to projection systems and caves that partially or completely surround the user/users (Louka 1998).

The VR software applications described by this paper are non-immersive systems that utilise standard PC's and require only keyboards and mice for input devices. This format was chosen for these applications due to the fact that non-immersive systems can run on almost any modern PCs, are flexible and straight forward to create and program and are relatively inexpensive for the user to run. Bell and Fogler (1997) emphasise this concept when they point out that undergraduate students rarely have access to expensive and complex VR systems.

2 USE OF 3D GRAPHICS AND VR IN THE MINING INDUSTRY

The mining VR research group at The University of Queensland has been involved in developing Virtual Reality applications for the benefit of the mining industry since 2000 (Kizil *et al.*, 2001; Kizil and Joy, 2001, Kizil, 2003a and 2003b and Kizil, Kerridge and Hancock, 2004). Applications have been developed in conjunction with various research centres and mining companies in the areas of:

- Data visualisation,
- Education and training,
- Environmental monitoring application,
- Accident reconstructions,
- Simulation applications,
- Risk analysis,
- Hazard awareness applications.

This paper gives an overview of the applications developed in education and training areas.

2.1 Virtual Reality in Education

Virtual Reality is increasingly being used as an educational tool. There are increasing demands today for ways and means to teach and train individuals without actually subjecting them to the hazards of particular simulations (Kizil, Kerridge and Hancock, 2004).

Virtual reality has been used for educational purposes in one form or another for nearly fifty years. The most well known example is that of an aircraft simulator, some which date back to the late 1950's (Mazuryk and Gervautz, 1996). It was not until 1965 however, that Ivan Sutherland constructed the first computerised virtual reality system – consisting of a head mounted display system that produced simple wireframe graphics in stereoscopic vision (Johnson, 2000). Nowadays, computerised VR is used for education in many different fields, such as aviation, military, medical science, engineering, research, mining and design and planning.

The attractiveness of using VR for education is well stated by Bell and Fogler (1997), *"Within a VR simulation, students are free to explore and to examine their environment from any vantage point they desire... With this newfound freedom to explore, students can analyze their problems and evaluate possible alternatives in ways never before possible."*

Kizil *et al.* (2004) and Kizil and Joy (2001) state that although VR should not be considered a substitute for real world training, it does allow for the reduction of the cost of training and improves safety. The use of VR in the initial training stages allows personnel to be taught to use equipment in a controlled and safe (both for the personnel and the equipment) environment. In addition, equipment down time due to training is reduced.

Both Schofield (2001) and The Advisory Group on Computer Graphics (1995) agree

that a principal strength of VR is that it can provide practical experience and training without the need for onsite training or the use of real equipment. The Advisory Group on Computer Graphics (1995) further clarifies this concept by listing the advantages of using VR for education: "A VR system has many strengths that cannot be ignored and include:

- Flexibility.
- Inherently safe.
- Wide application.
- Intuitive interaction.
- Motivating.
- They will exploit interactivity.
- We all learn faster by 'doing' rather than reading.
- People learn from mistakes.
- More efficient learning by enhanced sense of presence.
- Students can get a better understanding of process.

Although the advantages of using VR for education are clear, there are important factors that must be considered when producing an educational virtual reality application as discussed by Bell and Fogler (1997). The first is to understand the strengths and weaknesses of VR, which should not be used to present data already adequately shown in existing media types (e.g. books). Instead, the unique properties of VR should be utilised to produce a learning tool that would not be possible or as effective using other media. As VR is a predominantly a graphical environment, it is best used to demonstrate complex three-dimensional concepts and to provide illustrations of ideas. VR simulations are excellent tools for training, simulation of abnormal or dangerous conditions and solving complex problems (Kerridge *et al.*, 2003).

2.1.1 UQEMSimVent

UQEMSimVent is a Virtual Reality based application that is designed to simulate the process of conducting a pressure and quantity ventilation survey in the University of Queensland's Experimental Mine (UQEM). Undergraduate Mining

Engineering students undertake one of these surveys during their practical classes for mine ventilation. However, students only get one chance to perform such a survey, and the learning experience is often compromised by the need to instruct relatively large groups of students all at once. In addition, students are often unprepared for the practical class and do not understand the principals behind what is being demonstrated while they are collecting data they are supposed to later analyse. By providing a simulation of the same experience, students are free to revisit the practical lesson at a time and learning pace that suits them, and collect (simulated) data that is accurate and not compromised by the realities of group learning (Kizil *et al.*, 2004).

UQEMSimVent recreates the experience of a ventilation survey on an ordinary desktop PC. During the simulation, the user is presented with a first person view as demonstrated in Figure 4. The user is free to navigate around the virtual mine controlling their movement with the keyboard and their viewing direction with the mouse - similar to most first person computer games. UQEMSimVent allows the user to open and close doors within and to change regulators the mine in order to change the simulated ventilation network. Just as in real life, these actions affect the airflow throughout the simulated mine. Finally, in order to conduct the pressure and quantity survey the operator is able to use a vane anemometer, pressure transducer and tape measure as shown in Figure 5.



Figure 4. UQEMSimVent screen capture.

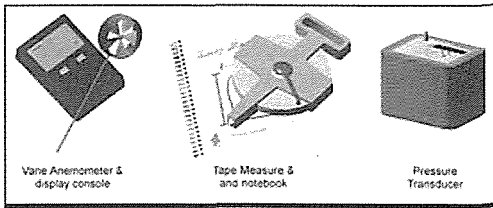


Figure 5. "Virtual" ventilation equipment used to perform a simulated network survey in UQEMSimVent.

The ability to navigate around the mine, change the ventilation network characteristics of the mine, and conduct pressure and quantity measurements allows students to:

- Characterise the UQEM's ventilation network,
- Use simulated data measured within the VR application to analyse the airflow through the UQEM's ventilation network, and
- Change some aspect of the ventilation network (e.g. door or regulator) and then measure the change in air movement that results from the changes to the network.

2.1.2 Virtual Mining Methods

Teaching mining methods to students is a challenge for many mining academics. The difficulty lies in representing 3D environments and constructions with 2D images and drawings. Since the purpose of VR is to intuitively convey 3D concepts and environments through 3D graphics and user interaction, it is the ideal solution to this problem.

As part of the mine planning teaching module developed with support from the Minerals Council of Australia (MCA)-Minerals Tertiary Education Council (MTEC), a series of six subsidiary teaching modules have been developed that outline various conventional mining methods (Kerridge *et al.*, 2003).

The methods featured are;

- Block Caving,
- Open Pit Mining,
- Strip Mining,

- Longwall Mining,
- Sublevel Stopping and
- Cut and Fill Mining.

While the teaching modules utilise traditional written text and graphics, it is the fully embedded 3D animations (Figure 6) and interactive virtual models that will enable students to rapidly learn the design and production aspects of the featured mining methods (Figure 7).

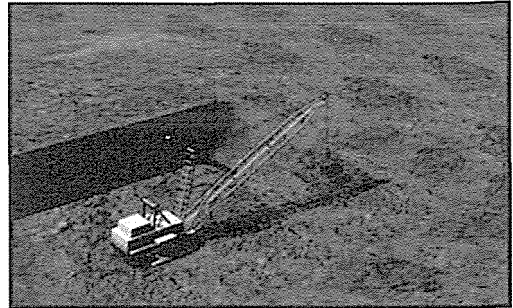


Figure 6. A scene from strip mining animation

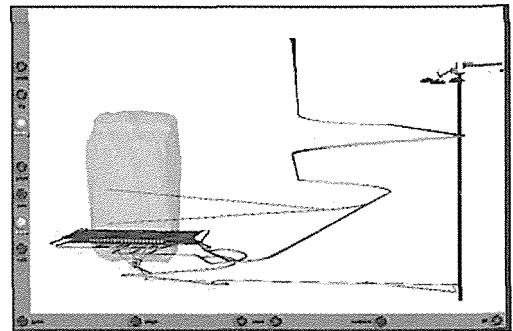


Figure 7. An interactive 3D VR model

Where appropriate each mining method module details the development, production and ventilation of a mine that uses the featured mining method. Equipment usage and method variations are also covered for each method. Each module is presented as a web based, multimedia document (Figure 8) and accessible as part of a virtual mining method website and as a CD-ROM distributed to each student.

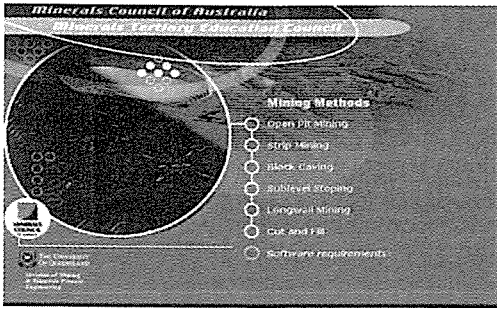


Figure 8. A screenshot of virtual mining methods website.

2.1.3 Instron Rock Testing Simulation

InstronVR has been developed to simulate Instron rock testing machine and Uniaxial Compressive Strength (UCS) testing practical at the University of Queensland (Kizil, 2004). The aim of this simulation is to let students perform UCS tests on a number of rock samples from the comfort of their computer laboratory (Figure 9). The simulation allows students to individually operate the equipment and perform the tests as opposed to the traditional approach of students observing a demonstration of the machine at the UQEM.

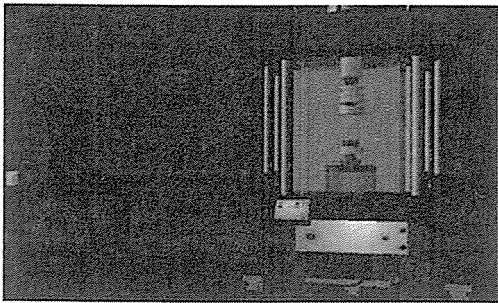


Figure 9. InstronVR: virtual UCS rock testing simulation.

Currently implemented in the project are UCS tests for sandstone and marble, and a post peak behaviour test for a sample of coalcrete (concrete and coal mixture).

During the practical the machine is already set up to perform the test, so set-up of test conditions using the control panel is not required.

Students are required to turn on the Instron machine and its computer and then choose a sample for testing. The test process cannot start until all the safety and operational requirements are met. After the test, the simulation produces a result file in Excel format, which students can save to a floppy disc for further analysis and interpretation in their practical report.

2.2 Virtual Reality in Training

Training is of great importance to the minerals industry in improving safety and productivity due to high injury and fatality rate (Quinlan and Bohle, 1995, MCA 1998 and 1999). Although there is no substitute for real world training, VR offers the necessary tools to reduce the cost of training and improve safety.

By using VR in the initial stages of training, personnel can be taught to use equipment in a controlled and safe (both for the personnel and the equipment) environment. In addition, equipment down time due to training and the risk of damage to expensive equipment during training are reduced. Figure 10 illustrates the benefits of using VR in training.

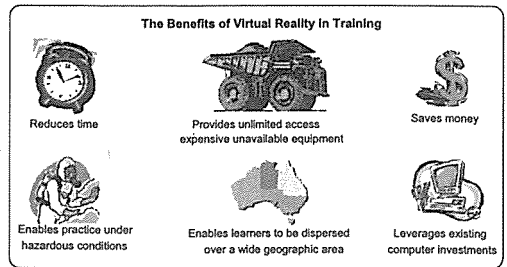


Figure 10. The benefits of using VR for training

Virtual reality can be used to train individuals to perform tasks in dangerous situations and hostile environments, such as in an underground mine accident or toxic gas environment (Denby and Schofield, 1999; Squelch, 2001 and Schofield *et al*, 1994). In addition to the assurance of safety, the use of a virtual training environment gives the trainer total control over many aspects of the

trainee's performance (Schofield *et al*, 1994). The virtual environment can be readily modified, either to provide new challenges through adjusting levels of difficulty or to provide training prompts to facilitate learning.

2.2.1 CRC Mining Drill Rig Training Simulator

BigTED virtual drill rig simulator developed by UQ Mine VR group is a good example of such training systems (Figure 11). The aim of the project was to create a 3D model of the CRC Mining's laboratory drill rig and consequently create a VR simulation with the model.

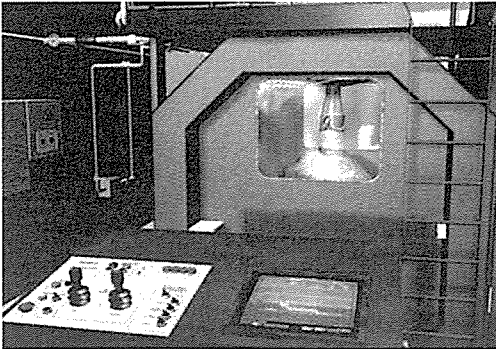


Figure 11. BigTED drill rig training simulation

The simulation includes the basic operating principles of the rig and some hazard identification situations. It is used in training users to operate the rig and all associated equipment. This involves starting up the rig and its power systems, basic operation of the rig using its control panel, and turning off the system when drilling is completed.

BigTED has a fully functional control system which can be used to operate the rig, provide hazard identification exercises, with detailed 3D models and realistic surround sound (Kizil *et al.*, 2001). The simulation is made to emulate, as closely as possible, the actual drill rig.

BigTED has a number of components which are replicated in the VR simulation.

These include the drill rig itself, the power pack, the associated control panels, the mains power board, the air compressor, and the rig's water, compressed air and hydraulic piping system. BigTED was developed in a 3D CAD package and assembled in SafeVR.

SafeVR provides real-time user interaction in a simulated virtual environment, and is a revolutionary new tool that may be used to create training applications quickly and simply on a PC. This powerful software has been developed by the AIMS Research Unit at The University of Nottingham, UK (AIMS, 2002).

BigTED combines two different simulations:

- Equipment inspection and
- Operator training.

In equipment inspection mode, the user navigates around the lab and inspects the rig, pipes, cables and sensors for any damage. The user is assessed based on the number of hazards identified and correctly dealt with.

In the operator training mode, the user is allowed to operate the rig in the same manner as in real life. The operation of the drill rig involves turning on the power, air and water supply in the right order and positioning the drill bit on the rock sample. The machine responds to any mistakes made by the operator with pop-up text messages providing instructions on the correct procedures.

2.2.2 Barring Down Training Simulator

Mining by nature is a hazardous occupation. Unfortunately, accidents still happen in the industry. About 60% of the fatalities happen in underground mines are related to roof falls.

The rock is drilled and blasted for development and production in underground. The blasted rocks need to be removed before the roof can be supported. Scaling down of loose rocks is therefore important before this task can begin.

The virtual barring down simulation system (Figure 12) was developed to provide improved hazard identification training for underground workers, primarily in relation to

rock fall related hazards during barring down exercises.

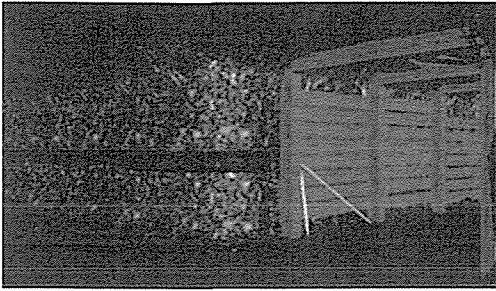


Figure 12. Barring down simulation.

The major aims of this simulation are to:

- Expose a trainee to various hazardous situations without actually risking his/her life,
- Take the trainee through a mine and test his/her ability to do a risk assessment in hazardous situations whilst tracking his/her individual scoring progress,
- Provide training in highly dangerous operation of scaling down rocks.

The simulation is still in the early development stage. An improved version of this model could be used to train people about the barring down exercise to prevent rock fall injuries and save lives.

There is also a cost benefit. \$600 M is lost each year, in Australian longwall mines alone through unforeseen geotechnical problems for which even a 10% improvement will save \$60 M per annum (Galvin, 1996).

The simulator provides sound and visual effects to the trainee to identify loose material. The trainee is required to successfully negotiate his/her way around the model identifying the hazards and selecting appropriate corrective actions prior to scaling.

3 CONCLUSIONS

Inadequate or insufficient training is often blamed for most of mining fatalities. There is no doubt that the use of VR based training will reduce these injuries and fatality numbers. Justifying the use of VR in the

minerals industry to improve safety is difficult to sell without hard evidence and quantified numbers.

When considering all these costs, the money invested in a VR model to train mine workers will be recovered in a very short time period with a bonus of improved safety record to the company.

The Mining VR research group is committed to use this technology to develop further applications for the mining industry.

REFERENCES

- AIMS, 2002. Aims Solutions, UK. <http://www.aims-solutions.co.uk>. Accessed August 2002.
- Aukstakalnis, S. and Blatner, D. 1992. *Silicon Mirage: The Art and Science of Virtual Reality*, Peach Pit Press ISBN 0-938151-82-7.
- Bell, J T and Fogler, H S, 1997. Ten steps to developing virtual reality applications for engineering education, in *Proceedings American Society for Engineering Education 1997*, Annual Conference on CDROM, session 3213 (American Society for Engineering. Education: Washington D.C.).
- Denby, B. and Schofield, D. 1999. Role of Virtual Reality in Safety Training of Mine Personnel. *Mining Engineering*, October, pp 59-64.
- Filiguzzi, MT., Orr, TJ and Ruff, TM. 2000. Virtual Reality for Mine Safety Training, *Applied Occupational and Environmental Hygiene*. 15(6): 465-469.
- Galvin, JM. 1996. Impact of Geology on Longwall Mining: A 20 Year Case Study: in *Geology in Longwall Mining. Paper with Symposium Proceedings, Coalfield Geology Council of New South Wales Australia*. ISBN 0 947333 90 8.
- Johnson, A, 2000. Introduction to Virtual Reality, *Electronic Visualization Laboratory, University of Illinois at Chicago*, CS 528 / EECS 590 Lecture notes, Illinois.
- Kerridge, A., Kizil, M S. and Howarth, D. 2003. Use of Virtual Reality in Mining Education. *The AusIMM Young Leader's Conference*, 30 Apr-1 May 2003. Brisbane, Australia
- Kizil, MS. and Joy J. 2001. What can Virtual Reality do for Safety? *Queensland Mining Industry Health and Safety Conference: Managing Safety to Have a Future*. Queensland Mining Council Publication. pp173-181. 26-29 Aug, Townsville.

- Kizil, MS., Hancock, MG and Edmunds, OT. 2001. Virtual Reality as a Training Tool. *Proceedings of the Australian Institute of Mining and Metallurgy Youth Congress*. 2-6 May 2001. pp 9-12. Brisbane, Queensland.
- Kizil MS. 2003a. Virtual Reality Applications in the Australian Minerals Industry. *31st Int. Symposium on Computer Applications in the Minerals Industries Held under the auspices of the South African Institute of Mining and Metallurgy*. 14-16 May 2003. Cape Town, South Africa.
- Kizil MS. 2003b. Visualising the Future in Mining with Virtual Reality. *NSW Minerals Council, Environment Workshop. Change for the Better*. 2nd – 4th July, Mudgee, NSW.
- Kizil, MS. 2004. Applications of Virtual Reality in the Minerals Industry. *INFOMINA, V International Symposium of Information Technology Applied in Mining*, 14-17 September, Lima, Peru.
- Kizil, MS. Kerridge, AP, and Hancock, MG, 2004. Use of Virtual Reality in mining education and training. *Proceedings of the 2004 CRC Mining Research and Effective Technology Transfer Conference*, 15-16 June 2004, Noosa.
- Louka, M, 1998. <http://www.ia.hiof.no/~michaell/home/vr/vrhi098/index.html>. What is Virtual Reality, May.
- Maciel, A, 2004. <http://vrlab.epfl.ch/~amaciel> Virtual Reality Lab: Haptic Sound Generation, May.
- Mazuryk, T and Gervautz, M, 1996. Virtual Reality History, Applications, Technology and Future, in *Institute of Computer Graphics Vienna University of Technology*, Vienna, Technical Report # TR-186-2-96-06.
- MCA. 1998. Minerals Council of Australia, Safety and Health Performance Report of the Australian Minerals Industry, 1997-98.
- MCA. 1999. Minerals Council of Australia, Annual Safety and Health Performance Report of the Australian Minerals Industry, Survey Report.
- Quinlan, M. and Bohle, P. 1995. Work, Health and Safety, Inquiry into Occupational Health and Safety, Industry Commission, Volume 2, Report 47, 11 September 1995.
- Schofield, D., Denby, B. and McClarnon, D. 1994. Computer Graphics and Virtual Reality in the Mining Industry, *Mining magazine*, p284-286, Nov.
- Squelch, A. 2001. Virtual Reality for Mine Safety Training in South Africa. *The Journal of the South African Institute of Mining and Metallurgy*. July. Pp 209-216.
- Teachers, 2002. http://www.teachers.ash.org.au/mrlaneis/ozedweb_a_index_power_point.htm. Accessed August 2002.
- The Advisory Group on Computer Graphics. 1995. <http://www.agocg.ac.uk/>. Accessed Mar 2005.

Miscellaneous

Physical Modeling of Joints Spacing Effects on Penetration Rate of Rotary Drilling in Open Pit Mines

H.S. Hoseinie

Faculty of Mining Eng. & Geophysics, Shahrood University of Tech., Shahrood, Iran.

Y. Pourrahimian & H. Aghababaei

Faculty of Mining Eng., Sahand University of Tech., Tabriz, Iran.

ABSTRACT Drilling is one of the most expensive stages of open pit mining and has many complexities. In drilling process, many parameters interact simultaneously each other, where studying each parameter requires recognition of the effects of other characteristics of rock mass and its material. In this paper, the main aim has been directed to investigate the effects of joint spacing among the structural parameters of rock mass. For this purpose, in order to study the condition of drilling in jointed rocks with different spacings, jointed rock masses with spacing of 10, 20, 30, 50 and 100 centimeters physically were modeled in laboratory by using cemented blocks. Penetration rate of cross bit has been measured by using rotary drilling system. According to the numerical results obtained from experiments, by increasing of joints spacing, penetration rate (m/min) of drill bit in jointed rock masses increases logarithmically.

1 INTRODUCTION

Drilling, like the other exploitation stages, has direct and close relation with rock mass would be affected by geomechanical characteristics of the rock material as well as rock mass. Therefore, recognition of drilling environment and in situ rock mass properties would be great help in choosing type of drilling system, number of machinery and the mine production rate. In discussion about the effects of rock material properties on the drilling process, many investigators have described the rocks behavior, using the various parameters. (Akun & Karpuz, 2005), (Aliha & Aiatolahy, 2005), (Bickel & Kuesel, 1982), (Clark, 1979), (Drake, 2004), (Ersoy & Waller, 1995a), (Ersoy & Waller, 1995b), (Funy, 1981), (Ghasemi et al, 2005), (Hoseinie et al, 2006), (Jung et al, 1994), (Jimeno et al, 1995), (Kaiser & McCreath, 1994), (Kahraman, 1999), (Kahraman et al, 2000), (Miranda & Mello-Mendes, 1983), (Osanloo, 1998), (Ostovar, 2000), (Pathinkar & Misra, 1980), (Protodyakonov, 1962),

(Rabia & Brook, 1980), (Rao & Misra, 1998), (Serradj, 1996), (Singh, 1969), (Singh, 1990), (Singh et al, 1998), (Singh et al, 2006), (Thuro, 1997), (Tanaino, 2005), (Wijk, 1991), (Wilbur, 1982), (Zhu, 1988).

In most studies on drilling, importance of rock, structure and mass have been emphasized. Although in classification system presented by Wilbur the rock mass condition has been seriously consider for the first time, however, the most subjects presented in which have quality aspect and quantitative effects of rock mass characteristics have been considered to a lesser degree.

In discussion on rock mass, joints, as the most important factor of instability of rock masses, have the most significant effects on the drilling process. Investigation of rock material without recognition of physical and spatial conditions of discontinuities would result in complicated problems on drilling process of rock masses. The most important specifications of joints that have effects on

drilling are spacing, dipping, continuity, filling, weathering and roughness of the joint surfaces.

2 INTRODUCTION

Considering simultaneous effect of various factors relating to rock material and the rock mass in the drilling process, laboratory testing of the effect of one factor on the quality of drillability of rock samples may be encountered with many errors. Therefore, the best method of surveying one parameter, without the effect of the other parameters, is physical modeling of rock masses by artificial materials such as concrete. Since in physical modeling of rock masses both rock material and its mass structure are very important, for studying of joints characteristics effects on drilling penetration, it is essential that characteristics of rock material to be constant. Regarding the concrete properties, one can easily obtain concretes with preplanned properties by modifying makeup ratio of aggregate, water, cement and dimensions of particles. Hence due to all conditions as well as molding ability, concrete is the best material for physical modeling of jointed rock masses (Hoseinie et al, 2006).

In the present project, as earlier mentioned, it was essential, due to laboratory conditions, that one assume the main parameters relating to concrete material for models to be constant. In physical modeling with concrete, considering parameters relating to rock materials involved in drilling; density, dimensions of grains, uniaxial compressive strength (UCS) and hardness are assumed to be constant parameters. Table 1 shows physical parameters of concrete utilized in physical modeling.

After completing of molding and processing, all samples were tested for uniaxial compressive strength (UCS), density and hardness. The results reveal that 90% of samples were in agreement with the theoretical designs of models.

Table 1. Physical specifications of concrete for physical modeling.

Texture	Porphyric
Maximum grain size (mm)	4.76 (mesh No.4)
Density (g/cm ³)	2.6
UCS (MPa)	75
Elastic modulus (GPa)	3.9

Regarding the volume, strength, flexibility of blocks and rate of bar loaded on physical models, AtlasCopco (512 HC) drilling machine with rotary system was finally selected for drilling studies. At jointed and crushed zones in open pit mines, rotary system is the best-applied system of drilling (Ostovar, 2000). Therefore, because of less spacing of modeled rock masses, rotary system and cross bit were select for studying drilling times.

3 INVESTIGATION ON JOINTS SPACING EFFECTS IN DRILLING

Drilling in jointed rock masses, in comparison with drilling in intact rocks, is a challenging. Drillability and penetration of rock mass are affected by joint spacing. Investigations show that, in open pit mine drilling, the most digging problems are at zones with joints of less than one meter and especially less than 0.5 m spacing. Therefore, during investigation of spacing effects on drilling time in rock masses, joints with spacing of 10, 20, 30, 50 and 100 centimeters have been studied. For physical modeling of joints above mentioned, 20 concrete blocks with constant makeup of Table 1 was providing. Numbers, volume and weight of each series of blocks have given in detail in Table 2.

Table 2. Specifications of block models

Spacing (cm)	Number of blocks	Dimension (cm)	Weight (kg)
10	10	50*50*10	65
20	5	50*50*20	130
30	3	50*50*30	195
50	2	50*50*50	325

In investigation the effect of joint spacing on the drilling of rock mass, drilling time of one meter of intact concrete has been the base of calculation and comparison. Before starting the drilling of jointed rock masses, the drilling time of one meter of concrete was first recorded, and then by placing blocks with spaces of 10, 20, 30, and 50 centimeters

into the steel mold, the time of one-meter drilling under the above conditions was recorded in second. Figure 1 shows the physical modeling (two sample concrete block) and drilling procedure of models. The relation between drilling rate and joint spacing was present as a curve in Figure 2.

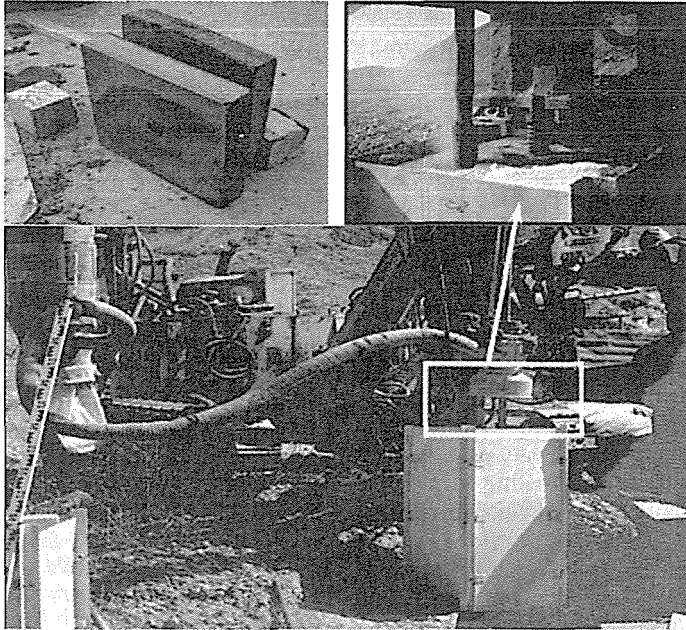


Figure 1. Physical modeling and drilling procedure of models

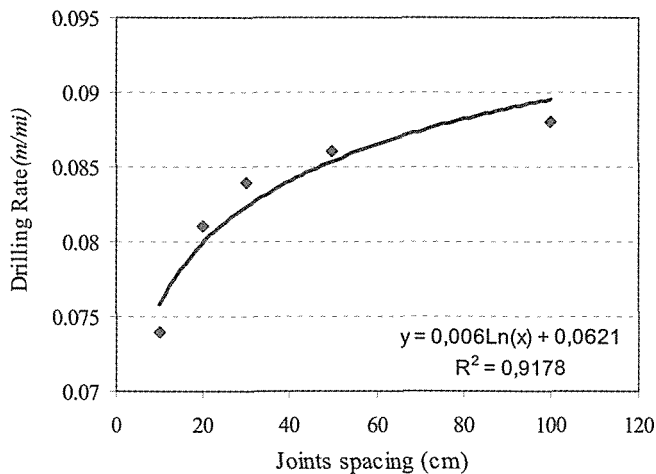


Figure 3. Relation between drilling rate and joints spacing.

The equation clearly reveals that in spacing less than one meter, drilling rate would logarithmically increase with increasing of spacing.

4 CONCLUSION

Considering physical modeling as well as the numerical results obtained from it, the following cases are emphasized as the basic results of this project:

- 1) Discontinuities, especially joints, are the most important structural factor, which is controlling rock mass behavior under the drilling process. Therefore, neglecting this factor as well as the rock material properties, the rock mass behavior would become unpredictable.
- 2) Considering the results obtained from models, it is clear that by increasing joints spacing, drilling time would decrease and thus, at the same ratio, drilling efficiency would enhance.
- 3) The equation resulted from drilling of physical models reveals that in spacing less than one meter, drilling rate would logarithmically increase with increasing joint spacing.
- 4) The critical condition from viewpoint of spacing occurs in the joints with spacing of 10 cm and less. This condition is the suitable model for surveying of crushed zones (very low RQD) in mines.

5 ACKNOWLEDGEMENT

The authors wish to acknowledge the full financial support provided by Sahand University of Technology. Grateful thanks are recorded to Dr. H. Afshin (Faculty of Civil Eng.). The co-operation of Mr. Karbasi, Mr. Mohamadzade and Eng. Gheibie in performing part of physical modeling in the rock mechanics laboratory of the Sahand University of Technology is also acknowledged.

REFERENCES

- Akun, M. E. & Karpuz, C. 2005. Drillability studies of surface-set diamond drilling in Zonguldak region sandstones from Turkey, *International Journal of Rock Mechanics and Mining Sciences*, Vol. 42, pp. 473-479.
- Aliha, M.R. & Aiatolahy, M.R. 2005. Application of fracture mechanism optimizing of rock cutting in drilling operation. *Proceedings Iranian Drilling Symposium. Arak University, Iran, March 2005.*
- Bickel, J. O. & Kuesel, T. R. 1982. Tunnel Engineering Handbook. Van Nostrand Reinhold Company.
- Clark, G. B. 1979. Principles of rock drilling. *Colorado School of Mines Quarterly*, 74: 91-93.
- Drake, R. 2004. Bench drilling techniques and equipment selection manual, Ingersol-Rand Company.
- Ersoy, A. & Waller, M. D. 1995a. Textural characterization of rocks. *J. of Engineering Geology*, June, Vol. 39, Issues 3-4, 123-136.
- Ersoy, A. & Waller, M.D. 1995b. Prediction of drill-bit performance using multi-variable linear regression analysis. *Transactions of the Institution of Mining and Metallurgy, Section A: Mining Industry*, Vol. 104, May-August, pp. A101-114. .
- Funy, R. 1981. Drilling (*Surface Coal Mining Technology*), NDC Publishers.
- Ghasemi, A.M., Memmariyan, H. & Mehinrad. A. 2005 Investigation of factors affecting drill bit abrasion in percussive drilling. *Proceedings Iranian Drilling Symposium, Arak University, Arak, Iran, March 2005.*
- Hoseinie, S. H., Pourrahimian, Y. & Aghababaei, H. 2006a. Analyzing and physical modeling of joints dipping effects on penetration rate of rotary drilling in open pit mines. *15th International Symposium on Mine Planning and Equipment Selection (MPES2006)*. Torino, Italy. 1007-1013.
- Jung, S. J., Prisbrey K. & Wu., G. 1994. Prediction of rock hardness and drillability using acoustic emission signatures during indentation. *International Journal of Rock Mechanics and Mining Science & Geomechanics Abstracts*, Vol. 31, Issue 5, October, 561-567.
- Jimeno, C. L., Jimeno, E. L. & Carcedo, F. J. A. 1995. *Drilling and Blasting of Rocks*. A.A. Balkema, Rotterdam.
- Kaiser. P. K & McCreath. D. R. 1994. Rock mechanics considerations for drilled or bored excavations in hard rock. *Tunnelling and Underground Space Technology*, Vol. 9, Issue 4, October, 425-437.
- Kahraman, S. 1999. Rotary and percussive drilling prediction using regression analysis. *International Journal of Rock Mechanics and Mining Sciences*, 36: 981-989

- Kahraman, S., Balci, C., Yazici, S. & Bilgin, N. 2000. Prediction of the penetration rate of rotary blast hole drilling using a new drillability index. *International Journal of Rock Mechanics and Mining Sciences*, 37: 729-743.
- Miranda, A. & Mello-Mendes, F. 1983. Drillability and drilling methods. *Proceedings 5th Congress of the Int. Soc. of Rock Mechanics*, Melbourne, Australia. 195-200.
- Osanloo, M. 1998. *Drilling Methods*. Sadra Pub Tehran.
- Ostovar, R. 2000. *Blasting in Mines*. Vol.1, 4th edn, Amir Kabir University of Technology, Jahad Daneshgahy Pub. Tehran.
- Pathinkar, A. G. & Misra, G. B. 1980. Drillability of rocks in percussive drilling from "energy per unit volume" as determined with a microbit. *Journal of Mining Engineering*, 32: 1407-1410.
- Tanaino, A. S., 2005. Rock classification by drillability. Part 1: Analysis of the available classification. *Journal of Mining Science*, Vol. 41, No. 6, pp. 541-549.
- Thuro, K. 1997. Drillability prediction- geological influences in hard rock drill and blast tunneling. *Geol Runsch* 86: 426-438.
- Protodyakonov, M. M. 1962. Mechanical properties and drillability of rocks. *Proceedings of 5th US Symposium on Rock Mechanics, University of Minnesota, Minnesota, USA, May*, 103-118.
- Rabia, H. & Brook, W. 1980. An empirical equation for drill performance prediction. *Proceedings 21st US Symposium on Rock Mechanics, University of Missouri, Missouri, USA*, 103-111.
- Rao, K.U.M. & Misra, B. 1998. *Principles of Rock Drilling*, Balkema, Rotterdam.
- Serradj, T. 1996. Method of assessment of rock drillability incorporating the Protodyakonov index. *Transactions of the Institution of Mining and Metallurgy, Section A: Mining Industry*, Vol. 105, September-December, A175-A179.
- Singh, DP. 1969. Drillability and physical properties of rocks. In: *Proceedings of the Rock Mechanics Symposium, University of Sydney, Australia*, 29-34.
- Singh, S. P. 1990. Rock drillability comparison by different methods. In: *Proceedings 2nd Int. Symposium on Mine Planning and Equipment Selection, Calgary, November*, Pub Rotterdam, A.A Balkema, 489-494.
- Singh S. P, Ladouceur. M & Rouhi. F. 1998. Sources, implication and control of blasthole deviation. *7th International Symposium on Mine Planning and Equipment Selection*. A.A Balkema, Pub Rotterdam, pp. 391-397.
- Singh, T. N, Gupta, A. R. & Sain, R. 2006. A comparative analysis of cognitive system for the prediction of drillability of rocks and wear factor. *Geotechnical and Geological Engineering*, 24: 299-312.
- Tanaino, A. S., 2005. Rock classification by drillability. Part 1: Analysis of the available classification. *Journal of Mining Science*, Vol. 41, No. 6, pp. 541-549.
- Thuro, K. 1997. Drillability prediction- geological influences in hard rock drill and blast tunneling. *Geol Runsch* 86: 426-438.
- Wijk.G. 1991. Rotary drilling prediction. *International Journal of Rock Mechanics and Mining Science* Vol. 28, Issue 1, Jan, 35-42.
- Wilbur, L. 1982. *Rock Tunnel Engineering Handbook*. Edited by BickeL and kuesel, Publication of Van Norstrand Reinhold Company, 123-207.
- Zhu S.T. 1988. Experimental study of drillability for rotary rock bits. In: *Proceeding International Symposium on Mine Planning and Equipment Selection, Calgary, 3-4 November*, A.A Balkema, Pub Rotterdam, 375-381.

Dragline Dynamic Modeling for Efficient Excavation

N. Demirel

Middle East Technical University, Ankara, Turkey

S. Frimpong

University of Missouri-Rolla, Rolla, MO, USA

ABSTRACT Overburden excavation is an integral component of the surface mine production chain. In large mines, the walking dragline is a dominant strip machine. Production engineers and operators must be guided by appropriate strategies to preserve the structural and operating performance of this equipment to justify its high capital investment. The dragline performance is a function of spatial kinematics and dynamics of its front-end assembly. In this study, the authors develop kinematics and dynamic modeling of a dragline front-end assembly using vector loop and simultaneous constraint methods. Detailed analysis of the simulation results show that the maximum closure error from the vector loop is 4×10^{-8} . The angular accelerations of the drag and hoist ropes are close to zero. The respective maximum drag, cutting and hoist forces are 100 kN, 200 kN, and 75 kN. The results provide a solid basis for developing appropriate simulation technologies for efficient dragline operations.

1 INTRODUCTION

Walking draglines are massive and expensive excavators, which have been extensively used in strip mining operations for overburden removal. Draglines are constructed for heavy-duty cyclic operation. Due to its massive structure and a heavy suspended load, the components of the dragline front-end assembly are under dynamic forces, moments, and stresses that arise due to the accelerating inertia in the mechanism. Inefficient dragline operations introduce significant stresses and strains along the boom which may result in additional maintenance costs and could lead catastrophic structural failure. Also, the lack of knowledge or clear understanding of the main parameters affecting the boom strength and durability may cause mine operators to run the machine under its capacity which have a negative impact on the overall performance of the dragline. Therefore, production engineers and operators must be

guided by appropriate strategies to preserve the operating performance and to ensure the machine longevity in order to justify high capital investment, which ranges between \$ 30 million to \$ 100 million (Townson et al., 2003; Wescott, 2004).

The dragline front-end consists of massive and interrelated structures, such as boom, drag, and hoist ropes, and rigging mechanism, which altogether cause the translational and rotational motion in 3-D space. Efficient use of draglines requires a thorough knowledge of the powered functions, the translational and rotational motions, and machine-formation interactions within the operating environment.

Kinematics analysis is performed to investigate dragline front-end motion in 2-D spaces. The vector loop representation is used to characterize the dragline front-end geometry and to provide mathematical expressions for the kinematics model, which explores the relationships between position, velocity, and acceleration vectors that

capture the 2-D space motions. The simultaneous constraint method is used to build the dynamic model of the front-end assembly to capture the forces, moments, and torques incident on the focus areas during excavation. Based on the kinematics and dynamic simulations, component stress modeling and analysis could be performed using finite element methods (FEM) in a mechanical event and system simulation environment to simulate the stress distribution along the dragline boom under different operating performance and field conditions.

2 BACKGROUND LITERATURE

Kinematics and dynamic modeling of excavators has been studied and reported extensively. Work on coordinated control of excavators began in the mid-1980s by Lawrence et al. (1993). In this work, an excavator end-point is controlled in cylindrical task space coordinates by an operator rotating with the arm and using a single joystick (Papadulos and Sarkar, 1996). Bullock et al. (1990) and Bernold (1991) studied the forces between the soil and a tool (bucket) during digging operations and developed static force/torque relations. Khoshzaban et al. (1992) developed kinematics equations for machine positioning. Several researchers have developed the kinematic equations of positioning for a front-end loader. Hansen (1993) presented a generalized dimensional synthesis of planar mechanisms with revolute and translational joints by solving a set of vector loop equations. Haneman et al. (1992) developed a physical model to determine the reliability of a dragline bucket and rigging performance. Koivo (1994) investigated the kinematics of the backhoe and loader construction excavator to provide a basis for achieving automatic computer-controlled operations using homogenous transformation matrices that relate the adjacent coordinate frames. Frimpong and Hu (2003) developed kinematics and dynamic models as a basis for hydraulic shovel situation. Frimpong and Chang

(2004) have advanced the dynamic and kinematics model of a cable shovel using an exponential and Kane's algorithms. The kinematics model for a hydraulic shovel has been developed using transformation matrix method to describe the motion of the machine (Frimpong and Chang, 2004). Shi and Joseph (2004) developed a kinematics and dynamic modeling of a cable shovel crowd arm based on Newton's first and second laws, and they introduced a new curved dipper design concept. Awuah-Offei et al. (2005) developed innovative kinematics and dynamic simulation modeling of a cable shovel to optimize specific energy consumption in the excavation of oil sands.

Despite these improvements, existing models and the current body of knowledge lack the robust fundamental theories required for comprehensive dragline simulation, reliability, and completeness. Therefore, dynamic modeling and simulation of a dragline front-end is still an emerging research frontier.

3 DRAGLINE DYNAMIC MODELING

Draglines operate in a dynamic environment that leads to variable loads and stresses on the machine, and thus, the knowledge of dragline dynamics should provide enough information to make appropriate predictions of the outcome of any achievable cycle. Dynamic model is built to capture dynamic forces that arise due to the accelerating inertia in the mechanism to characterize the machine performance. The simultaneous constraint method is used to build the dynamic model of the dragline front-end. The rationale for using the simultaneous constraint method is that the formulation of the mechanism does not require choosing a set of generalized coordinates to describe the system. It provides a more direct solution procedure using differential calculus. In this method, kinematics constraints and Newton-Euler equations are solved in a system of simultaneous linear equations.

3.1 Kinematic Modeling

The dragline kinematics model is developed to investigate its front-end spatial motion

during the machine operation. The kinematics modeling employs the vector loop method to provide mathematical expressions for the kinematics relationships among the components of the mechanism during its motion. A vector loop is a closed loop of vectors that represents the key parameters in the mechanism, which include the length between joints as well as their orientations. The schematic diagram (Fig. 1a) of a dragline front-end has been used to extract the vector loop representation to characterize the front-end assembly as shown in Figure 1b.

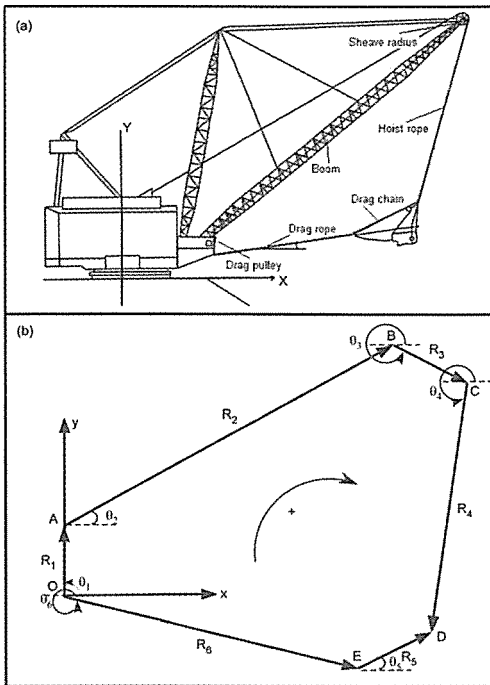


Figure 1. Dragline kinematics: (a) dragline front-end assembly, (b) vector loop representation.

From a fundamental theory of geometry, the vector loop closure equation is given by equation (1).

$$\sum_{i=1}^n \vec{R}_i = 0 \tag{1}$$

The vector loop closure equation is written for dragline front-end assembly as in equation (2).

$$\vec{R}_1 + \vec{R}_2 + \vec{R}_3 + \vec{R}_4 - \vec{R}_5 - \vec{R}_6 = 0 \tag{2}$$

Vector \vec{R}_i ($i=1, \dots, 6$) represents link i in 2-D space as a function of its scalar magnitude (r_i) in meter and the orientation from the x-axis (θ) in degree. The position equations are formed in x and y directions as in equations (3) and (4).

$$r_1 c \theta_1 + r_2 c \theta_2 + r_3 c (\theta_4 + \frac{\pi}{2}) + r_4 c \theta_4 - r_5 c \theta_5 - r_6 c \theta_6 = 0 \tag{3}$$

$$r_1 s \theta_1 + r_2 s \theta_2 + r_3 s (\theta_4 + \frac{\pi}{2}) + r_4 s \theta_4 - r_5 s \theta_5 - r_6 s \theta_6 = 0 \tag{4}$$

In equations (3) and (4) linear displacements are represented by r_i and angular displacements are represented by θ_i for all links.

After obtaining position equations, velocity equations are obtained by taking the first derivative of the displacement equations with respect to time and can be expressed in terms of a matrix format as in equation (5).

$$\begin{bmatrix} -r_3 c \theta_4 - r_4 s \theta_4 & r_6 s \theta_6 \\ -r_3 s \theta_4 + r_4 c \theta_4 & -r_6 c \theta_6 \end{bmatrix} \times \begin{bmatrix} \omega_4 \\ \omega_6 \end{bmatrix} = \begin{bmatrix} -\dot{r}_3 c \theta_4 + \dot{r}_3 c \theta_4 - r_5 s \theta_5 \omega_5 + \dot{r}_6 c \theta_6 \\ -\dot{r}_3 s \theta_4 + \dot{r}_3 s \theta_4 + r_5 c \theta_5 \omega_5 + \dot{r}_6 s \theta_6 \end{bmatrix} \tag{5}$$

In equation (5) \dot{r}_i represents the linear velocity of the link i and ω_4 and ω_6 represent angular velocities of the hoist and drag ropes respectively.

Similarly acceleration vectors are obtained by taking the second derivative of the position equations with respect to time as in equation (6).

$$\begin{bmatrix} -r_3 c \theta_4 - r_4 s \theta_4 & r_6 s \theta_6 \\ -r_3 s \theta_4 + r_4 c \theta_4 & -r_6 c \theta_6 \end{bmatrix} \times \begin{bmatrix} \alpha_4 \\ \alpha_6 \end{bmatrix} = \begin{bmatrix} -\ddot{r}_3 c \theta_4 - \dot{r}_3 c \theta_4 - 2\dot{r}_3 s \theta_4 \omega_4 + r_5 c \theta_5 \omega_5^2 + \ddot{r}_6 c \theta_6 - 2\dot{r}_6 s \theta_6 \omega_6 \\ -\ddot{r}_3 s \theta_4 + \dot{r}_3 s \theta_4 + \ddot{r}_3 c \theta_4 - 2\dot{r}_3 c \theta_4 \omega_4 - r_5 s \theta_5 \omega_5^2 - \ddot{r}_6 s \theta_6 + 2\dot{r}_6 c \theta_6 \omega_6 \\ r_5 c \theta_5 \alpha_5 - \dot{r}_5 s \theta_5 - 2\dot{r}_5 c \theta_5 \omega_5 + r_5 s \theta_5 \omega_5^2 + \ddot{r}_5 s \theta_5 + 2\dot{r}_5 c \theta_5 \omega_5 \\ -r_5 s \theta_5 \alpha_5^2 + r_5 c \theta_5 \alpha_5 + \ddot{r}_5 s \theta_5 + 2r_5 c \theta_5 \omega_5 - r_5 s \theta_5 \omega_5^2 \end{bmatrix} \tag{6}$$

The reason for choosing the angular velocities and accelerations of hoist and drag ropes respectively as state variables is that the operation of dragline stripping is mostly controlled by the drag and hoist ropes.

3.2 Dynamic Modeling

Draglines operate in a dynamic environment that leads to variable loads and forces on the machine components, and thus, the knowledge of dragline dynamics should provide enough information to make appropriate predictions of the outcome of any achievable operating cycle. The

dynamic forces that arise due to accelerating inertia in the mechanism are computed for characterizing the dynamic performance of the machine.

Focus areas of the dragline front-end dynamic model and analysis include the boom, the drag and hoist ropes, and the rigging mechanism. Simultaneous constraint method is used for the dynamic modeling in this study. For the purpose of dynamics, it is important that the frame of reference be an inertial reference frame. In this study the inertial frame is fixed to the machine to allow the measurement of displacement, velocity, and acceleration of machinery equipment.

The kinematics model equations form the foundation of the dynamic model. Next, the accelerations of the link centers of mass information are generated by using an approach similar to the vector loop. The resultant force/acceleration relationships are combined with the acceleration relationships that reflect the constraints of the mechanism. Finally, all equations are assembled into a sparse matrix in a more compact form that is solved within MATLAB and SIMULINK as part of full dynamic simulation of the mechanism.

3.2.1 Force Equations

Force equations are obtained by applying the general form of Newton-Euler equations to each individual link as illustrated in Figure 2 to relate the forces on each link to its individual acceleration. The generalized set of Newton's second law equations is given in equation (7).

$$\begin{cases} \sum_i^n F_{i,x} = M_i A_{ci,x} \\ \sum_i^n F_{i,y} = M_i A_{ci,y} \\ \sum_{i=1}^n \tau_i = I_i \alpha_i \end{cases} \quad (7)$$

It states that the acceleration of an object, produced by a net force, is directly proportional to the magnitude of the net force, in the same direction as the net force.

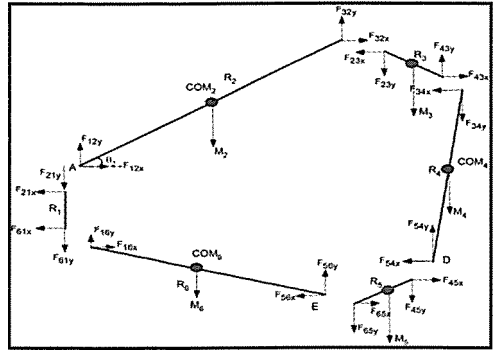


Figure 2. Free body diagrams of front-end components.

It should be noted that I_i is the moment of inertia about center of mass (COM) of the link. Often the moment is known with respect to different axis. If that is the case, then the parallel axis theorem is applied to compute the appropriate value as in equation (8).

$$I_{i,new} = I_i + M_i d^2 \quad (8)$$

The dynamic and static links are determined first prior to generating the force equations on each link. In that case the boom attachment point to the machine house (link R₁), the boom (link R₂), and the pulley diameter (link R₃) are fixed parts of the dragline front-end. Therefore, static limit equilibrium force equations are applied to these links. However, links R₄, R₅, and R₆ are dynamic parts and the accelerations of their centers of mass should be determined as a basis for developing the force equations. The relationship between mass and weight of each part is established by the characteristic gravitational acceleration, which has a magnitude g and is directed toward the center of the earth. The weights, M_i ($i=1$ to n) are vector quantities that are related to their respective masses and the gravitational acceleration by $M = mg$.

3.2.2 Center of Mass (COM) Equations

Since the positions of the front-end components are varying during its motion, it should be noted that the center of mass

(COM) and acceleration of COM variables also change depending on the machine kinematics. Application of Newton-Euler equations to model the various forces on link i requires the equations for the COM accelerations. These equations relate the kinematics state of the mechanism (link displacement, velocity, and accelerations) with the acceleration components of the centers of mass of the links, which are required in the force equations. In general, those accelerations that do not appear in the vector loop equation must be derived and will relate the acceleration of COM of each link to the other motion variables. The components' COM accelerations are derived for the links that have masses, such as the hoist rope (R_4), rigging (R_5), and the drag rope (R_6). To derive the COM acceleration equations of the two links, a vector relationship could be derived by inspection as in equation (9).

$$\begin{cases} A_{c2} = \ddot{R}_{c2} \\ A_{c3} = \ddot{R}_2 + \ddot{R}_{c3} \end{cases} \quad (9)$$

In equation, A_{c2} is the acceleration of the center of mass of the link 2. In order to generate a link's COM acceleration a vector relationship is utilized in which the vector sum of the previous links and the distance to the center of mass of the link information are summed with its corresponding second derivative generated for use in subsequent analysis. The general forms of COM accelerations of dragline front-end components in x and y directions are generated for each link in the dragline front-end mechanism. The main components of the COM acceleration equation is the distance between the end of the link and the center of its mass, angular position from the horizontal axis, angular velocity and angular acceleration of the link.

3.2.3 Formation Cutting Resistance Model

The force required to insert a tool into a formation is of major interest for the design and automation of earthmoving machinery (Blouin et al., 2001). The dragline bucket is

attached to the front-end by a rigging mechanism and the tension forces along the drag and hoist ropes are directly related to dynamic forces acting on the bucket. Therefore, the knowledge of dragline bucket forces in excavation operation is necessary to develop the dynamic model of the dragline front-end assembly.

The discrete element method (DEM) technique explicitly models the dynamic motion and mechanical interaction of each particle (body) throughout simulation. It also provides a detailed description of the positions, velocities, and forces acting on each particle at discrete points in time during the analysis.

The formation cutting resistance model is developed by using the mechanical relationships among soil-soil interactions and soil-tool (bucket teeth) interactions. Since time-dependent behavior can be modeled by spring-dashpot model, it is used in the simulations. Two basic parameters, namely stiffness and damping ratio, are essential using the spring-dashpot model. The collision force model by Cleary (1998) is adopted in modeling this process.

In this study, the soil is defined as the assembly of 2-D circular elements. Soil particles are modeled as mono-size circular discs kinematics parameters, which change through the digging process simulation as time in Figure (3).

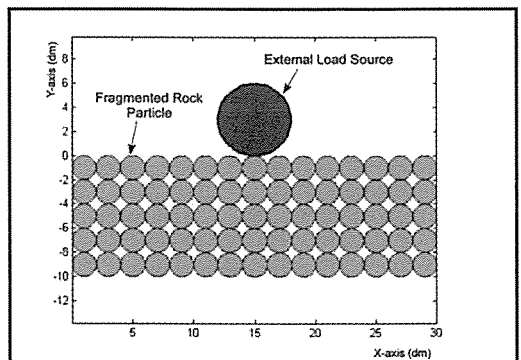


Figure 3. Rectangular clusters of circular discs.

3.3 Model Validation

In order to validate the model, error check analysis has been performed. For this purpose, a new function is introduced in a vector sense as shown in equation (10) that takes the displacement variables as input and return a value that represents the error inherent in the computation.

$$\bar{E} = \bar{R}_1 + \bar{R}_2 + \bar{R}_3 + \bar{R}_4 - \bar{R}_5 - \bar{R}_6 \tag{10}$$

The norm of \bar{E} is a scalar that indicates the absolute error in the loop closure. In this study, the acceptance tolerance limit chosen as 10E-6, and error check is done within that tolerance for two reasons. First, the units of the front-end components and the possible error are in meters. The selected error tolerance is equivalent to a micrometer, which is negligibly small when the typical dragline size is considered. Second, it is not applicable to measure distances precisely after three decimal points. The resulting error, while increasing steadily over time due to the high-order terms in Taylor Series expansion, starts at exactly zero, which indicated that the initial conditions were well posed and never achieved a value greater than 10E-6 m through the course of the simulation time as shown in Figure 4.

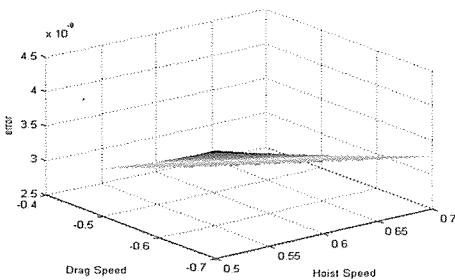


Figure 4. Truncation error through simulation time.

4 NUMERICAL SOLUTION ENVIRONMENT

The models developed results in a set of differential algebraic equations (DAEs), which are time-dependent, second-order

ordinary differential equations (ODEs) in the form of a set of linear algebraic equations. The solution procedure followed two steps. At first, the values of the time-dependent variables were obtained from an ODE solver. The values of the time-dependent variables are used to solve the linear system concurrently with the ODE solver, which is Runge-Kutta (4,5) (Dormand and Prince, 1980) embedded algorithm with automatic step-size control in MATLAB, at each iteration step. The linear equation system was solved using Gaussian elimination with partial pivoting. The numerical accuracy or truncation errors and stability issues have been properly assessed to ensure accurate solutions. The simulation models have been built using block modeling in MATLAB 7.0 and SIMULINK 6.0 (MATLAB, 2004). Essentially the algorithm combines linear solver, numerical integration, simulation, and analysis of the kinematics and dynamic model equations over time.

5 SIMULATION RESULTS

The simulation is initiated by defining the dragline model (Fig. 5) and passing the input data from user-written script file. The input file contains information that characterizes the dragline 3-D geometry. Then the SIMULINK block model is called by a command defined in function and then the results are post-processed and plotted on the relevant graphs. The post-processor script provides a platform for visualizing the obtained results on relevant graphs, which include kinematics parameters, simulation error through experimentation time, and forces.

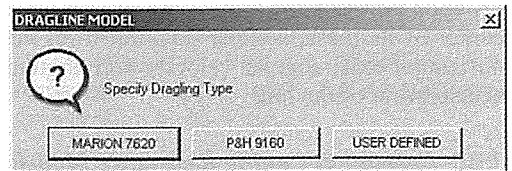


Figure 5. MATLAB GUI for dragline definitions in the main program.

The numerical experimentations are carried out for the MARION 7620 dragline, which has a bucket capacity of 15 to 27 m³, a boom length of 91.4 m, and a boom angle of 32°. A Dell Precision 670 dual processor desktop computer with a 3.0 GHz Intel Pentium 4 (Hyper-Threaded) central processing unit is used for numerical experimentation. An important aspect of a kinematics simulation is the appropriate assignment of initial conditions to the integrators. Typically, this requires that the position and velocity problem be solved by hand for at least one position of the mechanics. Table 1 contains the selected initial conditions for the model. The initial conditions are selected to ensure machine stability, optimum muck pile engagement, and motion control.

Table 1. Initial conditions chosen for simulation.

Operating Parameters	Symbol	Initial Value
Hoist Rope Speed	\dot{r}_4	0.5-0.7 (m/sec)
Drag Rope Speed	\dot{r}_6	-0.7- -0.5 (m/sec)
Linear Hoist Acceleration	\ddot{r}_4	0.01 (m/sec ²)
Linear Drag Chain Acceleration	\ddot{r}_5	0 (m/sec ²)
Linear Drag Acceleration	\ddot{r}_6	-0.03 (m/sec ²)
Angular Drag Chain Acceleration	α_5	0.05 (rad/sec ²)

From the detailed simulation experimentation and analysis of results from the kinematics models, it was found out that there is a negative correlation between the linear displacement of the drag and hoist ropes. However, the angular displacement and velocity of the drag and hoist ropes are positively correlated. The linear change in both drag and hoist ropes are 0.85 m/sec and 0.75 m/sec respectively.

Angular accelerations of both the drag and hoist ropes are close to zero and remains constant throughout the simulation (α_4 : $1.06 \cdot 10^{-3} \leq \alpha_4 \leq 1.08 \cdot 10^{-3}$ and α_6 : $-0.75 \cdot 10^{-3} \leq \alpha_6 \leq -1.3 \cdot 10^{-3}$) as depicted in Figure 6.

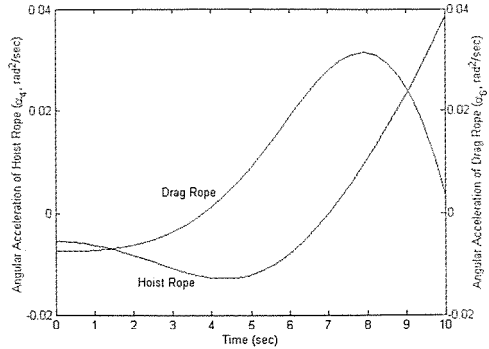


Figure 6. Angular acceleration of hoist rope (α_4) and drag rope (α_6) vs. time.

While the linear velocity of the drag rope increases in a negative direction, the linear velocity of the hoist rope increases in a positive direction. The results also showed that high drag rope speed leads to low bucket filling time and vice versa.

As the resistive force acting on the bucket is a function of the bucket position into the formation, it is essential to incorporate the bucket trajectory. The bucket trajectory is obtained using the bucket kinematics as illustrated in Figure 7.

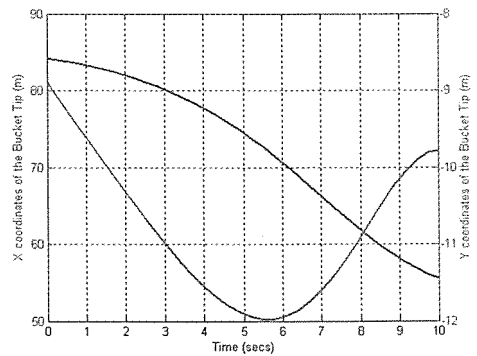


Figure 7. Bucket trajectory into formation.

Both drag and hoist speeds have an impact on angular acceleration of the hoist rope, which copes primarily with bending on rope drums, points sheaves, deflections sheaves, and the tension force imposed by the bucket and its load (Golosinski, 1994). Figure 8

represents the angular acceleration of the hoist rope with respect to the given initial values of drag and hoist speeds.

Important engineering data related to machine dynamics could be economically determined at a faster rate by simulating reality with a virtual prototype of a physical system. Simulation results of a dynamic model revealed that the maximum drag force, which is approximately 200 kN, occurs in a simulation time of 20 sec.

It is also important to note that the tension along the hoist rope is sensitive to the weight of the material in the bucket. The maximum hoist force, which is approximately 75 kN, occurs in a simulation time of 15 sec at which the bucket is filled completely. Also, the higher weight of the bucket leads to a higher initial force between the tool and the material.

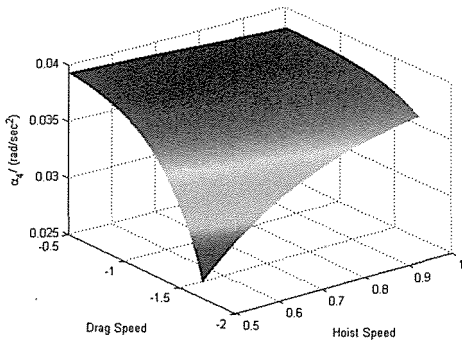


Figure 8. Angular acceleration of hoist rope (α_4), hoist and drag rope velocities (\dot{r}_4 and \dot{r}_6) vs. time.

The research findings showed that the maximum cutting resistant force, which is approximately 100 kN, occurs when the bucket teeth are fully engaged with the formation in a simulation time of 2.5 sec. The cutting resistant force decreases with simulation time because the cutting tool-particle collision force decreases with simulation time as shown in Figure 9. At the beginning of the simulation, the cutting resistance force is close to zero because there is no contact at the teeth of the dragline

bucket. The cutting resistant force decreases with simulation time because the cutting tool-particle collision force decreases with simulation time.

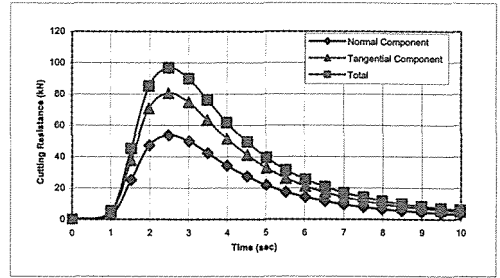


Figure 9. Cutting resistance force.

The solution to the bucket rigging dynamics was obtained after generating the cutting resistance force. Figure 10 shows the solutions to the bucket rigging dynamic problem. In these results, the center of mass for components is assumed to be located at half of the length of the component. The drag and hoist rope forces increase and decrease through simulation time.

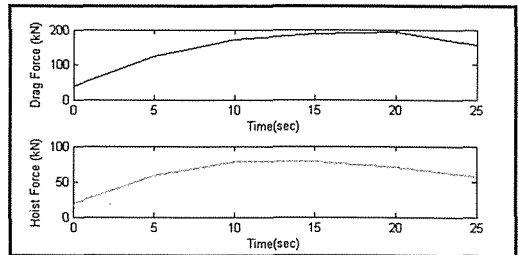


Figure 10. Bucket rigging dynamics for drag and hoist.

Since the numerical kinematics and dynamics models were developed for the 2-D dragline front-end assembly, the dynamics modeling results illustrate force generated during the planar motion of the dragline front-end. The drag force is a function of bucket displacement, cutting resistant force, and the material weight in the bucket. The maximum drag force, which is approximately 200 kN, occurs in a

simulation time of 20 sec. According to motor characteristics, increasing the drag force decreases the drag velocity (ACARP, 1999). This was confirmed by the results obtained from drag rope kinematics simulation results, which shows the decrease in the linear velocity of the drag rope through simulation time.

In Figure 10, the change in the hoist force is also given through simulation time. Since the formation digging process is mostly governed by the drag rope, the hoist rope force can be considered as a function of the material weight in the bucket. The maximum hoist force, which is approximately 75 kN, occurs in a simulation time of 15 sec. Since the hoist rope is a connection between the suspended load and the dragline boom, the hoist force is critical parameter in determining the stress loading on the dragline boom. Therefore, the change in the bucket payload and the linear and angular acceleration of the hoist rope affect the results significantly.

The force distribution on each dragline front-end component was also simulated to understand its load distribution. Figure 11 shows the MARION 7620 dragline boom dynamics during the excavation. The results showed that the forces exerted on the boom sheave are compressive forces and the forces exerted on the boom foot are tensile forces. Since the swing motion is not included in the study, the swing torque on the boom structure is eliminated from the calculations.

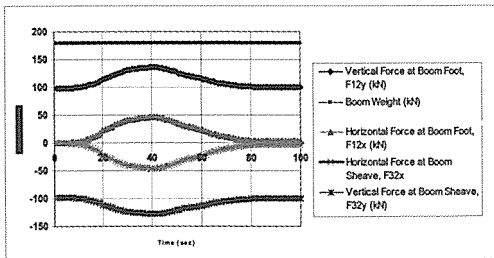


Figure 11. Boom dynamic forces.

The result showed that the weight of the boom is the biggest force component in the dynamics of the boom and it is critical for

determining the stress loading of the boom. The vertical and horizontal force components (F_{12x} and F_{12y}) at the boom foot are the forces required to connect the body of the boom to the machine house. Therefore, estimating these forces is critical for the welding process. On the other hand, the vertical and horizontal force components (F_{32x} and F_{32y}) at the boom sheave are the forces applied to the boom sheave and they are critical for stress loading.

Figure 12 shows the results of the hoist rope dynamics. The maximum hoist tension is found out to be 45 kN which takes place close to the boom sheave. The results showed that the maximum tension along the hoist rope occurs when the bucket is fully loaded due to the gravitational force and accelerating inertia of the bucket and its payload. The vertical and horizontal force components (F_{34x} and F_{34y}) are the forces on the hoist rope at the pulley. Estimating these forces is significant in estimating the required rope strength and required safety factor of the rope. Knowledge of these forces provides further insight into the appropriate rope strand selection. On the other hand, the vertical and horizontal force components (F_{54x} and F_{54y}) are the forces applied at the connection point of the rope to the bucket rigging mechanism, which is subject to oscillation during the operation.

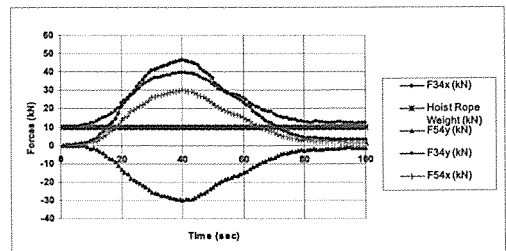


Figure 12. Hoist rope dynamics.

Figure 13 shows the drag rope forces as functions of the bucket and rigging kinematics and formation cutting resistant force. The vertical component of the drag rope tension increases continuously through the simulation time because the material inside the bucket increases within the same

time period. The drag rope is constantly under the effect of tension forces in Figure 13.

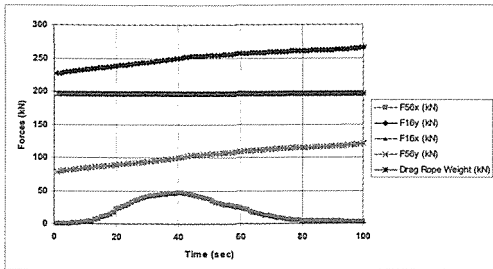


Figure 13. Drag rope dynamics.

In actual operating conditions, the usual practices for preventing the drag rope wear is to keep the drag rope always tight enough to prevent severe drag rope-ground interaction. Otherwise, the drag ropes are exposed to severe abrasion, especially at the pit crest, rope deformation, and inside breaking (Golosinski, 1994). The horizontal components of the drag rope tension increases until the digging process are completed; after the bucket is filled the horizontal tension decreases.

6 CONCLUSIONS

This research study advances a pioneering effort in dragline front-end simulation incorporating tool-formation interaction for efficient excavation. It contributed to the existing knowledge and advanced the research frontiers in dragline kinematics modeling and dynamic simulation.

This research study combines the use of an analytical literature review, kinematics and dynamic modeling, computer simulation, and detailed analysis of simulation results to achieve the research objectives. Numerical and computational techniques provided detailed information on all links and joints concerning the translational and rotational motion, displacement, velocity, and acceleration, as well as, forces, torques, and bending moments associated with these forces.

From detailed simulation experimentation and analysis of results from the kinematics

models, the following conclusions have been drawn: The vector loop methodology is a useful approach to derive kinematics relationships among the different components of the mechanical system having a closed loop structure. The maximum closure error was found to be about 4×10^{-8} , which is less than the required tolerance of 1×10^{-6} . The simulation results showed that there is a negative correlation between the kinematics properties of hoist and drag ropes. While the angular displacement of the hoist rope increases, that of the drag rope decreases. Similarly, if the angular velocity of the hoist rope increases, then the velocity of drag rope decreases with the same nonlinear characteristics. Also, for the same simulation time, angular acceleration of the hoist rope increases, however, the angular acceleration of the drag rope decreases.

The dynamic modeling results provided the forces exerted on the main dragline front-end components during a simulated digging operation. The research findings illustrated that the operating speed and operator performance impact the machine dynamical performance significantly. The discrete element method is proved to be an efficient tool to explicitly described the dynamics of assemblies of particles and the mechanical interaction processes between the soil particles and dragline bucket teeth.

Based on these pioneering initiatives, the results are expected to provide a solid basis for developing appropriate simulation technologies for efficient and economic dragline operations. Virtual simulation can optimize productivity by finding an optimized set of parameters for a particular dragline, which could take months to complete with physical simulations. The results could also be used for appropriate safety requirements and to provide guidelines for increasing machine reliability and maintainability for longevity and efficiency. Advances in dragline boom stress-strain, suspension monitoring and fatigue analysis will decrease operating and maintenance costs with significant benefits to industry.

7 RECOMMENDATIONS

Although this research study has made a significant contribution to efficient dragline excavation, its longevity and productivity, several areas require improvements through further research. The following areas are suggested for further research investigations:

Three-dimensional kinematics and dynamic models for generating a set of optimized 3-D dragline geometries for design and operation could significantly improve and add to the body of knowledge in this research area. The research findings could be used as a basis to yield an optimized set of 3-D geometry for dragline selection and operations in random multivariable fields through factorial experimental design and experimentation.

The experiments should be designed to provide knowledge on (i) an optimized set of dragline parameters; (ii) effective and efficient interactions with the formation; and (iii) minimized dragline boom stress and suspension during the operation to achieve maximum utilization.

The results could be used to provide solutions to important dragline problems such as component vibration and boom suspension. During the swing motion, the bucket is not limited within the vertical boom plane. It can experience out-of-plane oscillations caused by the swing acceleration. Therefore, the mechanics of this bucket oscillation must be incorporated into the dragline dynamics for more realistic and more accurate results. The dragline kinematics and dynamic characteristics could be monitored by using onboard instrumentations to provide real-time data to calibrate and to verify the theoretical models.

ACKNOWLEDGEMENT

The authors kindly acknowledge the financial support provided by the Robert H. Quenon Endowment Fund, USA and the Natural Sciences and Engineering Research Council (NSERC), Canada.

REFERENCES

- Awuah-Offei, K., Frimpong, S. and Askari-Nasab, H., 2005. Dynamic Simulation of Cable Shovel Specific Energy in Oil Sands Excavation, Computer Applications in the Minerals Industry (CAMI 2005), Banff, Alberta.
- ACARP 1999. Modeling Dragline Bucket Dynamics and Digging (Including Bucket Filling and Animations), *Australian Coal Association Research Program (ACARP) Research Project C3048, Final Report*, January, Earth Technology Pty. Ltd., 153 pp.
- Bernold, L. E., 1991. Experimental Studies on Mechanics of Lunar Excavation, *Journal of Aerospace Engineering*, ASCE, v. 4, No. 1: 9-22.
- Blouin, S., Hemami, A. and M. Lipsett, 2001. Review of Resistive Force Models for Earthmoving Process," *Journal of Aerospace Engineering*, Vol. 14, No. 3, American Society of Civil Engineers, New York, NY, USA, pp. 102-110.
- Bullock, D. M., Apte, S. and I. J. Oppenheim, 1990. Force and Geometry constraints in Robot Excavation, *Space 90: Engr. Constr. And Operations in Space*, NY.
- Cleary, P. W., 1998. The Filling of Dragline Buckets, *Math. Engng. Ind.*, Vol. 7, No. 1, pp. 1-24.
- Dormand, J. R. and P. J. Prince, 1980. A Family of Embedded Runge-Kutta Formulae, *Journal of Computational and Applied Mathematics*, Vol. 6(1), Elsevier B. V., Oxford, UK, pp. 19-26.
- Frimpong, S. and Y. Hu, 2003. Hydraulic Shovel Simulator in Surface Mining Excavation Engineering, *12th MPES*, Kalgoorlie, West Australia (April).
- Frimpong, S. and Z. Chang, 2004. KANEXP03 Cable Shovel Dynamics and PID Control Scheme for Efficient Surface Mining Excavation, Submitted to *SME Mining Engineering*, © SME, Littleton, CO.
- Golosinski, T. S., 1994. Performance of Dragline Hoist and Drag Ropes, *Mining Engineering*, Vol. 46, No. 11, pp. 1285-1288.
- Haneman, D. K., H. Hayes and G. I. Lumley, 1992. Dragline Performance Evaluations for Tarong Coal Using Physical Modeling, *Third Large Open Pit Mining Conference*; © The Australian Institute of Mining and Metallurgy, Mackay, Australia: 93-99.
- Hansen, M. R., 1993. An Automated Procedure for Dimensional Synthesis of Mechanisms, *Structural Optimization*, Vol. 5: 145-151.

- Hemami and Daneshmend, L., 1992. Force Analysis for Automation of the Loading Operation in a LHD-loader," *Proc., 1992 IEEE Int. Conf. on Robotics and Automation*, IEEE, Piscataway, N.J.: 645-650.
- Khoshzaban, M., Sassani, F. and Lawrence, P.D., 1992. Autonomous Kinematic Calibration of Industrial Hydraulic Manipulators, *Fourth International Symposium on Robotics and Manufacturing/The American Society of Mechanical Engineers*, Santa Fe, USA, 577-584, (November).
- Koivo, A. J., 1994. Kinematics of Excavators (Backhoes) for Transferring Surface Material, *Journal of Aerospace Engineering*, © American Society of Civil Engineering (ASCE) Vol. 7, No. 1: 17-32.
- Lawrence, P.D., Sassani, F., Sauder, B., Sepehri, N., Wallersteiner, U., and Wilson, J., 1993. Computer-Assisted Control of Excavator-Based Machines, *SAE off Highway Exposition*, Milwaukee, Wisconsin, USA, SAE Technical Paper #932486.
- MATLAB 7.0 User's Guide, 2004. *The Language of Technical Computing*, © The MathWorks Inc., 24 Prime Park Way, Natick, MA 01760.
- MSC. ADAMS, 2004. *MSC Software Corporation*, © MSC. ADAMS® Santa Ana, CA.
- Papadulos, E and S. Sarkar, 1996. On the Dynamic Modeling of an Articulated Electrohydraulic Forestry Machine, *Proceedings of the 1996 AIAA Forum on Advanced Developments in Space Robotics*, Madison, WI, (August 1-2).
- Shi, N. and T. G. Joseph, 2004. A New Canadian Shovel Dipper Design for Improved Performance, *Proc. of CIM Conference*, Edmonton, AB, Canada.
- Townson, P. G., Murthy, D. N. P. and H. Gurgenci 2003. Optimization of Dragline Load, *Case Studies in Reliability and Maintenance*, Ed. Wallace R. Blischke and D. N. Prabhakar Murthy, Wiley Series in Probability and Statistics, John Wiley & Sons Inc., New Jersey, USA, pp. 517-544.
- Westcott, P., 2004. Dragline and/or Truck/Shovel Assist: Some Technical and Business Considerations, Inaugural UNSW/Mitsubishi Lecture Notes, http://www.mining.unsw.edu.au/pdf/MitsubishiLect_Notes_2004.pdf (Last Accessed November 21, 2006).

Work of Mining Machines in Fault Tectonic Zones for the Conditions of Assarel Mine

L. Tsotsorkov, D. Nikolov & A. Kostov
Assarel-Medet JSC, Bulgaria

ABSTRACT “Assarel – Medet” JSC is the largest mining company in Republic of Bulgaria, with a considerable contribution to the mining industry development on a world scale. The company is the first Bulgarian enterprise from the highly-risky heavy industry, that have successfully implemented the integrated systems ISO 9001:2000, ISO 14001:1996 and OHSAS 18001/2003/ in 2003. During the last few years the mining equipment in “Assarel” open pit was basically replaced, as the biggest front loader in the world – CATERPILLAR 994 D was put into operation, as well as a single bucket hydraulic shovel LIEBHERR 994 E both with bucket capacity of 17 m³ and 130 t haulage trucks BelAZ 75 131.

Taking into consideration the significant investment made, the issue about the safe operation of the heavy mining equipment in fault tectonic zones of Assarel mine becomes a problem of the present day. The report covers in details the operation schemes, which need to be used during operation of highly productive mining machines in deposits that have a complex structure like mine “Assarel”, in order to increase the efficiency and work safety.

The copper deposit of Assarel is located in the Sredna Gora Mountain, district of Pazardzhik, 80 km eastward from the capital Sofia, and 10 km to the northwest of the town of Panagyurishte. The region of the deposit has a temperate mountain relief at an altitude of 800 to 1000 m.

The rocks, which build up the deposit, are primarily granatoides, andesites, asdesite tuffs, diorite and quartz diorite porphyrites, are strongly tectonically jointed and in some parts broken. During the process of ore formation, the exposed part of the cracks were filled with secondary minerals and formations such as quartzite, chloride, gypsum, clay materials, etc. At the same time the rocks were hydrothermally modified. This modification is strongest in the west half of the deposit where most of them are kaolinized and clayish.

In the south-west part, the rocks which lay under the South Asarelian fault are filled with a 2-3 mm thick gypsum layer. The engineering and geological peculiarity of these small cracks is that they do not have the same strength as the rocks. They do not have such big importance as the large cracks have for the slope angles in the pit.

The large cracks, which are visible in the mining headings, are impressive for their strength. Their number is small and they are distributed at irregular distances in 1-2 m up to 20-25 m and even more. In most cases their width is only few millimeters but in some cases, when it refers to strongly kaolinized rocks, it reaches 10-15 cm and they are filled with clay then. These cracks are characterized by the fact that there are tectonic slides on their walls. Those cracks, which are small tectonic faults, include relatively well expressed abnormal contact

surfaces which vary between porphyries and granites as well as tectonic broken zones whose width varies between 15 and 20 cm.

It becomes evident from the geological documentation (Anon, 1976) that 350 big cracks were found out for approximately 5,300 m mining headings, tectonic broken zones and abnormal contact surfaces i.e. such a tectonic fault is situated at the average of every 15 m of cutting.

The complex engineering and geological characteristics of the deposit is a prerequisite for the exclusive difficulties which are encountered in the mining activities.

For the sake of evaluation of the slopes in the Asarel pit and determining the slope angles, the stability can be regarded as general slope stability and stability of the individual benches or local areas.

The general slope stability and its slope angle are established based on: engineering and geological sections of a certain area, the litological composition of the rocks, their strength, the nature and degree of jointing, tectonic faults, the distribution, which is

close to the angle, the material which fills the tectonic cracks and faults, hydrostatic pressure distributed on the sliding surface.

The stability of the individual benches or local areas of the slope is impacted by the tectonic faults in the certain slope area of bench, the total intensity of the rocks cracking, the rocks susceptibility to weathering, the orientation of the slope distribution in the cases of large tectonic cracks, the filtration pressure caused by water flowing along the bench slope.

The main physical and mechanical properties of the rocks which determine their stability in the slopes are the characteristics of the shear resistance – the cohesion and the internal friction factor (Table 1, Straka and Ilieva, 1995). It is known that these characteristics change with time and in cases when the rocks bedding conditions are modified. The mining headings made are the ones that most significantly change the rocks bedding conditions in the area of weathering, which borders the bench slopes.

Table 1. Physical – mechanical properties of the rocks in Assarel Mine based on data from June 1996.

Rock type	Bulk density g/cm ³	Water content %	Tensile strength kN/m ²	Cohesion kN/m ²	Internal friction angle (°)
Propylites	2.49	0.8	66,000	2,260	39.8
Quartzites	2.33	0.7	35,000	1,510	35.8
Alunite-diaspore quartzites	2.49	1.0	-	80	30
Tectonic clay	2.15	8.2	-	50	27.2
Sericite quartzites in tectonic hidden zone	2.26	3.0	-	80	23

The following most frequently observed cases for weakened benches in the conditions of the Assarel mine are the following:

1. An area of the mined bench is chapped by tectonic faults or cracks, the distribution of which coincides or is close to the bench distribution by azimuth and the wall of mining serves as its slope as in Figure 1.

In order to assess its stability, the magnitudes of the restraining and shearing forces along the vertical plane sections, which are normal towards the area distribution, have to be assessed. The distance between the sections is assumed to be 5 or 10 m depending on distribution homogeneity of the bench parameters and the formula for the factual stability factor η_{ϕ} is used:

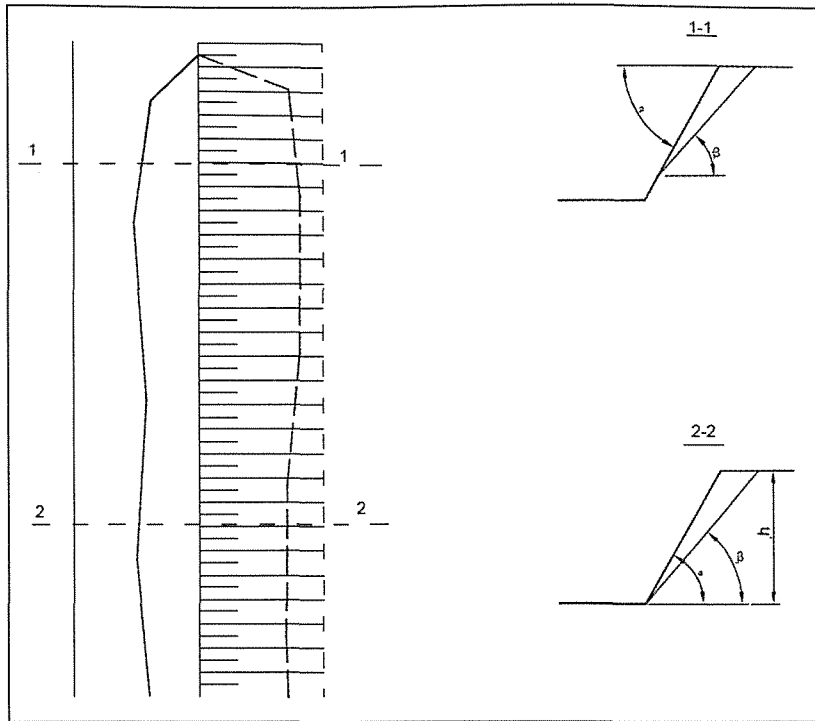


Figure 1.

$$\eta_{\phi} = \frac{P \cos \beta \operatorname{tg} \varphi' + c' S}{P \sin \beta}$$

where:

P stands for the weight of the possible caving prism, which is confined by two adjacent sections, N;

c' - stands for the relative cohesion by rocks contact surface, N/m^2 ;

φ' - stands for the angle of internal friction along the contact surface, $^{\circ}$;

β - stands for the cracks or tectonic faults slope angles, $^{\circ}$;

S - stands for the sliding surface average area, m^2 .

2. In many cases when shaping the bench in the boundary contour along with the tectonic faults, a system of cracks or faults whose slope is orientated towards the mining wall with angles bigger than the contact surface friction angle are also exposed, which form blocks Figure 2.

The following method is used for determining the stability of such blocks: based on data from the instrumental survey, the weight of the pyramid P, the area of the surfaces S_1 and S_2 , the slope angles of the planes β_1 and β_2 and the angle ω between them, measured in the horizontal plane (along the berm) are measured. In the event of caving, the block will move along the intersection line of the sliding plane and as a result, the so-called "chute" is formed. The calculation is done for the section A-A. The inclination angle of the "chute" in this case will be determined analytically using a formula, derived on the basis of graphical plotting:

$$\operatorname{arctg} \delta = \frac{\sin \operatorname{arctg} \left(\operatorname{ctg} \omega + \frac{\operatorname{ctg} \beta_1}{\operatorname{ctg} \beta_2 \sin \omega} \right)}{\operatorname{ctg} \beta_2}$$

This formula is valid when $\beta_2 < 90^{\circ}$.

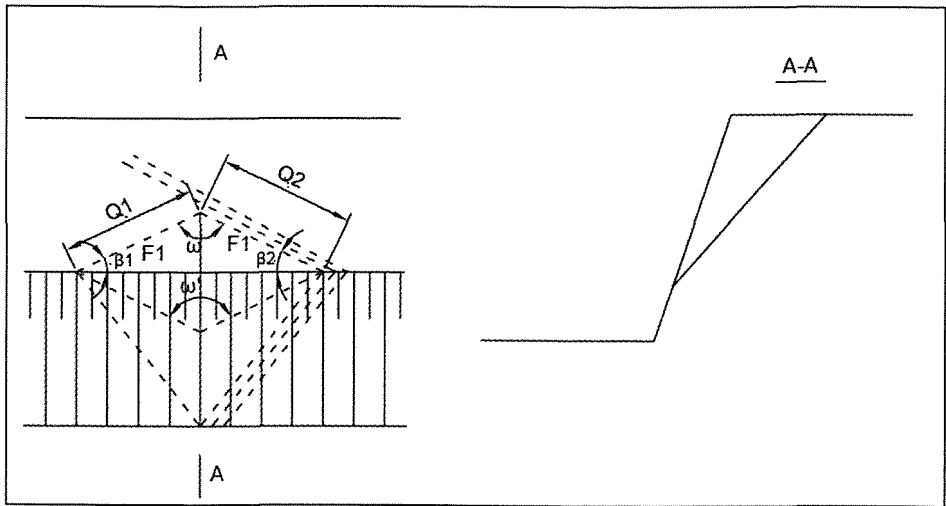


Figure 2.

The block stability is determined based on the following relation:

$$\eta_{\phi} = \frac{P \cos \delta \operatorname{tg} \varphi' + c'(S_1 + S_2)}{P \sin \delta}$$

In case, there is an abrupt difference between the friction angles along the contacts of the surfaces, the pyramid weight is divided into two parts – in proportion to the surfaces of the sliding planes projections upon the horizontal plane.

$$P_1 = \frac{a_1 \operatorname{ctg} \beta_1}{a_1 \operatorname{ctg} \beta_1 + a_2 \operatorname{ctg} \beta_2} \quad ,N;$$

$$P_2 = P \frac{a_2 \operatorname{ctg} \beta_2}{a_1 \operatorname{ctg} \beta_1 + a_2 \operatorname{ctg} \beta_2} \quad ,N,$$

where a_1 and a_2 stand for the lengths of the cracks, which are measured along the berm.

The final formula for the stability factor will be as follows:

$$\eta_{\phi} = \frac{(P_1 \operatorname{tg} \beta_1' + P_2 \operatorname{tg} \beta_2') \cos \delta + c'(S_1 + S_2)}{P \sin \delta}$$

3. Together with those two cases, the slope benches are chapped by displacements or faults, crossing them in plan at acute angles towards the slope distribution and with slope

angles versus the mining wall of $30 \div 35^\circ$, if the fault is filled with clays at angles of $12 \div 15^\circ$. Such areas break the continuity of the transportation berms and they are hazardous for people and machines. The hazard evaluation is calculated using the formula (Gavrillova et al., 1978):

$$\operatorname{tg} \varphi'_n \leq \operatorname{tg} \beta' = \cos \delta \operatorname{tg} \beta$$

where:

φ'_n stands for the angle of internal friction along the weakening surface reporting the safety factor;

β' - stands for the angle projection of the slope angle upon the vertical plane, which is a normal to the slope distribution;

δ - stands for the angle between the weakening surface and the slope distribution direction;

β - stands for the slope angle of the weakening surface.

The mining activities in these areas are exclusively difficult and hazardous not only for the mining equipment shovels, drills, front-end loaders, trucks but also for the maintenance personnel.

When mining activities are started in these areas, the equipment productivity is reduces and there is a high percent of risks for emergency situation sliding of big rock

pieces, spontaneous cavings, etc. The risk grows higher when the mining activities go in depth and reach the places of heavy hydrogeological conditions. Taking into account that the current mining activities have reached those hazardous zones, it is desirable that an immediate commitment for resolving this issue is made. Any failure to resolve it might cause operation suspension for a large period of time. Due to this fact, the following problems need to be solved in order to ensure the slope and benches stability for the safe operation of mining equipment for the conditions of pit Assarel:

- ❖ Carrying out of systematic monitoring of the slopes, bench slopes and berms width.

- ❖ Detailed studying of the engineering and geological conditions related to the stability of the individual areas of the benches.

- ❖ Zonating of the mining field depending on the structural faults and indicating the areas, which contain cracks, failures and tectonic faults.

- ❖ Preparation of passports for the shaping and strengthening of the berms.

- ❖ Preparation of passports and operation schemes for the respective type of mining equipment in the bench areas, which contain faults.

The deformations monitoring of the bench slopes, chapped by weakened surfaces, inclined towards the mining wall is performed by periodical instrumental surveys for the situation of the survey poles, put on the berms. For the sake of convenience, the monitoring stations are supplied with 2÷3 profile survey lines, put in parallel on the slope edges. The movement of the survey poles is determined based on the deviations from the line on the horizontal surface and along the way of geometrical leveling in the vertical surface. Instrumental monitoring need to be performed once or twice per month. The accuracy when determining the movements in the vertical plane has to be within 5 mm, and in the horizontal plane 10 mm. The continuous increase of the movement up to 20 mm in the vertical plane and up to 30 mm in the horizontal plane is an indication that the slope stability is close to

its boundary state (Hristov, 1995). The monitoring will enable us to identify the zones and areas where eventual slope deformations could occur and to take anti-failure measures.

The study of the engineering and geological conditions in order to prepare a passport for the benches shaping is performed for a area band with width of 80÷100 mm within the contour of each bench. The engineering and geological zoning which is performed at the stage of the pit design based on the data from the detailed geological study is usually inadequate. In this regard, when new benches are mined, new detailed study of the rocks jointing in situ needs to be carried out.

The anticipated slope deformation and prevention measures, drilling and blasting activities when reaching the boundary contour, the way of bench shaping need to be reflected in the passports.

One of the most responsible tasks of the engineering and technical staff is the passport preparation for the mining equipment operation in the weakened zones of the benches. They have to be prepared in particular of each type of equipment as the operation scheme and manner of the respective piece of equipment when reaching a faulty zone, the necessary monitoring by the equipment operator and the engineering and technical staff in charge, as well as the safety measures have to be reflected in them. Some of the operation schemes are shown on Figure 3, which can be applied for the conditions of pit Assarel with the loading equipment which is currently in operation: shovels LIEBHERR 994 BE, RH 120 C and front-end loaders CAT 992 D and 994 D.

The conjunction between parallel and cross cuttings is preferred in these schemes for the sake of safe mining material digging in the faulty zones.

The analysis of the performed studies serves as a ground to draw the following conclusions:

- The engineering and geological conditions of pit Asarel are a prerequisite for the occurrence of failures and bench slopes deformations;

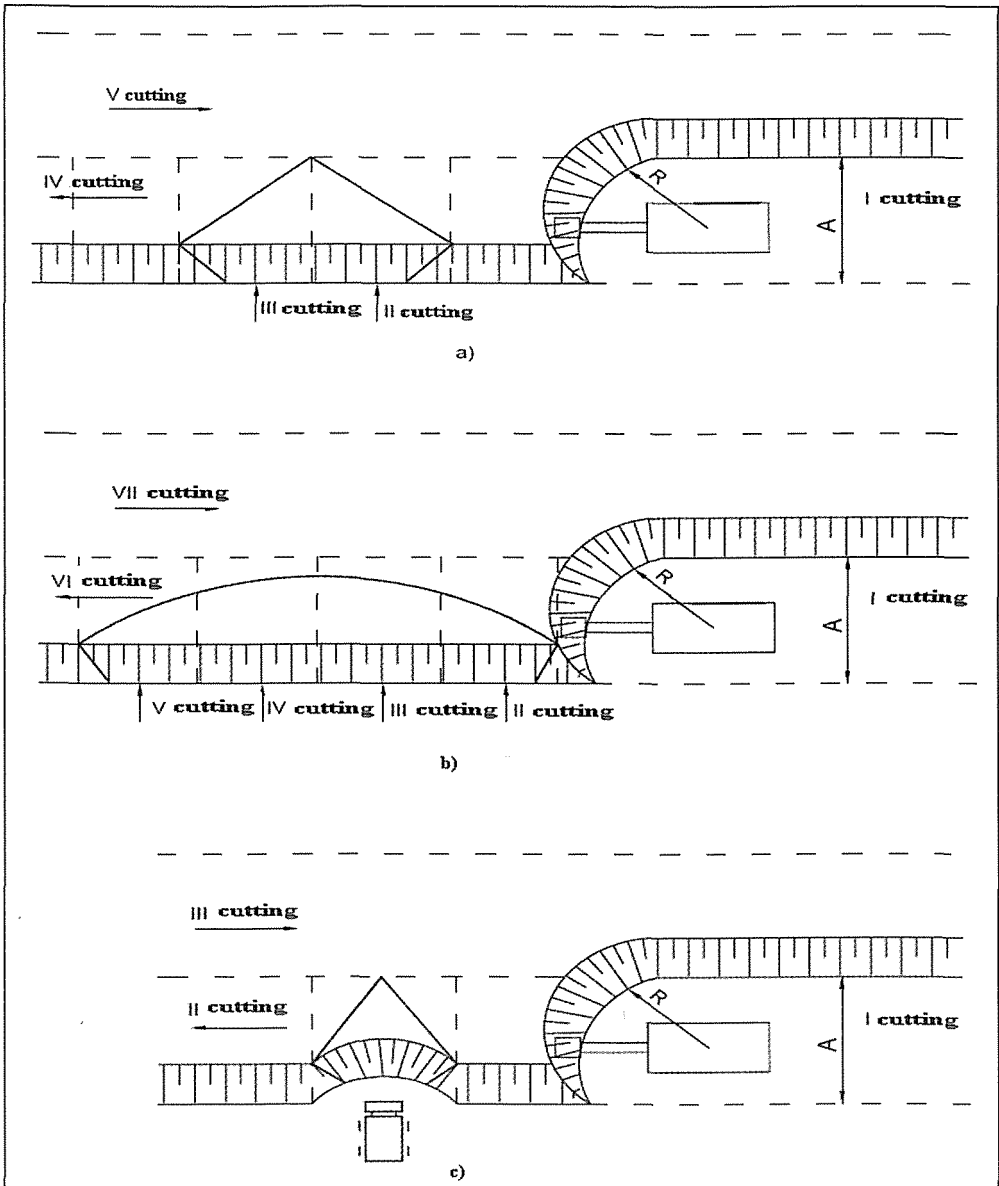


Figure 3.

- Due to the fact that the mining activities have gone indepth in the pit and they have reached the failure zones, monitoring and strengthening activities of these zones need to be undertaken when reaching these zones.
- Safe and efficient operation of people and equipment, when reaching those areas, and slope stability when mining deeper in the pit, have to be ensured;
- Taking into account the structural jointing of the massif in the deposit of Asarel contributes to reducing the

negative impact by the mining and material removal upon the environment, which is one of the requirements of the executive body of Assarel-Medet JSC in order for the “bottlenecks” in the particular activities and differentiated units to be studied. (Tsotsorkov, 1996).

REFERENCES

- Anon, 1976. Geological report for a detailed study of deposit Assarel.
- Gavrlova, R. B., Fissenko G. L., Revazov M. A., Galustian E. L., Hristov S. G., 1978, Artificial strengthening of instable slope areas, Technica©, Sofia.
- Hristov S. G., 1995, Instruction for monitoring the slopes deformations in pit Asarel and undertaking measures for ensuring their stability, Sofia.
- Straka, U., Ilieva L. 1995, Re-evaluation and update of the engineering and geological situation in pit Assarel, Sofia.
- Tsotsorkov, L. D. 1996, Foundations of Corporate Culture, Sofia.



AUTHOR INDEX

- Abadi, H.D.J. 143
Afshar, A. 33
Aghababaei, H. 229, 259
Albuquerque, R. 113
Aliasghari, H. 217
Ataman, N. 85
Aziz, N. 15, 209
Aziz, N.I. 21
- Badino, V. 197
Balci, C. 161
Benzer, H. 79
Berry, R. 217
Bilgin, N. 161
Blengini, G.A. 197
Boz, E. 57
Breslin, J.A. 3
- Caladine, R. 209
Cardu, M. 67, 127
- Çopur, H. 161
- Dağ, A. 151
Demirel, N. 265
Deniz, V. 57
Dezyani, H. 33
Düzyol, İ. 161
- Esen, S. 79
- Farzanegan, A. 103
Frimpong, S. 265
- Garbarino, E. 67, 197
Gürtunca, R.G. 3
- Hoseinie, H.S. 259
- Irannajad, M. 93, 103
- Jalalifar, H. 15
Joy, J. 47
- Kaymak, U. 151
Keilich, W. 21
Kızıl, G.V. 47
Kızıl, M. 247
Kostov, A. 277
Kushavand, B. 137
Kuyucak, N. 185
- Lever, P.J.A. 121
- Majdi, A. 137
Mancini, R. 67
Man'ko, A.V. 221
Mehdilo, A. 93
- Namin, F.S. 143
Nikbakhtan, B. 229
Nikolov, D. 277
- Özbayoğlu, G. 85
- Papini, R. 113
Peres, A. 113
Pourrahimian, Y. 137, 229, 259
- Rashidi, S. 103
Royanfar, A. 41
- Sarı, M. 121
Sauku, H. 241
Shahriar, K. 33, 41, 143
Strawson, C. 47
- Tank, E. 57
Tercan, A.E. 151
Tiryaki, B. 171
Tome, L. 209
Tsotsorkov, L. 277
Tumaç, D. 161
Tütmez, B. 151
- Umucu, Y. 57
- Vyas, D. 209
- Zavaglia, K. 197